ChemPubSoc Europe

DOI: 10.1002/chem.201502655

CHEMISTRY
A European Journal
Communication

Asymmetric Synthesis

Catalytic Asymmetric Reactions of 4-Substituted Indoles with Nitroethene: A Direct Entry to Ergot Alkaloid Structures

Simone Romanini,[a] Emilio Galletti,[a] Lorenzo Caruana,[a] Andrea Mazzanti,[a] Fahmi Himo,[b] Stefano Santoro,*[c] Mariafrancesca Fochi,*[a] and Luca Bernardi*[a]

Abstract: A domino Friedel–Crafts/nitro-Michael reaction between 4-substituted indoles and nitroethene is presented. The reaction is catalyzed by BINOL-derived phosphoric acid catalysts, and delivers the corresponding 3,4-ring-fused indoles with very good results in terms of yields and diastereo- and enantioselectivities. The tricyclic benzo[*cd*]indole products bear a nitro group at the right position to serve as precursors of ergot alkaloids, as demonstrated by the formal synthesis of 6,7-secoagroclavine from one of the adducts. DFT calculations suggest that the outcome of the reaction stems from the preferential evolution of a key nitronic acid intermediate through a nucleophilic addition pathway, rather than to the expected "quenching" through protonation.

Ergot alkaloids have been the subject of longstanding interest.[1] Besides being the causative agents of the serious disease ergotism and used as hallucinogenic drugs, ergot alkaloids and derivatives have seen their powerful biological activities subdued for medical purposes. Pharmaceutical usefulness arises from subtle modifications of their naturally occurring structures, which feature a distinctive tricyclic 4-amino-1,3,4,5-tetrahydrobenzo[*cd*]indole framework with a modified methallyl residue at the 5-position, often fused within an additional ring (Figure 1 a). Biosynthetically derived from tryptophan through intriguing enzymatic pathways,[2] total syntheses of several members of this class of natural compounds have been reported, with the archetype lysergic acid having been the most pursued.[3] Concurrently, the construction of the synthetically challenging 1,3,4,5-tetrahydrobenzo[*cd*]indole scaffold has recently received considerable attention, even in its unadorned and racemic/achiral forms.[4] In this context, we have reported an enantioselective approach to this scaffold, based on the organocatalytic domino reaction of indoles **1** bearing a Michael acceptor at the 4-position with α,β-unsaturated aldehydes.[5]

The domino reaction of these substrates **1** with nitroethene[6] **2** leads to benzo[*cd*]indoles **3** having the nitro group at a strategic position to serve as precursors of ergot alkaloids (Figure 1 b). This reaction has been attempted with a view to ergot synthesis. However, results were disappointing and the reaction was thus discarded in favor of less direct routes for compounds related to **3**.[4d,7,8] We hypothesized that recent advances in the activation of nitro compounds by weak H-bond donor catalysts[9] could offer a solution for this transformation, giving also an unprecedented stereocontrolled access to compounds **3**. However, initial experiments (Figure 1 c) showed that thiourea catalysts that were useful in simpler Friedel–Crafts (FC) reactions[10] were not able to promote any reaction between substrates **1 a**–**c** and nitroethene **2**, possibly due to the known[5a] poor nucleophilicity of indoles **1**. A more acidic BINOL-derived phosphoric acid[11] catalyst, such as **PA1**, proved instead to be useful. Substrate **1 a** furnished with promising enantioselectivity and as a single *trans*-diastereoisomer the desired product **3 a** with moderate (70 %) conversion. This result was somewhat unexpected. The reaction should proceed through a nitronate/nitronic acid, formed upon the FC addition. In principle, the **PA** catalyst should be able to easily "quench" this species through protonation, due to its acidity.[12] Indeed, the presence of a competition between nitro-Michael and "quenching" pathways was revealed by the exclusive formation of the side product **3′** not only in the reaction with indole **1 b** featuring a weak ester Michael acceptor, but also with **1 c** bearing an *N*-acyl pyrrole, an efficient moiety for nitro-Michael reactions (Figure 1 c).[13] It is worth stressing that only few examples of organocatalytic domino reactions[14] have dealt with this type of sequential process (H-bond-promoted addition of a neutral nucleophile triggering a subsequent transformation),[15] none of which has involved a phosphoric acid as catalyst.

Prior to embarking on the study and optimization of the reaction, we decided to resort to a computational approach to shed some light on the reaction pathway of this unusual phos-

[a] *S. Romanini, E. Galletti, Dr. L. Caruana, Prof. A. Mazzanti, Prof. M. Fochi, Prof. L. Bernardi*
Department of Industrial Chemistry "Toso Montanari"
University of Bologna, V. Risorgimento 4, 40136 Bologna (Italy)
E-mail: mariafrancesca.fochi@unibo.it
luca.bernardi2@unibo.it

[b] *Prof. F. Himo*
Department of Organic Chemistry, Arrhenius Laboratory
Stockholm University, 10691 Stockholm (Sweden)

[c] *Dr. S. Santoro*
Department of Chemistry, Biology and Biotechnology
University of Perugia, V. Elce di Sotto 8, 06123 Perugia (Italy)
E-mail: stefano.santoro@unipg.it

Supporting information for this article is available on the WWW under http://dx.doi.org/10.1002/chem.201502655.

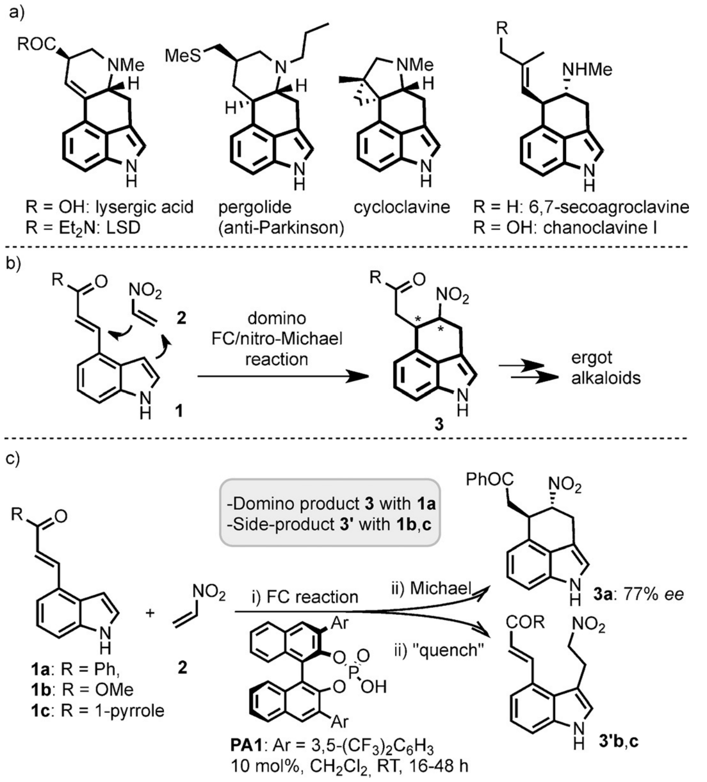

Figure 1. Ergot alkaloid structures and domino reaction of indoles **1** with nitroethene **2**. a) Some naturally occurring and semisynthetic ergot alkaloid derivatives (the 1,3,4,5-tetrahydrobenzo[*cd*]indole framework is highlighted); b) Friedel–Crafts (FC)-triggered nitro-Michael reaction en route to ergot alkaloids; c) preliminary results: thioureas do not promote the reaction. Phosphoric acids can catalyze the reaction, by two competing pathways (nitro-Michael vs. intermediate "quench").

phoric acid-catalyzed transformation. Previous computational studies of the phosphoric acid-catalyzed FC addition of indoles to nitroalkenes[16] focused on the C–C bond-forming step, neglecting subsequent H-transfer events (i.e., rearomatization and nitronate protonation) that are crucial in this cascade process, dictating its evolution. Here, several pathways following the first C–C bond formation can, in principle, be envisaged. The FC reaction might evolve through a H-relay process releasing the catalyst and a chiral indolenine. Alternatively, catalyst-coordinated nitronic acid intermediates could form upon indole rearomatization or N–H abstraction. Besides, indole rearomatization might occur prior to or after the Michael addition step. These hypotheses were evaluated by DFT calculations using the B3LYP-D functional (see the Supporting Information for details), studying the full catalytic cycle for the reaction between nitroethene **2** and the methyl ketone derivative **1d**, chosen as a model of substrates bearing a ketone Michael acceptor. We used the phosphoric acid derived from [1,1′-biphenyl]-2,2′-diol as a model of BINOL-derived chiral phosphoric acids (Figure 2).

First, two possibilities were found for the initial nucleophilic attack of the indole on electrophile **2**. In the first case (**TS1**) the catalyst coordinates to both the nitro group and the indole N–H, whereas in the second (**TS1′**), it coordinates to the nitro group and the C3–H of the indole. In both cases, protonation of the nitro group occurs concertedly with the expected C–C bond formation.[17] The reaction occurring through **TS1** is favored by 6.4 kcal mol^{-1} over **TS1′**, in line with the previously determined pathway followed in related FC processes.[16a] While N–H abstraction was not productive, a TS for the indole rearomatization through C3-deprotonation (**TS2**) was located, associated with

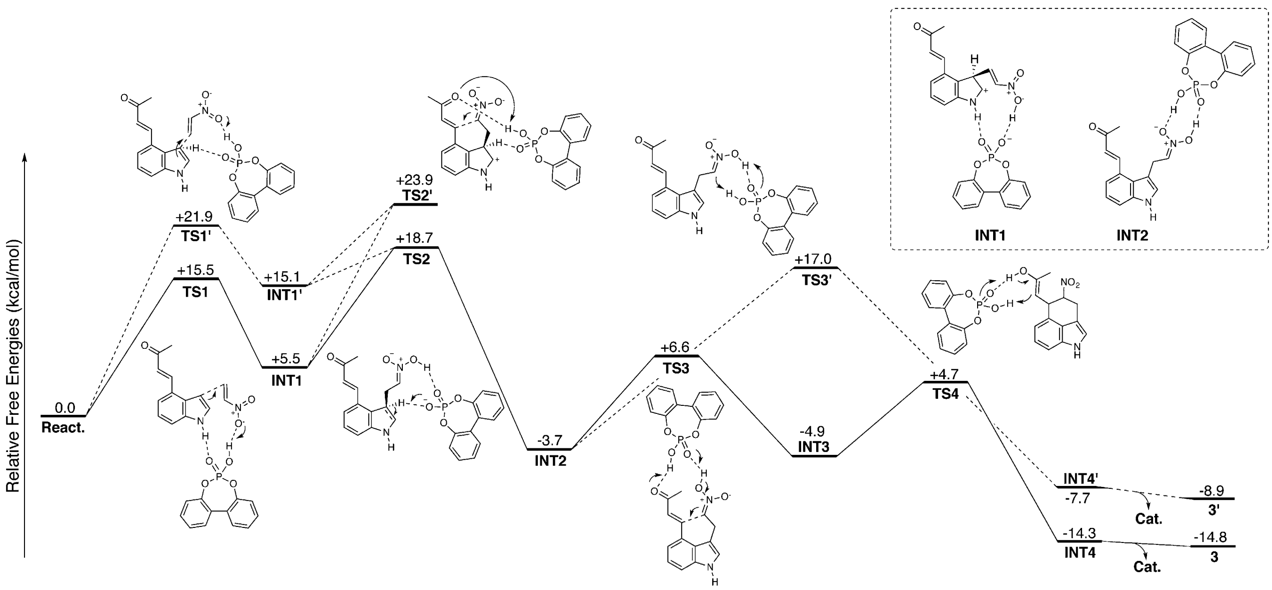

Figure 2. Free energy profile for the formation of products **3d** and **3′d** from the reaction between (*E*)-4-(1*H*-indol-4-yl)but-3-en-2-one (**1d**) and nitroethene **2**. See the Supporting Information for optimized ball-and-stick structures.

an energy barrier of 18.7 kcal mol^{-1} relative to the reactants. This step does not occur through a proton-relay process releasing the catalyst, but leads instead to intermediate **INT2**. Alternatively, we have found that a direct cyclization could occur before rearomatization through **TS2**′. However, the energy barrier for this possibility is higher than that for the rearomatization (23.9 vs. 18.7 kcal mol^{-1}), which makes this option less likely.[18] After the rearomatization, a nitro-Michael addition can occur with the catalyst coordinating to both the nitro group and the carbonyl moiety (**TS3**). In this step, associated with a low energy barrier (10.3 kcal mol^{-1}), the deprotonation of the nitro group and the protonation of the carbonyl occur concertedly with the *trans*-selective C–C bond formation.[19] After cyclization through **TS3**, a keto–enol tautomerization is required to generate final product **3 d**. We found that the catalyst can also promote this process through **TS4**, with a low barrier.

As discussed above, the formation of cyclized product **3** is in competition with the formation of side-product **3**′. This can be formed if **INT2** evolves through a nitronic acid–nitro tautomerization, instead of the cyclization. A transition state (**TS3**′) with an energy barrier of 20.7 kcal mol^{-1} relative to **INT2**, and involving the catalyst, was identified for this tautomerization. The energy required for this step is likely overestimated by our calculations,[20] with **TS3**′ being the best approximation we have found. Nevertheless, given the exclusive formation of cyclized product **3 d**, it can be concluded that the energy required for this tautomerization should be higher than about 13 kcal mol^{-1} relative to **INT2**.[20]

To summarize, the reaction occurs through a nucleophilic attack of the indole **1** on nitroethene **2**, followed by a rearomatization occurring before the cyclization and ensuing keto–enol tautomerization. The catalyst is involved in all steps, including the stereodetermining cyclization event, accounting for the enantioenrichment of product **3 a** when an enantiopure catalyst was used (Figure 1 c). A rather high energy barrier associated with the nitronic acid–nitro tautomerization step (nitronate “quench”) makes the cyclization to the desired products **3** possible and prevailing even with an acidic catalyst, provided that a highly reactive Michael acceptor is employed (i.e., **TS3** energy is sufficiently low).

To optimize the catalytic asymmetric version of the reaction, we screened various chiral phosphoric acid catalysts[11] and reaction conditions, using **1 a** as substrate in the reaction with nitroethene **2** (see the Supporting Information and Scheme 1). This screening initially identified catalyst **PA2** [(*R*)-TRIP, 10 mol %], a solvent that is non-coordinating but able to solubilize indole **1 a** (CH_2Cl_2), and ambient temperature as suitable conditions to afford **3 a** with very good results. We then tested dehydrating agents as additives, in order to increase the catalyst activity. Activated molecular sieves (3, 4, or 5 Å) gave scarcely reproducible results, and surprisingly shifted occasionally the reaction pathway towards the open-chain adduct **3**′**a**.[21] The obtainment of **3**′**a** allowed us to perform a control experiment (see the Supporting Information) confirming the expected[12] and computed (Figure 2) incapability of the catalyst to resume **3**′**a** to **3 a**. Instead, we found that $MgSO_4$ as drying agent had a beneficial effect, allowing a reduced catalyst loading and a lower reaction temperature, leading to increased enantioselectivity.

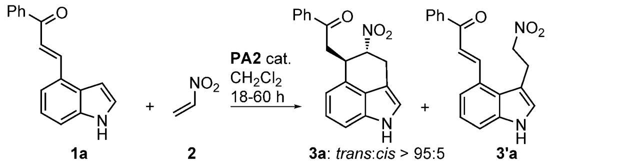

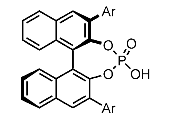

PA2: Ar = 2,4,6-(i-Pr)$_3C_6H_2$

Conditions	Results
10 mol% cat., RT	**3a**:**3'a** >9:1, >90% conv., 94% *ee*
10 mol% cat., RT, 3, 4 or 5 Å MS	**3a**:**3'a** >9:1-<1:9, >90% conv., 84-95% *ee*
5 mol% cat., 0 °C dry $MgSO_4$	**3a**:**3'a** >9:1, >90% conv. 97% *ee*

Scheme 1. Representative screening results.

Table 1. Scope of the catalytic enantioselective domino reaction.[a]

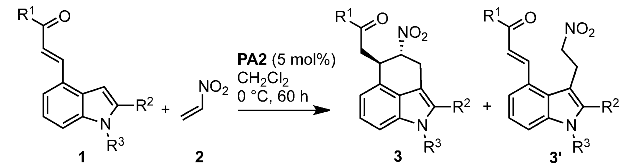

Entry	1	R^1	R^2	R^3	Yield[b] [%]	*ee*[c] [%]
1	**1 a**	Ph	H	H	**3 a**: 95	97
2[d]	**1 b**	OMe	H	H	**3**′**b**: 62	–
3[d]	**1 c**	pyrrol-1-yl	H	H	**3**′**c**: 94	–
4	**1 d**	Me	H	H	**3 d**: 96	54
5	**1 e**	4-MeOC_6H_4	H	H	**3 e**: 91	97
6	**1 f**	4-BrC_6H_4	H	H	**3 f**: 95	97
7	**1 g**	4-MeC_6H_4	H	H	**3 g**: 98	98
8	**1 h**	2-naphthyl	H	H	**3 h**: 98	>99
9	**1 i**	*t*Bu	H	H	**3 i**: 90	93
10[e]	**1 j**	$CH(OMe)_2$	H	H	**3 j**: 82	96
11	**1 k**	Ph	Me	H	**3 k**: 90	94
12[f]	**1 l**	Ph	H	Me	**3 l**: 75	95
13[g]	**1 m**	Ph	H	allyl	**3 m**: 70	93

[a] Conditions: indole **1** (0.10 mmol), **PA2** (0.005 mmol, 5 mol %), nitroethene **2** (1.5 M toluene solution, 0.15 mmol), dry $MgSO_4$ (30 mg), CH_2Cl_2 (300 μL), 0 °C, 60 h, then filtering through a plug of silica gel, solvent evaporation, and analysis by ^{1}H NMR spectroscopy; d.r. of products **3** was found to be >95:5 in all cases. [b] After chromatography on silica gel. [c] Determined by chiral stationary phase HPLC. [d] In the presence of 4 Å MS instead of $MgSO_4$, RT, 24 h. [e] RT, 24 h. [f] 0.225 mmol **2**. [g] **PA2** (0.0075 mmol, 7.5 mol %), RT.

We then applied these conditions to substrates **1 a**–**m** bearing different Michael acceptor groups and indole cores. The results (Table 1) show that, besides the simple phenyl derivative **1 a** (entry 1), other electronically/sterically different aryl acceptors in **1 e**–**h** provided the corresponding products **3 e**–**h** with excellent results (entries 5–8). The ester and *N*-acyl pyrrole derivatives **1 b** and **1 c** gave exclusively the open-chain adducts **3**′**b** and **c**, even under the optimized conditions. Molecular sieves provided better yields than $MgSO_4$ in these simple FC reactions (Table 1, entries 2 and 3).[21] The methyl ketone substrate **1 d** unfortunately gave a reduced enantioselectivity in the product **3 d** (Table 1, entry 4). However, the reaction scope is not restricted to Michael acceptors bearing aryl groups. Substrates **1i** and **1j**, bearing a *tert*-butyl and a dimethoxymethyl substituent at the ketone, respectively, afforded the products **3i** and **j** with excellent results (Table 1, entries 9 and 10), suggesting that it is the bulkiness of the acceptor that is essential to achieving excellent enantiocontrol in this reaction. As expected, the 2-methylindole derivative **1k** performed very well in the reaction (Table 1, entry 11). In contrast with simpler FC reactions, wherein catalyst coordination to the indole N–H is generally required for enantioselectivity,[16] the computed pathway of this transformation predicts this interaction to be absent in the stereodetermining step (Figure 2, **TS3**), while being useful for reactivity, as it is related to the RDS (**TS1** vs. **TS1′**). Indeed, the products **3l** and **m**, derived from the *N*-alkyl substrates **1l** and **m**, were obtained with excellent enantioselectivities, although slightly modified conditions were required to achieve good yields (Table 1, entries 12 and 13).

Treatment of **3a** with NaOH in MeOH caused equilibration favoring the *cis* stereoisomer **4a** [Eq. (1)]. DFT calculations indicated that this *cis* isomer (**4a**) is more polar than the *trans* (**3a**), and thus accounted for **4a** being favored in a polar medium such as MeOH. Equilibration occurred through a selective epimerization at the α-nitro stereogenic center and not through a retro-nitro-Michael pathway that would have led to racemization. We determined the relative configuration of compounds **3a** and **4a** as *trans* and *cis*, respectively, by a thorough computational (DFT) and NMR analysis (see the Supporting Information). Their absolute configuration was inferred as shown by comparing the calculated (TD-DFT) with the experimental Electronic Circular Dichroism (ECD) spectra.[22]

To increase the synthetic utility of this methodology, we thought to convert one of the ketone groups of compounds **3** into a more versatile ester group. However, all attempts to effect a Baeyer–Villiger oxidation on **3e** failed, presumably due

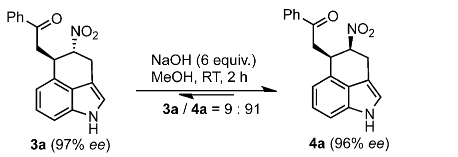

(1)

to the sensitivity of the benzo[*cd*]indole structure to oxidative conditions. Thus, we investigated other indole substrates featuring masked unsaturated esters/amides[23] as Michael acceptors at the 4-position. After considerable experimentation (see the Supporting Information), we found that an alkylidene malonate could serve as suitable acceptor moiety for the reaction. Using a different catalyst **PA3**, substrate **1n** bearing this group provided the corresponding product **3n** with synthetically useful results (Scheme 2). The malonate ester could be converted in three steps and with a small loss of diastereoenrichment into the previously inaccessible ester-substituted adduct **3b**. This compound, in racemic form, is the key intermediate in a reported synthesis of 6,7-secoagroclavine.[8a]

In summary, indoles **1** bearing a Michael acceptor at the 4-position react well with nitroethene **2** in the presence of chiral phosphoric acid catalysts, delivering the corresponding tricyclic

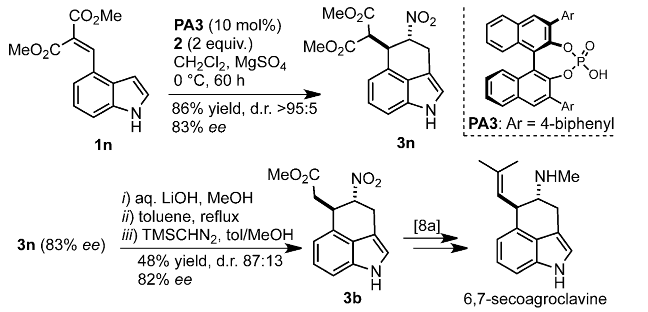

Scheme 2. Reaction with substrate **1n** and elaboration of product **3n**.

trans products **3** with very good results. As revealed by DFT calculations, the reaction is a unique example of evolution of a nitronate/nitronic acid intermediate towards a nucleophilic pathway, in favor of the ordinary "quench" of this intermediate through protonation. The benzo[*cd*]indole products **3** feature a nitro group at a strategic position to serve as ergot alkaloid precursors. Since diastereoisomer equilibration in MeOH favors the *cis* isomers (**4**), all four stereoisomers of the tricyclic system can be potentially accessed with this methodology.

Acknowledgements

We acknowledge financial support from University of Bologna (RFO). Donation of chemicals from Dr Reddy's Chirotech Technology Centre (Cambridge, UK) is gratefully acknowledged. F.H. acknowledges financial support from the Göran Gustafsson Foundation and the Knut and Alice Wallenberg Foundation. S.S. acknowledges financial support through a Programma Giovani Ricercatori "Rita Levi Montalcini" fellowship. We are grateful to Prof. Carmen Nàjera for a gift of (*R*)-BINOL and to Prof. Giovanni Piersanti for useful discussion.

Keywords: asymmetric synthesis · Brønsted acids · indoles · nitroalkenes · organocatalysis

[1] C. L. Schardl, D. G. Panaccione, P. Tudzynski in *The Alkaloids, Vol. 63* (Ed.: G. A. Cordell), Academic Press, San Diego, **2006**, pp. 45–86.

[2] a) H. G. Floss, *Tetrahedron* **1976**, *32*, 873; b) D. D. Schwarzer, P. J. Gritsch, T. Gaich, *Synlett* **2013**, *24*, 1025; c) C. Wallwey, S.-M. Li, *Nat. Prod. Rep.* **2011**, *28*, 496.

[3] a) M. Somei, Y. Yokoyama, Y. Murakami, I. Ninomiya, T. Kiguchi, T. Naito in *The Alkaloids, Vol. 54* (Ed.: G. A. Cordell), Academic Press, San Diego, **2000**, pp. 191–257; b) H. Ohno, H. Chiba, S. Inuki, S. Oishi, N. Fujii, *Synlett* **2014**, 179; c) S. Umezaki, S. Yokoshima, T. Fukuyama, *Org. Lett.* **2013**, *15*, 4230, and references therein.

[4] a) I.-K. Park, J. Park, C.-G. Cho, *Angew. Chem. Int. Ed.* **2012**, *51*, 2496; *Angew. Chem.* **2012**, *124*, 2546; b) D. Shan, Y. Gao, Y. Jia, *Angew. Chem. Int. Ed.* **2013**, *52*, 4902; *Angew. Chem.* **2013**, *125*, 5002; c) S. P. Breazzano, Y. B. Poudel, D. L. Boger, *J. Am. Chem. Soc.* **2013**, *135*, 1600; d) V. Lanke, K. R. Prabhu, *Org. Lett.* **2013**, *15*, 6262; e) T. Miura, Y. Funakoshi, M. Murakami, *J. Am. Chem. Soc.* **2014**, *136*, 2272; for oxindoles, see: f) T. Piou, A. Bunescu, Q. Wang, L. Neuville, J. Zhu, *Angew. Chem. Int. Ed.* **2013**, *52*, 12385; *Angew. Chem.* **2013**, *125*, 12611.

[5] a) L. Caruana, M. Fochi, M. Comes Franchini, S. Ranieri, A. Mazzanti, L. Bernardi, *Chem. Commun.* **2014**, *50*, 445; for catalytic enantioselective approaches to other 3,4-fused indoles, see: b) D.-J. Cheng, H.-B. Wu, S.-

K. Tian, *Org. Lett.* **2011**, *13*, 5636; c) Q.-L. Xu, L.-X. Dai, S.-L. You, *Chem. Sci.* **2013**, *4*, 97; d) H. Schönherr, J. L. Leighton, *Org. Lett.* **2012**, *14*, 2610.
[6] D. Ranganathan, C. B. Rao, S. Ranganathan, A. K. Mehrotra, R. Iyengar, *J. Org. Chem.* **1980**, *45*, 1185.
[7] a) W. Oppolzer, E. Francotte, K. Bättig, *Helv. Chim. Acta* **1981**, *64*, 478; b) L. I. Kruse, M. D. Meyer, *J. Org. Chem.* **1984**, *49*, 4761.
[8] a) F. Yamada, Y. Makita, M. Somei, *Heterocycles* **2007**, *72*, 599; b) N. Hatanaka, O. Ozaki, M. Matsumoto, *Tetrahedron Lett.* **1986**, *27*, 3169.
[9] Reviews: a) Z. Zhang, P. R. Schreiner, *Chem. Soc. Rev.* **2009**, *38*, 1187; b) R. R. Knowles, E. N. Jacobsen, *Proc. Natl. Acad. Sci. USA* **2010**, *107*, 20678; c) Y. Takemoto, *Chem. Pharm. Bull.* **2010**, *58*, 593; d) L. S. Aitken, N. R. Arezki, A. Dell'Isola, A. J. A. Cobb, *Synthesis* **2013**, 2627.
[10] S. Lancianesi, A. Palmieri, M. Petrini, *Chem. Rev.* **2014**, *114*, 7108.
[11] Reviews: a) D. Kampen, C. M. Reisinger, B. List in *Topics in Current Chemistry, Vol. 291: Asymmetric Organocatalysis* (Ed.: B. List), Springer-Verlag, Heidelberg, **2010**, pp. 395–456; b) T. Akiyama, *Chem. Rev.* **2007**, *107*, 5744; c) M. Terada, *Synthesis* **2010**, 1929; d) J. Yu, F. Shi, L.-Z. Gong, *Acc. Chem. Res.* **2011**, *44*, 1156; e) A. Zamfir, S. Schenker, M. Freund, S. B. Tsogoeva, *Org. Biomol. Chem.* **2010**, *8*, 5262; f) D. Parmar, E. Sugiono, S. Raja, M. Rueping, *Chem. Rev.* **2014**, *114*, 9047.
[12] For the same reason, as verified in a control experiment (see the Supporting Information), a phosphoric acid should be unable to resume undesired **3′** to tricyclic **3**. Thus, the nitronate "quench" is an irreversible process. Phosphoric acid-catalyzed direct additions proceeding through enol/nitronic acid intermediates have been reported, but only in the presence of a base (e.g., imine), at high temperature, or with enol-rich substrates (e.g., cyclohexanone): a) Q.-X. Guo, H. Liu, C. Guo, S.-W. Luo, Y. Gu, L.-Z. Gong, *J. Am. Chem. Soc.* **2007**, *129*, 3790; b) M. Rueping, A. P. Antonchick, *Org. Lett.* **2008**, *10*, 1731; c) G. Pousse, F. Le Cavelier, L. Humphreys, J. Rouden, J. Blanchet, *Org. Lett.* **2010**, *12*, 3582; d) I. Felker, G. Pupo, P. Kraft, B. List, *Angew. Chem. Int. Ed.* **2015**, *54*, 1960; *Angew. Chem.* **2015**, *127*, 1983; e) X. Yang, F. D. Toste, *J. Am. Chem. Soc.* **2015**, *137*, 3205; f) M. Yamanaka, M. Hoshino, T. Katoh, K. Mori, T. Akiyama, *Eur. J. Org. Chem.* **2012**, 4508; g) A. R. Burns, A. G. E. Madec, D. W. Low, I. D. Roy, H. W. Lam, *Chem. Sci.* **2015**, *6*, 3550.
[13] B. Vakulya, S. Varga, T. Soós, *J. Org. Chem.* **2008**, *73*, 3475.
[14] Reviews: a) C. Grondal, M. Jeanty, D. Enders, *Nat. Chem.* **2010**, *2*, 167; b) H. Pellissier, *Adv. Synth. Catal.* **2012**, *354*, 237; c) C. M. R. Volla, I. Atodiresei, M. Rueping, *Chem. Rev.* **2014**, *114*, 2390.
[15] a) X.-F. Wang, J.-R. Chen, Y.-J. Cao, H.-G. Cheng, W.-J. Xiao, *Org. Lett.* **2010**, *12*, 1140; b) C. C. J. Loh, I. Atodiresei, D. Enders, *Chem. Eur. J.* **2013**, *19*, 10822; c) J. C. Anderson, P. J. Koovits, *Chem. Sci.* **2013**, *4*, 2897.
[16] a) T. Hirata, M. Yamanaka, *Chem. Asian J.* **2011**, *6*, 510; for a related reaction with 4,7-dihydroindoles: b) C. Zheng, Y.-F. Sheng, Y.-X. Li, S.-L. You, *Tetrahedron* **2010**, *66*, 2875.
[17] **TS1′** evolves to intermediate **INT1′**, in which the anionic catalyst coordinates the nitronic acid and the C3–H of the indole (see the Supporting Information). However, this intermediate should be in rapid equilibrium with the more stable **INT1**, provided that the indole is unsubstituted at nitrogen. For *N*-substituted indoles, the first part of the process could occur through **TS1′**-**INT1′**-**TS2**.
[18] To locate **TS2′**, one proton had to be shifted from the protonated nitro group to the catalyst, to allow the protonation of the electrophilic ketone during the cyclization.
[19] The lowest energy pathway represented in Figure 2 leads to the formation of product *trans*-**3**. We also computed the pathway leading to the *cis* isomer, and we found it to be associated with higher energy barriers (see the Supporting Information), in agreement with the experimental results.
[20] We have also optimized the corresponding transition states for the reaction occurring on the ester-substituted indole **1b** that, when subjected to reaction conditions, only afforded product **3′b**. In this case, the barriers for the formation of the two products are closer in energy, mainly due to an increase in the energy required for the cyclization. The calculations, however, still predict the preferential formation of the cyclization product **3b**, in disagreement with the experiments. This could be an indirect proof that the barriers that we found for the tautomerizations giving the open-chain products **3′a** or **3′b** are slightly overestimated. Based on the experimental outcome of the reactions and on the calculated barriers for the cyclizations affording **3a** or **3b**, a more realistic value for the energy barriers of the tautomerization step lies between 13 and 18 $kcal\,mol^{-1}$. For additional discussion, see the Supporting Information.
[21] FC of indoles with nitroalkenes catalyzed by phosphoric acids are performed with MS: a) J. Itoh, K. Fuchibe, T. Akiyama, *Angew. Chem. Int. Ed.* **2008**, *47*, 4016; *Angew. Chem.* **2008**, *120*, 4080; b) K. Mori, M. Wakazawa, T. Akiyama, *Chem. Sci.* **2014**, *5*, 1799; c) Y.-F. Sheng, G.-Q. Li, Q. Kang, A.-J. Zhang, S.-L. You, *Chem. Eur. J.* **2009**, *15*, 3351. It can be speculated that molecular sieves (MS) have a role that goes beyond simple dehydration in these reactions. We hypothesize that MS serve as external proton sources providing an alternative pathway for the nitronic acid–nitro tautomerization. In some Lewis acid-catalyzed reactions, MS have been assumed to facilitate the reverse tautomerization (nitro–nitronic acid): d) C. Palomo, R. Pazos, M. Oiarbide, J. M. García, *Adv. Synth. Catal.* **2006**, *348*, 1161; e) M. Hasegawa, F. Ono, S. Kanemasa, *Tetrahedron Lett.* **2008**, *49*, 5220.
[22] A. Mazzanti, D. Casarini, *WIREs Comput. Mol. Sci.* **2012**, *2*, 613.
[23] D. Monge, H. Jiang, Y. Alvarez-Casao, *Chem. Eur. J.* **2015**, *21*, 4494.

Received: July 7, 2015
Published online on October 21, 2015

CHEMISTRY
A European Journal

Supporting Information

Catalytic Asymmetric Reactions of 4-Substituted Indoles with Nitroethene: A Direct Entry to Ergot Alkaloid Structures

Simone Romanini,[a] Emilio Galletti,[a] Lorenzo Caruana,[a] Andrea Mazzanti,[a] Fahmi Himo,[b] Stefano Santoro,*[c] Mariafrancesca Fochi,*[a] and Luca Bernardi*[a]

chem_201502655_sm_miscellaneous_information.pdf

Table of contents:

Selected additional studies in the catalytic asymmetric reactions

Optimization of the catalytic asymmetric reaction with substrate 1a

Table S1. Screening of chiral phosphoric acid catalysts **PA1-PA8** in the reaction between substrate **1a** and nitroethene **2**, representative results.[a]

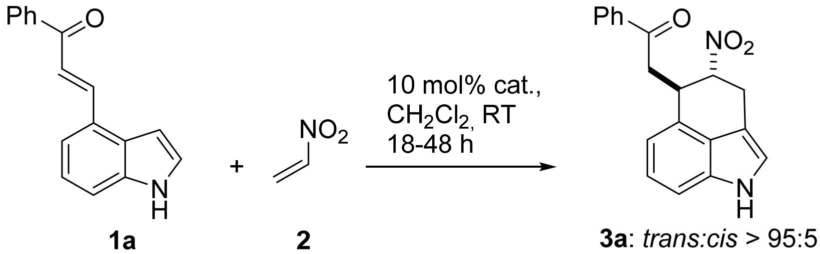

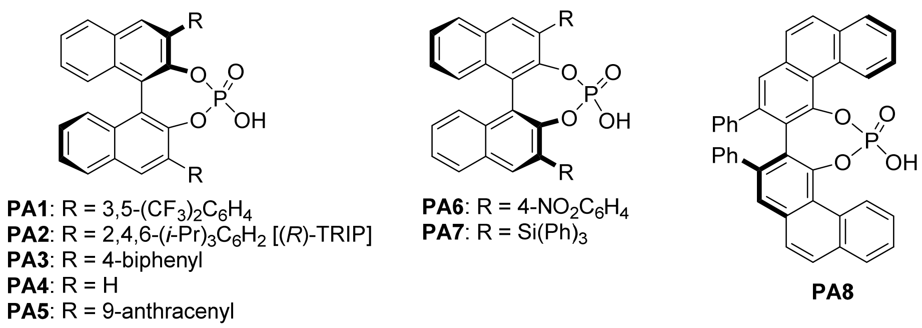

Entry	Catalyst	time (h)	Conversion (%)[b]	*ee* (%)[c]
1	**PA1**	48	90	77
2	**PA2**	18	>90	94
3	**PA3**	48	88	5
4	**PA4**	22	>90	59
5	**PA5**	22	>90	92
6	**PA6**	22	>90	27
7	**PA7**	22	>90	93
8	**PA8**	22	>90	31

[a] Conditions: **1a** (0.05 mmol), catalyst **PA1-PA8** (0.005 mmol, 10 mol%), nitroethene **2** (1 – 1.5 M solution in toluene, 0.075 mmol), CH_2Cl_2 (0.25 mL), RT, then filtration on a plug of silica gel, evaporation and NMR analysis, showing the presence of a single diastereoisomer in all cases. [b] Determined by ^{1}H NMR analysis of the crude. [c] Determined by chiral stationary phase HPLC.

As shown in Table S1, all BINOL and VAPOL derived phosphoric acid catalysts tested were found to be able to promote the domino reaction between substrate **1a** and **2**, with the (*R*)-TRIP catalyst **PA2** giving the best result in terms of enantioselectivity. It must be noted however that also the BINOL derived catalysts **PA5** and **PA7**, derived from BINOL and bearing a 9-anthracenyl and a triphenylsilyl group at 3,3' position, respectively, gave very good enantioselectivity in the reaction.

Table S2. Screening of reaction conditions with the (*R*)-TRIP catalyst **PA2**, representative results.[a]

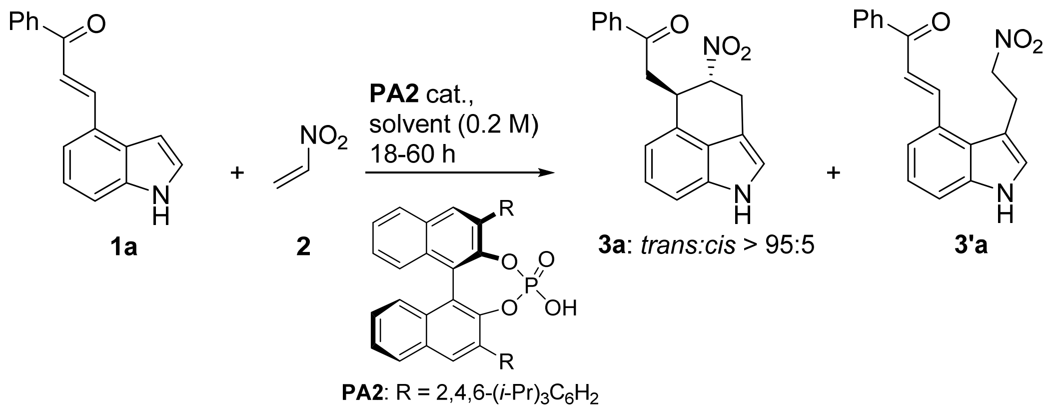

Entry	Cat. mol%	Solvent	Additive	T (°C)	t (h)	Conv. (%)[b]	3a:3'a[b]	*ee* (%)[c]
1	10	CH_2Cl_2	-	RT	18	80	>9:1	95
2	10	CH_2Cl_2	-	RT	60	>90	>9:1	95
3	10	toluene	-	RT	60	87	>9:1	95
4	10	THF	-	RT	48	<10	-	-
5	10	EtOAc	-	RT	48	<10	-	-
6	10	CH_3CN	-	RT	48	22	>9:1	nd
7	5	CH_2Cl_2	-	RT	48	83	>9:1	95
8	5	CH_2Cl_2	-	0	48	59	>9:1	96
9	5	CH_2Cl_2	4 Å MS - powder	0	60	>90	>9:1	96
10	5	CH_2Cl_2	4 Å MS - powder	0	60	>90	1:5	nd
11	5	CH_2Cl_2	5 Å MS - powder	0	60	>90	>9:1	84
12	5	CH_2Cl_2	5 Å MS - powder	0	60	>90	<1:9	-
13	5	CH_2Cl_2	3 Å MS - spheres	0	60	>90	<1:9	-
14	5	dry CH_2Cl_2	-	0	60	76	>9:1	97
15	5	dry CH_2Cl_2	$MgSO_4$	0	60	>90	>9:1	97
16	2.5	dry CH_2Cl_2	$MgSO_4$	0	60	70	>9:1	97

[a] Conditions: indole derivative **1a** (0.05 mmol), catalyst **PA2**, nitroethene **2** (1 – 1.5 M solution in toluene, 0.075 mmol), solvent (0.25 mL), then filtration on a plug of silica gel, evaporation and NMR analysis, showing the presence of a single diastereoisomer of **3a** in all cases. [b] Determined by ^1H NMR spectroscopy on the crude mixture. [c] Determined by chiral stationary phase HPLC analysis.

Different solvents were initially tested (entries 1-6), showing the necessity of employing non-coordinating solvents such as CH_2Cl_2 or toluene in the reaction. CH_2Cl_2 was selected for further optimization, since toluene did not efficiently solubilize substrate **1a**, and experiments not reported in Table S2 showed that this low solubilizing power resulted in even lower conversions with other substrates **1**. Lowering the catalyst loading to 5 mol% worsened the conversion, especially when the reaction was performed at 0 °C (entries 7,8). Thus, drying agents were tested, in order to increase catalyst activity. Molecular sieves of different pore sizes and shapes, commonly employed in phosphoric acid catalyzed reactions, were first employed (entries 9-13). Although these drying agents did indeed increase the observed conversion, results turned out to be irreproducible, leading in some cases even to the preferential formation of the undesired side-product **3'a**. Thus, dry

CH_2Cl_2 (freshly distilled from CaH_2) without additives was used as solvent, however without giving any substantial improvement (entry 14). It was finally found that a different drying agent ($MgSO_4$, pre-dried under vacuum with a heat-gun prior to the reaction) allowed to reach full conversion in the desired product **3a**, even at 0 °C with 5 mol% catalyst loading, providing a small improvement in the enantiomeric excess of the product **3a** (entry 15). Since a further lowering of the catalyst loading gave insufficient conversion (entry 16), conditions reported in entry 15 were taken as optimal to carry out the catalytic asymmetric domino reaction.

Control experiment with side-product 3’a

The obtainment of the side-product **3’a** in some of the reactions performed in the presence of molecular sieves allowed to perform the following control experiment (Scheme S1), which showed unequivocally that catalyst **PA2** is unable to resume **3’** to **3** (see the article for a relevant discussion).

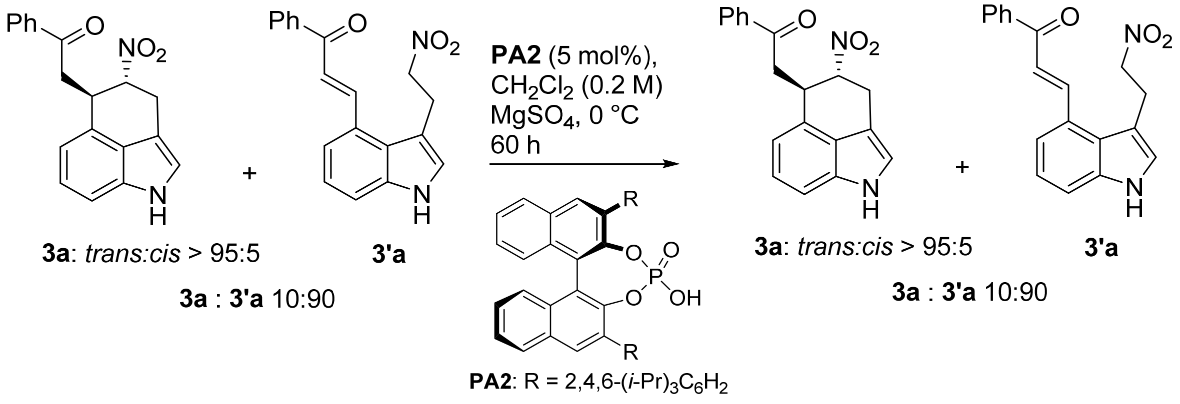

Scheme S1 Control experiment with a mixture enriched in side-product **3’a**.

Products elaboration: failure of the oxidative conversion of arylketone to ester

We carried out several attempts to unveil an ester function from arylketone **3e**. Usual protocols, useful even with complex chiral compounds bearing multiple stereogenic centres,[1] are based on the Bayer-Villiger oxidation, with *m*-CPBA as oxidizing agent. However, none of the conditions tested with *m*-CPBA afforded the desired ester product (Scheme S2). No evidence of the cleavage of the aryl-CO bond was found. We invariably observed either unreacted starting compound **3e**, or extensive decomposition resulting in intractable reaction mixtures. Since these conditions are usually compatible with γ-nitro aryl ketones,[1] we attributed these failures to the presence of the electron rich benzo[*cd*]indole core. We set up to protect of the indole NH with an electron-withdrawing group (Boc and Ts), which however proved to be much more challenging than expected, and could not be achieved with satisfactory and reproducible results. Thus, we tested different (milder) oxidative protocols on the unprotected compound **3e**, namely Dakin-type oxidations which involve aqueous H_2O_2 or UHP in basic reaction media (hydroxide bases). These latter protocols did not afford the desired ester product neither. Epimerization at the α-nitro stereogenic centre was instead observed, due to the highly basic reaction medium (Scheme S2).

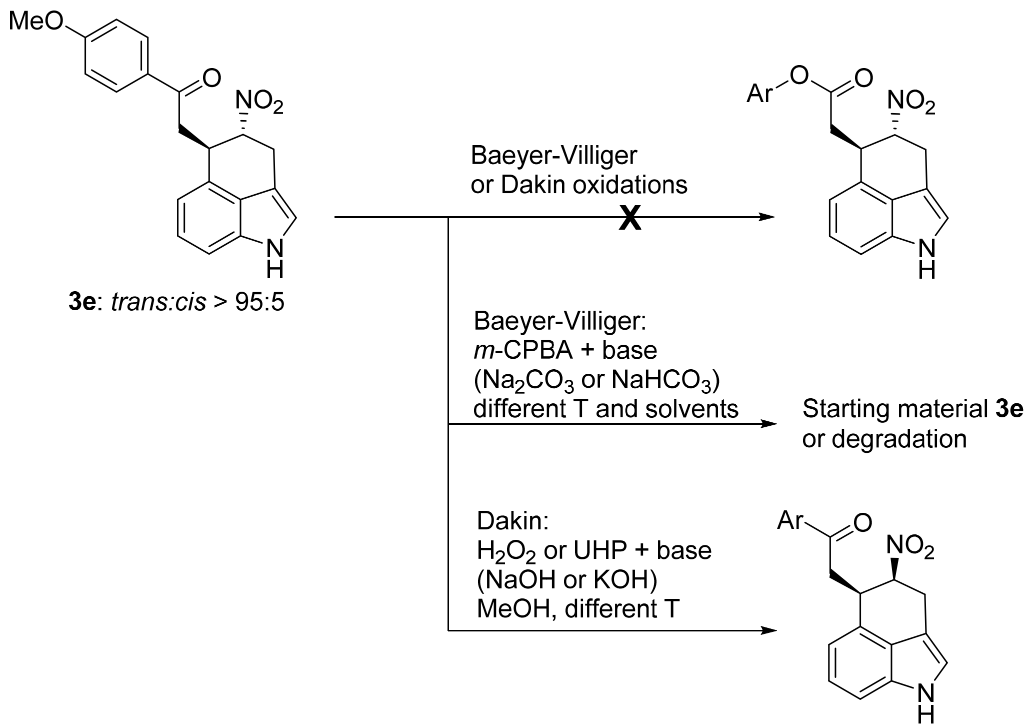

Scheme S2 Attempts of conversion of the arylketone **3e** to an ester under oxidative conditions.

---

[1] Q. Dai, A. Harman, J. C.-C. Zhao, *Chem. Eur. J.* **2013**, *19*, 1666.

Different unsaturated ester surrogates as Michael acceptors in substrates 1: selected results in the reactions with nitroethene 2 using catalyst PA2

All attempts to convert the ketone moiety of product **3e** into an ester failed, and the reactions with substrate **1b** bearing a methyl ester as the Michael acceptor did not provide the desired product **3b**. Thus, to increase the synthetic usefulness of our protocol, we decided to test other ester surrogates (or masked esters) in the reaction. On the other hand, due to poor reactivity of α,β-unsaturated esters, the recourse to moieties able to activate a double bond for a conjugate addition, and then to be converted into a carboxylate ester, is a common practice in catalytic asymmetric synthesis.[2] To select promising candidates, we explored literature data dealing with FC conjugate addition of indoles, and nitro-Michael reactions. We reasoned that *i*) masked esters useful for nitro-Michael reactions would possess the right reactivity to favor the desired product **3** vs side-product **3'**, and that *ii*) masked esters useful for FC addition of indoles would guarantee compatibility between the unmasking step and the indole moiety of our products **3**. However, our choice had to be restricted to compounds readily prepared from 4-formylindole. This synthetic restrain forced us to abandon some otherwise promising candidates, such as acylphosphonates and acylsilanes, and resulted in the candidates shown in Figure S1. Starting from 4-formylindole, the 1-pyrrole and the 1-methylimidazole derivatives were prepared through Wittig olefinations, whereas the pyridyn-2-yl-*N*-oxide, the α-hydroxyketone, the Meldrum's acid and the malonate derivatives through Knoevenagel condensations. DCC-mediated couplings of the amine/amide/alcohol with the carboxylic acid derived from ester substrate **1b** upon hydrolysis gave the hexafluoro-*iso*-propyl ester, the pyrrolidin-2-one, the oxazolidin-2-one and the succinimide substituted acceptors. The same ester **1b** was reduced and then oxidized to give the aldehyde derivative. All these compounds were tested in the reaction using **PA2** (5-10 mol%) as catalyst, as reported in Table S3.

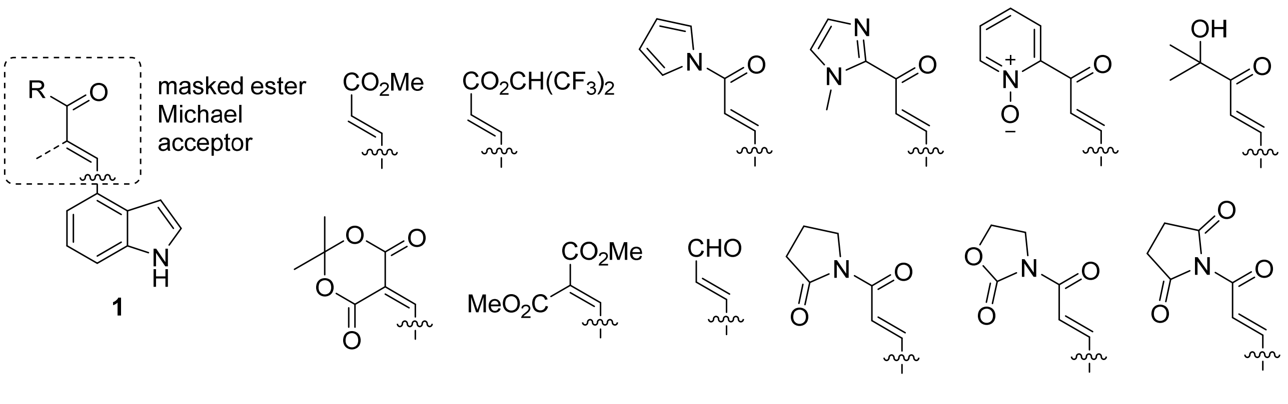

Figure S1 Selected masked unsaturated esters installed at the 4-position of indole.

[2] D. Monge, H. Jiang, Y. Alvarez-Casao, *Chem. Eur. J.* **2015**, *21*, 4494.

Table S3. Screening of different ester surrogates with catalyst **PA2**, representative results.[a]

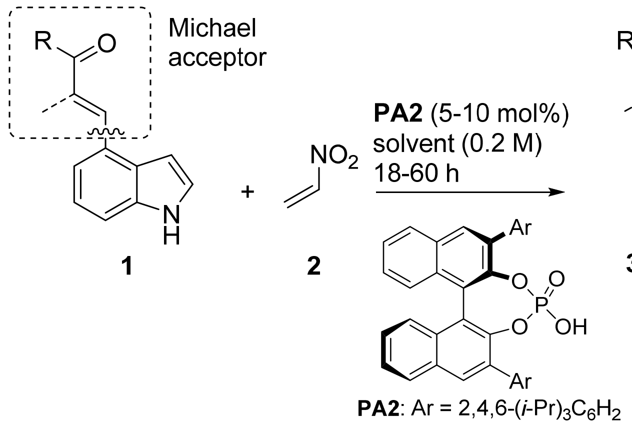

Entry	Michael acceptor	Solvent	Additive	T (°C)	t (h)	Conv. (%)[b]	3:3'[b]	*ee* 3 (%)[c]
1	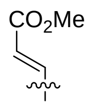	CH_2Cl_2	-	RT	18	50	<5:95	-
2		toluene	-	55	20	55	<5:95	-
3		CH_2Cl_2	$MgSO_4$	RT	20	>90 (35)[d]	<5:95	-
4		CH_2Cl_2	MS 4 Å	RT	24	>90 (62)[d]	<5:95	-
5	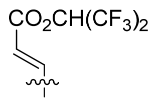	CH_2Cl_2	-	RT	18	35	<5:95	-
6	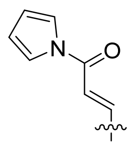	CH_2Cl_2	-	RT	60	nd	<5:95	-
7		CH_2Cl_2	$MgSO_4$	RT	24	49	<5:95	-
8		CH_2Cl_2	MS 4 Å	RT	24	>95 (94)[d]	<5:95	-
9		toluene	MS 4 Å	90	60	>90	60:40[e]	rac/rac
10	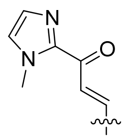	CH_2Cl_2	-	RT	60	15	1:1	-
11		CH_2Cl_2	MS 4 Å	RT	60	70	1:2	-
12	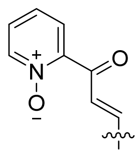	CH_2Cl_2	$MgSO_4$	RT	72	<20	>90:10	nd
13		DCE	$MgSO_4$	50	20	>90	>90:10	nd
14	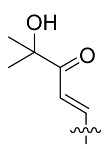	CH_2Cl_2	$MgSO_4$	0	60	>95	>95:5	55
15	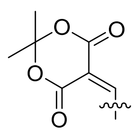	CH_2Cl_2	-	RT	60	<10	-	-
16		toluene	MS 4 Å	60	20	dec.	-	-
17		toluene	$MgSO_4$	60	20	dec.	-	-

Entry	Michael acceptor	Solvent	Additive	T (°C)	t (h)	Conv. (%)[b]	3:3'[b]	*ee* 3 (%)[c]
18	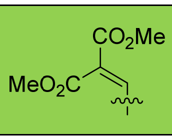	CH_2Cl_2	-	RT	60	>90	>95:5	12
19	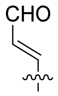	CH_2Cl_2	-	RT	60	dec.	-	-
20	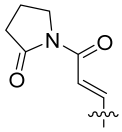	CH_2Cl_2	-	RT	72	<20	<5:95	-
21	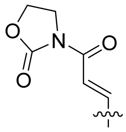	CH_2Cl_2	-	RT	72	<10	-	-
22		DCE	-	55	24	50	<5:95	-
23	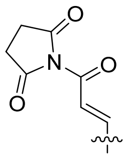	CH_2Cl_2	-	RT	60	<10	-	-
24		DCE	-	55	60	<10	-	-

[a] Conditions: indole derivative (0.05 mmol), catalyst **PA2** (5-10 mol%), nitroethene **2** (1 – 1.5 M solution in toluene, 0.075-1.0 mmol), solvent (0.25 mL), then filtration on a plug of silica gel, evaporation and NMR analysis. [b] Determined by ^{1}H NMR spectroscopy on the crude mixture. [c] Determined by chiral stationary phase HPLC analysis. [d] Yield of isolated product after chromatography on silica gel. [e] Product **3** obtained as a diastereomeric mixture (ca 1:1).

As shown in Table S3, an electron-poor hexafluoro-*iso*-propyl ester (entry 5) was not sufficient to drive the reaction towards the desired product **3**, giving results comparable to the methyl ester (entries 1-4). An *N*-acyl pyrrole did not give useful results neither (entries 6-8). With this substrate, it was found that the desired product **3** could be obtained by running the reaction at higher temperatures (entry 9). However, the product was afforded as a diastereomeric mixture and in racemic form. We speculated that thermodynamic equilibration between the open chain side-product **3'** and tricyclic **3** occurred at these temperatures. Moving to 1-methyl-2-acyl imidazole as the activating moiety for the double bond, this compound was poorly reactive (entries 10-11), possibly due to the strong interactions between the acidic catalyst and the basic imidazole, "quenching" the catalyst and preventing the first step of the reaction (the FC). Even if some reactivity could be gained using molecular sieves as drying agents, nearly equimolar mixtures of product **3** and side-product **3'** were invariably obtained. A pyridin-2-yl-*N*-oxide ketone was then tested, considering that this ketone moiety can render an ester under (harsh) basic hydroxide conditions,[3] thus avoiding the oxidative Baeyer-Villiger process. The low solubility of this substrate prevented the reaction from occurring at RT, however the corresponding product **3** could be cleanly obtained by working at 55 °C in DCE (entries 12-13). It was not possible to determine the ee of this product by the available CSP HPLC. In any case, this substrate was abandoned after some preliminary tests directed at the cleavage of the pyridinyl-ketone bond in the product (hydroxides, high temperatures), led only to decomposition, without giving any evidence of the formation of the desired carboxylic acid. Palomo's α-hydroxy ketone showed also very good reactivity and selectivity towards the desired domino product **3** but only poor enantioselectivity (entry 14). Unfortunately, a screening of phosphoric acid catalysts **PA1**-**PA8** failed to improve the enantioselectivity of the reaction with this substrate. Possibly, the hydroxyl proton of this ketone interferes with the H-bond interactions between catalyst and substrates in the stereodetermining nitro-Michael step. Moving to a substrate bearing a highly activated Meldrum's acid derived Michael acceptor installed on the indole, this compound did not react with nitroethene in the presence of catalyst **PA2** (entries 15-17). Apparently, the strong electron withdrawing nature of this Michael acceptor completely suppressed the FC reactivity of the indole moiety. By increasing the reaction temperature, decomposition occurred. A substrate **1** bearing a less activated dicarbonyl Michael acceptor, such as an alkylidene malonate, showed instead excellent reactivity and selectivity towards the desired tricyclic product **3**, which was afforded with good results in terms of conversion, but only poor enantioselectivity (entry 18). The enantioselectivity could be dramatically improved by changing the catalyst structure (see next section), and this masked ester turned out to be the substrate of choice. An aldehyde as activating moiety in the Michael acceptor was instead not suitable, since it mainly decomposed in the presence of the acidic phosphoric acid catalyst **PA2** (entry 19). Moving to amides and imides as Michael acceptors, not only these substrates proved to be poorly reactive, but they gave mainly the undesired side-product **3'** when some reactivity could be gained by increasing the reaction temperature (entries 20-24).

[3] P. K. Singh, V. K. Singh, *Org. Lett.* **2008**, *10*, 4121.

Optimization of the catalytic asymmetric reaction with substrate 1n

Table S4. Screening of chiral phosphoric acid catalysts **PA1-PA8** in the reaction between substrate **1n** and nitroethene **2**, representative results.[a]

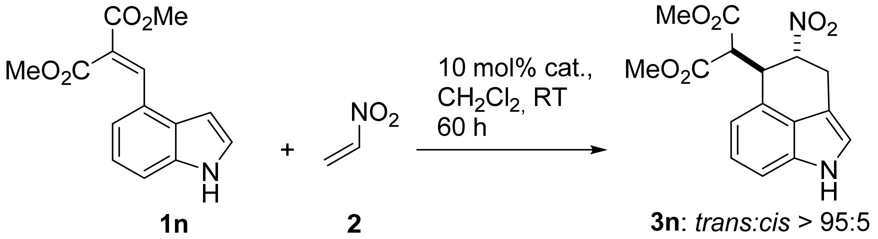

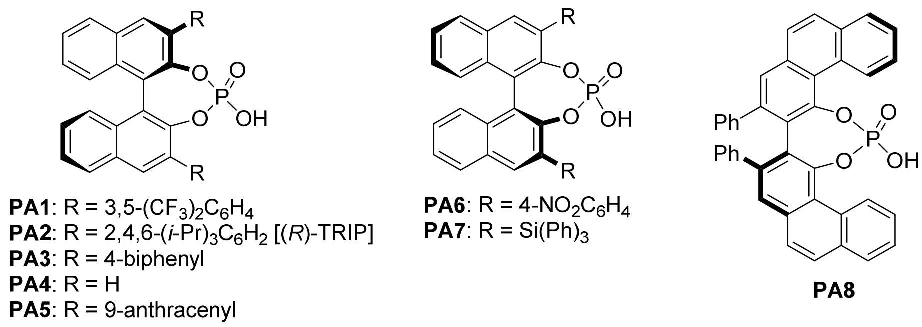

Entry	Catalyst	Conversion (%)[b]	*ee* (%)[c]
1	**PA1**	>90	rac
2	**PA2**	>90	12
3	**PA3**	>90	70
4	**PA4**	>90	nd
5	**PA5**	>90	23
6	**PA6**	>90	10
7	**PA7**	>90	7
8	**PA8**	>90	10

[a] Conditions: **1n** (0.05 mmol), catalyst **PA1-PA8** (0.005 mmol, 10 mol%), nitroethene **2** (1 – 1.5 M solution in toluene, 0.10 mmol), CH_2Cl_2 (0.20 mL), RT, then filtration on a plug of silica gel, evaporation. [b] Determined by TLC analysis of the crude. [c] Determined by chiral stationary phase HPLC.

As shown in Table S4, all phosphoric acid catalysts tested afforded the desired tricyclic adduct **3n**. However, only the 3,3'-(4-biphenyl) substituted derivative **PA3** gave this product with moderate enantioselectivity (entry 3). This catalyst was thus selected for further optimization (Table S5).

Table S5. Screening of reaction conditions in the reaction of substrate **1n** with nitroethene **2** catalyzed by **PA3**, representative results.[a]

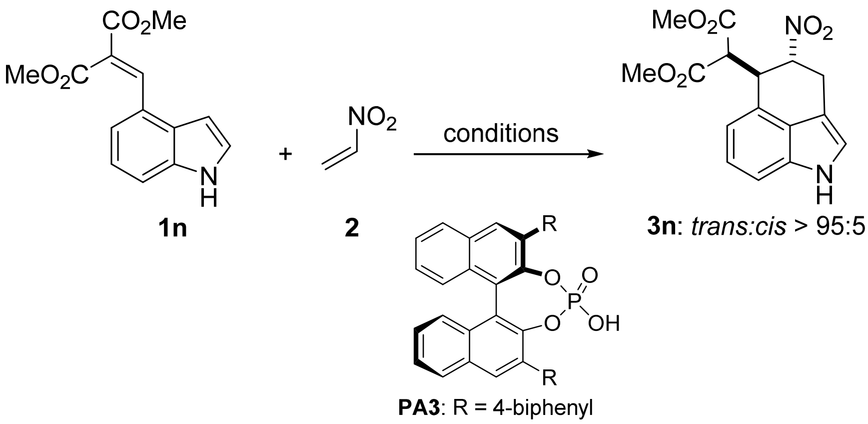

Entry	Solvent	Additive	T (°C)	t (h)	Conversion (%)[b]	*ee* (%)[c]
1	CH_2Cl_2	-	RT	60	>90	70
2	toluene	-	RT	20	ca 80	65
3	CH_2Cl_2	-	0	84	63	83
4	CH_2Cl_2	$MgSO_4$	0	60	91	83
5	CH_2Cl_2	$MgSO_4$	-25	60	54	90
6[d]	CH_2Cl_2	$MgSO_4$	0	60	70	83

[a] Conditions: **1n** (0.05 mmol), catalyst **PA3** (0.005 mmol, 10 mol%), nitroethene **2** (1 – 1.5 M solution in toluene, 0.10 mmol), dry solvent (0.15 mL), then filtration on a plug of silica gel, evaporation and NMR analysis. [b] Determined by ^{1}H NMR spectroscopy on the crude mixture. [c] Determined by chiral stationary phase HPLC analysis. [d] 5 mol% catalyst loading.

Having selected catalyst **PA3**, some experiments were carried out to improve the result in terms of enantioselectivity. As shown in Table S5, dichloromethane as solvent gave better results than toluene (entries 1,2). The enantioselectivity could be improved to a satisfactory level at the expense of the conversion by cooling the reaction mixture to 0 °C (entry 3). As in the reactions with the other substrates **1** catalyzed by **PA2**, the employment of $MgSO_4$ as a mild drying agent allowed to reach at 0 °C satisfactory results also in terms of conversion (entry 4). Since a further lowering of reaction temperature (entry 5) or of catalyst loading (entry 6) was found to be unpractical, the conditions reported in entry 4 were considered as optimal for this substrate **1n**.

Experimental details and products characterization

General Methods. ^{1}H, ^{13}C NMR spectra were recorded on a Varian AS 400 or 600 spectrometer. Chemical shifts (δ) are reported in ppm relative to residual solvent signals for ^{1}H and ^{13}C NMR.[4] ^{13}C NMR spectra were acquired with ^{1}H broad band decoupled mode. Chromatographic purifications were performed using 70-230 mesh silica. Mass spectra were recorded on a micromass LCT spectrometer using electrospray (ES) ionisation techniques. Optical rotations were measured on a Perkin-Elmer 241 polarimeter. The Electronic Circular Dichroism spectra were recorded on a Jasco J-810 spectropolarimeter. The enantiomeric excess (ee) of the products was determined by chiral stationary phase HPLC, using a UV detector operating at 254 nm. The absolute and relative configuration of compound **3a** and **4a** was determined as outlined in the dedicated section. We assume a similar reaction pathway for compounds **3d-m**, leading to the same relative and absolute configuration. Since a different catalyst was used, the absolute configuration of **3n** was not assigned, whereas its *trans* relative configuration was confirmed by comparison with reported ^{1}H NMR spectrum after decarboxylation (see below).

Materials. Analytical grade solvents and commercially available reagents were used as received, unless otherwise stated. Dichloromethane for the catalytic reactions was dried by filtration on a plug of basic alumina, and distillation from CaH_2 prior to use. 1*H*-Indole-4-carbaldehyde was purchased from Apollo Scientific. 2-Methyl-1*H*-indole-4-carbaldehyde,[5] 1-methyl and 1-allyl-1*H*-indole-4-carbaldehydes[6] were prepared according to the literature. Indole substrates **1a-i,k-m** were synthesised through Wittig olefination, detailed as follows: the phosphonium salts, unless commercially available, were obtained by refluxing an equimolar mixture of triphenyl phosphine and the appropriate alkyl halides for a few hours in toluene or acetonitrile, and collected by filtration; the phosphorous ylides were then obtained by adding CH_2Cl_2 and the phosphonium salts in a separating funnel containing 2 M aq. NaOH; after five minutes of vigorous shaking, the organic phase was collected, dried over $MgSO_4$, filtered and evaporated affording the ylides. The ylide used in the preparation of substrate **1c** was obtained following a modified literature method.[7] Finally, the

[4] H. E. Gottlieb, V. Kotlyar, A. Nudelman, *J. Org. Chem.* **1997**, *62*, 7512.
[5] J. M. Muchowski, *J. Heterocyclic Chem.* **2000**, *37*, 1293.
[6] M. Antoine, P. Marchand, G. Le Baut, M. Czech, S. Baasner, E. Gunther, *J. Enzyme Inhib. Med.* **2008**, *23*, 686.
[7] B. Vakulya, S. Varga, T. Soós, *J. Org. Chem.* **2008**, *73*, 3475; the following modifications were applied: crude di(1*H*-pyrrol-1-yl)methanone was used directly after evaporation (no precipitation) in the second step, and *n*-BuLi instead of PhLi was used in the second step.

Wittig olefination between the indole-4-carbaldehyde and the appropriate phosphorous ylide[8] was carried out in toluene or a toluene/1,4-dioxane mixture (8:2), at reflux temperature for 18-48 h;[9] substrates **1** were purified by column chromatography and obtained as pure *E*-isomers in the case of compounds **1a,c-i,k-m,** and with a 96:4 *E*/*Z* ratio in the case of **1b**. Substrate **1j** was prepared by an aldol condensation with pyruvic aldehyde dimethyl acetal, modifying a reported procedure.[9,10] Substrate **1n** was prepared by a Knoevenagel condensation following a literature protocol.[11] Nitroethene **2** was obtained and stored as a toluene solution by modifying the reported procedure,[12] as outlined below. (*R*)-TRIP catalyst **PA2** was prepared from (*R*)-BINOL using reported procedures.[13] The 3,3'-(4-biphenyl)-substituted (*R*)-BINOL derived phosphoric acid catalyst **PA3** was prepared according to the literature.[14] Racemic samples of products **3** for HPLC analysis were obtained by using diphenylphosphoric acid as catalyst (20 mol%) in CH_2Cl_2 as solvent, at RT for 24-48 h.

Preparation and storage of nitroethane 2.[12] Phthalic anhydride (2.8 g, 18.8 mmol) and 2-nitroethanol (0.97 mL, 12.6 mmol) are added to a Claisen apparatus, connected to a vacuum pump through a trap, and equipped after the trap with a vacuum control (Mohr clamp) and a vacuum gauge. The system is evacuated to 110 mBar, the trap immersed in a Dewar filled with liquid nitrogen, and the Claisen flask heated to 140-150 °C (pre-heated oil bath). The solid mixture turns into a brown liquid in a few minutes. Heating at this temperature is continued until ca half of the liquid in the Claisen flask is distilled. The heating temperature is then raised to 180 °C and kept at this temperature for about 10 minutes. The oil bath is then removed, the system carefully brought back to ambient pressure, and the cold trap placed under a nitrogen atmosphere and left warming to RT. Then, the yellow liquid collected in the trap is transferred by means of a Pasteur pipette and with the aid of small toluene portions into a vial. This solution is dried on powdered $CaCl_2$, and filtered on a short plug of cotton in another vial. The concentration of nitroethane **2** in the resulting solution is determined by ^{1}H NMR analysis (integration of nitroethane vs toluene peaks; in the calculation it is assumed that the density of this solution is the same as toluene), if needed adjusted

[8] F. Yamada, Y. Makita, M. Somei, *Heterocycles* **2007**, *72*, 599.
[9] Olefination reactions can be conveniently followed by TLC using 2,4-dinitrophenylhydrazine stain.
[10] S.-K. Tian, R. Hong, L. Deng, *J. Am. Chem. Soc.* **2003**, *125*, 9900; modification: MeOH/H_2O 3:1 was used as solvent (0.70 M), and K_2CO_3 (1 mol%) was also added in the reaction. Reflux, reaction time: 18 h.
[11] H. Chen, Y. Li, C. Sheng, Z. Lv, G. Dong, T. Wang, J. Liu, M. Zhang, L. Li, T. Zhang, D. Geng, C. Niu, K. Li, *J. Med. Chem.* **2013**, *56*, 685.
[12] D. Ranganathan, C. B. Rao, S. Ranganathan, A. K. Mehrotra, R. Iyengar, *J. Org. Chem.* **1980**, *45*, 1185.
[13] M. Klussmann, L. Ratjen, S. Hoffmann, V. Wachaure, R. Goddard, B. List, *Synlett* **2010**, 2189; for the last step (phosphoric acid formation): L. He, M. Bekkaye, P. Retailleau, G. Masson, *Org. Lett.* **2012**, *4*, 3158.
[14] The procedure reported for a 9-phenantryl catalyst was applied: W. Hu, J. Zhou, X. Xu, W. Liu, L.-z. Gong, *Org. Synth.* **2011**, *88*, 406.

to a 1-1.5 M concentration by adding more toluene and checked again by ^{1}H NMR. The solution of known concentration can be stored in a freezer (-25 °C) for several months without apparent degradation/changes in concentration, as checked by ^{1}H NMR.

General procedure for the catalytic asymmetric reaction of indoles 1 with nitroethene 2. To a Schlenk tube equipped with a magnetic stirring bar, $MgSO_4$ (30 mg) is added. This salt is carefully thermally activated under vacuum for 5 minutes and then allowed to cool to RT. After backfilling the Schlenk tube with nitrogen, the indole derivative **1** (0.10 mmol) is added, followed by the (*R*)-TRIP catalyst **PA2** (3.8 mg, 0.0050 mmol, 5.0 mol%), and CH_2Cl_2 (300 μL). The mixture is cooled to 0 °C and allowed to stir for 5 minutes, then nitroethene **2** (0.15 mmol, x μL of a 1-1.5 M toluene solution) is added in one portion. The mixture is then stirred at this temperature for 60 h, then filtered through a short plug of silica gel, and the plug washed with Et_2O (4x). After concentration of the solvents, the residue is analysed by ^{1}H NMR spectroscopy to determine the diastereomeric ratio of the adducts **3**. Finally, the residue is purified by chromatography on silica gel, affording pure products **3**.

1-((4*R*,5*R*)-4-Nitro-1,3,4,5-tetrahydrobenzo[*cd*]indol-5-yl)-1-phenylethanone (3a)

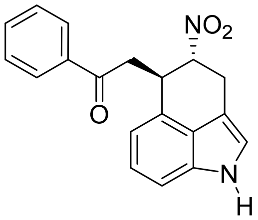

Following the general procedure, the title compound was obtained as a white solid in 95% yield, after chromatography on silica gel (CH_2Cl_2). ^{1}H NMR analysis of the crude mixture showed the presence of a single diastereoisomer. The enantiomeric excess of the product was determined by chiral stationary phase HPLC (Chiralpak AS column, *n*-hexane/*i*-PrOH 80:20, flow 0.75 mL/min, λ 254 nm, t_{maj} = 35.4 min, t_{min} = 30.4 min, 97% ee).^{1}H NMR ($CDCl_3$, 400 MHz) δ = 8.06 (br s, 1H), 7.96-7.93 (m, 2H), 7.62-7.56 (m, 1H), 7.50-7.44 (m, 2H), 7.21 (br d, J = 8.0 Hz, 1H), 7.14 (br t, J = 8.0 Hz, 1H), 6.96-6.93 (m, 1H), 6.83 (d, J = 7.1 Hz, 1H), 5.24 (dt, J_t = 5.8 Hz, J_d = 4.4 Hz, 1H), 4.65 (q, J = 6.2 Hz, 1H), 3.79 (dd, J = 16.0, 5.7 Hz, 1H), 3.43 (dd, J = 18.1, 6.0 Hz, 1H), 3.40 (ddd, J = 16.2, 4.3, 1.1 Hz, 1H), 3.33 (dd, J = 18.1, 7.1 Hz, 1H); ^{13}C NMR ($CDCl_3$, 100 MHz) δ = 197.2, 136.5, 133.7, 133.5, 129.6, 128.8, 128.1, 124.8, 123.6, 118.9, 116.0, 109.5, 107.3, 85.4, 41.9, 36.9, 25.1; $[\alpha]_D^{25}$ = -107 (c = 0.586 in CH_2Cl_2); ESIMS = 343 (M + Na^+).

Methyl 3-(3-(2-nitroethyl)-1*H*-indol-4-yl)acrylate (**3'b**)

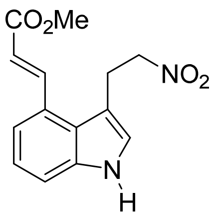

Following the general procedure but performing the reaction at RT for 24 h in the presence of 4 Å MS (45 mg) instead of $MgSO_4$, the title compound was obtained as a pale yellow solid in 62% yield, after chromatography on silica gel (CH_2Cl_2). ^{1}H NMR analysis of the crude mixture showed a 96:4 *E*/*Z* ratio, corresponding to the *E*/*Z* ratio of the starting substrate **1b**. ^{1}H NMR ($CDCl_3$, 400 MHz) δ = [signals of the *E*-isomer] 8.36 (d, J = 16.1 Hz, 1H), 8.29 (br s, 1H), 7.44-7.37 (m, 2H), 7.27-7.18 (m, 1H), 7.13 (br s, 1H), 6.48 (d, J = 15.7 Hz, 1H), 4.70 (t, J = 6.8 Hz, 2H), 3.84 (s, 3H), 3.65 (t, J = 6.5 Hz, 2H); ^{13}C NMR ($CDCl_3$, 100 MHz) δ = [signals of the *E*-isomer] 167.4, 142.6, 137.2, 127.6, 124.9, 124.7, 122.6, 119.3, 118.8, 113.4, 110.3, 75.8, 51.8, 25.7; ESIMS = 297 (M + Na^+).

(*E*)-3-(3-(2-Nitroethyl)-1*H*-indol-4-yl)-1-(1*H*-pyrrol-1-yl)prop-2-en-1-one (**3'c**)

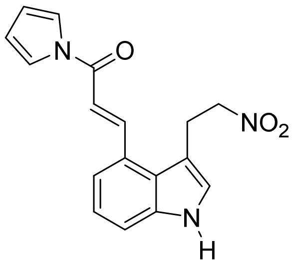

Following the general procedure but performing the reaction at RT for 20 h in the presence of 4 Å MS (45 mg) instead of $MgSO_4$, the title compound was obtained as a yellow solid in 94% yield, after chromatography on silica gel (CH_2Cl_2). ^{1}H NMR analysis of the crude mixture showed a single *E* stereoisomer. ^{1}H NMR (acetone-d_6, 400 MHz) δ = 10.55 (br s, 1H), 8.77 (d, J = 15.2 Hz, 1H), 7.78-7.72 (m, 3H), 7.62-7.58 (m, 2H), 7.43 (br s, 1H), 7.25 (t, J = 8.1 Hz, 1H), 6.42-6.40 (m, 2H), 4.97 (t, J = 7.5 Hz, 2H), 3.77 (t, J = 7.45 Hz, 2H); ^{13}C NMR (acetone-d_6, 100 MHz) δ = 163.6, 146.2, 138.7, 128.2, 126.8, 126.4, 122.6, 120.9, 119.7, 117.5, 115.3, 115.2, 113.7, 110.8, 76.4, 26.4; ESIMS = 332 (M + Na^+).

1-((4*R*,5*R*)-4-Nitro-1,3,4,5-tetrahydrobenzo[*cd*]indol-5-yl)propan-2-one (3d)

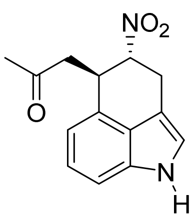

Following the general procedure, the title compound was obtained as a pale yellow solid in 96% yield, after chromatography on silica gel (CH_2Cl_2). ^{1}H NMR analysis of the crude mixture showed the presence of a single diastereoisomer. The enantiomeric excess of the product was determined by chiral stationary phase HPLC (Chiralpak AS column, *n*-hexane/*i*-PrOH 80:20, flow 0.75 mL/min, λ 254 nm, t_{maj} = 30.1 min, t_{min} = 24.6 min, 54% ee).^{1}H NMR ($CDCl_3$, 400 MHz) δ = 8.05 (br s, 1H), 7.21-7.11 (m, 2H), 6.93 (br s, 1H), 6.83 (br d, J = 7.1 Hz, 1H), 5.07 (dt, J_t = 6.2 Hz, J_d = 4.8 Hz, 1H), 4.39 (br q, J = 5.9 Hz, 1H), 3.71 (dd, J = 16.1, 6.3 Hz, 1H), 3.35 (dd, J = 17.0, 4.5 Hz, 1H), 2.90 (dd, J = 17.6, 6.0 Hz, 1H), 2.80 (dd, J = 18.2, 6.0 Hz, 1H), 2.19 (s, 3H); ^{13}C NMR ($CDCl_3$, 100

MHz) δ = 205.7, 133.6, 129.2, 124.7, 123.5, 118.8, 115.7, 109.5, 107.2, 85.5, 46.2, 36.8, 30.4, 25.3; $[\alpha]_D^{25}$ = -47 (c = 0.436 in CH_2Cl_2); ESIMS = 281 (M + Na^+).

1-(4-Methoxyphenyl)-2-((4*R*,5*R*)-4-nitro-1,3,4,5-tetrahydrobenzo[*cd*]indol-5-yl)ethanone (3e)

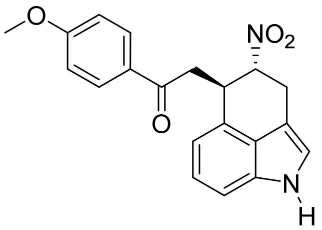

Following the general procedure, the title compound was obtained as a white solid in 91% yield, after chromatography on silica gel (CH_2Cl_2 + 1% Et_2O). ^{1}H NMR analysis of the crude mixture showed the presence of a single diastereoisomer. The enantiomeric excess of the product was determined by chiral stationary phase HPLC (Chiralpak AS column, *n*-hexane/*i*-PrOH 80:20, flow 0.75 mL/min, λ 254 nm, t_{maj} = 63.9 min, t_{min} = 53.1 min, 97% ee).^{1}H NMR ($CDCl_3$, 600 MHz) δ = 8.12 (br s, 1H), 7.95-7.90 (m, 2H), 7.19-7.10 (m, 2H), 6.94-6.90 (m, 3H), 6.88 (d, J = 7.2 Hz, 1H), 5.23 (br q, J = 5.6 Hz, 1H), 4.63 (br q, J = 6.2 Hz, 1H), 3.86 (s, 3H), 3.77 (dd, J = 16.8, 6.8 Hz, 1H), 3.47-3.36 (m, 2H), 3.24 (dd, J = 17.8, 6.8 Hz, 1H); ^{13}C NMR ($CDCl_3$, 150 MHz) δ = 195.7, 163.8, 133.6, 130.4, 129.6, 129.5, 124.7, 123.4, 118.9, 115.9, 113.8, 109.5, 107.2, 85.4, 55.5, 41.6, 37.0, 24.9; $[\alpha]_D^{25}$ = -140 (c = 0.472 in CH_2Cl_2); ESIMS = 373 (M + Na^+).

1-(4-Bromophenyl)-2-((4*R*,5*R*)-4-nitro-1,3,4,5-tetrahydrobenzo[*cd*]indol-5-yl)ethanone (3f)

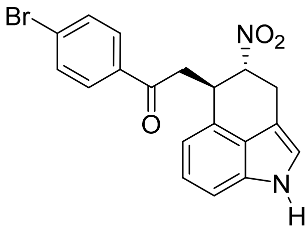

Following the general procedure, the title compound was obtained as white solid in 95% yield, after chromatography on silica gel (CH_2Cl_2). ^{1}H NMR analysis of the crude mixture showed the presence of a single diastereoisomer. The enantiomeric excess of the product was determined by chiral stationary phase HPLC (Chiralpak AS column, *n*-hexane/*i*-PrOH 80:20, flow 0.75 mL/min, λ 254 nm, t_{maj} = 39.4 min, t_{min} = 35.8 min, 97% ee).^{1}H NMR ($CDCl_3$, 400 MHz) δ = 8.01 (br s, 1H), 7.74-7.70 (m, 2H), 7.54-7.49 (m, 2H), 7.15-7.02 (m, 2H), 6.89 (br s, 1H), 6.79-6.74 (m, 1H), 5.13 (dt, J_t = 5.7 Hz, J_d = 4.4 Hz, 1H), 4.53 (q, J = 6.1 Hz, 1H), 3.70 (dd, J = 16.8, 6.3 Hz, 1H), 3.39-3.29 (m, 2H), 3.20 (dd, J = 18.2, 6.3 Hz, 1H); ^{13}C NMR ($CDCl_3$, 100 MHz) δ = 196.1, 135.2, 133.7, 132.0, 129.6, 129.3, 128.8, 124.7, 123.5, 119.0, 115.9, 109.6, 107.2, 85.4, 41.6, 36.9, 25.2; $[\alpha]_D^{25}$ = -85 (c = 0.580 in CH_2Cl_2); ESIMS = 421-423 (M + Na^+).

2-((4*R*,5*R*)-4-Nitro-1,3,4,5-tetrahydrobenzo[*cd*]indol-5-yl)-1-(*p*-tolyl)ethanone (3g)

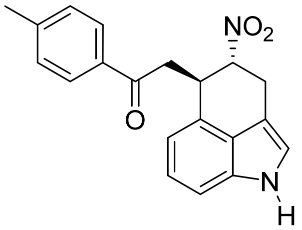

Following the general procedure, the title compound was obtained as a white solid in 98% yield, after chromatography on silica gel (CH_2Cl_2). ^{1}H NMR analysis of the crude mixture showed the presence of a single diastereoisomer. The enantiomeric excess of the product was determined by chiral stationary phase HPLC (Chiralpak AS column, *n*-hexane/*i*-PrOH 80:20, flow 0.75 mL/min, λ 254 nm, t_{maj} = 35.8 min, t_{min} = 30.5 min, 98% ee). ^{1}H NMR ($CDCl_3$, 400 MHz) δ = 8.06 (br s, 1H), 7.88-7.81 (m, 2H), 7.29-7.08 (m, 4H), 6.94 (br s,1H), 6.90-6.84 (m, 1H), 5.22 (q, J = 5.6 Hz, 1H), 4.62 (q, J = 6.2 Hz, 1H), 3.77 (dd, J = 16.7, 5.8 Hz, 1H), 3.53-3.35 (m, 2H), 3.27 (dd, J = 18.0, 7.2 Hz, 1H), 2.40 (s, 3H); ^{13}C NMR ($CDCl_3$, 100 MHz) δ =196.8, 144.5, 134.1, 133.7, 130.0, 129.4, 128.2, 124.8, 123.5, 119.0, 116.0, 109.5, 107.3, 85.4, 41.8, 37.0, 25.1, 21.7; $[\alpha]_D^{25}$ = -186 (c = 0.560 in CH_2Cl_2); ESIMS = 357 (M + Na^+).

1-(Naphthalen-2-yl)-2-((4*R*,5*R*)-4-nitro-1,3,4,5-tetrahydrobenzo[*cd*]indol-5-yl)ethanone (3h)

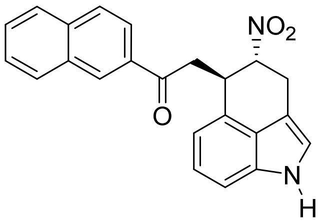

Following the general procedure, the title compound was obtained as a white solid in 98% yield, after chromatography on silica gel (CH_2Cl_2). ^{1}H NMR analysis of the crude mixture showed the presence of a single diastereoisomer. The enantiomeric excess of the product was determined by chiral stationary phase HPLC (Chiralpak AS column, *n*-hexane/*i*-PrOH 80:20, flow 0.75 mL/min, λ 254 nm, t_{maj} = 46.2 min, t_{min} = 27.0 min, >99% ee). ^{1}H NMR ($CDCl_3$, 400 MHz) δ = 8.44 (br s, 1H), 8.12-8.01 (m, 2H), 7.95-7.85 (m, 3H), 7.65-7.51 (m, 2H), 7.23-7.11 (m, 2H), 7.02-6.90 (m, 2H), 5.27 (br q, J = 5.3 Hz, 1H), 4.70 (q, J = 5.9 Hz, 1H), 3.79 (dd, J = 16.8, 6.0 Hz, 1H), 3.61 (dd, J = 17.9, 5.7 Hz, 1H), 3.50-3.40 (m, 2H); ^{13}C NMR ($CDCl_3$, 100 MHz) δ = 197.1, 135.8, 133.8, 133.7, 132.4, 130.0, 129.6, 128.8, 128.7, 127.8, 127.0, 124.8, 123.7, 123.6, 119.0, 116.1, 110.0, 107.3, 85.4, 42.0, 37.0, 25.1; $[\alpha]_D^{25}$ = -110 (c = 0.793 in CH_2Cl_2); ESIMS = 393 (M + Na^+).

3,3-Dimethyl-1-((4*R*,5*R*)-4-nitro-1,3,4,5-tetrahydrobenzo[*cd*]indol-5-yl)butan-2-one (3i)

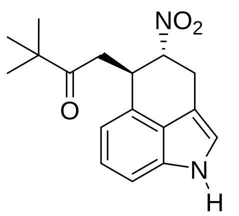

Following the general procedure, the title compound was obtained as a white solid in 90% yield, after chromatography on silica gel (CH_2Cl_2). ^{1}H NMR analysis of the crude mixture showed the presence of a single diastereoisomer. The enantiomeric excess of the product was determined by chiral stationary phase HPLC (Chiralpak AS column, *n*-hexane/*i*-PrOH 80:20, flow 0.75 mL/min, λ 254 nm, t_{maj} = 13.5 min, t_{min} = 11.3 min, 93% ee).^{1}H NMR ($CDCl_3$, 400 MHz) δ = 8.03 (br s, 1H), 7.23-7.12 (m, 2H), 6.97 (br s, 1H), 6.81 (br d, J = 6.9 Hz, 1H), 5.10 (q, J = 6.9 Hz, 1H), 4.43 (q, J = 6.2 Hz, 1H), 3.77 (dd, J = 16.6, 5.9 Hz, 1H), 3.32 (br dd, J = 16.4, 4.5 Hz, 1H), 2.96 (dd, J = 18.2, 5.9 Hz, 1H), 2.83 (dd, 18.3, 7.0 Hz, 1H), 1.13 (s, 9H); ^{13}C NMR ($CDCl_3$, 100 MHz) δ = 213.0, 133.7, 129.7, 124.7, 123.5, 118.8, 116.0, 109.4, 107.3, 85.2, 44.3, 40.1, 36.6, 26.4, 24.9; $[\alpha]_D^{25}$ = -93 (c = 0.500 in CH_2Cl_2); ESIMS = 323 (M + Na^+).

1,1-Dimethoxy-3-((4*R*,5*R*)-4-nitro-1,3,4,5-tetrahydrobenzo[*cd*]indol-5-yl)propan-2-one (3j)

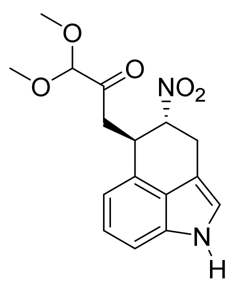

Following the general procedure, but performing the reaction at RT for 24 h, the title compound was obtained as a white solid in 82% yield, after chromatography on silica gel (CH_2Cl_2). ^{1}H NMR analysis of the crude mixture showed the presence of a single diastereoisomer. The enantiomeric excess of the product was determined by chiral stationary phase HPLC (Chiralpak AS column, *n*-hexane/*i*-PrOH 80:20, flow 0.75 mL/min, λ 254 nm, t_{maj} = 27.5 min, t_{min} = 18.8 min, 96% ee). ^{1}H NMR ($CDCl_3$, 400 MHz) δ = 8.03 (br s, 1H), 7.25-7.10 (m, 2H), 6.96 (br s, 1H), 6.86 (br d, J = 7.0 Hz, 1H), 5.09 (dt, J_t = 6.1 Hz, J_d = 4.5 Hz, 1H), 4.43 (s, 1H), 4.42 (q, J = 6.1 Hz, 1H), 3.73 (br dd, J = 16.1, 5.9 Hz, 1H), 3.42 (s, 3H), 3.40 (s, 3H), 3.44-3.35 (m, 1H), 3.05 (dd, J = 19.3, 6.5 Hz, 1H), 3.00 (dd, J = 19.7, 6.3 Hz, 1H); ^{13}C NMR ($CDCl_3$, 100 MHz) δ = 203.0, 133.7, 129.2, 124.7, 123.5, 118.8, 115.9, 109.5, 107.4, 104.5, 85.4, 55.2, 55.1, 40.0, 36.1, 25.3; $[\alpha]_D^{25}$ = -36 (c = 0.39 in CH_2Cl_2); ESIMS = 341 (M + Na^+).

2-((4*R*,5*R*)-2-Methyl-4-nitro-1,3,4,5-tetrahydrobenzo[*cd*]indol-5-yl)-1-phenylethanone (3k)

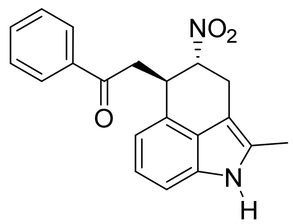

Following the general procedure, the title compound was obtained as a white solid in 90% yield, after chromatography on silica gel (CH_2Cl_2). ^{1}H NMR analysis of the crude mixture showed the presence of a single diastereoisomer. The enantiomeric excess of the product was determined by chiral stationary phase HPLC (Chiralpak AS column, *n*-hexane/*i*-PrOH 80:20, flow 0.75 mL/min, λ 254 nm, t_{maj} = 33.4 min, t_{min} = 26.1 min, 94% ee).^{1}H NMR ($CDCl_3$, 400 MHz) δ = 8.00-7.92 (m, 2H), 7.80 (br s, 1H), 7.62-7.56 (m, 1H), 7.50-7.43 (m, 2H), 7.12-7.01 (m, 2H), 6.83 (br d, J = 6.3 Hz, 1H), 5.19 (br q, J = 6.0 Hz, 1H), 4.58 (br q, J = 5.9 Hz, 1H), 3.65 (dd, J = 16.2, 6.2 Hz 1H), 3.45 (dd, J = 17.9, 5.8 Hz, 1H), 3.35-3.22 (m, 2H), 2.35 (s, 3H); ^{13}C NMR

($CDCl_3$, 100 MHz) δ = 197.3, 136.6, 133.5, 133.3, 129.2, 128.7, 128.5, 128.1, 125.8, 122.4, 115.8, 108.7, 103.4, 85.5, 41.8, 36.9, 24.7, 11.6; $[\alpha]_D^{25}$ = -184 (c = 0.524 in CH_2Cl_2); ESIMS = 357 (M + Na^+).

2-((4*R*,5*R*)-1-Methyl-4-nitro-1,3,4,5-tetrahydrobenzo[*cd*]indol-5-yl)-1-phenylethanone (3l)

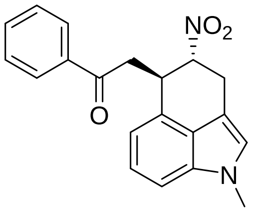

Following the general procedure but using 2.25 equiv. of nitroethene **2**, the title compound was obtained as a white solid in 75% yield, after chromatography on silica gel (CH_2Cl_2). ^1H NMR analysis of the crude mixture showed the presence of a single diastereoisomer. The enantiomeric excess of the product was determined by chiral stationary phase HPLC (Chiralpak AS column, *n*-hexane/*i*-PrOH 80:20, flow 0.75 mL/min, λ 254 nm, t_{maj} = 46.8 min, t_{min} = 35.9 min, 95% ee).^1H NMR ($CDCl_3$, 400 MHz) δ = 7.97-7.92 (m, 2H), 7.61-7.54 (m, 1H), 7.49-7.42 (m, 2H), 7.19-7.12 (m, 2H), 6.88-6.80 (m, 2H), 5.22 (br q, J = 5.6 Hz, 1H), 4.63 (br q, J = 6.1 Hz, 1H), 3.78 (dd, J = 16.5, 5.8 Hz, 1H), 3.75 (s, 3H), 3.47 (dd, J = 18.1, 5.8 Hz, 1H), 3.40 (dd, J = 16.2, 4.1 Hz, 1H), 3.30 (dd, J = 18.1, 7.0 Hz, 1H); ^{13}C NMR ($CDCl_3$, 100 MHz) δ = 197.1, 136.5, 134.8, 133.5, 129.7, 128.7, 128.1, 125.1, 123.6, 123.1, 115.4, 107.8, 105.9, 85.4, 41.9, 36.9, 32.9, 25.0; $[\alpha]_D^{25}$ = -102 (c = 0.332 in CH_2Cl_2); ESIMS = 357 (M + Na^+).

2-((4*R*,5*R*)-1-Allyl-4-nitro-1,3,4,5-tetrahydrobenzo[*cd*]indol-5-yl)-1-phenylethanone (3m)

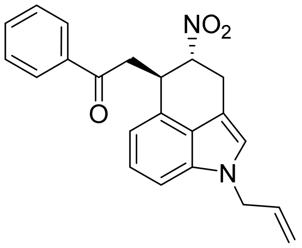

Following the general procedure but using 7.5 mol% (*R*)-TRIP catalyst, 2 equiv. of nitroethene **2** and at RT, the title compound was obtained as a white solid in 70% yield, after chromatography on silica gel (CH_2Cl_2). ^1H NMR analysis of the crude mixture showed the presence of a single diastereoisomer. The enantiomeric excess of the product was determined by chiral stationary phase HPLC (Chiralpak AS column, *n*-hexane/*i*-PrOH 80:20, flow 0.75 mL/min, λ 254 nm, t_{maj} = 31.8 min, t_{min} = 26.1 min, 93% ee). ^1H NMR ($CDCl_3$, 400 MHz) δ = 7.96 (bd, J = 8.1 Hz, 2H), 7.58 (bt, J = 7.0 Hz, 1H), 7.46 (bt, J = 7.3 Hz, 2H), 7.15-7.12 (m, 2H), 6.89-6.84 (m, 2H), 6.03-5.95 (m, 1H), 5.28-5.10 (m, 3H), 4.72-4.65 (m, 2H), 4.63 (bq, J = 6.1 Hz, 1H), 3.78 (dd, J = 16.1, 6.1 Hz, 1H), 3.48 (dd, J = 17.9, 5.8 Hz, 1H), 3.41 (dd, J = 15.8, 4.2 Hz, 1H), 3.32 (dd, J = 17.6, 7.1 Hz, 1H); ^{13}C NMR ($CDCl_3$, 100 MHz) δ = 197.1, 136.5, 134.2, 133.5, 133.5, 129.8, 128.7, 128.0, 125.3, 123.1, 122.5, 117.5, 115.5, 108.2, 106.3, 85.4, 49.1, 41.9, 36.9, 25.1; $[\alpha]_D^{25}$ = -75 (c = 0.334 in CH_2Cl_2); ESIMS = 360 (M + Na^+).

Dimethyl 2-((4*R,5*R**)-4-nitro-1,3,4,5-tetrahydrobenzo[cd]indol-5-yl)malonate** (**3n**)

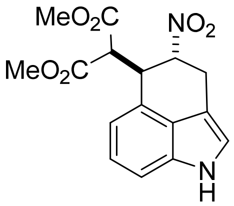

Following the general procedure but using 10 mol% 3,3'-(4-biphenyl) (*R*)-BINOL derived phosphoric acid catalyst **PA3** and 2 equiv. of nitroethene **2**, the title compound was obtained as a pale yellow foam in 86% yield, after chromatography on silica gel (CH_2Cl_2). ^{1}H NMR analysis of the crude mixture showed the presence of a single diastereoisomer. The enantiomeric excess of the product was determined by chiral stationary phase HPLC (Chiralpak ADH column, *n*-hexane/*i*-PrOH 90:10, flow 0.75 mL/min, λ 254 nm, t_{maj} = 41.2 min, t_{min} = 44.1 min, 83% ee). ^{1}H NMR ($CDCl_3$, 400 MHz) δ = 8.06 (br s, 1H), 7.20 (br d, J = 8.3 Hz, 1H), 7.11 (br t, J = 8.0 Hz, 1H), 6.96 (br s, 1H), 6.91 (br d, J = 7.0 Hz, 1H), 5.22 (br q, J = 3.4 Hz, 1H), 4.80 (dd, J = 10.9, 3.4 Hz, 1H), 3.90 (dd, J = 17.8, 3.0 Hz, 1H), 3.80 (s, 3H), 3.61 (s, 3H), 3.57 (d, J = 10.5 Hz, 1H), 3.34 (br dd, J = 17.5, 4.3 Hz, 1H); ^{13}C NMR ($CDCl_3$, 100 MHz) δ = 167.8, 167.5, 133.9, 125.4, 124.5, 123.2, 119.3, 117.8, 110.4, 106.5, 83.1, 55.8, 53.1, 52.7, 40.2, 23.6; $[\alpha]_D^{25}$ = +87 (c = 0.520 in CH_2Cl_2); ESIMS = 355 (M + Na^+).

Preparation of compound 4a (1-((4*S*,5*R*)-4-nitro-1,3,4,5-tetrahydrobenzo[*cd*]indol-5-yl)-1-phenylethanone) via base promoted epimerisation.

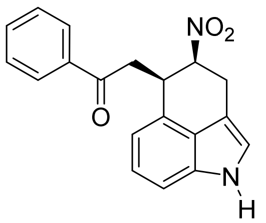

In a vial equipped with a magnetic stirring bar, compound **3a** (0.072 mmol, 97% ee) was dissolved in MeOH (200 μL), and the resulting solution cooled to 0 °C with stirring. A NaOH solution in MeOH (268 μL of a solution prepared dissolving 96 mg NaOH in 1.5 mL of MeOH, 0.43 mmol, 6 equiv.) was added, the reaction allowed to warm to RT. After 2 h stirring, it was judged by TLC (*n*-hexane/Et_2O 3/7) that the diastereomeric mixture had reached the equilibrium composition. The mixture was diluted with Et_2O, sat. aq. NH_4Cl was added, the phases separated, and the aqueous phase extracted with EtOAc (3 x). The combined organic extracts were dried by filtration on a Celite® plug, evaporated and analysed by ^1H NMR spectroscopy, which showed a 91:9 diastereomeric ratio favouring the *cis*-isomer **4a**. The product was purified by chromatography on silica gel (*n*-hexane/EtOAc 35:65), affording an analytically pure sample of the title compound as a white solid accompanied by its diastereomeric mixture with the starting **3a** (overall 92% yield). The enantiomeric excess of the product was determined by chiral stationary phase HPLC (Chiralpak ADH column, *n*-hexane/*i*-PrOH 80:20, flow 0.75 mL/min, λ 254 nm, t_{maj} = 23.2 min, t_{min} = 20.4 min, 96% ee), showing that epimerisation occurred without racemisation, under these conditions. Optical rotation was not measured due to the very small amount of diastereomerically pure compound available. ^1H NMR (acetone-d_6, 600 MHz) δ = 10.07 (br s, 1H), 8.01 (br d, J = 8.3 Hz, 1H), 7.60 (br t, J = 8.3 Hz, 1H), 7.49 (br t, J = 8.4 Hz, 1H), 7.21 (d, J = 8.3 Hz, 1H), 7.16 (br s, 1H), 7.02 (br t, J = 8.3 Hz, 1H), 6.86 (br d, J = 8.3 Hz, 1H), 5.32 (br quint, J = 4.0 Hz, 1H), 4.60 (br quint, J = 4.0 Hz, 1H), 3.67 (ddd, J = 15.9, 9.2, 1.7 Hz, 1H), 3.62 (br dd, J = 15.5, 7.4 Hz, 1H), 3.59 (dd, J = 15.9, 4.9 Hz, 1H), 3.36 (br dd, J = 17.6, 3.9 Hz, 1H); ^{13}C NMR (acetone-d_6, 150 MHz) δ = 198.7, 138.7, 135.6, 134.6, 131.9, 130.2, 129.6, 126.9, 124.0, 121.1, 117.0, 111.2, 108.9, 87.0, 41.0, 38.5, 31.1, 26.1; ESIMS = 343 (M + Na^+).

Preparation of compound 3b (methyl 2-((4*R,5*R**)-4-nitro-1,3,4,5-tetrahydrobenzo[*cd*]indol-5-yl)acetate) via hydrolysis, decarboxylation and esterification of 3n**[15] In a vial equipped with a magnetic stirring bar, compound **3n** (0.090 mmol) was suspended in MeOH (600 µL), and cooled to ca -10 °C (ice-acetone bath). An aq. 1 M LiOH solution (300 µL, 0.30 mmol, 3.3 equiv.) was added, and the resulting mixture stirred at the same temperature for 4 h, then at RT for additional 4 h. EtOAc was then added, followed by H_2O and 0.5 M aq. $KHSO_4$ until pH < 1. The organic phase was separated, and the aqueous phase extracted with EtOAc (3x). The combined organic phases were dried by filtration on a short plug of Celite® and evaporated to dryness under reduced pressure in a 50 mL round bottom flask. The thus obtained di-acid was suspended in toluene (2 mL), a magnetic stirring bar was added to the flask, a cooler was applied and the system heated to 110 °C using a pre-heated oil bath for 2 h. The mixture was then cooled to RT, and evaporated to dryness under reduced pressure. The residue was suspended in MeOH (1 mL) and toluene (1 mL), and a 2 M solution of $TMSCHN_2$ in Et_2O (120 µL, 0.24 mmol, CAUTION! Highly toxic and explosive) was added while stirring. The reaction mixture was left stirring at RT for 30 min, then evaporated to dryness under reduced pressure. The residue was purified by chromatography on silica gel (CH_2Cl_2), affording the title compound as a pale yellow solid in 48% yield over the three steps, and as a 87:13 diastereomeric mixture favouring the *trans*-isomer **3b** over the *cis*-isomer. The enantiomeric excess of the *trans*-product **3b** was determined by chiral stationary phase HPLC (Chiralpak ADH column, *n*-hexane/*i*-PrOH 90:10, flow 0.75 mL/min, λ 254 nm, t_{maj} = 30.4 min, t_{min} = 33.0 min, 82% ee), showing that racemization did not occur under these conditions. ^{1}H NMR ($CDCl_3$, 400 MHz) δ [signals of the *trans*-isomer] = 8.02 (br s, 1H), 7.23 (br d, J = 8.2 Hz, 1H), 7.17 (br t, J = 7.4 Hz, 1H), 6.98 (br s, 1H), 6.94 (br d, J = 7.1 Hz, 1H), 5.18 (dt, J_t = 6.4 Hz, J_d = 4.4 Hz, 1H), 4.35 (q, J = 6.7 Hz, 1H), 3.75 (dd, J = 15.7, 6.1 Hz, 1H), 3.72 (s, 3H), 3.43 (ddd, J = 16.0, 4.3, 0.9 Hz, 1H), 2.80 (dd, J = 16.6, 6.2 Hz, 1H), 2.76 (dd, J = 16.6, 6.5 Hz, 1H); ^{13}C NMR ($CDCl_3$, 100 MHz) δ [signals of the *trans*-isomer] = 171.5, 133.7, 128.6, 123.6, 118.8, 115.8, 109.7, 107.3, 85.4, 52.0, 37.9, 37.1, 25.4; ESIMS = 297 (M + Na^+). ^{1}H NMR spectroscopic data for this compound are in accordance with literature,[8] thus substantiating the assignment of the relative configuration of the major diastereoisomer **3b** (and of the parent compound **3n**) as 4,5-*trans*.

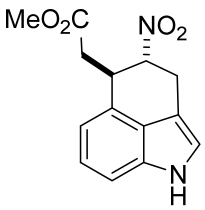

[15] Procedure adapted from: O. Marianacci, G. Micheletti, L. Bernardi, F. Fini, M. Fochi, D. Pettersen, V. Sgarzani, A. Ricci, *Chem. Eur. J.* **2007**, *13*, 8338. It turned out to be better to use MeOH instead of THF during the hydrolytic step.

Conformational analysis and determination of the relative and absolute configuration of compounds 3a and 4a

All the attempts to obtain good crystals of the prepared compounds **3** were not successful. For this reason the relative and absolute configuration was determined by a combination of conformational analysis and theoretical simulations of chirooptical spectra. Compound **3a** was selected as representative compound.

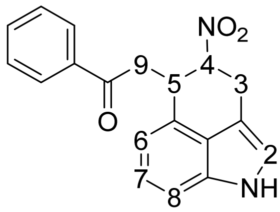

3a

Relative configuration

The relative stereochemistry of the two stereogenic centres at C-4 and C-5 of compound **3a** and of its diastereoisomer **4a** was determined by means of NMR spectroscopy. Full assignment of the ^{1}H and ^{13}C spectra was preliminarily achieved by bi-dimensional experiments (COSY, gHSQC and gHMBC), taken in $CDCl_3$ solutions for **3a** and acetone-d_6 for **4a**.

Compound 3a.

The two diastereotopic hydrogens belonging to C-3 were found at 3.45 ($^{2}J_{HH}$ = 16.9 Hz, $^{3}J_{HH}$ = 4.2 Hz) and 3.73 ppm ($^{2}J_{HH}$ = 16.9, $^{3}J_{HH}$ = 4.2 Hz) whereas the two diastereotopic hydrogens belonging to C-9 at 3.41 ppm ($^{2}J_{HH}$ = 18.2 Hz, $^{3}J_{HH}$ = 6.9 Hz) were assigned by long-range correlation with the carbonyl signal. The CH signal at 4.59 ppm was assigned to the H-5 hydrogen by long range correlation with the carbonyl signal, and the signal at 5.29 ppm was therefore assigned to H-4. The pattern of the latter is a quartet generated by three very similar $^{3}J_{HH}$ coupling constants (about 5.0 Hz) with H-5 and with H-3' and H-3". This feature suggests that H-5 should occupies a pseudo-equatorial position, where anti-periplanar dihedral angle with other hydrogens are not available. The signal of the NH (7.98 ppm) was assigned by the lack of correlation in the ^{1}H-^{13}C HSQC spectrum. DPFGSE-NOE experiments[16] were acquired in order to assign the relative stereochemistry at C-4 and C-5 (Figure S2).

[16] K. Stott, J. Stonehouse, J. Keeler, T-L. Hwang, A. J. Shaka, *J. Am. Chem. Soc.* **1995**, *117*, 4199.

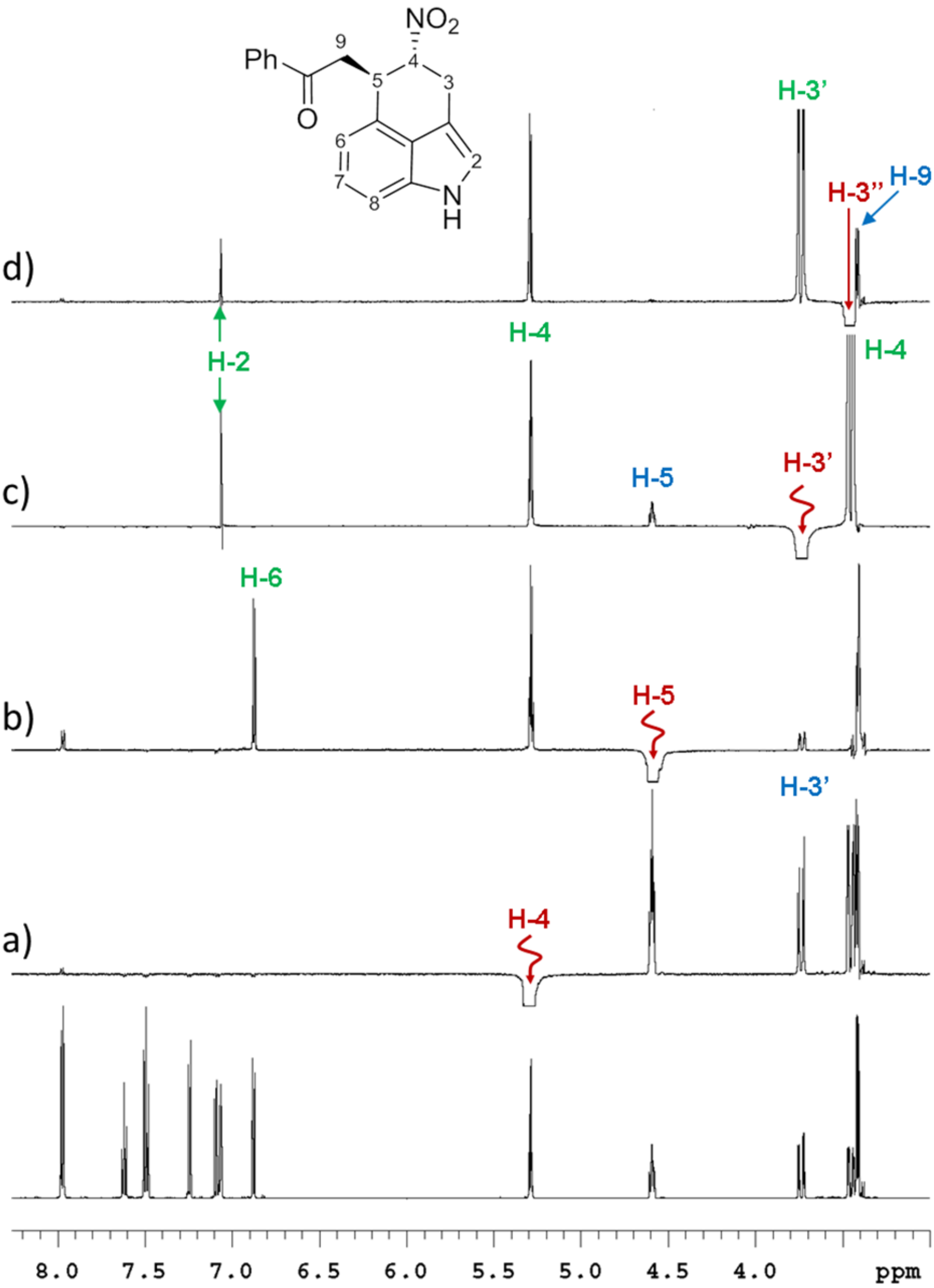

Figure S2: DPFGSE-NOE spectra of **3a** (600 MHz in $CDCl_3$, +25°C). Bottom: ^{1}H-NMR control spectrum. Traces a-d: red labels indicate the saturation point. Green labels indicate "control" NOEs, that have to be observed to assure reliable results. Blue labels indicate diagnostic NOEs.

On saturation of the H-4 signal (trace a), NOE enhancements with similar intensity were observed for H-5, H-3',H-3" and both the H-9 signals. On saturation of the H-5 signal (trace b), large NOEs were observed on H-4 and H-9 and only a small enhancement was observed for one of the H-3 hydrogens at 3.73 ppm (H-3'). The observed NOEs suggested that H-5 occupies a pseudo-equatorial position, otherwise a strong NOE should be observed on one of the H-3 signals, due to 1-3 diaxial relationship (the observation of the small NOE on H-3' is due to the presence of a second conformation with smaller population, see below). As a confirmation, the saturation of the signal of H-3" (in a pseudo-axial position) at 3.41 ppm yields a noticeable NOE enhancement on the H-9 hydrogens (trace d), that occupies a pseudo-axial position on the ring, too. All the NOE data thus agree to assign the 4*R**,5*R** relative configuration (i.e. a *trans* relationship).

Compound 4a

In the case of **4a** the signal of H-4 was found at 5.21 ppm, while that of H-5 was at 4.50 ppm (both CH signals were assigned by HSQC). The pattern of both signals was a doublet of triplets, with $^3J_{HH}$ = 8.6 and 4.3 Hz for H-4 and 8.5 and 4.3 Hz for H-5. The large coupling constant of H-4 corresponds to a ^3J with one of the H-3 hydrogens and that of H-5 is with one of the H-9 hydrogens. The H-4/H-5 ^3J coupling constant is 4.3 Hz. This small value implies that H-4 occupies a pseudo-axial position, where it can develop a large coupling constant with one of the H-3 hydrogen, the dihedral angle between them being close to 180°. On the other hand, the small ^3J between H-4 and H-5 suggests that the latter is in the equatorial position, with a H-C-C-H dihedral with H-4 close to 60°, thus a *cis* relationship of the substituents.

As a cross check, NOE spectra were acquired also for compound **4a** (Figure S3). On saturation of the H-4 signal a noticeable NOE effect was observed on one of the H-9 hydrogens (H-9', trace a). When H-5 was saturated the NOE was observed on H-3", i.e. the hydrogen that occupies the pseudo-axial position. This NOE is observable only when also H-5 is in a pseudo-axial position. On the other hand, when H-9' was saturated a NOE enhancement was observed for H-3'. Also this NOE can be effective only when the H-9 hydrogens are in a pseudo-axial position (and therefore H-5 in a pseudo-equatorial position). This mismatch clearly indicates that the observed NOEs are the result of averaging between two different conformations of the cycle (see below).

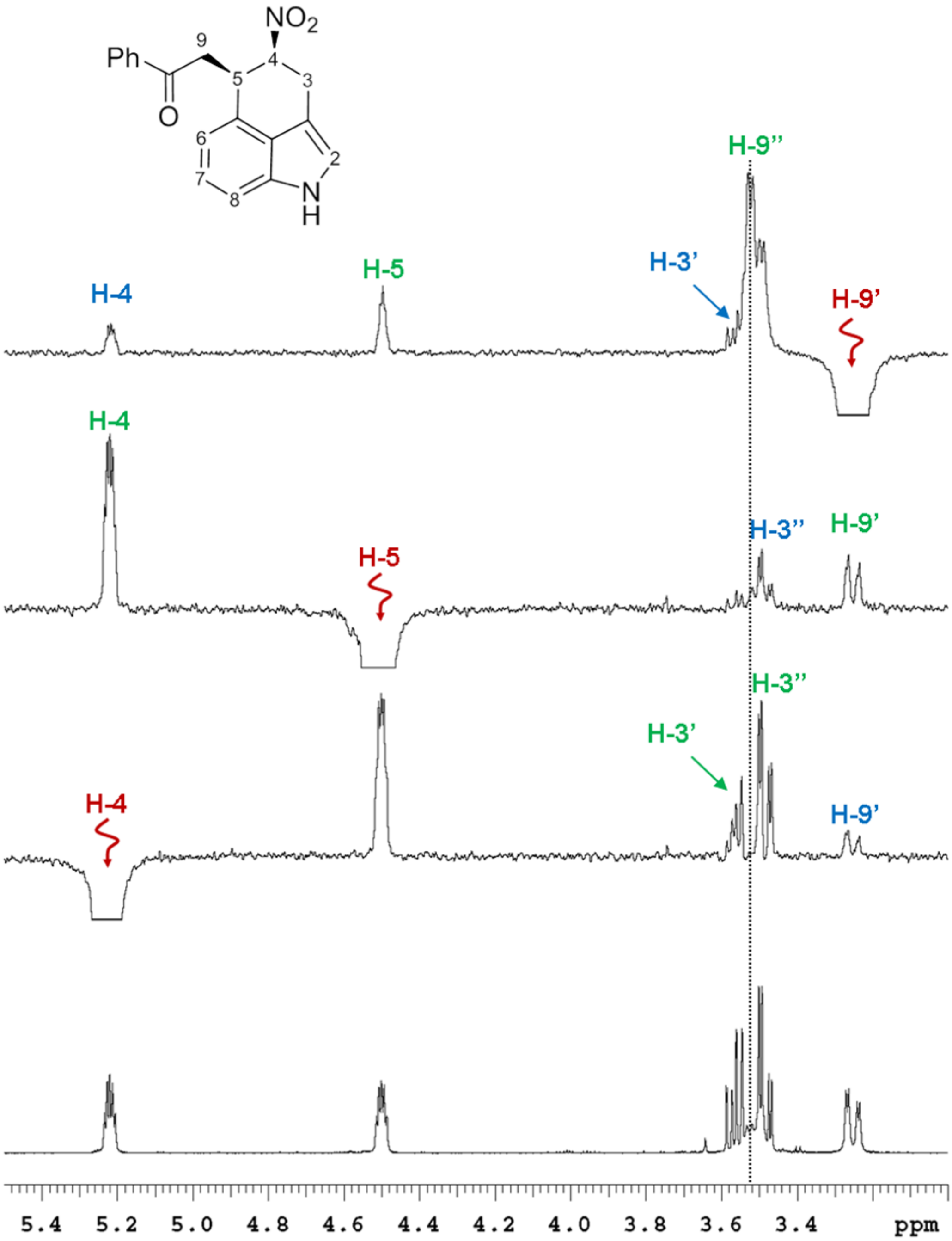

Figure S3: DPFGSE-NOE spectra of **4a** (600 MHz in acetone-d_6). Bottom: ^{1}H-NMR control spectrum. Red labels indicate the saturation point. Green label indicate "control" NOEs, that have to be observed to assure reliable results. Blue labels indicate diagnostic NOEs. The dotted line marks the chemical shift of the H-9'' hydrogen.

Variable Temperature NMR spectra of 4a

The NMR spectrum of **4a** recorded at +25 °C showed some broad signals (H-9"), probably due to the ring inversion that is not fast in the NMR timescale. To get information about the conformational rearrangement, a CD_2Cl_2 sample of **4a** was cooled to -80 °C. On lowering the temperature all the aliphatic signals (and some aromatic signals as well) broadened, reached the coalescence and split into two sets of signals below -50 °C. At -80 °C the ratio of the signals is 64:36 (Figure S4). In particular, the signal of H-4 was split into two signals at 5.12 ppm (major) and 5.50 ppm (minor) and the signal of H-5 was split into signals at 4.74 ppm (major) and 4.36 ppm (minor).

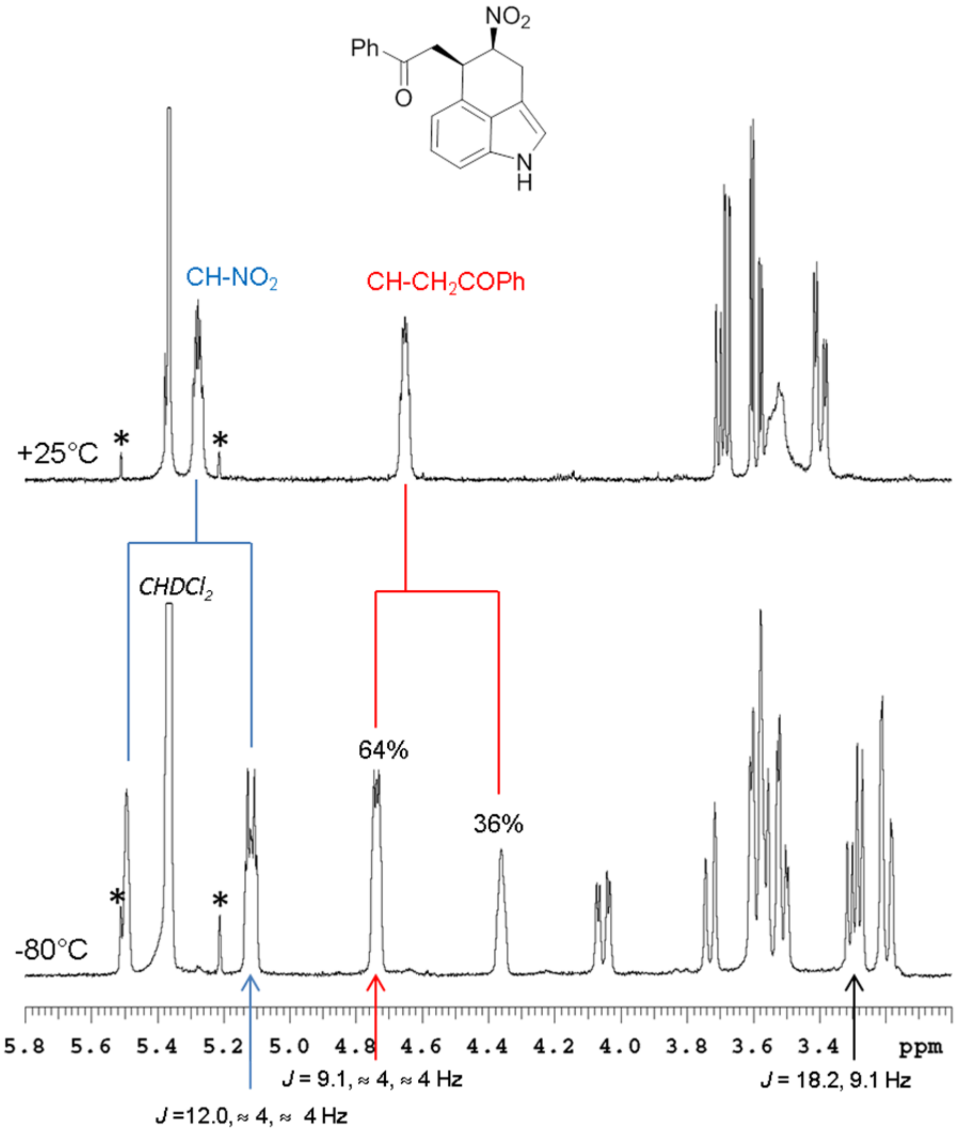

Figure S4. ^{1}H spectra (600 MHz in CD_2Cl_2,) of the aliphatic region of **4a**. Top trace: spectrum recorded at +25 °C. Bottom: spectrum recorded at -80 °C showing the presence of two conformers with 64:36 ratio. Asterisks in the spectra indicate the ^{13}C satellites of the residual signal of the deuterated solvent.

The pattern of the major signal of H-4 is a doublet of triplets with a very large coupling constant (12.0 Hz) with one of the H-3 hydrogens, indicating the *trans*-diaxial relationship of the two hydrogens. On the contrary, only small coupling constants are observed for the same signal of the minor conformer, confirming that in the minor conformation the H-4 is in a pseudo-equatorial position. The small H-4/H-5 coupling constant (≈ 4 Hz) confirmed the gauche relationship between the two hydrogens, thus a *cis* relationship (4*R**, 5*S** relative configuration). The energy barrier involved in the conformational exchange was evaluated at the coalescence temperature of the H-5 signal (-33 °C) as 11.0 ± 0.2 kcal/mol. The 64:36 ratio at -80 °C corresponds to a $\Delta G°$= 0.22 kcal/mol. Considering $\Delta G°$ invariant with the temperature and applying Boltzmann distribution, the conformational ratio to be considered at ambient temperature is 59:41.

Variable Temperature NMR spectra of 3a

The same VT-NMR approach was employed for compound **3a**. The ring inversion barrier was found to be lower with respect to **4a** and the conformers ratio was more unbalanced. On lowering the temperature below -50 °C a broadening of the lines of H-4 and H-5 was observed, reaching the maximum linewidth at -110 °C, eventually followed by a sharpening of the same lines. This is the classical behaviour of a conformational exchange within two widely unbalanced conformations.[17] At -140 °C a second set of signals was detected, accounting for a 97:3 ratio of the two conformations (Figure S5).

The line broadening of the signals due to the very low temperature did not allow for a direct measure of the coupling constants of H-4 and H-5, but the line of the H-4 signal (≈ 13 Hz at -140 °C) is too narrow to hide large coupling constants (if a line broadening is applied to the -50 °C spectrum the same signal has a linewidth of 14 Hz). This implies that in the more populated conformation the H-4 hydrogen occupies a pseudo-equatorial position, where only small coupling constants can be effective with the neighboring hydrogens. The 97:3 ratio at -140 °C corresponded to a $\Delta G°$ = 0.86 kcal/mol. If $\Delta G°$ is kept constant with the temperature the conformational ratio at ambient temperature is 81:19. The presence of a second populated conformation where H-5 is in the axial position well explains the weak NOE observed for H-3' (trace b of Figure S2).

[17] J. Sandstrom, *Dynamic NMR Spectroscopy*. Academic Press, **1982**, p. 81. See also L. Lunazzi, A. Mazzanti , D. Casarini , O. De Lucchi, F. Fabris, *J. Org. Chem.* **2000**, *65*, 883.

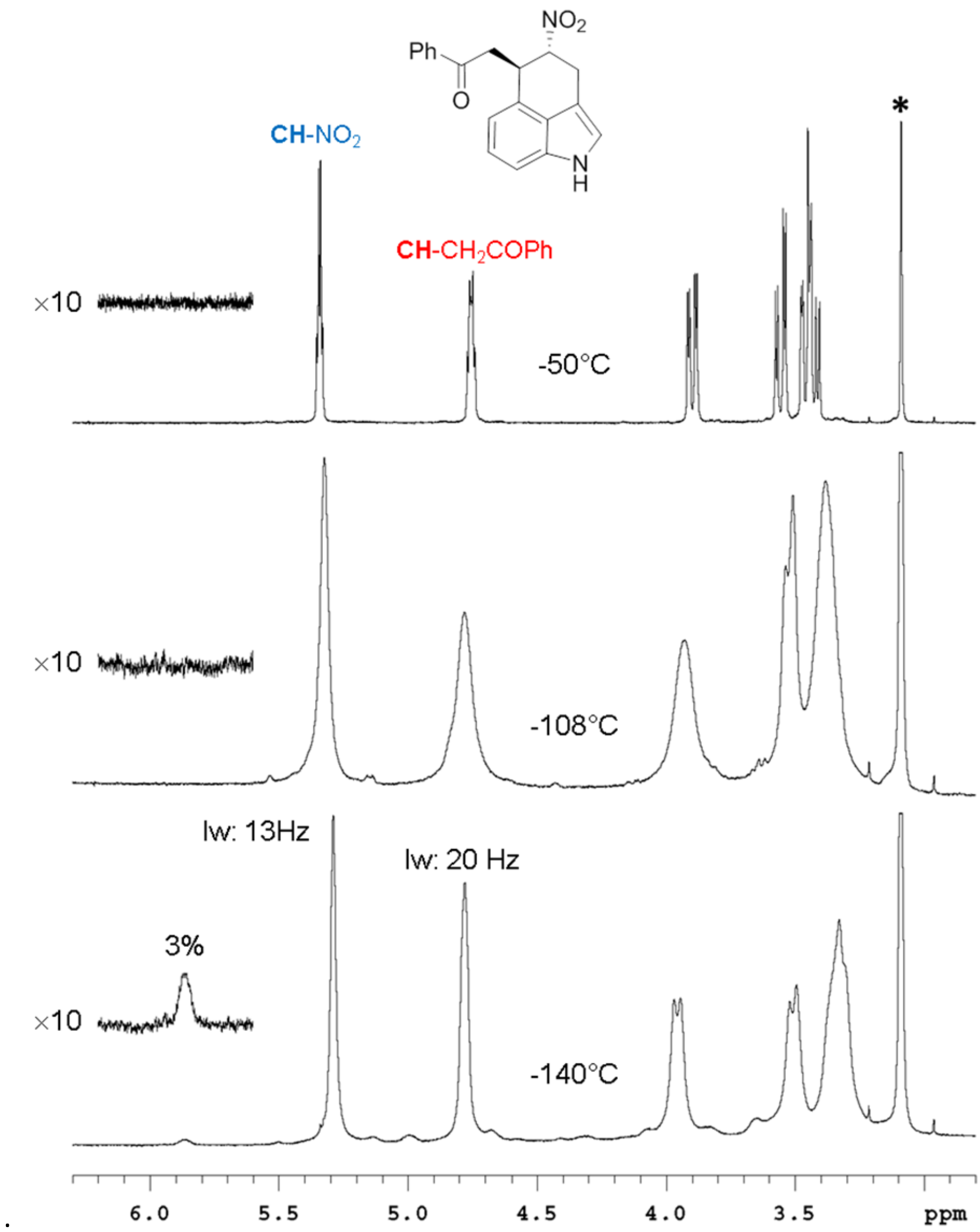

Figure S5. ^{1}H spectra ($CDFCl_2$, 600 MHz) of the aliphatic region of **3a**. Top trace: spectrum recorded at -50 °C. Bottom: spectrum recorded at -140 °C showing the presence of two conformations with 97:3 ratio (see the inset spectrum on the left). Asterisk in the spectra indicates an impurity of the deuterated solvent.

Conformational analysis of 3a and 4a

Although the rigidity of the heterocyclic core of compound **3a** and **4a** and the VT-NMR data provided very good information,[18] the conformational degrees of freedom due to the CH_2COPh moiety still represents an issue for the conformational analysis step needed to tackle the absolute configuration determination.

As the first stage, we performed a conformational search on compound **3a** (*trans*), with the 4*R**,5*R** relative configuration. The whole conformational space was explored by means of Monte Carlo searching together with the MMFF94 molecular mechanics force field as implemented in Titan 1.0.5 (Wavefunction inc.).

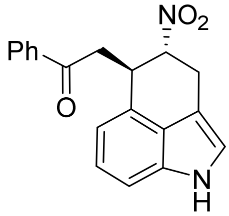

3a

All the conformations found by MM search within a 10 kcal/mol window were then optimized using DFT at the M06-2X/6-31++G(d,p) level and at the M06-2X/6-31+G(d,p) by including the solvent (acetonitrile) with the PCM model[19] using the Gaussian 09 suite of programs.[20] The harmonic vibrational frequencies of each optimized conformation were calculated at the same level to confirm their stability (no imaginary frequencies were observed) and to evaluate the relative energy of each conformation. After DFT minimization, four conformations were found to be enclosed in a 2 kcal/mol window, as reported in Table S6. All of them exhibit the same shape of the six-membered ring, that corresponds to a pseudo boat conformation with the carbon bearing the NO_2 group out of the plane. Two conformations have the CH in a pseudo-axial conformation while the second pair has the CH in the pseudo-equatorial position (i.e. NO_2 in the axial position). Within each pair the conformations are different because of the disposition of the CH_2COPh moiety (Figure S6). The relative electronic energies and enthalpies suggested that all these conformations should be

[18] P. L. Polavarapu, E. A. Donahue, G. Shanmugam, G. Scalmani, E. K. Hawkins, C. Rizzo, I. Ibnusaud, G. Thomas, D. Habeland, D. Sebastian, *J. Phys. Chem. A* **2011**, *115*, 5665.
[19] J. Tomasi, B. Mennucci, R. Cammi, *Chem. Rev.* **2005**, *105***,** 2999.
[20] Program Gaussian 09, rev A.02M. J. Frisch, G. W. Trucks, H. B. Schlegel, G. E. Scuseria, M. A. Robb, J. R. Cheeseman, G. Scalmani, V. Barone, B. Mennucci, G. A. Petersson, H. Nakatsuji, M. Caricato, X. Li, H. P. Hratchian, A. F. Izmaylov, J. Bloino, G. Zheng, J. L. Sonnenberg, M. Hada, M. Ehara, K. Toyota, R. Fukuda, J. Hasegawa, M. Ishida, T. Nakajima, Y. Honda, O. Kitao, H. Nakai, T. Vreven, J. A. Montgomery, Jr., J. E. Peralta, F. Ogliaro, M. Bearpark, J. J. Heyd, E. Brothers, K. N. Kudin, V. N. Staroverov, R. Kobayashi, J. Normand, K. Raghavachari, A. Rendell, J. C. Burant, S. S. Iyengar, J. Tomasi, M. Cossi, N. Rega, J. M. Millam, M. Klene, J. E. Knox, J. B. Cross, V. Bakken, C. Adamo, J. Jaramillo, R. Gomperts, R. E. Stratmann, O. Yazyev, A. J. Austin, R. Cammi, C. Pomelli, J. W. Ochterski, R. L. Martin, K. Morokuma, V. G. Zakrzewski, G. A. Voth, P. Salvador, J. J. Dannenberg, S. Dapprich, A. D. Daniels, Ö. Farkas, J. B. Foresman, J. V. Ortiz, J. Cioslowski, D. J. Fox, Gaussian, Inc., Wallingford CT, 2009.

populated.[21] Whereas the gas-phase calculations gave unreliable results, probably due to the large difference of the large dipole moment of the molecule in the different conformations, the PCM optimization showed a clear preference for one of the equatorial conformations, matching well the experimental observations.

Table S6. Relative energies of the four conformations of **3a** evaluated using ZPE-corrected enthalpies and PCM-M06-2X/6-31+G(d,p) using acetonitrile as solvent. Theoretical populations were calculated using Boltzmann distribution at 298 °K. Experimental ratios of the two pairs were determined by VT-NMR.

Conformation	ΔH° PCM-M06-2X /6-31+G(d,p)	Calcd. Populations	Exptl. Populations
Eq-1	**0.00**	68	81
Eq-2	2.29	1	
Ax-1	0.96	13	19
Ax-2	0.78	18	

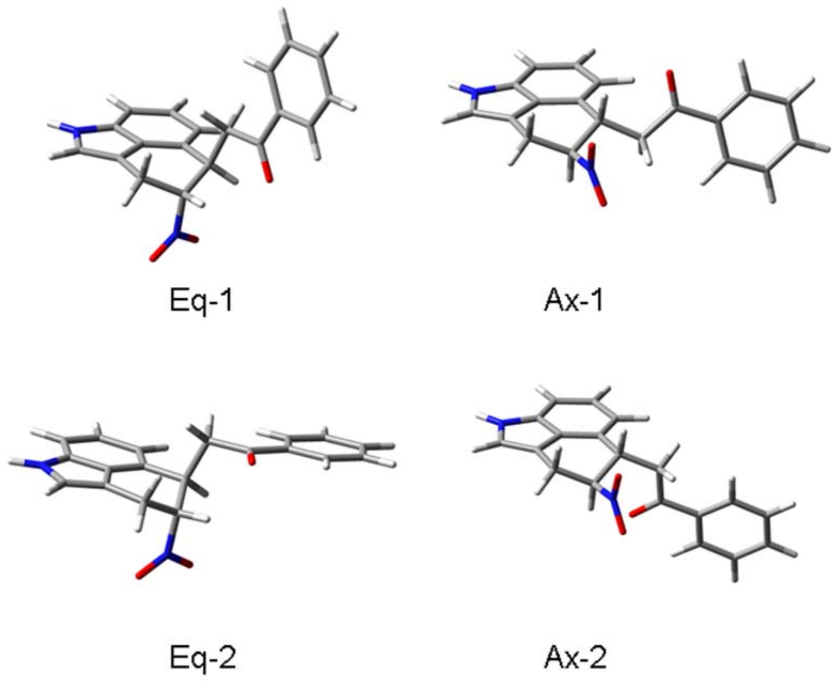

Figure S6. 3D view of the four conformations of compound **3a**.

In the case of compound **4a** (*cis*) the MM conformational search found three conformations the were subsequently optimized at the PCM-M06-2X/6-31+G(d,p) level using acetonitrile as the

[21] It has been pointed out that the calculations of entropy data are often thwarted by the existence of low-frequency vibrational modes, thus the calculation of the free Gibbs Energy is not reliable. See: a) Y. Lan, K. N. Houk, *J. Am. Chem. Soc.* **2010**, *132*, 17921. b) C. P. A. Anconi, C. S. Nascimento Jr, H. F. Dos Santos, W. B. De Almeida, *Chem. Phys. Lett.* **2006**, *418*, 459. c) J. P. Guthrie, *J. Phys. Chem. A* **2001**, *105*, 8495. d) M. W. Wong, *Chem. Phys. Lett.* **1996**, *256*, 391; e) S. E. Wheeler, A. J. McNeil, P. Muller, T. M. Swager, K. N. Houk, *J. Am. Chem. Soc.* **2010**, *132*, 3304.

solvent (Table S7 and Figure S7).

Table S7. Relative energies of the three conformations of **4a** evaluated using ZPE-corrected enthalpies and PCM-M06-2X/6-31+G(d,p) using acetonitrile as solvent. Theoretical populations were calculated using Boltzmann distribution at 298 °K. Experimental ratio of the two pair were determined by VT-NMR.

Conformation	ΔH° PCM-M06-2X /6-31+G(d,p)	Calcd. Population	Exptl. Population
Eq-1	**0.00**	41	45
Eq-2	0.43	19	
Ax-1	0.02	39	55

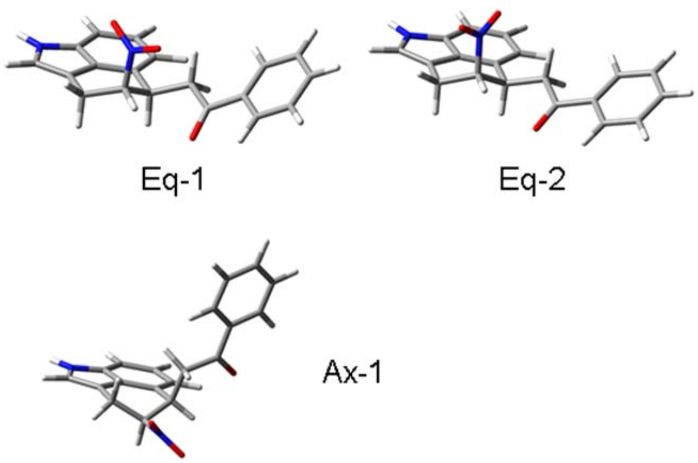

Figure S7. 3D view of the three conformations of compound **4a**.

Also in this case the calculations including the solvent (acetonitrile) well agree with the experimental populations. Within the pair in which the H-4 is equatorial the conformations are different because of the different dispositions of the nitro group with respect to the group in position 5. On the contrary, in the axial conformation the nitro group has only one preferred conformation.

Absolute configuration

Having in hand the relative configuration and suitable experimental data supporting the preferred conformations, the assignment of the absolute configuration was pursued by chirooptical methods.

The determination of the absolute configuration (AC) of chiral molecules using chirooptical techniques like optical rotation (OR), electronic circular dichroism (ECD), and vibrational circular dichroism (VCD) has gained feasibility and reliability because of the development of methods for the prediction of these properties based on density functional theory (DFT) and on its Time-Dependent formalism (TD-DFT).[22] In the present case the theoretical calculation of the electronic circular dichroism spectra (ECD) was selected for the absolute configuration assignment.

The electronic excitation energies and rotational strengths have been calculated for the isolated molecule in the gas phase for the four conformations of **3a** using TD-DFT with four different methods (functionals), to ascertain whether different computational approaches provide different shapes of the simulated spectra (see Figure S8).[23] Simulations were performed with the hybrid functionals BH&HLYP[24] and M06-2X,[25] with ωB97XD that includes empirical dispersion,[26] and CAM-B3LYP that includes long range correction using the Coulomb Attenuating Method.[27] The calculations employed the 6-311++G(2d,p) basis set that proved many times to be sufficiently accurate at a reasonable computational cost.[28] Rotational strengths were calculated in both length and velocity representation, the resulting values being very similar (RMS differences < 5%). For this reason the errors due to basis set incompleteness should be very small.[29] Although the spectra simulated within the same functional for the four conformations are quite different, they are nevertheless consistent with the simulation of a negative Cotton effect at about 190 nm (Figure S8).

---

[22] For reviews see: a) G. Bringmann, T. Bruhn, K. Maksimenka, Y. Hemberger, *Eur. J. Org. Chem.* **2009**, 2717. b) T. D. Crawford, M. C. Tam, M. L. Abrams, *J. Chem. Phys. A* **2007**, *111*, 12057. c) G. Pescitelli, L. Di Bari, N. Berova, *Chem. Soc. Rev.* **2011**, *40*, 4603. For a review on conformational analysis for the absolute configuration determination see: A. Mazzanti, D. Casarini, *WIREs Comput. Mol. Sci.* **2012**, *2*, 613.

[23] C. E. Check, T. M. Gilbert. *J. Org. Chem.* **2005**, *70*, 9828.

[24] In Gaussian 09 the BH&HLYP functional has the form: $0.5*E_X^{HF} + 0.5*E_X^{LSDA} + 0.5*\Delta E_X^{Becke88} + E_C^{LYP}$

[25] Y. Zhao, D. G. Truhlar, *Theor. Chem. Acc.* **2008**, *120*, 215.

[26] J-D. Chai, M. Head-Gordon, *Phys. Chem. Chem. Phys.* **2008**, *10*, 6615.

[27] T. Yanai, D. Tewand, N. Handy, *Chem. Phys. Lett.* **2004**, *393*, 51.

[28] a) G. Cera, M. Chiarucci, A. Mazzanti, M. Mancinelli, M. Bandini, *Org. Lett.* **2012**, *14*, 1350; b) F. Pesciaioli, P. Righi, A. Mazzanti, G. Bartoli, G. Bencivenni, *Chem. Eur. J.* **2011**, *17*, 2482; c) S. Duce, F. Pesciaioli, L. Gramigna, L. Bernardi, A. Mazzanti, A. Ricci, G. Bartoli, G. Bencivenni, *Adv. Synt. Catal.* **2011**, *353*, 860; d) L. Bernardi, M. Comes-Franchini, M. Fochi, V. Leo, A. Mazzanti, A. Ricci, *Adv. Synt. Catal.* **2010**, *352*, 3399.

[29] P. J. Stephens, D. M. McCann, F. J. Devlin, J. R. Cheesemanand, M. J. Frisch, *J. Am. Chem. Soc.* **2004**, *126*, 7514.

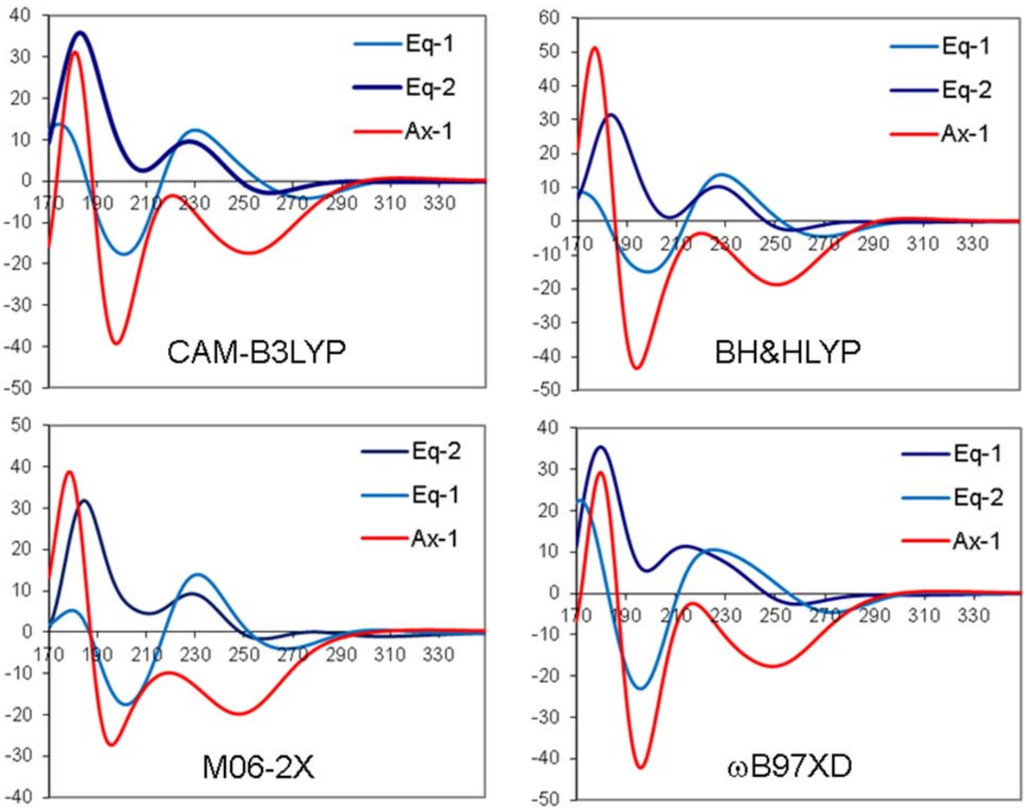

Figure S8.TD-DFT simulated spectra calculated for the four conformations of **3a** using four different functionals (CAM-B3LYP, BH&HLYP, M06-2X, ωB97-XD) and the same 6-311++G(2d,p) basis set. For each conformation the first 60 excited states were calculated, and the spectrum was obtained using a 0.33 eV line width at half height.

The population-weighted spectra to be compared with the experimental spectrum were obtained using the experimental ratio measured by VT-NMR. This accounts for the experimental ratio between the two conformations due to ring inversion, but NMR data do not provide information about the conformational ratio due to the different dispositions of the CH_2COPh moiety within each conformational pair. For this reason these ratios were calculated using the relative enthalpies within each pair, keeping constant the overall Eq:Ax ratio as 80:20. The final ratio employed for the to generate the conformationally averaged spectrum was 70:10:13:7 (**Eq-1:Eq-2:Ax-1:Ax-2**). As shown in Figure S9, the simulated spectra match very well the Cotton effects at 270, 230 and 200 nm when the 4*R*,5*R* absolute configuration was assumed in the calculations.

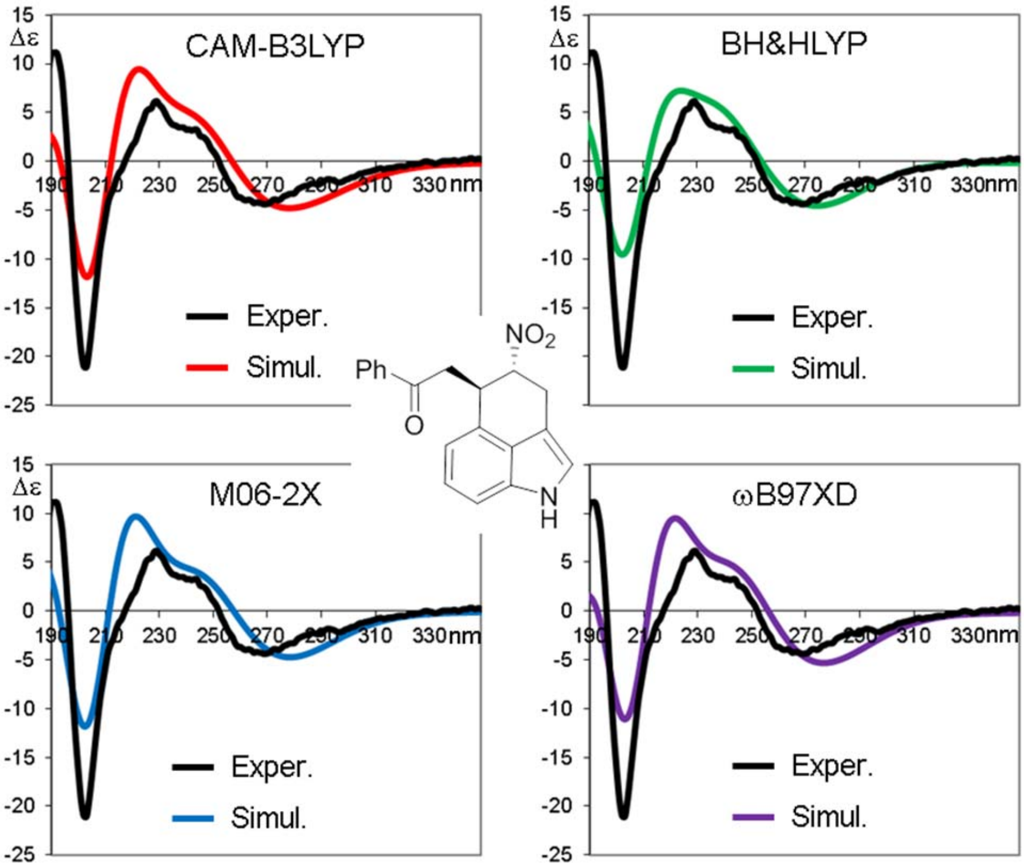

Figure S9 Simulations of the experimental ECD spectrum of **3a**. For each quarter, the black line correspond to the experimental spectrum (acetonitrile solution, $1.1 \cdot 10^{-4}$ M, 0.2 cm path length, Δε in Mol L^{-1} cm^{-1}) and the colored line to the TD-DFT simulation (6-311++G(2d,p) basis set). The simulated spectra were vertically scaled and red-shifted by 7-14 nm to get the best match with the experimental spectrum. All the simulations are for the 4*R*,5*R* absolute configuration.

The same theoretical approach were applied to compound **4a** (Figures S10 and S11). In this case the conformational ratio employed in the simulation of the experimental ECD spectrum was that derived from VT-NMR for the Eq:Ax ratio and that suggested by calculations for the Eq-1:Eq-2 ratio. The final population ratio employed was 32:15:53 (**Eq-1:Eq-2:Ax-1**). Again the simulated spectrum fitted very well the experimental one when the 4*S*,5*R* absolute configuration is considered. This result confirms that epimerization occurred at C-4.

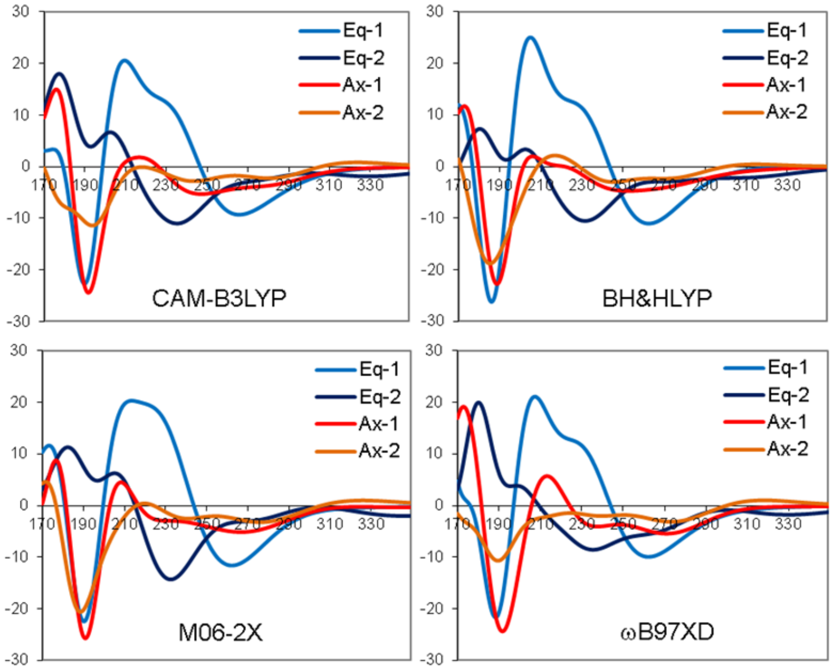

Figure S10. TD-DFT simulated spectra calculated for the four conformations of **4a** using four different functionals (CAM-B3LYP, BH&HLYP, M06-2X, ωB97-XD) and the same 6-311++G(2d,p) basis set. For each conformation the first 60 excited states were calculated, and the spectrum was obtained using a 0.33 eV line width at half height.

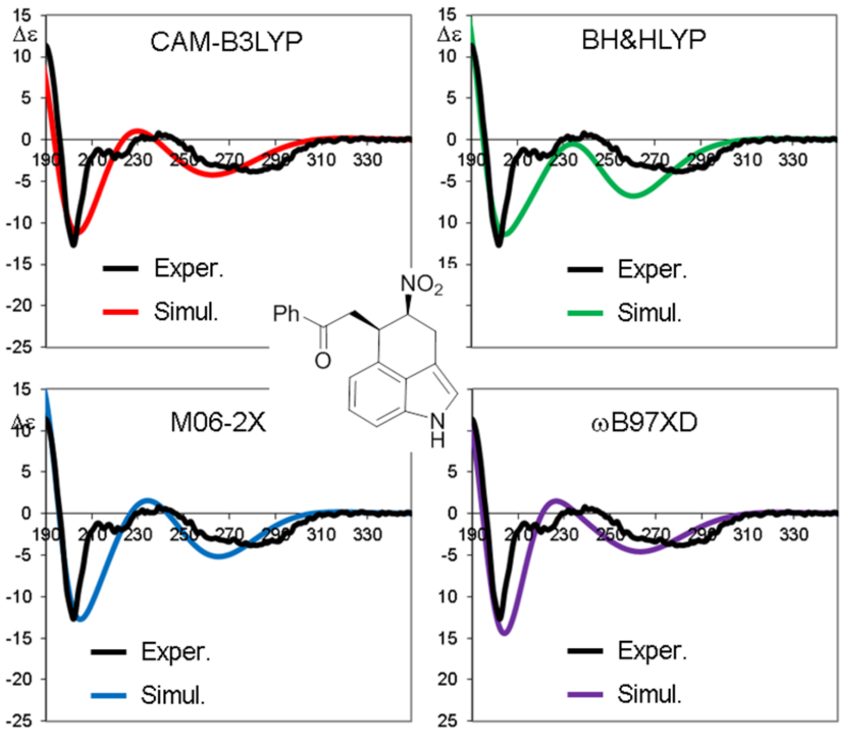

Figure S11 Simulations of the experimental ECD spectrum of **4a**. For each quarter, the black line correspond to the experimental spectrum (acetonitrile solution, $1.2 \cdot 10^{-4}$M, 0.2 cm path length Δε in Mol L^{-1} cm^{-1}) and the colored line to the TD-DFT simulation (6-311++G(2d,p) basis set). The simulated spectra were vertically scaled and red-shifted by 7-14 nm to get the best match with the experimental spectrum. All the simulations are for the 4*S*,5*R* absolute configuration.

Additional material: COSY of 4a at -80 °C:

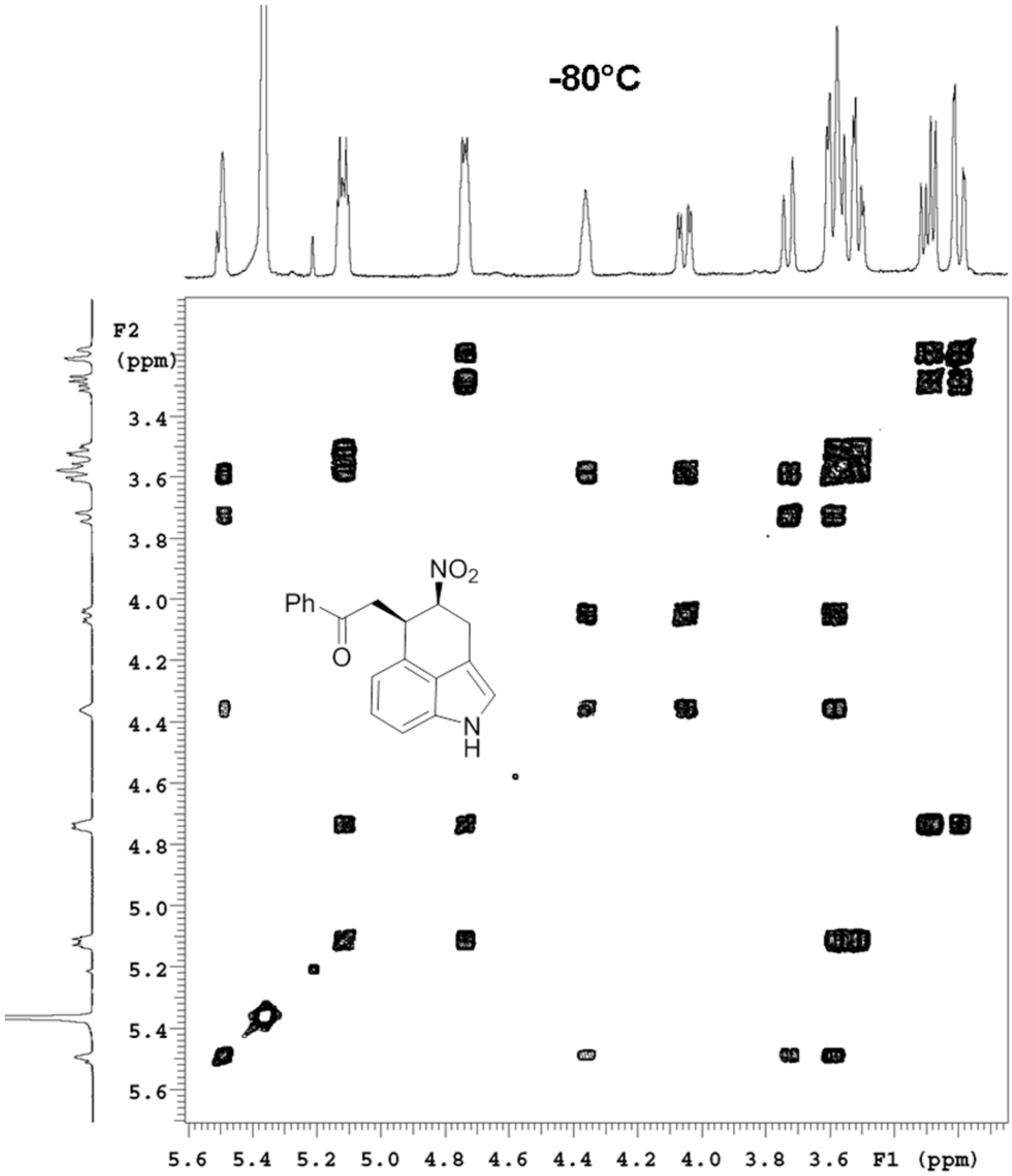

Computational studies on the reaction pathway

Computational methods

All calculations reported in the present mechanistic study were carried out using density functional theory with the B3LYP functional,[30] as implemented in the Gaussian09 program package.[31] Geometry optimizations were performed using the 6-31G(*d,p*) basis set for all atoms. Single-point energy calculations were then performed for each of these optimized structures with the 6-311+G(*2d,2p*) basis set. The stationary points were confirmed as minima (no imaginary frequencies) or transition states (only one imaginary frequency) by analytical frequency calculations at the same theory level as the geometry optimizations. All calculations, including geometry optimizations and frequency calculations, were performed in solvent phase using the conductor-like polarizable continuum model (CPCM)[32] method with the UFF radii and with the parameters for dichloromethane. The reported energies are Gibbs free energies, which include zero-point vibrational corrections, thermal and entropy corrections at 298 K, solvation energies and dispersion effects. The latter are calculated using the B3LYP-D3 method of Grimme,[33] with BJ damping.[34]

Pathway for the formation of product *cis*-4

For comparison, we optimized the transition states leading to the formation of the *cis* stereoisomer of the product, not observed under standard reaction conditions (Figure S12).

Starting from **INT2** the cyclization affording the *cis* product could occur through $\mathbf{TS3_{cis}}$. This is 3.6 kcal/mol higher in energy compared to the corresponding transition state (**TS3**) leading to the formation of the *trans* diastereoisomer. According to these results the reaction should afford exclusively *trans* product **3**, in agreement with the experiments.

---

[30] (a) A. D. Becke, *J. Chem. Phys.* **1993**, *98*, 5648. (b) C. Lee, W. Yang, R. G. Parr, *Phys. Rev.* **1988**, *B37*, 785.

[31] Gaussian 09, Revision A.02, Frisch, M. J.; Trucks, G. W.; Schlegel, H. B.; Scuseria, G. E.; Robb, M. A.; Cheeseman, J. R.; Scalmani, G.; Barone, V.; Mennucci, B.; Petersson, G. A.; Nakatsuji, H.; Caricato, M.; Li, X.; Hratchian, H. P.; Izmaylov, A. F.; Bloino, J.; Zheng, G.; Sonnenberg, J. L.; Hada, M.; Ehara, M.; Toyota, K.; Fukuda, R.; Hasegawa, J.; Ishida, M.; Nakajima, T.; Honda, Y.; Kitao, O.; Nakai, H.; Vreven, T.; Montgomery, J. A., Jr.; Peralta, J. E.; Ogliaro, F.; Bearpark, M.; Heyd, J. J.; Brothers, E.; Kudin, K. N.; Staroverov, V. N.; Kobayashi, R.; Normand, J.; Raghavachari, K.; Rendell, A.; Burant, J. C.; Iyengar, S. S.; Tomasi, J.; Cossi, M.; Rega, N.; Millam, N. J.; Klene, M.; Knox, J. E.; Cross, J. B.; Bakken, V.; Adamo, C.; Jaramillo, J.; Gomperts, R.; Stratmann, R. E.; Yazyev, O.; Austin, A. J.; Cammi, R.; Pomelli, C.; Ochterski, J. W.; Martin, R. L.; Morokuma, K.; Zakrzewski, V. G.; Voth, G. A.; Salvador, P.; Dannenberg, J. J.; Dapprich, S.; Daniels, A. D.; Farkas, Ö.; Foresman, J. B.; Ortiz, J. V.; Cioslowski, J.; Fox, D. J. Gaussian, Inc., Wallingford CT, **2009**.

[32] (a) A. Klamt, G. Schüürmann, *J. Chem. Soc., Perkin. Trans 2.* **1993**, 799. (b) J. Andzelm, C. Kölmel, A. Klamt, *J. Chem. Phys.* **1995**, *103*, 9312. (c) V. Barone, M. Cossi, *J. Phys. Chem. A* **1998**, *102*, 1995. (d) M. Cossi, N. Rega, G. Scalmani, V. Barone, *J. Comput. Chem.* **2003**, *24*, 669.

[33] S. Grimme, J. Antony, S. Ehrlich, H. Krieg, *J. Chem. Phys.* **2010**, *132*, 154104.

[34] S. Grimme, S. Ehrlich, L. Goerigk, *J. Comput. Chem.* **2011**, *32*, 1456.

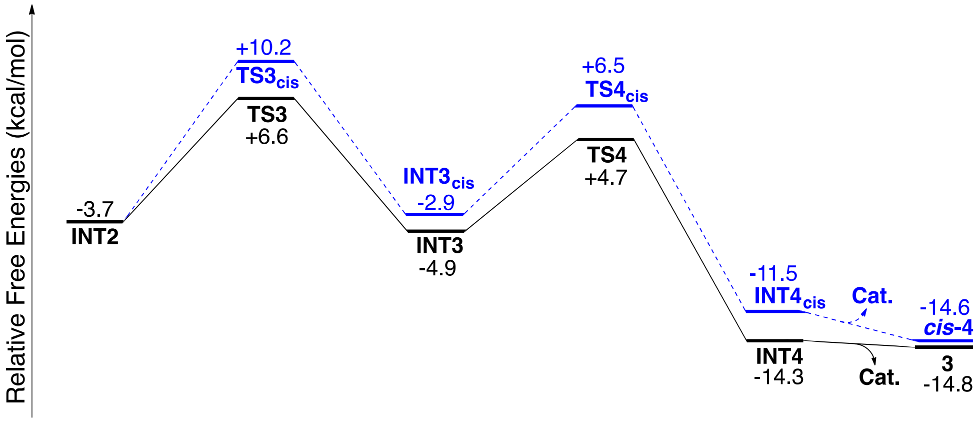

Figure S12: Free energy profile for the formation of *trans*-**3** its *cis* diastereoisomer, starting from **INT2**.

Reaction of ester-substituted indole 1b

Experimentally, the reaction on ester-substituted indole **1b** afforded exclusively the open-chain adduct **3'b**. To test whether the suggested mechanism can also account for this fact, we optimized the transition states for the cyclization (**TS3$_{ester}$**, analogous to **TS3**) and for the nitronic acid-nitro tautomerization giving the open-chain product (**TS3'$_{ester}$**, analogous to **TS3'**). The tautomerization has essentially the same energy barrier as when occurring on the ketone-substituted indole (Figure S13). As expected, the nature of the substituent does not affect this barrier, while it influences substantially the barrier for the cyclization. In fact, the cyclization occurring on the ester-substituted intermediate is ca. 8 kcal/mol higher in energy compared to the same step occurring on the ketone-substituted intermediate (**TS3$_{ester}$** vs. **TS3**). This is consistent with the notion that the ester is a weaker Michael acceptor than the ketone. However, the calculations still predict the formation of the cyclized product to be favored, in contrast to the experimental outcome. This inconsistency is probably due to the computed tautomerization **TS3'**, and can have different possible explanations. One possibility is that the computational approach used here leads to an overestimation of the energy of **TS3'$_{ester}$**. Another possibility is that the tautomerization leading to the open-chain adduct **3'b** occurs through a different mechanism, with the possible involvement of other species present in solution. Several other mechanistic possibilities were tested, including a tautomerization mediated by two or three water molecules, the involvement of one water molecule in the phosphoric acid catalyzed tautomerization, and possible stepwise processes. We found these possibilities to be associated with higher energy barriers. Moreover, due to the inclusion of more species (i.e. water molecules) or the separation of charged species, these results are likely to be associated with higher computational errors.

Since **TS3'** and **TS3'$_{\mathbf{ester}}$** are very similar, it is likely that our calculations give an overestimation of the energy computed for **TS3'** also for the ketone derived substrate. Considering the experimental outcome of the reactions and the calculated barriers for **TS3** and **TS3$_{\mathbf{ester}}$**, a more realistic value for the energy barriers of the tautomerization step lies between 13 and 18 kcal/mol. Nevertheless, we feel that the overall computational results give a reliable qualitative picture over the actual reaction pathway.

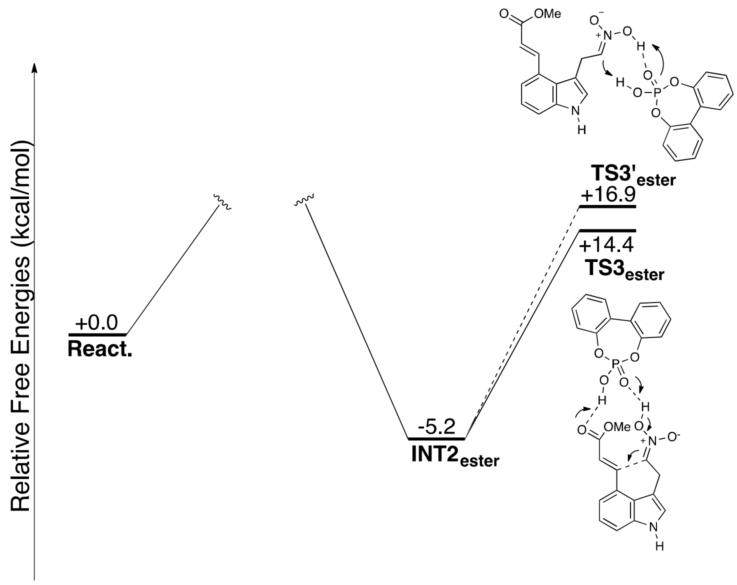

Figure S13: Selected points in the free energy profile for the reaction occurring on the ester-substituted indole **1b**.

Optimized structures and Cartesian coordinates of stationary points

- (*E*)-4-(1*H*-indol-4-yl)but-3-en-2-one (1d)

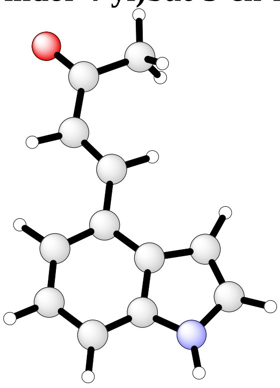

B3LYP/6-311+G(*2d*,*2p*) energy:
-594.0617100200 a.u.
ZPE: 0.200715 a.u.
Thermal correction to Gibbs Free Energy: 0.160812 a.u.
Dispersion correction: -30.86 kcal/mol

C	2.61315700	0.12750800	-0.00043900
C	1.29452000	-0.41827100	0.00013300
C	0.17799500	0.46323400	0.00160900
C	0.44262600	1.84260700	0.00271000
C	1.74996600	2.34956900	0.00214300
C	2.85756100	1.50217600	0.00050000
C	2.78903900	-2.11224600	-0.00235300
C	1.44128100	-1.84591900	-0.00152600
H	-0.38483500	2.54459200	0.00463800
H	1.90131700	3.42461700	0.00324600
H	3.86924100	1.89625900	0.00024200
H	4.50188100	-0.85450400	-0.00197800
H	3.30787100	-3.06007300	-0.00342200
H	0.65926300	-2.59129600	-0.00213200
N	3.49647000	-0.93076600	-0.00173500
C	-1.17282200	-0.08910700	0.00214200
H	-1.22159600	-1.17536300	0.00704700
C	-2.34199200	0.59134500	-0.00296700
H	-2.36869700	1.67803400	-0.00884000
C	-3.67568600	-0.03168000	-0.00145500
C	-3.80469900	-1.54662900	0.00628100
H	-3.32387000	-1.98772500	-0.87312700
H	-3.32601600	-1.97861600	0.89134600
H	-4.86314300	-1.80986700	0.00632300
O	-4.68154700	0.67922400	-0.00648200

- 2

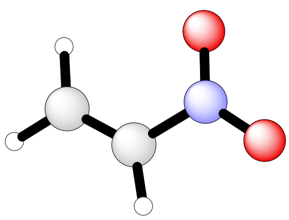

B3LYP/6-311+G(*2d*,*2p*) energy:
-283.1960730220 a.u.
ZPE: 0.055071 a.u.
Thermal correction to Gibbs Free Energy: 0.027286 a.u.
Dispersion correction: -5.39 kcal/mol

C	-1.87212600	0.05035500	0.00046700
H	-1.86185900	1.13409900	0.00159700
H	-2.82550100	-0.46507400	0.00036200
C	-0.74140500	-0.64616400	-0.00066800
H	-0.63904100	-1.72226600	-0.00162500
N	0.55362600	0.02825000	-0.00016200
O	1.54588500	-0.70512100	0.00061500
O	0.59564000	1.25891400	-0.00036500

- Catalyst

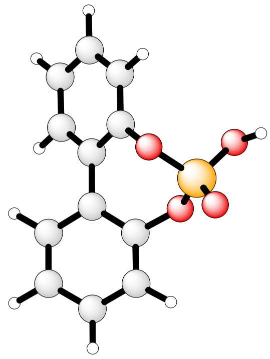

B3LYP/6-311+G(*2d*,*2p*) energy:
-1105.3294049100 a.u.
ZPE: 0.189888 a.u.
Thermal correction to Gibbs Free Energy: 0.150128 a.u.
Dispersion correction: -39.72 kcal/mol

P	0.07100900	2.07302500	-0.06762700
O	-0.64125500	3.06559800	-0.89812000
O	1.10193100	2.64804400	1.01513200
H	1.37892500	3.55197900	0.80102500
O	-0.78540200	1.12972500	0.92448900
O	0.87687200	1.01614900	-0.98984400
C	-1.50562200	0.04078100	0.41170000
C	-0.82191800	-1.11201800	-0.00822300
C	-2.89473700	0.11778100	0.43253400
C	-1.60624800	-2.20504800	-0.41728300
C	-3.64594300	-0.98331200	0.02287400
H	-3.36678100	1.03059900	0.77929800
C	-2.99830600	-2.14611600	-0.40206300
H	-1.10795700	-3.10405500	-0.76593100
H	-4.72987100	-0.93046600	0.03573500
H	-3.57653100	-3.00479000	-0.72819300
C	1.46567000	-0.13428600	-0.44792900
C	2.85487800	-0.21444200	-0.46425000
C	0.65805100	-1.19388700	-0.00208800
C	3.47854500	-1.38193700	-0.02563100
H	3.42636000	0.63129100	-0.83102900
C	1.31529100	-2.35709900	0.43641600
C	2.70515200	-2.45469200	0.42497800
H	4.56166300	-1.45046300	-0.03597400
H	0.71949800	-3.18575500	0.80576400

H	3.18351600	-3.36419500	0.77423300

- TS1

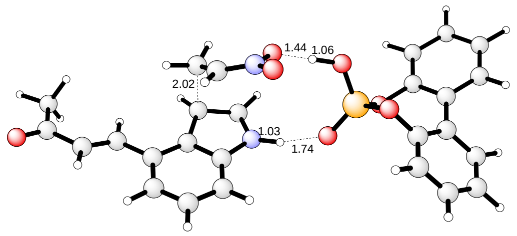

B3LYP/6-311+G(*2d*,*2p*) energy:
-1,982.5830246800 a.u.
ZPE: 0.448131 a.u.
Thermal correction to Gibbs Free Energy: 0.380628 a.u.
Dispersion correction: -89.67 kcal/mol

P	-2.31467500	-0.14438700	0.25388600
O	-1.23722600	0.72332800	-0.30241200
O	-1.92181800	-1.29880400	1.22265600
H	-0.89123900	-1.50397900	1.32885700
O	-3.44799500	0.62844400	1.11798900
O	-3.16429300	-0.76886200	-0.98148000
C	-4.38844900	1.44611200	0.48256400
C	-5.43139400	0.86541300	-0.25948100
C	-4.30559400	2.81931800	0.69563100
C	-6.40151100	1.73452900	-0.78886200
C	-5.28355200	3.65665100	0.15967000
H	-3.48523100	3.21065800	1.28752700
C	-6.33324300	3.11116900	-0.58375500
H	-7.20895600	1.31670800	-1.38202200
H	-5.22347100	4.72809600	0.32244400
H	-7.09465200	3.75717300	-1.00932200
C	-4.40344500	-1.38215800	-0.77537400
C	-4.49195800	-2.75530800	-0.98658700
C	-5.52825400	-0.59998000	-0.46172000
C	-5.73175300	-3.38608100	-0.88847200
H	-3.59246400	-3.30757400	-1.23637600
C	-6.76439500	-1.26335500	-0.36763700
C	-6.86964300	-2.63673400	-0.57882300
H	-5.80593600	-4.45655100	-1.05205700
H	-7.64767100	-0.68804300	-0.10844000
H	-7.83694100	-3.12186200	-0.49438200
C	2.56811900	1.16879600	-0.56751700
C	3.71864600	0.36013200	-0.68622700
C	4.99885100	0.93267000	-0.53124500
C	5.05106800	2.31808100	-0.28367100
C	3.89397700	3.09591700	-0.16690200
C	2.62260300	2.53452500	-0.30384700
C	1.83299200	-0.89189400	-1.04747900
C	3.24013300	-1.01426300	-0.85887000
H	6.01619100	2.80583800	-0.19816500
H	3.98821700	4.16005800	0.02382800
H	1.72297600	3.13418300	-0.21836100
H	0.45496000	0.62668700	-0.68258700
H	1.11287400	-1.66801100	-1.25753400
H	3.80840000	-1.81229000	-1.31991900
N	1.44782900	0.35448400	-0.78872300
C	6.19667200	0.09867200	-0.64323700
H	6.03516000	-0.89261100	-1.06035400
C	7.45046600	0.43810900	-0.27646300
H	7.66928500	1.40468400	0.17000100
C	8.63658400	-0.43111000	-0.41947500
C	8.49095100	-1.81821500	-1.01937100
H	7.79948400	-2.43044400	-0.43082700
H	8.09514000	-1.76560900	-2.03901000
H	9.46965900	-2.29882600	-1.03766100
O	9.73372200	-0.01824500	-0.04865200
C	3.18375800	-1.78675700	1.00867900
H	2.71826600	-2.72732300	0.73799200
H	4.26327700	-1.82663100	1.11301200
C	2.51844600	-0.97921900	1.94877400
H	2.99709500	-0.21842300	2.54690600
N	1.16587400	-1.03540400	2.09819000
O	0.56702700	-0.31765200	2.92567600
O	0.50050000	-1.86118500	1.34373000

- INT1

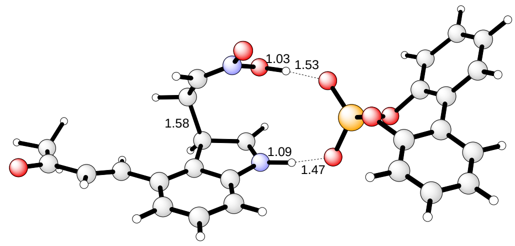

B3LYP/6-311+G(*2d*,*2p*) energy:
-1,982.6019542000 a.u.
ZPE: 0.450213 a.u.
Thermal correction to Gibbs Free Energy: 0.383843 a.u.
Dispersion correction: -89.79 kcal/mol

P	-2.16342500	-0.22794600	-0.17632100
O	-1.30932900	0.67897000	-1.03985500
O	-1.54364200	-1.37626300	0.57660700
H	-0.14333300	-2.00094600	0.63289400
O	-2.99689800	0.63533400	0.94289300
O	-3.37259900	-0.73042500	-1.16673000
C	-3.99396300	1.52727400	0.56406400
C	-5.23780600	1.04316900	0.11794900
C	-3.75753700	2.89014900	0.73515200
C	-6.24184700	1.99019700	-0.14907100
C	-4.77202700	3.80764300	0.46378300
H	-2.78454700	3.21083800	1.09206300
C	-6.01776100	3.35524000	0.02123000
H	-7.20475600	1.64272200	-0.51095000
H	-4.58855400	4.86936500	0.59708200
H	-6.81074000	4.06346700	-0.19800300
C	-4.54672700	-1.25991800	-0.64272800
C	-4.79163400	-2.62097900	-0.81546200
C	-5.49382600	-0.40788100	-0.04510500
C	-6.00445400	-3.16401400	-0.39252900
H	-4.03217700	-3.23287700	-1.29052900
C	-6.70703900	-0.98207100	0.37277200
C	-6.96438300	-2.34121400	0.20244300
H	-6.19629100	-4.22416800	-0.52634100
H	-7.44716800	-0.34896600	0.85258000
H	-7.90824600	-2.75783500	0.54010800
C	2.25513700	1.17214600	-0.70084000
C	3.46226000	0.46279700	-0.72931500
C	4.64887200	1.08829900	-0.32155400
C	4.54490200	2.43194400	0.10542500

C	3.32631500	3.10921600	0.13522400
C	2.14144000	2.48710300	-0.27482800
C	1.69505500	-0.83651300	-1.50571500
C	3.15490800	-0.94577300	-1.19664900
H	5.44389600	2.96332200	0.39810900
H	3.29954100	4.14126100	0.46852800
H	1.18888300	3.00461000	-0.26842200
H	0.15063000	0.54607800	-1.18244900
H	1.06577600	-1.61414000	-1.91536100
H	3.70417900	-1.23318700	-2.10238300
N	1.22255600	0.32724800	-1.19173500
C	5.92951600	0.37380400	-0.36903400
H	5.94540100	-0.51636600	-0.99321300
C	7.05753200	0.72188300	0.28097200
H	7.08962300	1.58652200	0.93879800
C	8.34397800	-0.00663100	0.19551500
C	8.45508500	-1.24824300	-0.66902200
H	7.75297300	-2.02071200	-0.33754000
H	8.22317200	-1.02143400	-1.71486700
H	9.47239000	-1.63502600	-0.60151500
O	9.30848400	0.40911800	0.83205200
C	3.40868700	-2.08813500	-0.13145600
H	3.01986900	-3.01885600	-0.55330600
H	4.49030000	-2.20107000	-0.03529300
C	2.85209000	-1.82743600	1.22949500
H	3.46942200	-1.49844200	2.05353000
N	1.58246200	-1.95537300	1.52860200
O	1.02640100	-1.72852500	2.62356400
O	0.77950400	-2.42326400	0.48883500

- TS2

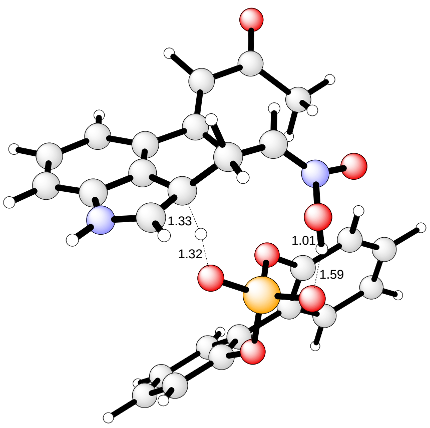

B3LYP/6-311+G(*2d*,*2p*) energy:
-1,982.5714623300 a.u.
ZPE: 0.446663 a.u.
Thermal correction to Gibbs Free Energy: 0.3824 a.u.
Dispersion correction: -94.86 kcal/mol

P	-1.02984400	-0.52989000	-1.64632800
O	0.23722600	-1.36449500	-1.44701800
O	-1.19141300	0.28582600	-2.89986600
H	0.11065300	1.12756800	-3.25712800
O	-2.33905700	-1.49338900	-1.52546000
O	-1.14641600	0.38395800	-0.29337500
C	-2.75160000	-2.02092300	-0.30141900
C	-3.32671500	-1.18516900	0.67488000
C	-2.66996600	-3.40106500	-0.13113700
C	-3.82306100	-1.80099000	1.83691400
C	-3.17051000	-3.98414300	1.03264100
H	-2.22807000	-4.00048700	-0.91992500
C	-3.74987100	-3.18093600	2.01796200
H	-4.25738200	-1.17743300	2.61235100
H	-3.10787000	-5.05960600	1.16643800
H	-4.13768300	-3.62647400	2.92870300
C	-2.35842500	1.02817800	-0.03365000
C	-2.43807900	2.40310300	-0.23814700
C	-3.42938200	0.28192400	0.48611800
C	-3.61042700	3.07513600	0.10930200
H	-1.58318400	2.91506200	-0.66888000
C	-4.59660400	0.98612700	0.82846000
C	-4.68722000	2.36570600	0.64866200
H	-3.68287400	4.14724700	-0.04544300
H	-5.44608300	0.43513400	1.22028500
H	-5.60270900	2.88398000	0.91654000
C	3.38075600	-2.42182700	0.27430100
C	2.94090300	-1.08210800	0.21937400
C	2.68572400	-0.41117000	1.43703500
C	2.95251300	-1.11053900	2.62747300
C	3.40899800	-2.43449900	2.64010200
C	3.61565700	-3.12783700	1.45147600
C	3.24482900	-1.90445900	-1.90256700
C	2.78400100	-0.72995800	-1.22345100
H	2.75120400	-0.61658300	3.57211100
H	3.57825100	-2.93090100	3.58987500
H	3.93943700	-4.16293200	1.43931500
H	3.79250400	-3.81582000	-1.30688200
H	3.32462800	-2.05964500	-2.97067200
H	1.49099700	-0.96135200	-1.40932000
N	3.53295600	-2.87197000	-1.04516600
C	2.09297900	0.93518800	1.50077100
H	1.31697100	1.14849600	0.76931600
C	2.42224900	1.86848400	2.41554600
H	3.22383600	1.68683100	3.12803600
C	1.79097300	3.20162100	2.55554700
C	0.60795600	3.57814800	1.68621000
H	0.84932900	3.54231900	0.61800100
H	-0.22448200	2.88545900	1.84806200
H	0.28945000	4.58863400	1.94604800
O	2.23271900	3.98206800	3.39590800
C	3.19470400	0.61681600	-1.87812500
H	3.19497000	0.46147700	-2.95888000
H	4.22761500	0.82526700	-1.58061800
C	2.38656300	1.83233500	-1.55885300
H	2.65160900	2.49473100	-0.74736900
N	1.33623600	2.21089500	-2.23873200
O	0.58719400	3.19230000	-2.00202100
O	1.05856400	1.46148700	-3.38570800

- INT2

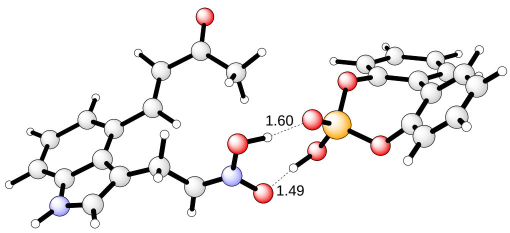

B3LYP/6-311+G(*2d*,*2p*) energy:
-1,982.6173128200 a.u.
ZPE: 0.450213 a.u.

Thermal correction to Gibbs Free Energy: 0.383325 a.u.
Dispersion correction: -89.03 kcal/mol

H	-0.05595200	-1.87069800	-0.78933800
C	7.01313400	-0.51256900	0.37674500
C	5.64087900	-0.31386000	0.03457600
C	5.16162600	1.02269100	-0.09159900
C	6.07179200	2.06622500	0.13920000
C	7.41244900	1.83344500	0.47919800
C	7.90535900	0.53816800	0.60247300
C	6.08294600	-2.53149400	0.09779100
C	5.07043200	-1.63054700	-0.14523800
H	5.71764700	3.09048900	0.08622100
H	8.07018000	2.67816700	0.65876900
H	8.94100500	0.34826800	0.86717300
H	8.12861100	-2.30902200	0.61241700
H	6.05655700	-3.61159500	0.05947400
H	-0.52492700	-0.93877700	1.40712600
N	7.24259400	-1.87001000	0.41459600
C	3.76586900	1.30943300	-0.42883400
H	3.04657500	0.53589200	-0.17752500
C	3.30374900	2.43914400	-1.00946300
H	3.98347800	3.22895400	-1.31970000
C	1.88698500	2.72307200	-1.30275200
C	0.81506200	1.72021700	-0.91370300
H	1.01277600	0.72834300	-1.33245100
H	0.76552800	1.60750800	0.17486800
H	-0.14994400	2.07540300	-1.27720800
O	1.58296600	3.78017000	-1.85573400
C	3.67136300	-2.03013300	-0.53361200
H	3.68656000	-3.06192300	-0.91192400
H	3.29647000	-1.42339900	-1.36492600
C	2.70188500	-1.96291800	0.61223500
H	3.02266800	-1.95997700	1.64549200
N	1.41461300	-1.95888500	0.45368500
O	0.54419100	-1.97816900	1.40669000
O	0.94873500	-1.98336200	-0.84073900
P	-2.27149300	-0.70587300	0.15050900
O	-1.36342700	-0.33131200	1.37098500
O	-1.62004400	-1.54136200	-0.90604600
O	-2.82880500	0.66127400	-0.49745300
O	-3.57828200	-1.35669000	0.84371300
C	-3.75268400	1.47876000	0.17143300
C	-5.08067700	1.05122900	0.33697300
C	-3.32327100	2.74297200	0.56326600
C	-5.97510700	1.96316300	0.92516700
C	-4.23434200	3.62622900	1.14126500
H	-2.28808700	3.02193400	0.40051700
C	-5.56299500	3.23378600	1.32122000
H	-7.00369200	1.65546700	1.08470400
H	-3.90539500	4.61366300	1.44893500
H	-6.27648400	3.91333600	1.77633700
C	-4.78070600	-1.44720100	0.12604400
C	-5.21613900	-2.71185400	-0.25702500
C	-5.54093400	-0.28831300	-0.10060500
C	-6.45129900	-2.84499100	-0.89074200
H	-4.59037500	-3.57185100	-0.04477000
C	-6.78057600	-0.45395200	-0.74325900
C	-7.23319400	-1.71275600	-1.13327400
H	-6.79789700	-3.82789900	-1.19350800
H	-7.38337500	0.42459100	-0.95025700
H	-8.19228800	-1.80859500	-1.63224800

- TS3

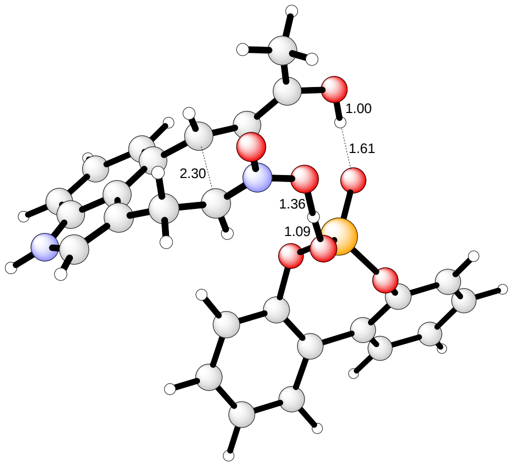

B3LYP/6-311+G(*2d*,*2p*) energy:
-1,982.5928126400 a.u.
ZPE: 0.449875 a.u.
Thermal correction to Gibbs Free Energy: 0.386586 a.u.
Dispersion correction: -96.21 kcal/mol

H	-0.18642700	-1.76414900	-1.48955900
C	-3.85628300	2.62818000	0.87453900
C	-3.60841900	1.31336300	0.40166900
C	-2.97136800	0.36297600	1.23064800
C	-2.56833400	0.78505200	2.50395800
C	-2.83256100	2.09135600	2.96005100
C	-3.48288400	3.03027200	2.16150800
C	-4.53561600	2.49535800	-1.26788100
C	-4.03395700	1.25012400	-0.96284700
H	-2.08765300	0.07785100	3.17227900
H	-2.52755800	2.36851700	3.96441100
H	-3.68214100	4.03434300	2.52330200
H	-4.72305100	4.28798600	-0.14097100
H	-4.94637000	2.86880200	-2.19539100
H	0.29419500	-3.18003000	1.25620700
N	-4.44600400	3.31863300	-0.16279100
C	-2.81368600	-1.03536000	0.78756700
H	-3.72464000	-1.54556300	0.48328700
C	-1.71760900	-1.80809700	1.19602400
H	-0.82731400	-1.28228400	1.52727800
C	-1.62490400	-3.19695200	1.11601500
C	-2.75543000	-4.15224400	0.89182800
H	-3.71749900	-3.65637300	0.78139600
H	-2.55665000	-4.74691000	-0.00261000
H	-2.79964200	-4.83714700	1.74563000
O	-0.48076200	-3.81186500	1.34241000
C	-3.85638400	0.04109200	-1.83721800
H	-3.83050400	0.33475600	-2.89604500
H	-4.68731500	-0.66556200	-1.73761000
C	-2.58044800	-0.66879100	-1.46625100
H	-1.64948000	-0.12069000	-1.41168400
N	-2.44297300	-1.98446500	-1.77041400
O	-1.27906300	-2.55704200	-1.61335500
O	-3.42461400	-2.71273700	-2.04256600
P	1.66411000	-1.15588600	-0.23336300
O	0.72452200	-1.16683000	-1.46812000

O	1.50790100	-2.21674700	0.80954100
O	1.55811800	0.28452100	0.50957000
O	3.12215900	-1.10158200	-0.93492400
C	1.94498300	1.46331900	-0.13582700
C	3.30831900	1.72523300	-0.35514900
C	0.95186900	2.38594200	-0.45284700
C	3.63793400	2.96942100	-0.92127300
C	1.30937900	3.61280600	-1.01112600
H	-0.08303300	2.13767800	-0.24305000
C	2.65574100	3.90297900	-1.24616000
H	4.68137600	3.19276000	-1.12029600
H	0.53932200	4.33590400	-1.26065100
H	2.94094400	4.85303000	-1.68684700
C	4.23582800	-0.62292400	-0.23539500
C	5.23337800	-1.53524000	0.09608500
C	4.36442500	0.75350000	0.01777600
C	6.40532900	-1.08009900	0.69935300
H	5.08349500	-2.58446200	-0.13431300
C	5.55636300	1.18229600	0.62828200
C	6.56575000	0.28231600	0.96422300
H	7.18649800	-1.78705100	0.96015300
H	5.67735000	2.23724000	0.85346600
H	7.47270100	0.64345700	1.43871400

- INT3

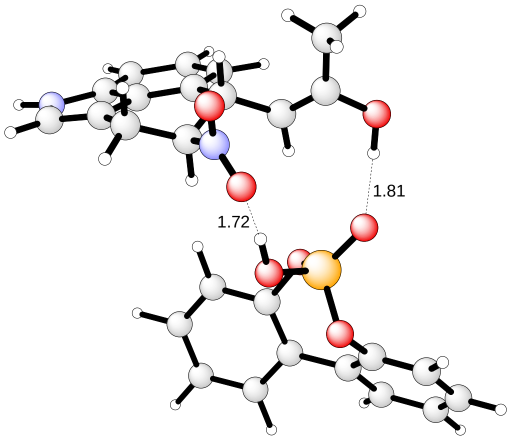

B3LYP/6-311+G(*2d*,*2p*) energy:
-1,982.6206251500 a.u.
ZPE: 0.45501 a.u.
Thermal correction to Gibbs Free Energy: 0.39076 a.u.
Dispersion correction: -92.81 kcal/mol

H	0.18715900	-1.49678300	-1.84348600
C	-4.22335900	2.51657500	0.77501400
C	-3.84333300	1.24995500	0.28213000
C	-3.22006000	0.28287100	1.07912000
C	-2.98301300	0.61693500	2.40846300
C	-3.37698500	1.88055100	2.91110300
C	-3.99508300	2.84800500	2.11815400
C	-4.73128400	2.38731700	-1.42936600
C	-4.16946200	1.17655100	-1.10347000
H	-2.49519600	-0.09405200	3.06840300
H	-3.18375500	2.10708500	3.95582000
H	-4.27853700	3.81206300	2.52921600
H	-5.13896400	4.13185200	-0.27682700
H	-5.11323900	2.75693600	-2.37043800
H	0.33077500	-3.03942800	1.42783800
N	-4.77193600	3.19301400	-0.29718500
C	-2.88703000	-1.04737600	0.40907500
H	-3.76637000	-1.69959800	0.47507100
C	-1.68174300	-1.73328100	0.98929700
H	-0.77662600	-1.13092800	1.02074500
C	-1.59426400	-3.01305300	1.40612200
C	-2.71446100	-4.00452800	1.54107800
H	-3.69619500	-3.56303200	1.36994600
H	-2.57390000	-4.83394700	0.83933600
H	-2.69640400	-4.43077000	2.55012000
O	-0.41166700	-3.56967000	1.78777500
C	-3.85893100	-0.08452200	-1.85389900
H	-3.58988300	0.10428900	-2.89851100
H	-4.70969700	-0.77568800	-1.85601800
C	-2.67503800	-0.77490200	-1.13186100
H	-1.75786500	-0.20261700	-1.27442200
N	-2.41039100	-2.10523700	-1.78575200
O	-1.25755500	-2.37715700	-2.15946100
O	-3.34290400	-2.88743700	-1.89572800
P	1.87644100	-1.13627200	-0.47249900
O	1.04104800	-0.99528800	-1.80908200
O	1.62598900	-2.32620600	0.37990200
O	1.66505200	0.20864700	0.40220100
O	3.35802800	-0.96683400	-1.08432000
C	2.05647400	1.46459300	-0.08244100
C	3.42160200	1.78043400	-0.18337000
C	1.05539900	2.39048200	-0.35925700
C	3.74601200	3.08725000	-0.58847400
C	1.40809200	3.67988600	-0.75621700
H	0.01796200	2.09515000	-0.24581900
C	2.75659200	4.02664300	-0.87159600
H	4.79213500	3.35624700	-0.69499600
H	0.63250100	4.40713200	-0.97415500
H	3.03831100	5.02623900	-1.18699700
C	4.41691000	-0.54125200	-0.26797500
C	5.42059000	-1.46118400	0.01801400
C	4.48358500	0.79939800	0.14560600
C	6.53821500	-1.04887700	0.74294600
H	5.31883300	-2.48012500	-0.33930300
C	5.62132400	1.18442700	0.87677200
C	6.63685400	0.27711500	1.17176300
H	7.32481200	-1.76100100	0.97087400
H	5.69364500	2.20854800	1.22883600
H	7.50062900	0.60356600	1.74213200

- TS4

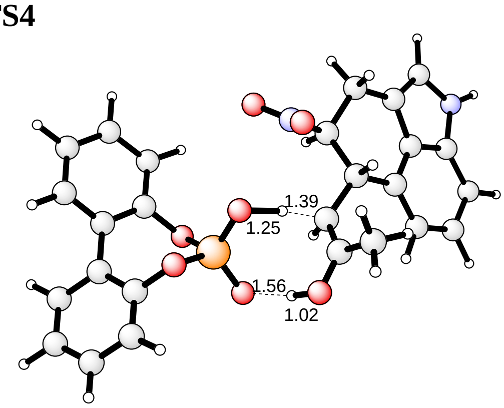

B3LYP/6-311+G(*2d*,*2p*) energy:
--1,982.59905156 a.u.
ZPE: 0.449926 a.u.
Thermal correction to Gibbs Free Energy: 0.38640 a.u.

Dispersion correction: -94.06 kcal/mol

H	0.34596600	-0.65650100	0.87539200
C	5.99374800	0.08470300	-1.35561200
C	4.88204800	0.26259300	-0.50401900
C	3.93815300	-0.74286300	-0.26390900
C	4.13989100	-1.95644400	-0.91549200
C	5.26252600	-2.14556800	-1.75800600
C	6.20250300	-1.14418500	-1.99693600
C	5.99516000	2.20413100	-0.55607600
C	4.89311100	1.59629900	-0.00614300
H	3.43737700	-2.77555900	-0.79701800
H	5.38853400	-3.10877600	-2.24386700
H	7.04855200	-1.31436000	-2.65547300
H	7.50136100	1.49679200	-1.88706200
H	6.37294000	3.21090300	-0.44837900
H	-0.23167000	-2.84215800	-0.05864000
N	6.66484500	1.29105300	-1.36303000
C	2.79905100	-0.39608700	0.70138300
H	3.13491300	-0.60838500	1.72241200
C	1.53461200	-1.20429000	0.41474400
H	1.22333600	-1.17256800	-0.63257200
C	1.34246100	-2.46339600	1.01436800
C	2.09169500	-2.94519300	2.21889600
H	1.96956500	-2.23152200	3.04025000
H	1.71316300	-3.91879500	2.52965600
H	3.16194200	-3.01671600	2.00412400
O	0.39738100	-3.27559800	0.62011800
C	3.80038900	2.02154400	0.92589200
H	3.52494700	3.07342300	0.80431700
H	4.09091400	1.87870300	1.97523500
C	2.54789700	1.13914800	0.65054900
H	2.09753400	1.42618200	-0.30105400
N	1.52706700	1.55657300	1.68996700
O	0.77773800	2.48391000	1.39578600
O	1.54813400	0.99494600	2.78410400
P	-1.79723600	-0.78952600	-0.00629800
O	-0.82150700	-0.24472600	1.05502300
O	-1.33590400	-1.99930300	-0.77886700
O	-2.18812800	0.35210400	-1.09515600
O	-3.18713400	-0.99528700	0.81101900
C	-2.92171400	1.47897900	-0.71059900
C	-4.29571800	1.35630700	-0.44216700
C	-2.26987900	2.70899800	-0.69360300
C	-5.00381100	2.53902000	-0.16629200
C	-2.99815400	3.86559600	-0.41614000
H	-1.20529800	2.74394400	-0.89746500
C	-4.36835500	3.77929800	-0.15651200
H	-6.06325000	2.47338300	0.06113800
H	-2.49544300	4.82749800	-0.40084900
H	-4.93978800	4.67521000	0.06491800
C	-4.40350500	-1.09987500	0.12790300
C	-5.04981700	-2.33292500	0.13765900
C	-4.97909500	0.04098800	-0.45862000
C	-6.30963700	-2.45232800	-0.44839300
H	-4.56336000	-3.17715900	0.61428500
C	-6.24888100	-0.11002400	-1.04281300
C	-6.90928400	-1.33717500	-1.03915300
H	-6.81728400	-3.41173000	-0.44331000
H	-6.70991400	0.74972300	-1.51893900
H	-7.88687300	-1.42390400	-1.50283600

- INT4

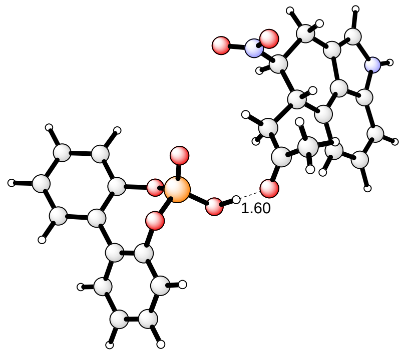

B3LYP/6-311+G(*2d*,*2p*) energy:
-1,982.63437263 a.u.
ZPE: 0.454373 a.u.
Thermal correction to Gibbs Free Energy: 0.385955 a.u.
Dispersion correction: -90.63 kcal/mol

H	1.40229300	0.64290800	1.66249700
C	5.66584700	-1.10610100	-1.97113100
C	5.00985200	-0.36816800	-0.96246900
C	3.91218500	-0.86424100	-0.24824400
C	3.47542300	-2.14367500	-0.58354300
C	4.14092300	-2.89365800	-1.58392700
C	5.23590100	-2.40109900	-2.29172200
C	6.62494000	0.93771500	-1.79649100
C	5.62009700	0.91448100	-0.86001800
H	2.61577900	-2.59185800	-0.09587900
H	3.77466900	-3.89031500	-1.81166500
H	5.72111600	-2.99581100	-3.05933700
H	7.30516800	-0.51398100	-3.19995000
H	7.32762300	1.71619100	-2.05750300
H	-0.61900700	-1.61595500	0.68059500
N	6.66006800	-0.28307500	-2.46007300
C	3.33736100	0.05966100	0.82171100
H	3.90199100	-0.08265100	1.75147600
C	1.84021500	-0.19463700	1.10175600
H	1.27830000	-0.25879500	0.16662800
C	1.51136200	-1.40939000	1.95018200
C	2.40083300	-1.76787600	3.11008900
H	2.62912100	-0.88117800	3.71028000
H	1.91571000	-2.52614800	3.72483700
H	3.35428600	-2.16154700	2.73985400
O	0.49520800	-2.07231500	1.73126500
C	5.08526600	1.88855400	0.14521100
H	5.15862200	2.92656200	-0.19512000
H	5.62018000	1.81933200	1.10006000
C	3.59587500	1.54288000	0.40838200
H	2.98014000	1.81330500	-0.45031000
N	3.10871200	2.44419300	1.52191100
O	2.21387000	3.24567800	1.26402600
O	3.63903200	2.31886200	2.62579900
P	-2.13819700	-0.05007500	0.59850400
O	-1.43326800	0.83812700	1.55127300
O	-1.35424000	-1.31194800	0.05932300
O	-2.60066500	0.58408100	-0.82096200
O	-3.54075800	-0.55818900	1.24292300
C	-3.70351800	1.44243200	-0.88424300
C	-5.00267600	0.92089000	-0.76115900

C	-3.46728500	2.78472400	-1.16782700
C	-6.07180300	1.81706500	-0.93588600
C	-4.54767600	3.64995900	-1.33758300
H	-2.44337800	3.12968300	-1.26327900
C	-5.85218800	3.16311900	-1.22166900
H	-7.08646400	1.44682600	-0.82782600
H	-4.36906100	4.69763100	-1.55799200
H	-6.69793600	3.83192100	-1.34642900
C	-4.49794700	-1.22376200	0.47147400
C	-4.73752000	-2.56633100	0.75146300
C	-5.24732300	-0.51421800	-0.48268800
C	-5.75186800	-3.23909600	0.07094200
H	-4.13502700	-3.06100100	1.50566700
C	-6.26211200	-1.21865400	-1.15414500
C	-6.51519500	-2.56196300	-0.88354200
H	-5.94233400	-4.28587300	0.28578200
H	-6.84537700	-0.70136000	-1.90958000
H	-7.30218200	-3.08062800	-1.42191900

- TS1'

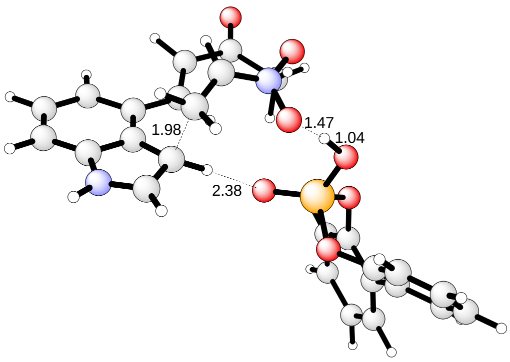

B3LYP/6-311+G(*2d*,*2p*) energy:
-1,982.5719127000 a.u.
ZPE: 0.44906 a.u.
Thermal correction to Gibbs Free Energy: 0.382495 a.u.
Dispersion correction: -91.48 kcal/mol

C	-4.68314100	-1.18803100	-2.05263100
C	-3.77344900	-0.60677100	-1.14298900
C	-3.99770900	0.70735800	-0.67938300
C	-5.14979300	1.36053400	-1.15955800
C	-6.04609600	0.74826200	-2.04227800
C	-5.82878900	-0.54772100	-2.51322900
C	-3.04663200	-2.69499000	-1.73114900
C	-2.75630200	-1.62410300	-0.83732300
H	-5.33805300	2.38551800	-0.85894700
H	-6.91643300	1.30006300	-2.38207700
H	-6.50925700	-1.02301500	-3.21146300
H	-4.64960100	-3.11810800	-2.99525400
H	-2.51302300	-3.62629000	-1.86204100
H	-1.73083200	-1.38515800	-0.56993600
N	-4.19278000	-2.46175200	-2.37444700
C	-3.03937100	1.36112300	0.21953200
H	-2.04744400	0.91438400	0.25210500
C	-3.29102800	2.45890900	0.96422600
H	-4.27486300	2.92171200	0.97441400
C	-2.30977100	3.14952300	1.82799600
C	-0.90515500	2.59949600	1.96761500
H	-0.93329700	1.62593900	2.47019200
H	-0.43450400	2.44429500	0.99260600
H	-0.30946100	3.29612600	2.55929400
O	-2.65745200	4.16291300	2.43333200
C	-3.24679700	-2.45439700	0.89133900
H	-2.56274800	-3.29336100	0.84017500
H	-4.28589800	-2.69683700	0.69282200
C	-3.02773400	-1.54255800	1.94442600
H	-3.77131800	-0.86081200	2.32851200
N	-1.78180800	-1.36859300	2.46299100
O	-1.56930900	-0.53834400	3.37628300
O	-0.81021000	-2.08380900	1.99080100
P	1.43453400	-0.24226200	0.35250900
O	0.17272700	0.02802400	-0.38505900
O	1.33674100	-0.80925600	1.81070700
H	0.44634800	-1.32160400	1.98534000
O	2.41146900	1.02958300	0.61174100
O	2.36905100	-1.23604700	-0.53735600
C	3.16002200	1.57517900	-0.43468800
C	4.28287900	0.88668300	-0.92618100
C	2.81511800	2.84576200	-0.88814000
C	5.05363600	1.53422300	-1.90771300
C	3.59941800	3.46426100	-1.86124700
H	1.94687400	3.33789500	-0.46340200
C	4.72103900	2.80556900	-2.37126600
H	5.91582800	1.01815800	-2.31843500
H	3.33371300	4.45451500	-2.21762100
H	5.33261900	3.27801400	-3.13349700
C	3.70647200	-1.46208600	-0.20391200
C	4.05974500	-2.72981600	0.25103700
C	4.66218700	-0.45446400	-0.42120800
C	5.40043300	-3.02122900	0.50044300
H	3.28218500	-3.47290900	0.39178700
C	6.00569700	-0.77607000	-0.15962600
C	6.37454100	-2.04108700	0.29372800
H	5.68017300	-4.00810500	0.85555500
H	6.76317800	-0.01132800	-0.30046600
H	7.41927000	-2.25860200	0.49237500

- INT1'

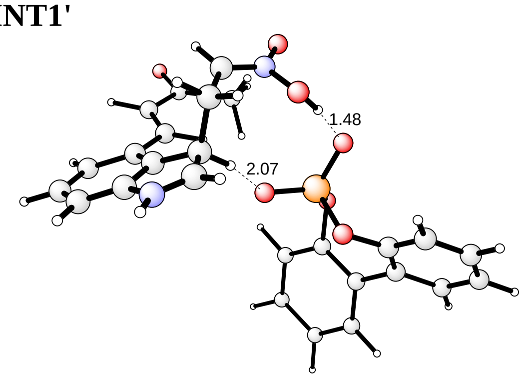

B3LYP/6-311+G(*2d*,*2p*) energy:
-1,982.58463926 a.u.
ZPE: 0.451584 a.u.
Thermal correction to Gibbs Free Energy: 0.385640 a.u.
Dispersion correction: -92.22 kcal/mol

C	-4.05754300	-1.06972200	-2.39753100
C	-3.44286300	-0.63166000	-1.21652200
C	-3.64203500	0.69295600	-0.79387200
C	-4.51556200	1.48210700	-1.57405500
C	-5.14558800	0.99696000	-2.72192000

C	-4.91383100	-0.30400300	-3.17533500
C	-2.79966400	-2.80779300	-1.70742000
C	-2.64400500	-1.78305600	-0.64728000
H	-4.67204500	2.51805500	-1.29358200
H	-5.79968000	1.65146700	-3.28791700
H	-5.36275100	-0.68367200	-4.08607000
H	-3.88743300	-2.95456800	-3.44211900
H	-2.36783900	-3.80069900	-1.73108300
H	-1.58037600	-1.52879600	-0.48585100
N	-3.61243100	-2.39733700	-2.63690000
C	-2.90650200	1.25524700	0.34863100
H	-1.94817500	0.78367200	0.55641300
C	-3.31207300	2.30934600	1.08365300
H	-4.27376600	2.78640100	0.90879300
C	-2.53213900	2.92968700	2.18120400
C	-1.18318400	2.35890900	2.56394100
H	-1.29928100	1.34890100	2.97568500
H	-0.51963000	2.27722000	1.69740000
H	-0.72592800	3.00587500	3.31397600
O	-3.00526000	3.90045400	2.76869400
C	-3.20632800	-2.41131800	0.70879100
H	-2.73188400	-3.38691800	0.82974700
H	-4.28167000	-2.56490800	0.59165500
C	-2.96829000	-1.57550700	1.91548500
H	-3.71937300	-0.91983100	2.33200500
N	-1.82306100	-1.57697100	2.55425500
O	-1.52283600	-0.88845100	3.55989600
O	-0.87218700	-2.45734100	2.07848500
P	1.31001800	-0.48668300	0.46391800
O	0.03426100	-0.24078800	-0.28697400
O	1.29205400	-1.21244100	1.79623500
H	0.02288200	-1.92501200	2.06578700
O	2.14248300	0.90788900	0.76320700
O	2.33558100	-1.23590700	-0.59340600
C	2.74954400	1.62002600	-0.26071000
C	3.93019400	1.13471100	-0.85638900
C	2.22241500	2.86530200	-0.60300400
C	4.56033800	1.95325500	-1.80980500
C	2.86854400	3.65737100	-1.55153600
H	1.31871600	3.20489900	-0.10808200
C	4.04203400	3.19971000	-2.15615800
H	5.46247200	1.59109400	-2.29359400
H	2.45616500	4.62651600	-1.81537000
H	4.54834200	3.80760100	-2.89961800
C	3.69340200	-1.31629400	-0.32240900
C	4.23377200	-2.55767500	0.01127500
C	4.50649000	-0.17850800	-0.48176700
C	5.61076900	-2.68905200	0.18843100
H	3.56628900	-3.40657700	0.11581500
C	5.89082400	-0.33859000	-0.29728500
C	6.44124900	-1.57602600	0.03220000
H	6.03126400	-3.65576300	0.44835900
H	6.53579700	0.52895000	-0.39979800
H	7.51349700	-1.66911900	0.17443200

- TS2'

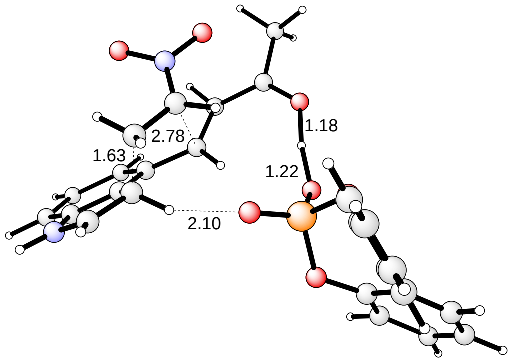

B3LYP/6-311+G(*2d*,*2p*) energy:
-1,982.56344092 a.u.
ZPE: 0.447091 a.u.
Thermal correction to Gibbs Free Energy: 0.380891 a.u.
Dispersion correction: -93.75 kcal/mol

C	4.18888600	-1.84660900	1.88392900
C	3.32140300	-1.09755200	1.08165400
C	3.36907700	0.30287500	1.11989600
C	4.32202500	0.88212200	1.98483800
C	5.17327000	0.10650000	2.77736700
C	5.12445600	-1.29141600	2.74643600
C	2.97407900	-3.34705900	0.72194000
C	2.52870600	-2.03238800	0.22603000
H	4.37353400	1.96344100	2.06017700
H	5.87878800	0.59862000	3.43835800
H	5.77663800	-1.89980600	3.36274100
H	4.40922000	-3.99044300	2.05158600
H	2.64743700	-4.32538700	0.39245600
H	1.43862200	-1.90110900	0.27843600
N	3.92005300	-3.21337000	1.61702000
C	2.44796300	1.09017800	0.30369600
H	1.46620500	0.66033400	0.15188700
C	2.75147400	2.30801500	-0.23190300
H	3.75949000	2.70042500	-0.14791600
C	1.86988400	3.02549900	-1.10874100
C	2.40349600	4.20042400	-1.87742200
H	3.46060000	4.07790100	-2.11225600
H	1.82791100	4.33336700	-2.79482600
H	2.28130500	5.10479900	-1.26725500
O	0.62687200	2.78773300	-1.25006200
C	2.85907300	-1.90202300	-1.36794000
H	2.26800300	-2.69468800	-1.83629100
H	3.92172500	-2.09615700	-1.51587400
C	2.51786000	-0.58243100	-1.91812900
H	-0.00737000	2.10287000	-0.52776600
N	3.47733700	0.27923600	-2.33006100
O	3.10710600	1.37085700	-2.88488900
O	4.71211200	0.04369100	-2.13685700
H	1.50516000	-0.29531200	-2.15520500
P	-1.35837500	0.13693200	0.04435300
O	-0.41162100	-0.99880300	-0.15597100
O	-0.81163900	1.56194700	0.21412100
O	-2.47789900	0.27466700	-1.14733400
O	-2.28972300	-0.19439700	1.34770500
C	-3.45770900	-0.70338400	-1.29519800
C	-4.53226800	-0.75351300	-0.38829100
C	-3.38769700	-1.54966500	-2.39977700

C	-5.54332100	-1.69772500	-0.63823500
C	-4.40587200	-2.47592100	-2.62400200
H	-2.54230800	-1.46183100	-3.07388500
C	-5.48571900	-2.54920100	-1.74021200
H	-6.37552200	-1.76936000	0.05538900
H	-4.35381900	-3.13642300	-3.48399700
H	-6.27875700	-3.27198900	-1.90482500
C	-3.49760600	0.46078800	1.57122400
C	-3.58188800	1.31998100	2.66489600
C	-4.61632200	0.17082200	0.76831800
C	-4.80281200	1.91227000	2.98576200
H	-2.69091300	1.50187300	3.25638100
C	-5.83385000	0.78260700	1.11498700
C	-5.93175200	1.64084000	2.20857400
H	-4.86977400	2.58184700	3.83766000
H	-6.70827500	0.58991800	0.50101100
H	-6.88467600	2.10231500	2.44812800

- TS3'

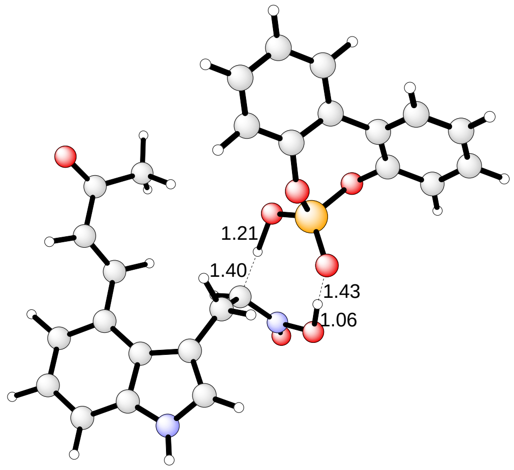

B3LYP/6-311+G(*2d*,*2p*) energy:
-1,982.5779839900 a.u.
ZPE: 0.445815 a.u.
Thermal correction to Gibbs Free Energy: 0.378861 a.u.
Dispersion correction: -90.23 kcal/mol

H	-0.26896800	-2.82369500	0.14599700
C	5.55523200	-1.32728100	-1.06553900
C	4.45412700	-0.55667900	-0.58283300
C	4.70707900	0.77139500	-0.13021200
C	6.02912500	1.24032700	-0.18849900
C	7.08613200	0.45356400	-0.66904300
C	6.86516300	-0.84541500	-1.11558100
C	3.71026100	-2.58286400	-1.26463100
C	3.27796700	-1.38610400	-0.73308500
H	6.24718000	2.23493700	0.18655400
H	8.09167700	0.86232800	-0.67984800
H	7.67689600	-1.46406000	-1.48575500
H	5.61361900	-3.29796300	-1.86468200
H	3.13367400	-3.45853200	-1.52801500
H	0.24475700	-0.68019000	1.19817400
N	5.06702200	-2.55377000	-1.45912100
C	3.64301300	1.62053800	0.40960000
H	2.79420500	1.10506600	0.84677100
C	3.62608400	2.97179400	0.42016300
H	4.42281500	3.54756000	-0.04423100
C	2.55933000	3.79779200	1.01613600
C	1.39467400	3.13498900	1.73297700
H	0.85390400	2.44290300	1.07903600
H	1.74724600	2.55831100	2.59487200
H	0.70893800	3.90988000	2.07792300
O	2.62656300	5.02422200	0.93570800
C	1.83944200	-1.08707500	-0.41061000
H	1.18279700	-1.67400800	-1.05522900
H	1.60354800	-0.04124600	-0.62616300
C	1.46954200	-1.34432500	1.06461800
H	2.14718300	-0.92541500	1.80573700
N	1.20423500	-2.65326800	1.44153600
O	1.57099000	-3.15866700	2.48612700
O	0.44643400	-3.42453700	0.64517600
P	-1.80153400	-0.76197000	0.18477600
O	-0.80866800	-0.08859300	1.15950300
O	-1.32680100	-2.05658100	-0.43438500
O	-2.20037700	0.22161000	-1.03465100
O	-3.17130300	-0.88224800	1.03631600
C	-2.95997800	1.37878400	-0.81093200
C	-4.32717100	1.27021300	-0.50681400
C	-2.33347900	2.60762300	-0.99496200
C	-5.05262500	2.46930500	-0.39226700
C	-3.07934700	3.77997500	-0.87602300
H	-1.27730600	2.62899600	-1.24070900
C	-4.44174300	3.70830100	-0.57478900
H	-6.10694200	2.41955200	-0.13923600
H	-2.59682500	4.74178700	-1.01744900
H	-5.02718500	4.61671000	-0.47451900
C	-4.39844400	-1.09038600	0.38964500
C	-5.02634600	-2.31837900	0.57431300
C	-4.99300200	-0.04292700	-0.33341500
C	-6.29197600	-2.52752700	0.02732400
H	-4.52287900	-3.08602700	1.15185400
C	-6.26849200	-0.28401100	-0.87389800
C	-6.91279500	-1.50680800	-0.69705400
H	-6.78762700	-3.48293500	0.16683400
H	-6.74663900	0.49911400	-1.45374000
H	-7.89520200	-1.66482400	-1.13059800

- INT4'

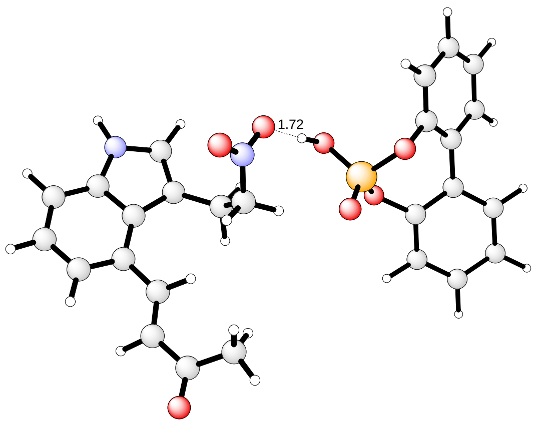

B3LYP/6-311+G(*2d*,*2p*) energy:
-1,982.6238272600 a.u.
ZPE: 0.452367 a.u.
Thermal correction to Gibbs Free Energy: 0.380762 a.u.
Dispersion correction: -87.41 kcal/mol

H	-0.86757300	-1.73446400	0.34791600
C	5.27608700	-2.12243500	-1.17136600
C	4.59889300	-0.96106400	-0.68691400
C	5.38199900	0.18547400	-0.35817500
C	6.77461800	0.09108300	-0.51443800
C	7.40391200	-1.06982300	-0.98458900
C	6.66201200	-2.19648800	-1.32437400
C	3.08281000	-2.57102800	-1.17309700
C	3.18619100	-1.27915200	-0.70214000
H	7.39135700	0.93783500	-0.23232100
H	8.48536800	-1.08961600	-1.07585300
H	7.13831000	-3.10109400	-1.68984000
H	4.51015600	-3.99650900	-1.82374900
H	2.19485400	-3.16522200	-1.33815500
H	0.76726600	0.11033600	1.42124200
N	4.32517200	-3.07890700	-1.44863200
C	4.77408500	1.42117400	0.13788200
H	3.79051900	1.32567600	0.58579900
C	5.31967000	2.65739900	0.09003100
H	6.28234600	2.83044200	-0.38404100
C	4.69894300	3.87766800	0.63645200
C	3.34706200	3.79842300	1.32583500
H	2.57916700	3.41397700	0.64607100
H	3.38470700	3.12798500	2.19069100
H	3.06230700	4.79748300	1.65797100
O	5.28359100	4.95565700	0.53016100
C	1.99146700	-0.45906200	-0.30109400
H	1.10458000	-0.82095000	-0.82903900
H	2.10491100	0.59002000	-0.59162600
C	1.67989500	-0.45534800	1.21085800
H	2.51142500	-0.10204600	1.81757600
N	1.41914000	-1.85410300	1.68836400
O	2.21108500	-2.36906100	2.45819500
O	0.41739100	-2.44828900	1.24974100
P	-2.27718100	-0.08787100	0.48453500
O	-1.40643700	0.70890500	1.38110900
O	-1.62499600	-1.37489500	-0.17950300
O	-2.83842600	0.61818300	-0.85679100
O	-3.62265400	-0.54073300	1.26285900
C	-3.89166300	1.54038300	-0.78185200
C	-5.19855700	1.08917300	-0.53247900
C	-3.60452300	2.87379000	-1.05769300
C	-6.22371000	2.05083200	-0.56907900
C	-4.64258600	3.80441300	-1.08920700
H	-2.57761500	3.16152300	-1.25530400
C	-5.95418100	3.38990800	-0.84443000
H	-7.24182300	1.73711400	-0.36129200
H	-4.42549100	4.84614700	-1.30271000
H	-6.76630500	4.10978200	-0.86081600
C	-4.69992000	-1.12231500	0.58165800
C	-4.98903900	-2.45667600	0.85126100
C	-5.49983500	-0.33758000	-0.26571200
C	-6.10987200	-3.04571100	0.26701900
H	-4.34130500	-3.01018600	1.52242300
C	-6.62182400	-0.95931700	-0.84179100
C	-6.92691500	-2.29360100	-0.58080700
H	-6.34062500	-4.08601000	0.47326700
H	-7.24842900	-0.38469500	-1.51653500
H	-7.79711200	-2.74722900	-1.04454500

- 3

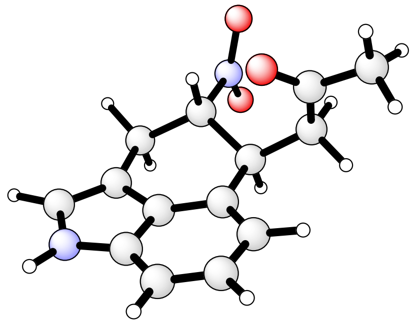

B3LYP/6-311+G(*2d*,*2p*) energy:
-877.294814288 a.u.
ZPE: 0.262879 a.u.
Thermal correction to Gibbs Free Energy: 0.217794 a.u.
Dispersion correction: -46.45 kcal/mol

H	-1.78772100	1.76767300	-1.53820500
C	2.97233600	0.24178500	0.12190000
C	1.64941100	-0.18866100	-0.11645800
C	0.64585600	0.66259300	-0.59428700
C	1.01400300	1.98149400	-0.84709700
C	2.34351900	2.41447300	-0.62235100
C	3.34031700	1.56965000	-0.13579500
C	2.78667200	-1.94674400	0.67583000
C	1.54440400	-1.56724500	0.22972300
H	0.29333100	2.70204000	-1.22198000
H	2.59283000	3.45040500	-0.83369600
H	4.34973500	1.93157000	0.03374900
H	4.62029500	-0.87971600	0.88069900
H	3.14502500	-2.89980400	1.03831700
N	3.65050000	-0.85901700	0.60589400
C	-0.72147500	0.02430500	-0.81869000
H	-0.73443100	-0.39558600	-1.83422700
C	-1.89672900	1.01585600	-0.74812200
H	-2.84054500	0.50947100	-0.99192000
C	-2.11258100	1.74126500	0.57600600
C	-3.10651100	2.88386900	0.54607900
H	-4.03871400	2.58043400	0.05807500
H	-3.31019100	3.22856800	1.56081100
H	-2.69357800	3.71259900	-0.04129200
O	-1.53151400	1.42598400	1.60213500
C	0.22823100	-2.26069700	0.04298300
H	0.05546800	-3.04099100	0.79175700
H	0.15981600	-2.73523300	-0.94324000
C	-0.89077000	-1.19522500	0.14574400
H	-0.99967900	-0.83762600	1.16706900
N	-2.21014200	-1.86141900	-0.17042400
O	-2.32807400	-2.40775800	-1.26756300
O	-3.09969200	-1.80710900	0.67705200

- 3’

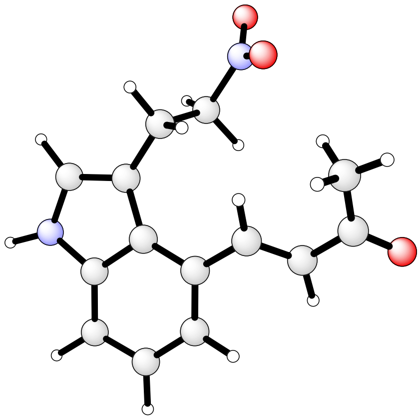

B3LYP/6-311+G(*2d*,*2p*) energy:
-877.2864919800 a.u.
ZPE: 0.261171 a.u.
Thermal correction to Gibbs Free Energy: 0.213902 a.u.
Dispersion correction: -43.36 kcal/mol

C	3.10729000	-0.21643900	0.00482600
C	1.69529900	-0.10674300	0.19102800
C	1.09672200	1.18097300	0.06253000
C	1.93497400	2.26393600	-0.24532900
C	3.31848400	2.11729600	-0.42326600
C	3.92757700	0.87297500	-0.29805300
C	2.31876700	-2.26756300	0.43797600
C	1.21374200	-1.44537800	0.46214900
H	1.50332300	3.25726700	-0.31038200
H	3.92198500	2.99155200	-0.64651200
H	4.99877300	0.75039000	-0.42554300
H	4.38328900	-1.91571300	0.10260700
H	2.37380700	-3.33563900	0.59594100
N	3.45010900	-1.53973000	0.16988800
C	-0.33748300	1.38986100	0.27705700
H	-0.83484400	0.66955000	0.91970800
C	-1.08228800	2.39231800	-0.24010900
H	-0.64943700	3.11839400	-0.92389600
C	-2.51639500	2.60983000	0.03249400
C	-3.24998600	1.69827900	1.00020600
H	-3.18421400	0.64844900	0.69634200
H	-2.81740700	1.77377400	2.00389600
H	-4.29803400	1.99808200	1.03982700
O	-3.10283200	3.53825000	-0.52333200
C	-0.18646300	-1.95205300	0.67871600
H	-0.13768100	-2.97771500	1.05891700
H	-0.72931400	-1.36883300	1.42698900
C	-0.99006500	-1.95548800	-0.63218500
H	-0.55918100	-2.61649400	-1.38175800
N	-2.39708700	-2.44132300	-0.40791200
O	-2.81824900	-3.34044200	-1.12946100
O	-3.04747100	-1.90629600	0.49099400
H	-1.09486500	-0.94860500	-1.04380800

- TS3$_{cis}$

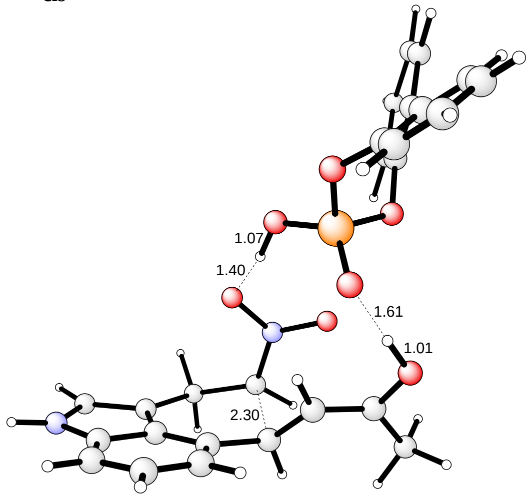

B3LYP/6-311+G(*2d*,*2p*) energy:
-1,982.5908302200 a.u.
ZPE: 0.45020 a.u.
Thermal correction to Gibbs Free Energy: 0.387819 a.u.
Dispersion correction: -94.64 kcal/mol

P	-1.51299400	-0.54859200	-0.35396300
O	-0.86856000	-1.63066300	0.45891700
O	-0.64860800	0.28643900	-1.33547200
H	0.27320800	0.73469300	-1.01994900
O	-2.65419500	-1.07928900	-1.37728900
O	-2.34042700	0.41275200	0.65583000
C	-3.92037900	-1.45184300	-0.91775700
C	-4.82790500	-0.47260700	-0.47411100
C	-4.27412800	-2.79459200	-1.02074800
C	-6.12147800	-0.90614400	-0.13401700
C	-5.56533800	-3.19435800	-0.67793100
H	-3.53740300	-3.50454600	-1.38098400
C	-6.49059400	-2.24610300	-0.23481700
H	-6.83738700	-0.17547100	0.22938800
H	-5.84418600	-4.24039100	-0.75693900
H	-7.49597300	-2.54976800	0.03942200
C	-3.22155800	1.37004000	0.14540400
C	-2.86534100	2.71054800	0.25799300
C	-4.45832600	0.96060400	-0.37997700
C	-3.76553900	3.69189900	-0.15599300
H	-1.89458900	2.95850400	0.67391000
C	-5.34457200	1.97200600	-0.79011600
C	-5.00702600	3.31982700	-0.67924300
H	-3.49676200	4.74021400	-0.07207000
H	-6.30191000	1.68852500	-1.21628200
H	-5.70957800	4.07876800	-1.00896100
C	5.56380700	-0.59888500	-1.59581200
C	4.76632000	-0.04397600	-0.55458600
C	4.11997100	-0.90069400	0.36267500
C	4.28210700	-2.28031800	0.18671800
C	5.09611100	-2.80620300	-0.83555900
C	5.75018000	-1.97718400	-1.74140100
C	5.50782400	1.63388400	-1.85472100
C	4.73790800	1.37420300	-0.74519600
H	3.79567000	-2.96071900	0.87852100
H	5.21149300	-3.88285300	-0.91556400
H	6.37000600	-2.38401300	-2.53462700

H	6.58420700	0.37449500	-3.18878300
H	5.73361500	2.57570400	-2.33494300
H	-0.31756200	-1.48325400	1.96515400
N	6.01698000	0.45340700	-2.35900500
C	3.30720400	-0.39945600	1.49932400
H	3.84761600	0.04799800	2.32815500
C	2.05201900	-0.98057500	1.72262900
H	1.60165600	-1.52601400	0.89917200
C	1.24930100	-0.78750100	2.84417400
C	1.66401400	-0.10231200	4.10633900
H	2.74148100	0.04272600	4.17348600
H	1.16898000	0.87351000	4.15560800
H	1.32434700	-0.68855000	4.96479700
O	0.01626300	-1.24603600	2.88557400
C	4.00399600	2.36851500	0.11232800
H	3.59194200	3.16629000	-0.51981300
H	4.70210100	2.85718800	0.80301500
C	2.90009700	1.80457800	0.97180900
H	2.83720700	2.12671100	2.00244600
N	1.66325500	1.55792400	0.46780300
O	0.69246700	1.38423900	1.24880200
O	1.52218900	1.33502000	-0.80145800

- INT3$_{cis}$

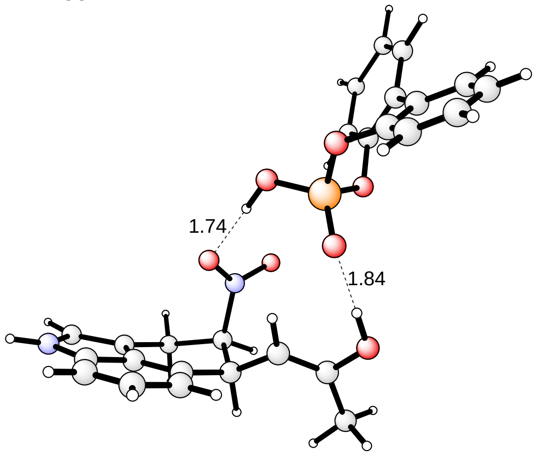

B3LYP/6-311+G(*2d*,*2p*) energy:
-1,982.6179722700 a.u.
ZPE: 0.454764 a.u.
Thermal correction to Gibbs Free Energy: 0.389985 a.u.
Dispersion correction: -92.03 kcal/mol

P	-1.66686000	-0.41561700	-0.51754100
O	-0.96036200	-1.60601700	0.02329000
O	-0.83147200	0.61100700	-1.38374500
H	0.08448500	0.81146100	-1.05744400
O	-2.85583400	-0.69180600	-1.57299900
O	-2.39444400	0.37786200	0.68823000
C	-4.10223200	-1.15461600	-1.12639600
C	-4.96627200	-0.28646600	-0.43730500
C	-4.47181500	-2.44952400	-1.47704600
C	-6.23913500	-0.78386100	-0.10666400
C	-5.74194900	-2.91382800	-1.13691300
H	-3.76665500	-3.06953900	-2.01983500
C	-6.62593100	-2.07759300	-0.45061600
H	-6.92269500	-0.14449500	0.44292100
H	-6.03627600	-3.92312000	-1.40639300
H	-7.61373100	-2.43444000	-0.17676700
C	-3.30498200	1.40965500	0.42242100
C	-2.93203000	2.70565000	0.76424200
C	-4.57642400	1.10090900	-0.08824800
C	-3.85028500	3.74315600	0.60544800
H	-1.93513600	2.87882700	1.15477800
C	-5.47990400	2.16774200	-0.23813100
C	-5.12642300	3.47128800	0.10523600
H	-3.56811300	4.75734600	0.86978900
H	-6.46487100	1.96541700	-0.64688200
H	-5.84375100	4.27520100	-0.02616900
C	5.65024700	0.07710800	-1.70358000
C	4.85420200	0.22748200	-0.54738100
C	4.16134600	-0.83734200	0.03646500
C	4.30310900	-2.08528500	-0.56424100
C	5.11925000	-2.24543600	-1.70904800
C	5.79868900	-1.18117200	-2.30275600
C	5.63858800	2.25508400	-1.08277300
C	4.85426600	1.59907600	-0.16498800
H	3.78159500	-2.94622300	-0.15656400
H	5.21081500	-3.23476400	-2.14842300
H	6.40672500	-1.32810400	-3.19011600
H	6.71718300	1.57308600	-2.78892200
H	5.90518600	3.29937800	-1.16450200
H	-0.14357800	-2.30988200	1.51842600
N	6.12516500	1.33845800	-2.00733000
C	3.33408100	-0.54339300	1.28253700
H	3.95935500	-0.74760100	2.16145700
C	2.07066900	-1.36394800	1.34518800
H	1.50719900	-1.40591600	0.41725100
C	1.52164600	-1.96368400	2.41875700
C	2.10906700	-2.08938500	3.79397600
H	3.12812500	-1.70527500	3.85164600
H	1.49068000	-1.55181200	4.52155400
H	2.11566700	-3.14292900	4.09480000
O	0.29954700	-2.56534900	2.35480500
C	4.11411600	2.01079100	1.06860300
H	3.68190000	3.01504800	1.00031400
H	4.78416900	2.02927300	1.93810800
C	3.00180900	0.99233800	1.44084300
H	2.68433200	1.16691300	2.46739500
N	1.74229300	1.29670300	0.66399600
O	0.76800800	1.71478600	1.27598800
O	1.73529100	1.06599400	-0.55753700

- TS4$_{cis}$

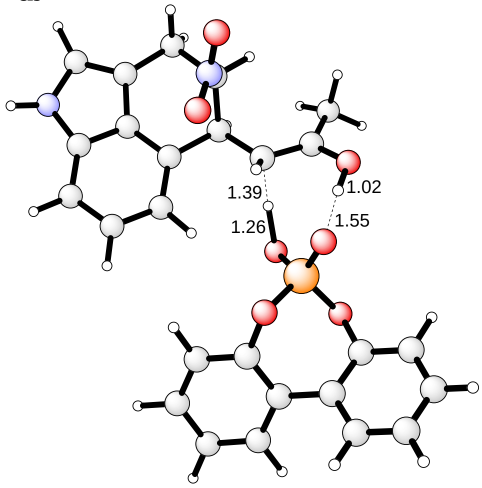

B3LYP/6-311+G(*2d*,*2p*) energy:

-1,982.5951714900 a.u.
ZPE: 0.449916 a.u.
Thermal correction to Gibbs Free Energy: 0.386415 a.u.
Dispersion correction: -94.66 kcal/mol

P	-1.82864900	-0.75508000	-0.00342600
O	-1.47097000	-1.87503700	0.94025900
O	-0.76639600	-0.38150900	-1.05731500
H	0.36747100	-0.87785100	-0.82164600
O	-3.16633400	-1.01110600	-0.89046600
O	-2.24187100	0.51837900	0.91712100
C	-4.42912700	-1.01512500	-0.28981300
C	-5.00766000	0.19531300	0.12839200
C	-5.11089300	-2.22682300	-0.21610800
C	-6.31941700	0.13792000	0.63164100
C	-6.41157300	-2.25282100	0.28596000
H	-4.61879700	-3.12865400	-0.56406500
C	-7.01587000	-1.06649100	0.70973800
H	-6.78577100	1.05409500	0.98019600
H	-6.94721000	-3.19498000	0.34572000
H	-8.02563000	-1.07954600	1.10770400
C	-2.93222800	1.61289300	0.38958100
C	-2.26450900	2.83370500	0.33678100
C	-4.28556200	1.48641000	0.03047000
C	-2.94550300	3.97220500	-0.09252000
H	-1.22685200	2.87743700	0.64943500
C	-4.94532100	2.65076700	-0.40119700
C	-4.28910700	3.87835700	-0.46385800
H	-2.42788100	4.92527800	-0.13571300
H	-5.98524900	2.57921000	-0.70407600
H	-4.82448200	4.75834800	-0.80610600
C	4.44622300	2.56673500	-0.06458300
C	4.19452600	1.19499000	-0.28215500
C	2.90082700	0.67318200	-0.42610700
C	1.84992500	1.58260700	-0.36296400
C	2.10248800	2.96214800	-0.15866300
C	3.38561500	3.48143500	-0.00261900
C	6.41263800	1.44421500	-0.07808400
C	5.43946700	0.49894300	-0.29125200
H	0.82292700	1.25455100	-0.47312300
H	1.25622600	3.64255900	-0.12218200
H	3.54816100	4.54269500	0.15837000
H	6.31635800	3.55103100	0.22420600
H	7.48671800	1.34678400	-0.00753500
H	-0.43135600	-2.87269100	0.35485900
N	5.81619900	2.69250900	0.05311900
C	2.82325800	-0.83049500	-0.69749400
H	2.95380000	-0.95044400	-1.78231300
C	1.50021400	-1.49431900	-0.30789000
H	1.20790700	-1.31388300	0.72782300
C	1.15928600	-2.78190900	-0.76692000
C	1.81209900	-3.50402600	-1.90502500
H	2.41399100	-2.84763400	-2.53247400
H	2.46424500	-4.28655700	-1.49835700
H	1.04886400	-3.99843100	-2.51001800
O	0.14372900	-3.43974500	-0.27217400
C	5.43877500	-0.98241900	-0.52130600
H	6.22558600	-1.50963200	0.02475800
H	5.57757400	-1.22451700	-1.58313600
C	4.06400600	-1.57642500	-0.11654100
H	4.04080800	-2.62401200	-0.41929000
N	4.03187600	-1.67411500	1.40918800
O	4.80404200	-2.48932700	1.91044100
O	3.27284200	-0.95559800	2.05181000

- INT4$_{cis}$

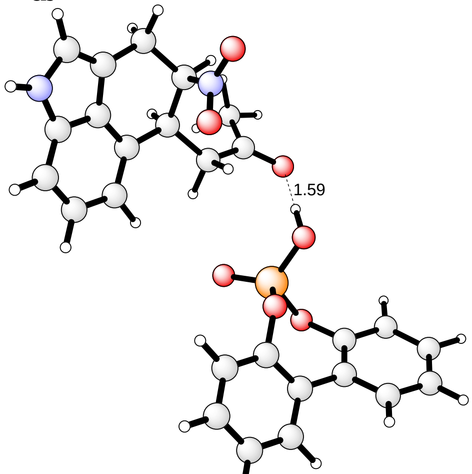

B3LYP/6-311+G(*2d*,*2p*) energy:
-1,982.6301404900 a.u.
ZPE: 0.454262 a.u.
Thermal correction to Gibbs Free Energy: 0.38746 a.u.
Dispersion correction: -91.36 kcal/mol

P	-2.05307200	-0.37945900	-0.47561800
O	-1.56110500	-1.56052900	0.44874600
O	-1.13412700	0.09685600	-1.53739800
H	1.20021500	-0.62520800	-1.38433500
O	-3.47823200	-0.80039700	-1.13190100
O	-2.48010900	0.67993000	0.67503500
C	-4.60262900	-1.05457100	-0.34080600
C	-5.26204200	0.00591900	0.30421300
C	-5.08559600	-2.35974600	-0.30186900
C	-6.44383500	-0.30316600	1.00060400
C	-6.26169800	-2.63599400	0.39454400
H	-4.54135900	-3.13700000	-0.82745300
C	-6.94139700	-1.60389200	1.04640600
H	-6.96429500	0.49219200	1.52485200
H	-6.64217700	-3.65200900	0.42754400
H	-7.85369200	-1.81228900	1.59636700
C	-3.39243900	1.70126300	0.38828300
C	-2.91507900	3.00853200	0.35546400
C	-4.75690200	1.39823000	0.24183700
C	-3.81132300	4.06090900	0.17157100
H	-1.85275400	3.18366000	0.48678600
C	-5.63626800	2.47949700	0.05594400
C	-5.17461200	3.79381400	0.02208600
H	-3.44466600	5.08214300	0.14459500
H	-6.69379900	2.27537500	-0.07921000
H	-5.87732100	4.60739200	-0.12779700
C	5.21754800	2.29940300	-0.19476800
C	4.77965200	0.95917500	-0.23644800
C	3.49938600	0.59050500	-0.66950100
C	2.65365200	1.61863600	-1.07290300
C	3.09553400	2.96518900	-1.04415700
C	4.36732500	3.33420100	-0.61093500
C	6.86107600	0.95336300	0.59054800
C	5.82080000	0.11980000	0.25936000

H	1.63980500	1.41778700	-1.40514200
H	2.40762900	3.74091700	-1.36811200
H	4.67513700	4.37508600	-0.59385400
H	7.09080500	3.06850900	0.47536900
H	7.83510900	0.73501300	1.00491900
H	-0.85551400	-2.15076900	0.02813500
N	6.50244200	2.26669800	0.30973900
C	3.22548500	-0.91368500	-0.68667600
H	3.64097900	-1.28932200	-1.63309100
C	1.72830100	-1.26676200	-0.66570400
H	1.28369100	-1.03688300	0.30466300
C	1.29674700	-2.66088100	-1.07205600
C	2.13021900	-3.48639600	-2.01538700
H	2.35773200	-2.90792200	-2.91770900
H	3.08908300	-3.75779400	-1.56158900
H	1.58938000	-4.39411800	-2.28337800
O	0.20536000	-3.09431900	-0.69247600
C	5.59342900	-1.36223500	0.31637600
H	6.08436400	-1.84547700	1.16496200
H	5.96473700	-1.86160500	-0.58789300
C	4.07062400	-1.65965000	0.38302900
H	3.92820300	-2.73840900	0.29728900
N	3.60857500	-1.38388400	1.81589600
O	4.05645600	-2.13861200	2.67645000
O	2.84449600	-0.45115400	2.04337000

-*cis*-4

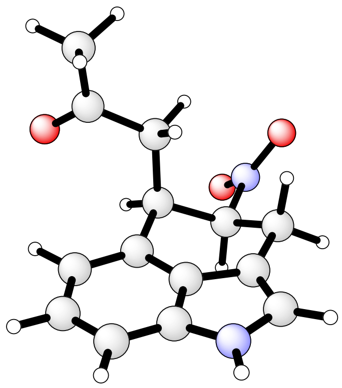

B3LYP/6-311+G(*2d*,*2p*) energy:
-877.2949781220 a.u.
ZPE: 0.262863 a.u.
Thermal correction to Gibbs Free Energy: 0.217635 a.u.
Dispersion correction: -46.08 kcal/mol

C	-2.93915700	0.14650200	0.06727400
C	-1.57429700	-0.20810700	0.01098800
C	-0.60148000	0.61744300	-0.56518700
C	-1.03134000	1.82911700	-1.09778000
C	-2.39911700	2.19093300	-1.03538500
C	-3.37112200	1.37202800	-0.45970300
C	-2.66026900	-1.90940100	0.97799300
C	-1.40785600	-1.50388200	0.58574600
H	-0.31721800	2.50641200	-1.55497200
H	-2.70326300	3.14475900	-1.45714200
H	-4.41340200	1.67479800	-0.43091800
H	-4.57231200	-0.97497400	0.85846800
H	-2.98936000	-2.82515000	1.44846800
N	-3.58301900	-0.91363800	0.67409800
C	0.83005400	0.09977900	-0.50475900
H	1.37835700	0.41631800	-1.39670800
C	-0.03496100	-2.11707800	0.61527100
H	-0.06023400	-3.20160700	0.46970700
H	0.47377200	-1.93805900	1.56857000
C	0.77055300	-1.46412900	-0.52717400
H	0.35616800	-1.76112600	-1.49222200
N	2.18729900	-1.99465300	-0.57651400
O	2.70754800	-2.39899600	0.46318500
O	2.75404600	-1.95863700	-1.66650400
C	1.57565600	0.65985900	0.72507300
H	2.46374800	0.05734100	0.96366500
H	0.94932100	0.62345100	1.62325700
C	2.08393500	2.08455800	0.52891700
O	2.17421900	2.59476900	-0.57625700
C	2.49123900	2.82349200	1.78499700
H	3.02955900	3.73691700	1.52797500
H	1.59089700	3.08415000	2.35460400
H	3.10647800	2.19102500	2.43314300

- Methyl (*E*)-3-(1*H*-indol-4-yl)acrylate (1b)

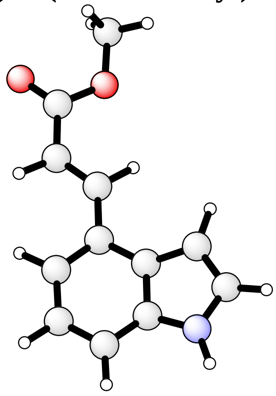

B3LYP/6-311+G(*2d*,*2p*) energy:
-669.3175452740 a.u.
ZPE: 0.206267 a.u.
Thermal correction to Gibbs Free Energy: 0.164432 a.u.
Dispersion correction: -31.25 kcal/mol

C	-3.00219000	0.03531300	-0.00001400
C	-1.63352800	0.43962000	-0.00003600
C	-0.61559000	-0.55362200	0.00116700
C	-1.02247800	-1.89763500	0.00255600
C	-2.37582900	-2.26501100	0.00257700
C	-3.38865800	-1.30644300	0.00125100
C	-2.94152200	2.28130400	-0.00243600
C	-1.62929400	1.87480300	-0.00161500
H	-0.27384900	-2.68330400	0.00416100
H	-2.63902100	-3.31830800	0.00381800
H	-4.43600300	-1.59308400	0.00133300
H	-4.77727600	1.21071700	-0.00174800
H	-3.35775300	3.27846900	-0.00365400
H	-0.77237900	2.53265400	-0.00224900
N	-3.76945900	1.18056400	-0.00144700
C	0.78483800	-0.14300800	0.00118100
H	0.96109100	0.92927300	0.00481500
C	1.87382900	-0.94178400	-0.00301600
H	1.80180900	-2.02432800	-0.00754400
C	3.25930100	-0.45067200	-0.00227500
O	4.23693800	-1.18548400	-0.00654800
O	3.35961900	0.90003800	0.00349100

C	4.69721000	1.42448400	0.00431200
H	4.58862200	2.50861700	0.00946800
H	5.24205700	1.09328100	0.89181400
H	5.23992000	1.10154500	-0.88753700

- INT2$_{ester}$

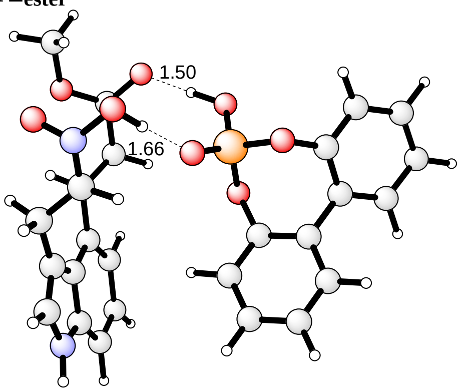

B3LYP/6-311+G(*2d*,*2p*) energy:
-2,057.8681330600 a.u.
ZPE: 0.456375 a.u.
Thermal correction to Gibbs Free Energy: 0.389158 a.u.
Dispersion correction: -95.49 kcal/mol

H	-0.88442600	-2.09589400	-1.71962200
C	-3.17102200	3.19840700	0.46055900
C	-3.18735300	1.77758500	0.32473100
C	-2.61566600	0.99443700	1.36705600
C	-2.05677200	1.66181700	2.46670100
C	-2.06704700	3.06202900	2.57109000
C	-2.62594000	3.85110200	1.57002400
C	-4.10669500	2.70581600	-1.51542000
C	-3.78531600	1.48836800	-0.95917700
H	-1.64076600	1.07420700	3.27919100
H	-1.64086100	3.53320600	3.45114700
H	-2.63922700	4.93413600	1.64571400
H	-3.86588600	4.71186500	-0.86293900
H	-4.56883800	2.91655300	-2.46973800
H	0.68925400	-2.74191700	1.04227800
N	-3.75052100	3.72906400	-0.66942400
C	-2.61322900	-0.46608900	1.29775100
H	-3.46587200	-0.94312500	0.82365600
C	-1.61734700	-1.26883900	1.73354700
H	-0.69100000	-0.86680700	2.12999800
C	-1.63897300	-2.71456300	1.50646100
O	-0.61161400	-3.40455800	1.39438100
C	-4.02840600	0.15946800	-1.62771100
H	-4.52008400	0.34119900	-2.59419500
H	-4.73302800	-0.46263100	-1.06236700
C	-2.77325300	-0.63796200	-1.83831000
H	-1.80093600	-0.18339700	-1.96632300
N	-2.83388100	-1.94373900	-1.83967800
O	-1.64898400	-2.68564500	-1.96750700
O	-3.85868800	-2.65718300	-1.73592600
P	1.54441500	-1.17354900	-0.29849400
O	0.42993800	-1.17448300	-1.29033900
O	1.58572400	-2.31376100	0.77190300
O	1.64200500	0.16575400	0.60804100
O	2.95762200	-1.21056700	-1.07238600
C	2.04144100	1.37506300	0.02200000

C	3.39161600	1.56384800	-0.31706900
C	1.08896100	2.38006600	-0.11548800
C	3.75270900	2.82695600	-0.81833700
C	1.47865500	3.62360200	-0.61236000
H	0.06479700	2.18159800	0.18138900
C	2.81240700	3.84492400	-0.96513100
H	4.78442500	2.99925600	-1.10820500
H	0.74209500	4.41317600	-0.72222400
H	3.12014900	4.80831300	-1.35922500
C	4.16066900	-0.84468200	-0.45298800
C	5.11872200	-1.83946300	-0.28229900
C	4.40590500	0.49924300	-0.12354400
C	6.37059900	-1.50400200	0.23192200
H	4.87533300	-2.85762000	-0.56590100
C	5.67687500	0.80569400	0.39495000
C	6.64875000	-0.17724000	0.56958500
H	7.12161100	-2.27575800	0.36724700
H	5.89054500	1.83136100	0.67850900
H	7.61860600	0.09131300	0.97616500
O	-2.85284800	-3.24064900	1.39422400
C	-2.94609100	-4.59789100	0.90020100
H	-3.98545300	-4.88528800	1.04897300
H	-2.69803800	-4.60091300	-0.16228700
H	-2.27823700	-5.25430800	1.45830300

- TS3$_{ester}$

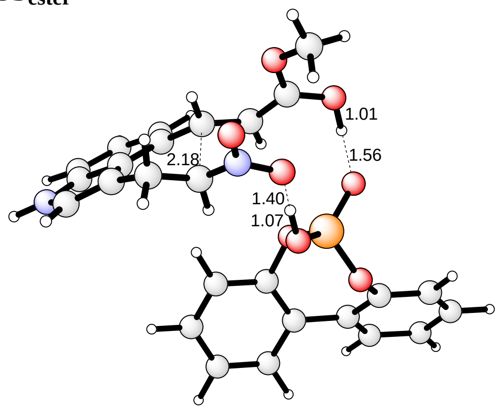

B3LYP/6-311+G(*2d*,*2p*) energy:
-2,057.8357778600 a.u.
ZPE: 0.455468 a.u.
Thermal correction to Gibbs Free Energy: 0.391497 a.u.
Dispersion correction: -97.66 kcal/mol

H	-0.16527300	-1.62553000	-1.47182500
C	-3.68195800	3.00156600	0.64122000
C	-3.47705900	1.64380000	0.28718800
C	-2.79469800	0.76500400	1.15503200
C	-2.30696200	1.29846800	2.35283500
C	-2.52559900	2.64932400	2.69538400
C	-3.21686700	3.51992400	1.85555700
C	-4.51860200	2.65845000	-1.42342800
C	-4.00365900	1.44594100	-1.02774800
H	-1.78911200	0.65178500	3.05391300
H	-2.14984500	3.01603500	3.64581400
H	-3.37962800	4.55731500	2.13156000
H	-4.61367600	4.55969100	-0.47396000
H	-4.99639700	2.94141800	-2.35082600
H	0.33084200	-3.04899000	1.18828100

N	-4.34018200	3.59084600	-0.41750000
C	-2.67841800	-0.67529100	0.81799000
H	-3.61782900	-1.21042500	0.69613100
C	-1.57817100	-1.42987000	1.26118300
H	-0.65017700	-0.93357300	1.51742600
C	-1.57636500	-2.82602800	1.25887400
O	-0.50706100	-3.56759900	1.41547600
C	-3.89441800	0.13986900	-1.76017200
H	-3.91551100	0.29733000	-2.84728600
H	-4.73214900	-0.52936600	-1.53378300
C	-2.61067800	-0.54630200	-1.35627600
H	-1.68073900	0.00488000	-1.41212300
N	-2.47374500	-1.87525400	-1.65510100
O	-1.30957900	-2.43410400	-1.50133500
O	-3.45461900	-2.60035700	-1.92891100
P	1.72859900	-1.15033500	-0.30911400
O	0.73818500	-1.05797600	-1.50588400
O	1.58657600	-2.29508300	0.64427500
O	1.67086800	0.22251200	0.55139600
O	3.15286300	-1.06153600	-1.06421400
C	2.04163200	1.44958200	-0.01231000
C	3.39619000	1.71470900	-0.27534800
C	1.04580300	2.40334100	-0.20124100
C	3.71432400	2.99788400	-0.75438800
C	1.39275800	3.66845200	-0.67451100
H	0.01952300	2.14884100	0.04118000
C	2.72974100	3.96378400	-0.95273900
H	4.74973300	3.22737600	-0.98564300
H	0.62138800	4.41719300	-0.82418500
H	3.00578100	4.94407100	-1.32817400
C	4.30309200	-0.64393000	-0.38123300
C	5.30376500	-1.58702200	-0.16722800
C	4.45687200	0.70782200	-0.03010300
C	6.50635300	-1.18851300	0.41541400
H	5.13219000	-2.61408300	-0.47062600
C	5.67955500	1.07882900	0.55722900
C	6.69298900	0.14808000	0.77674100
H	7.29062600	-1.91924400	0.58536900
H	5.82155800	2.11198400	0.85807900
H	7.62390300	0.46473600	1.23629500
O	-2.73032100	-3.46917100	1.16794100
C	-2.73752400	-4.81270000	0.63381100
H	-3.75371800	-5.17366800	0.78364600
H	-2.50592100	-4.75778300	-0.43277500
H	-2.02492200	-5.44862700	1.15806300

- TS3'$_{ester}$

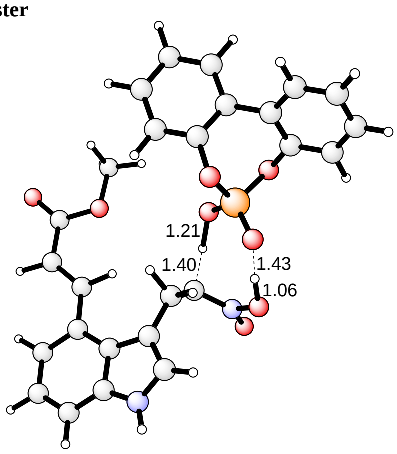

B3LYP/6-311+G(*2d*,*2p*) energy:
-2,057.8340608900 a.u.
ZPE: 0.45153 a.u.
Thermal correction to Gibbs Free Energy: 0.383638 a.u.
Dispersion correction: -91.33 kcal/mol

H	-0.25833100	-2.92586100	0.30574000
C	5.52439100	-1.47771200	-1.10926300
C	4.42729400	-0.68118700	-0.65867500
C	4.69249500	0.65891300	-0.24708000
C	6.02134400	1.10975400	-0.30410600
C	7.07217100	0.29768200	-0.75122300
C	6.83908100	-1.01136500	-1.16336600
C	3.67278700	-2.72812800	-1.26358900
C	3.24600400	-1.51101600	-0.77573700
H	6.25010900	2.11545900	0.03295000
H	8.08231000	0.69468100	-0.76827600
H	7.64655000	-1.64899800	-1.50986100
H	5.57227400	-3.47732400	-1.83414700
H	3.09124700	-3.61057400	-1.49118600
H	0.24724000	-0.70084300	1.17885800
N	5.02908600	-2.71389400	-1.46112500
C	3.61903700	1.52598900	0.23221400
H	2.68625800	1.04217400	0.49224300
C	3.64802900	2.86676400	0.38868400
H	4.51378000	3.47054100	0.13806600
C	2.50742800	3.64292100	0.90219900
O	2.52627300	4.85438100	1.06372900
C	1.80761500	-1.21273100	-0.44597100
H	1.15364200	-1.87002100	-1.02171900
H	1.53613000	-0.19645000	-0.74510000
C	1.47909600	-1.35426300	1.05484000
H	2.16853200	-0.86737000	1.74120400
N	1.24581700	-2.63340500	1.54068600
O	1.64778100	-3.04920600	2.61131300
O	0.47999900	-3.47580800	0.82851500
O	1.42241100	2.88126900	1.17696100
C	0.27207800	3.57535900	1.68632500
H	-0.06120000	4.34094000	0.98157600
H	-0.49452900	2.81135200	1.80880000
H	0.50004000	4.04735600	2.64545400
P	-1.81435500	-0.87654600	0.21211900
O	-0.82214200	-0.13592700	1.13692300
O	-1.34786200	-2.22083700	-0.29726100
O	-2.19510800	0.00693600	-1.08806900
O	-3.19114200	-0.91189100	1.05955100
C	-2.93325000	1.19186400	-0.96357600
C	-4.30317500	1.13315800	-0.65856200
C	-2.28336400	2.38998600	-1.24444700
C	-5.00732100	2.35032400	-0.64768700
C	-3.00851300	3.58111600	-1.22788300
H	-1.22531100	2.37190000	-1.48220000
C	-4.37336900	3.55877300	-0.92957500
H	-6.06333600	2.34045600	-0.39697900
H	-2.50837700	4.51915200	-1.44677400
H	-4.94279700	4.48253700	-0.90900000
C	-4.41956000	-1.14699500	0.42480100
C	-5.07137900	-2.34426100	0.70458400
C	-4.99266300	-0.14979700	-0.38213200
C	-6.33919800	-2.57331100	0.17090300
H	-4.58393500	-3.07219300	1.34396600

C	-6.27072600	-0.41045100	-0.90735600	H	-6.73238300	0.33212200	-1.55043500
C	-6.93852200	-1.60289700	-0.63598600	H	-7.92236000	-1.77702100	-1.05999700
H	-6.85309900	-3.50502500	0.38478900				

Copies of the ^{1}H and ^{13}C NMR spectra

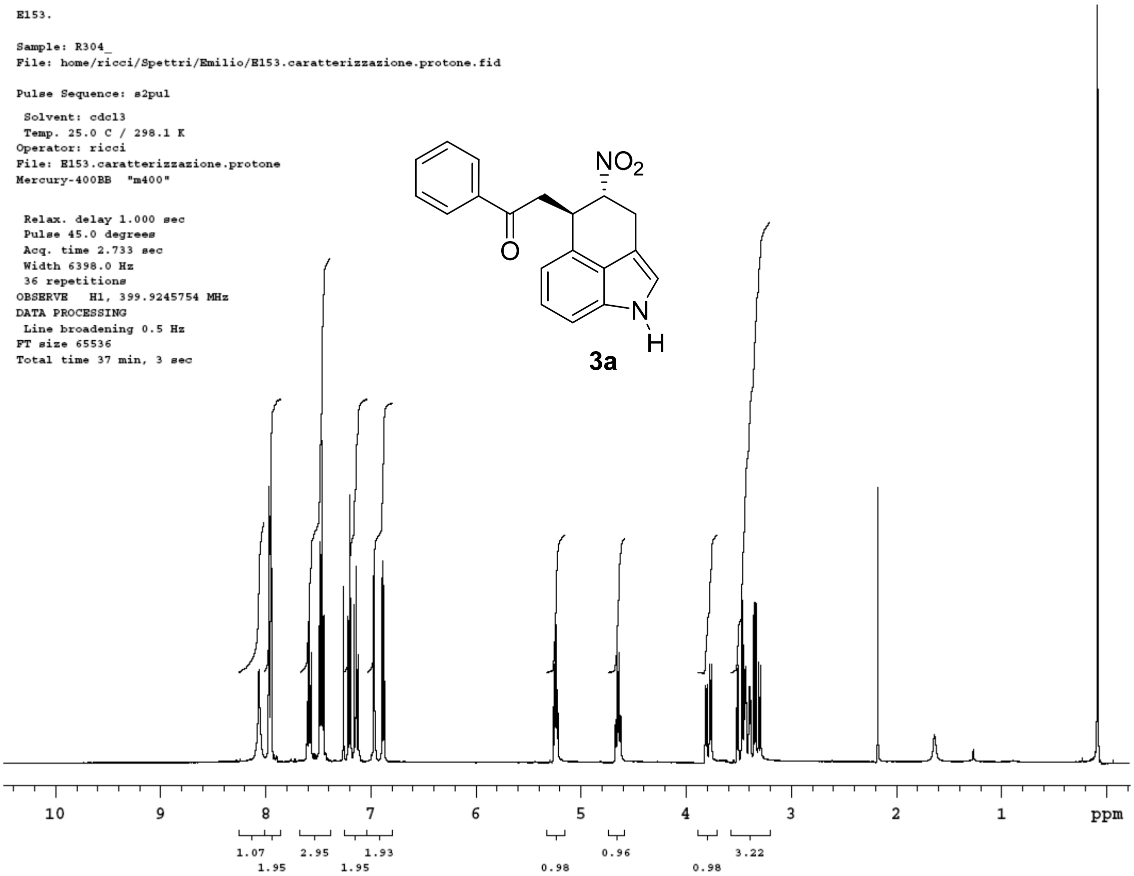

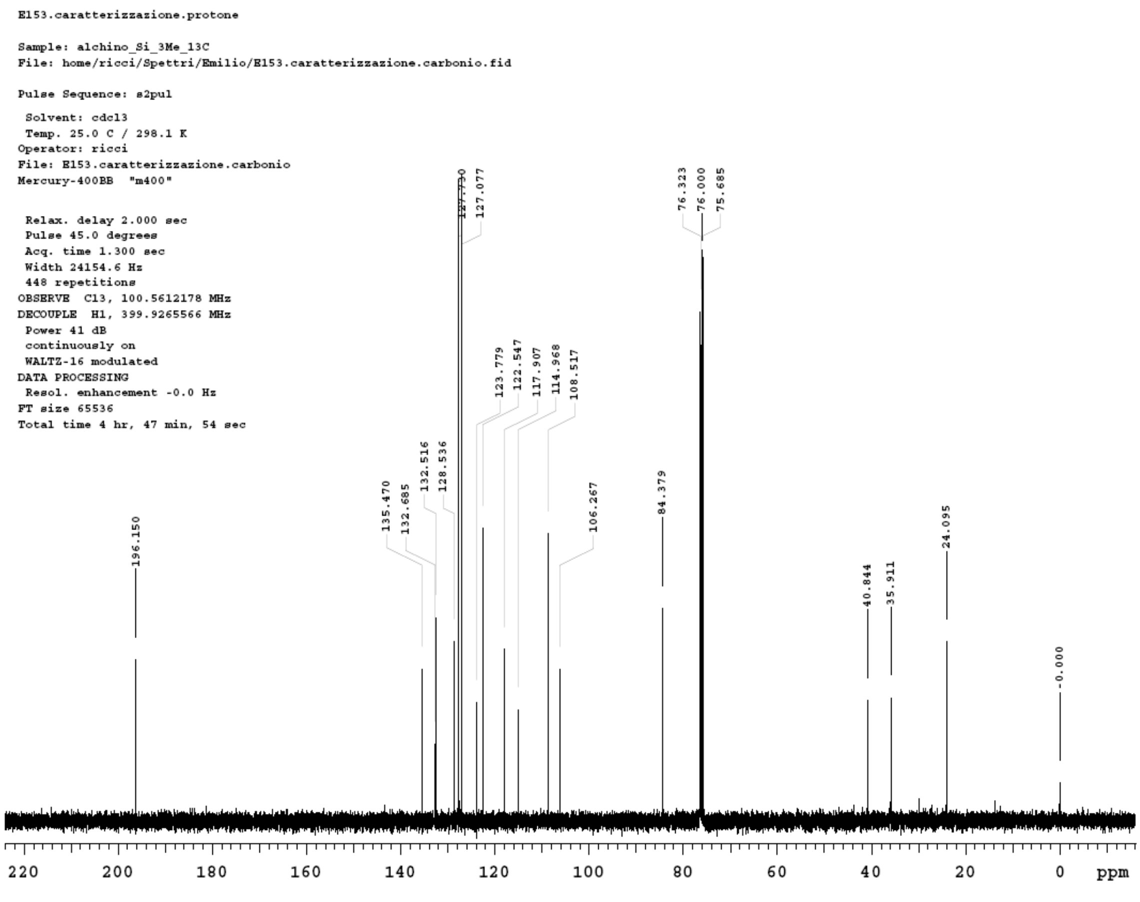

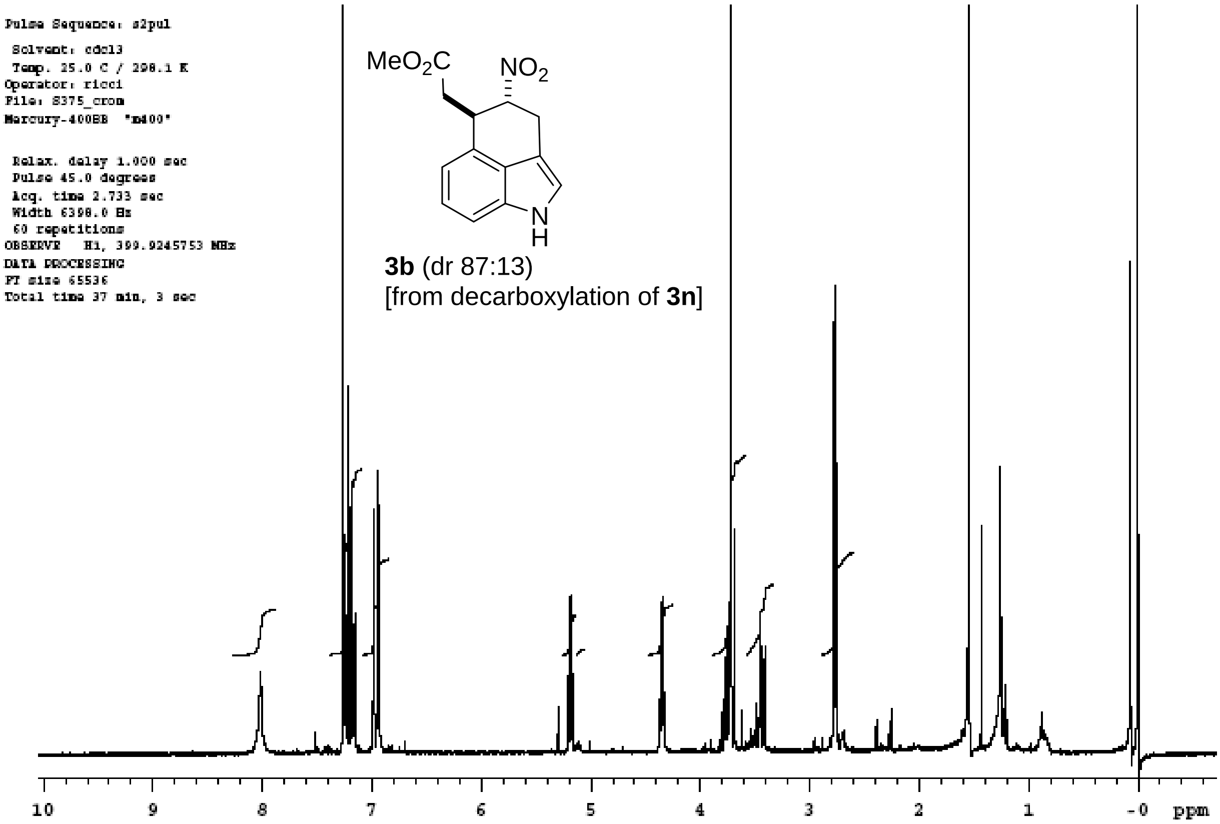
Pulse Sequence: s2pul
Solvent: cdcl3
Temp. 25.0 C / 298.1 K
Operator: ricci
File: S375_crom
Mercury-400BB "m400"
Relax. delay 1.000 sec
Pulse 45.0 degrees
Acq. time 2.733 sec
Width 6398.0 Hz
60 repetitions
OBSERVE H1, 399.9245753 MHz
DATA PROCESSING
FT size 65536
Total time 37 min, 3 sec
MeO2C
NO2
N
H
3b (dr 87:13)
[from decarboxylation of 3n]
10 9 8 7 6 5 4 3 2 1 -0 ppm

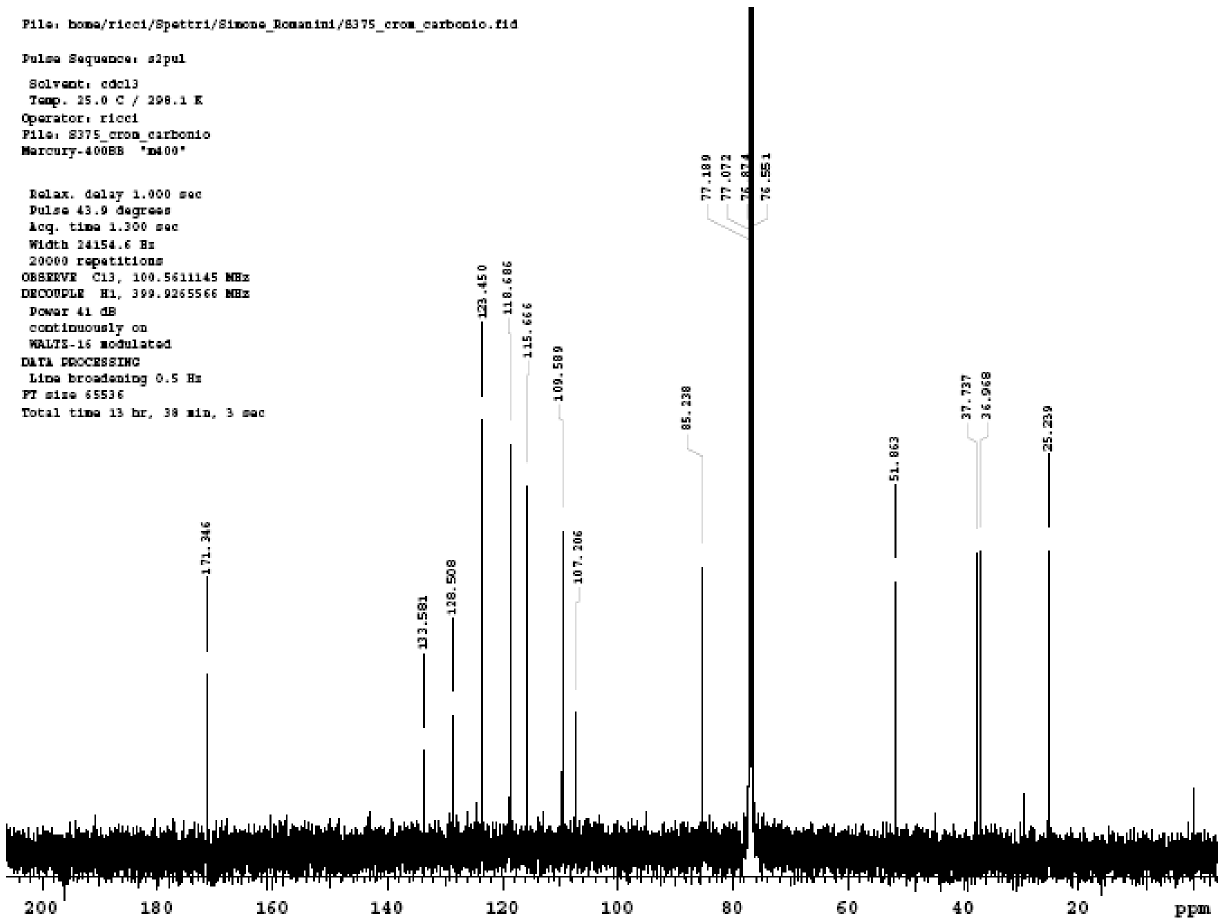
File: home/ricci/Spettri/Simone_Romanini/S375_crom_carbonio.fid
Pulse Sequence: s2pul
Solvent: cdcl3
Temp. 25.0 C / 298.1 K
Operator: ricci
File: S375_crom_carbonio
Mercury-400BB "m400"
Relax. delay 1.000 sec
Pulse 43.9 degrees
Acq. time 1.300 sec
Width 24154.6 Hz
20000 repetitions
OBSERVE C13, 100.5611145 MHz
DECOUPLE H1, 399.9265566 MHz
Power 41 dB
continuously on
WALTZ-16 modulated
DATA PROCESSING
Line broadening 0.5 Hz
FT size 65536
Total time 13 hr, 38 min, 3 sec
77.189
77.072
76.874
76.551
123.450
118.686
115.666
109.589
85.238
37.737
36.968
25.239
51.863
171.346
107.206
133.581
128.508
200 180 160 140 120 100 80 60 40 20 ppm

Std Proton parameters

File: home/ricci/Spettri/Simone/s171_H.fid

Pulse Sequence: s2pul
Solvent: cdcl3
Ambient temperature
Operator: ricci
File: s171_H
Mercury-400BB "m400"

Relax. delay 1.000 sec
Pulse 45.0 degrees
Acq. time 2.733 sec
Width 6398.0 Hz
28 repetitions
OBSERVE H1, 399.9245792 MHz
DATA PROCESSING
FT size 65536
Total time 4 min, 38 sec

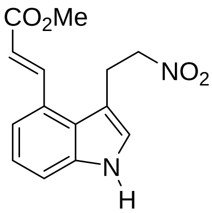

3'b

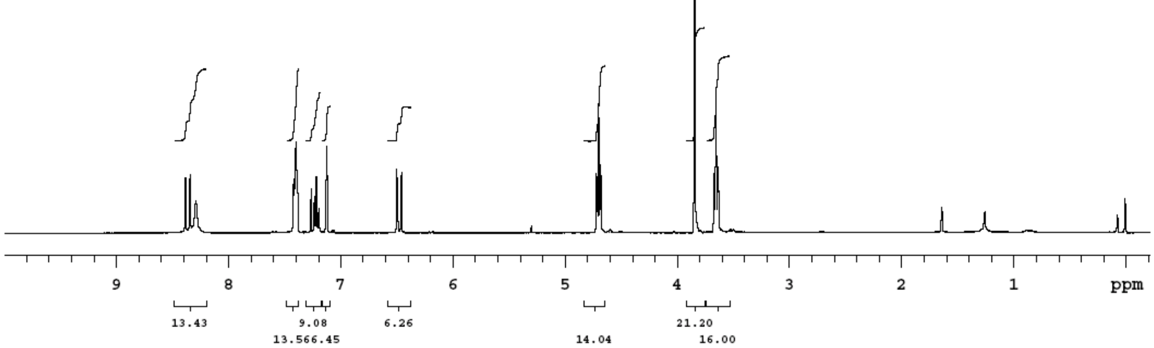

Std Carbon experiment

File: home/ricci/Spettri/Simone/s171_C.fid

Pulse Sequence: s2pul
Solvent: cdcl3
Ambient temperature
Operator: ricci
File: s171_C
Mercury-400BB "m400"

Relax. delay 1.000 sec
Pulse 45.0 degrees
Acq. time 1.300 sec
Width 24154.6 Hz
512 repetitions
OBSERVE C13, 100.5611145 MHz
DECOUPLE H1, 399.9265566 MHz
Power 41 dB
continuously on
WALTZ-16 modulated
DATA PROCESSING
Line broadening 1.0 Hz
FT size 65536
Total time 39 min, 54 sec

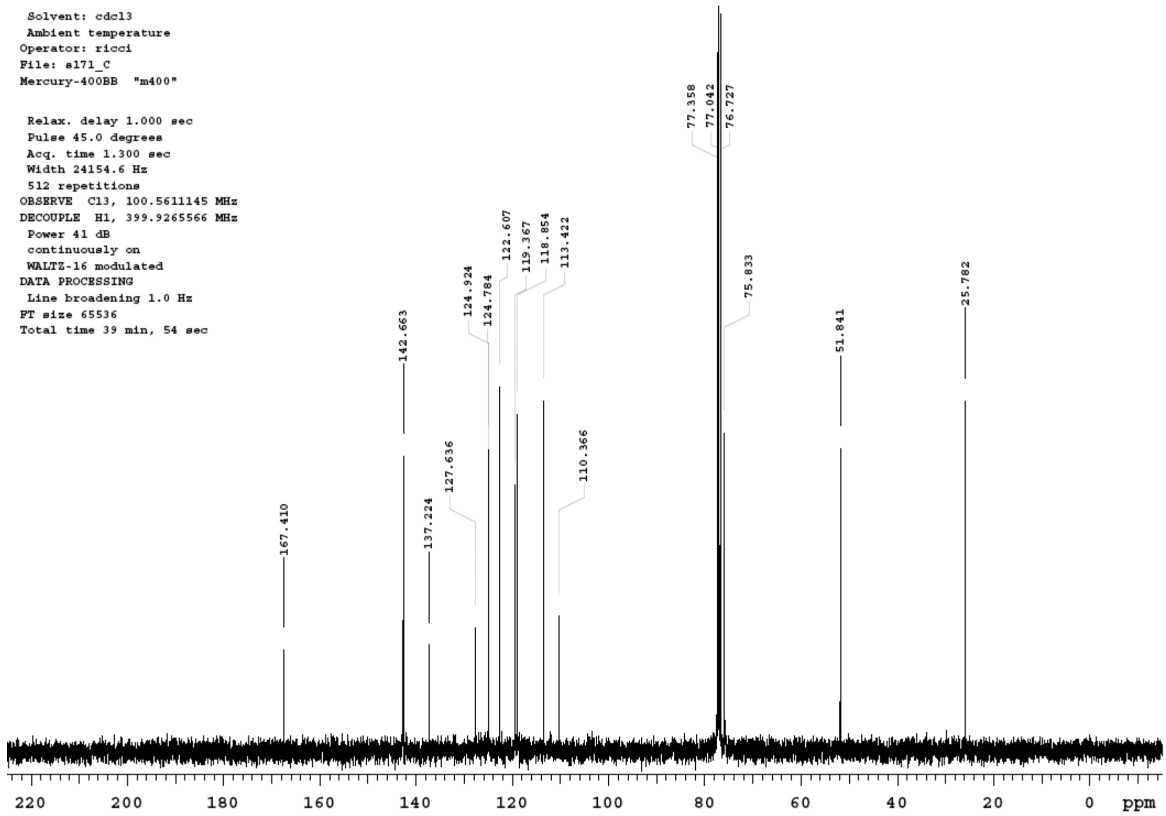

Std Proton parameters

Sample: s173
File: home/ricci/Spettri/Simone/s173_H.fid

Pulse Sequence: s2pul

Solvent: acetone
Ambient temperature
Operator: ricci
File: s173_H
Mercury-400BB "m400"

Relax. delay 1.000 sec
Pulse 45.0 degrees
Acq. time 2.733 sec
Width 6398.0 Hz
64 repetitions
OBSERVE H1, 399.9267101 MHz
DATA PROCESSING
FT size 65536
Total time 4 min, 38 sec

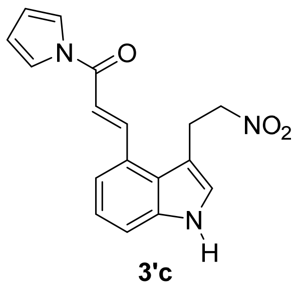

3'c

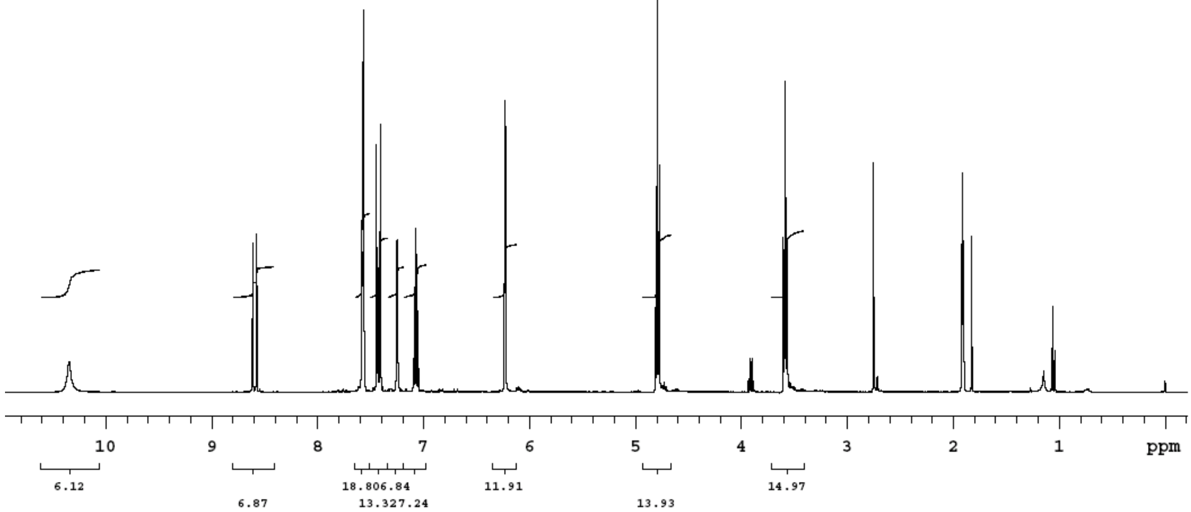

Std Carbon experiment

Sample: F20_13C
File: home/ricci/Spettri/Simone/s173_C.fid

Pulse Sequence: s2pul

Solvent: dmso
Ambient temperature
Operator: ricci
File: s173_C
Mercury-400BB "m400"

Relax. delay 1.000 sec
Pulse 44.6 degrees
Acq. time 1.300 sec
Width 24154.6 Hz
640 repetitions
OBSERVE C13, 100.5615922 MHz
DECOUPLE H1, 399.9284563 MHz
Power 41 dB
continuously on
WALTZ-16 modulated
DATA PROCESSING
Line broadening 0.5 Hz
FT size 65536
Total time 39 min, 54 sec

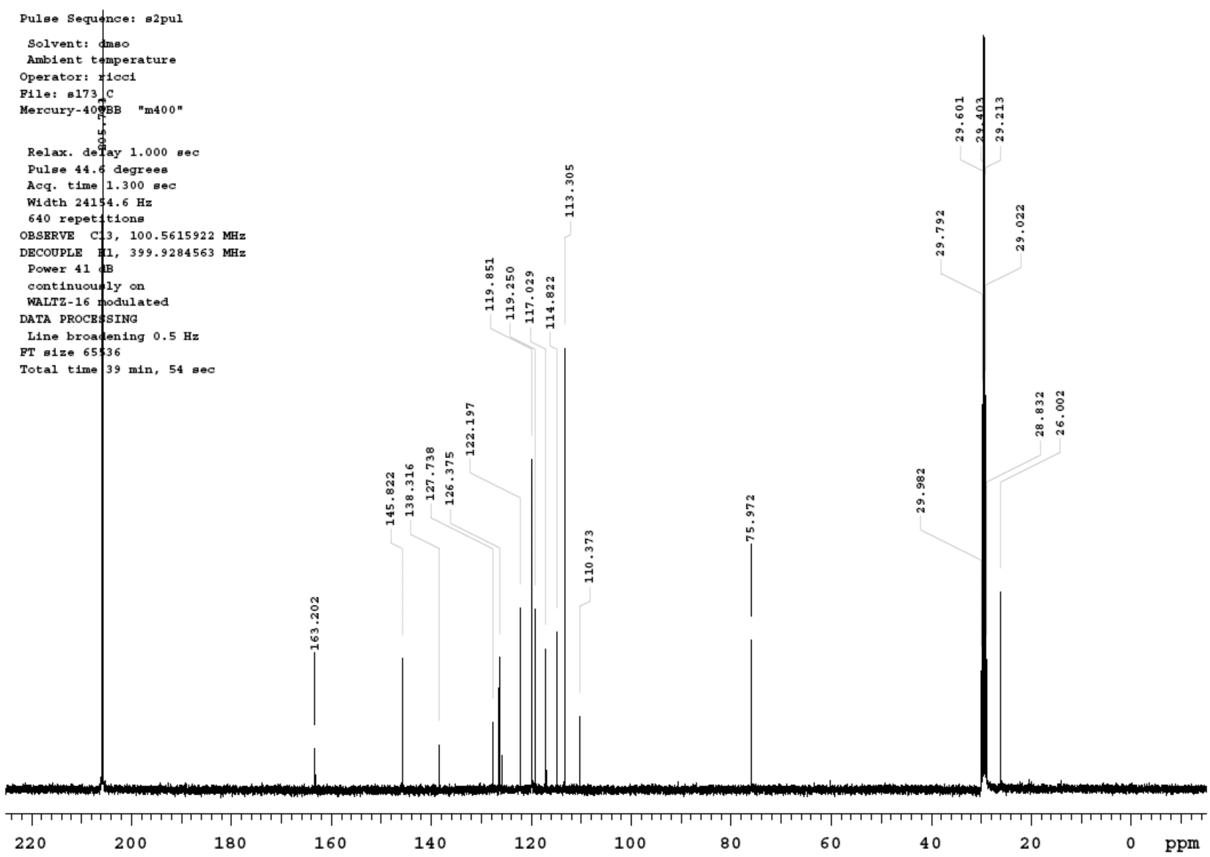

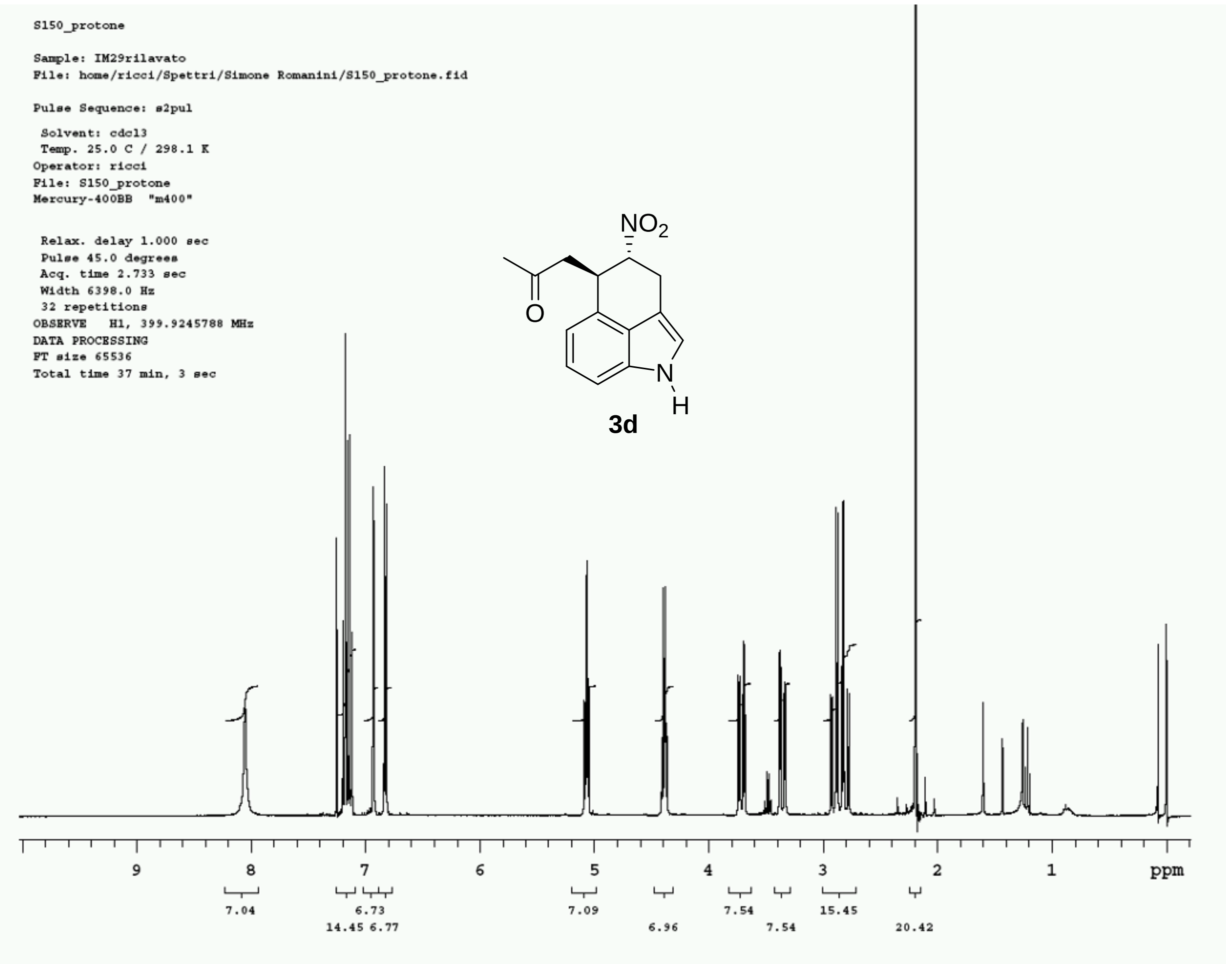
S150_protone
Sample: IM29rilavato
File: home/ricci/Spettri/Simone Romanini/S150_protone.fid
Pulse Sequence: s2pul
Solvent: cdcl3
Temp. 25.0 C / 298.1 K
Operator: ricci
File: S150_protone
Mercury-400BB "m400"
Relax. delay 1.000 sec
Pulse 45.0 degrees
Acq. time 2.733 sec
Width 6398.0 Hz
32 repetitions
OBSERVE H1, 399.9245788 MHz
DATA PROCESSING
FT size 65536
Total time 37 min, 3 sec
NO2
O
N
H
3d
9
8
7
6
5
4
3
2
1
ppm
7.04
14.45
6.73
6.77
7.09
6.96
7.54
7.54
15.45
20.42

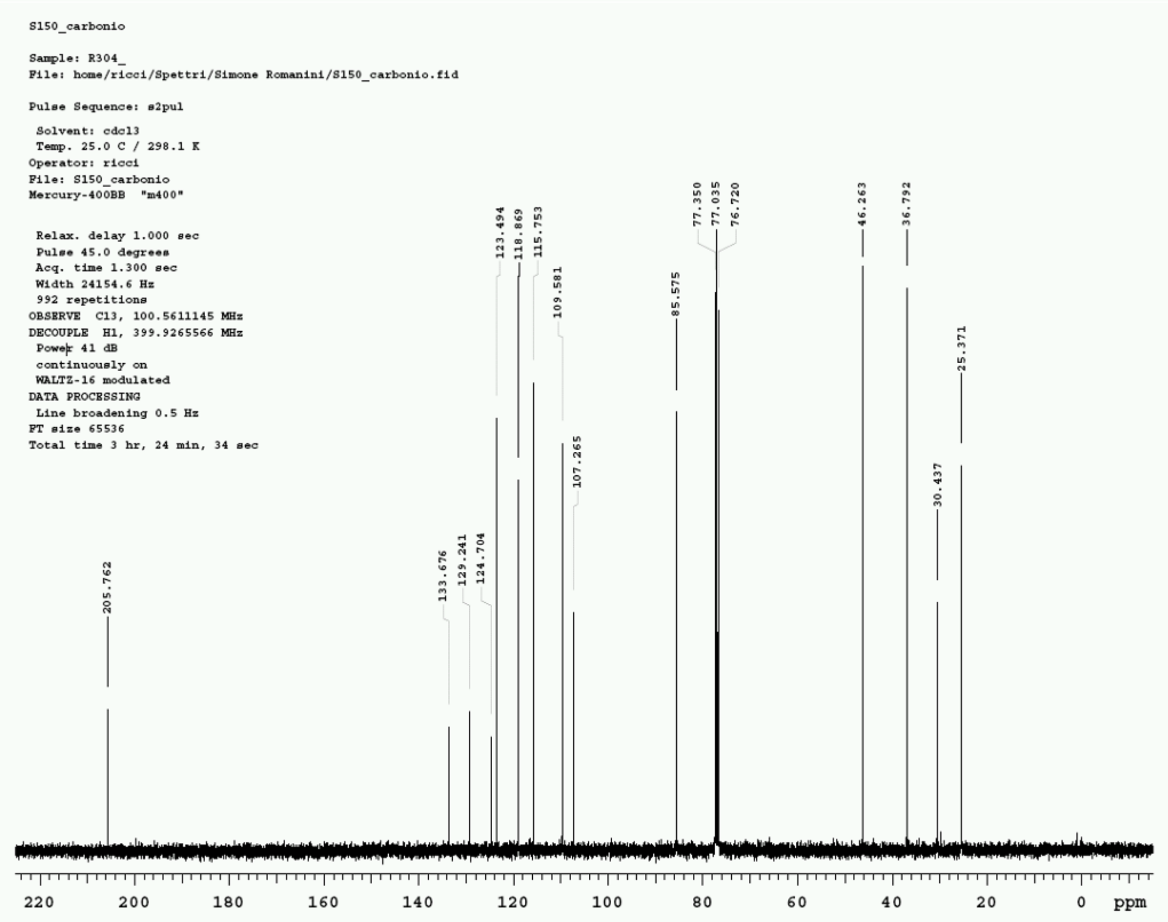
S150_carbonio
Sample: R304_
File: home/ricci/Spettri/Simone Romanini/S150_carbonio.fid
Pulse Sequence: s2pul
Solvent: cdcl3
Temp. 25.0 C / 298.1 K
Operator: ricci
File: S150_carbonio
Mercury-400BB "m400"
Relax. delay 1.000 sec
Pulse 45.0 degrees
Acq. time 1.300 sec
Width 24154.6 Hz
992 repetitions
OBSERVE C13, 100.5611145 MHz
DECOUPLE H1, 399.9265566 MHz
Power 41 dB
continuously on
WALTZ-16 modulated
DATA PROCESSING
Line broadening 0.5 Hz
FT size 65536
Total time 3 hr, 24 min, 34 sec
205.762
133.676
129.241
124.704
123.494
118.869
115.753
109.581
107.265
85.575
77.350
77.035
76.720
46.263
36.792
30.437
25.371
220
200
180
160
140
120
100
80
60
40
20
0
ppm

s27_h

Sample: s27
File: home/ricci/spettri/Siml/s27_H.fid

Pulse Sequence: s2pul

Solvent: cdcl3
Temp. 25.0 C / 298.1 K
Operator: ricci
File: s27_H
INOVA-600 "i600"

Relax. delay 1.000 sec
Pulse 45.0 degrees
Acq. time 2.995 sec
Width 9595.8 Hz
16 repetitions
OBSERVE H1, 599.7276389 MHz
DATA PROCESSING
FT size 65536
Total time 1 min, 12 sec

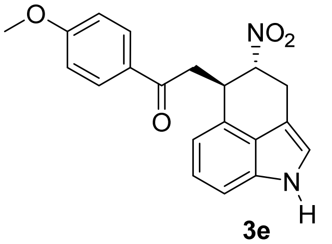

3e

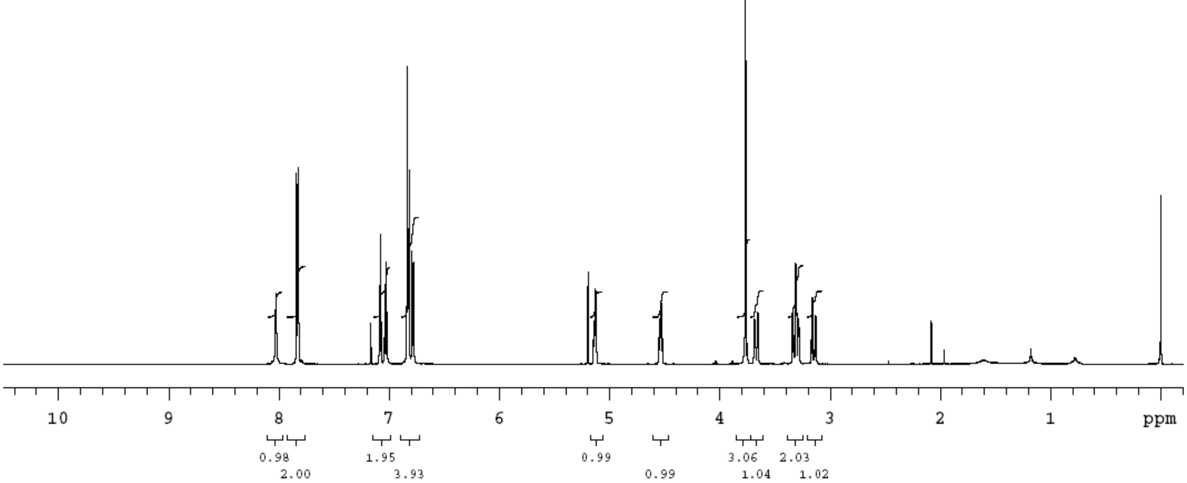

1600 std carbon parameters

Sample: s27
File: home/ricci/spettri/Siml/s27_C.fid

Pulse Sequence: s2pul

Solvent: cdcl3
Temp. 25.0 C / 298.1 K
Operator: ricci
File: s27_C
INOVA-600 "i600"

Relax. delay 1.000 sec
Pulse 45.0 degrees
Acq. time 1.000 sec
Width 36199.1 Hz
2040 repetitions
OBSERVE C13, 150.8016298 MHz
DECOUPLE H1, 599.7305861 MHz
Power 39 dB
continuously on
WALTZ-16 modulated
DATA PROCESSING
Line broadening 1.0 Hz
Sq. sine bell 1.000 sec
Shifted by -1.000 sec
FT size 131072
Total time 1 hr, 23 min, 43 sec

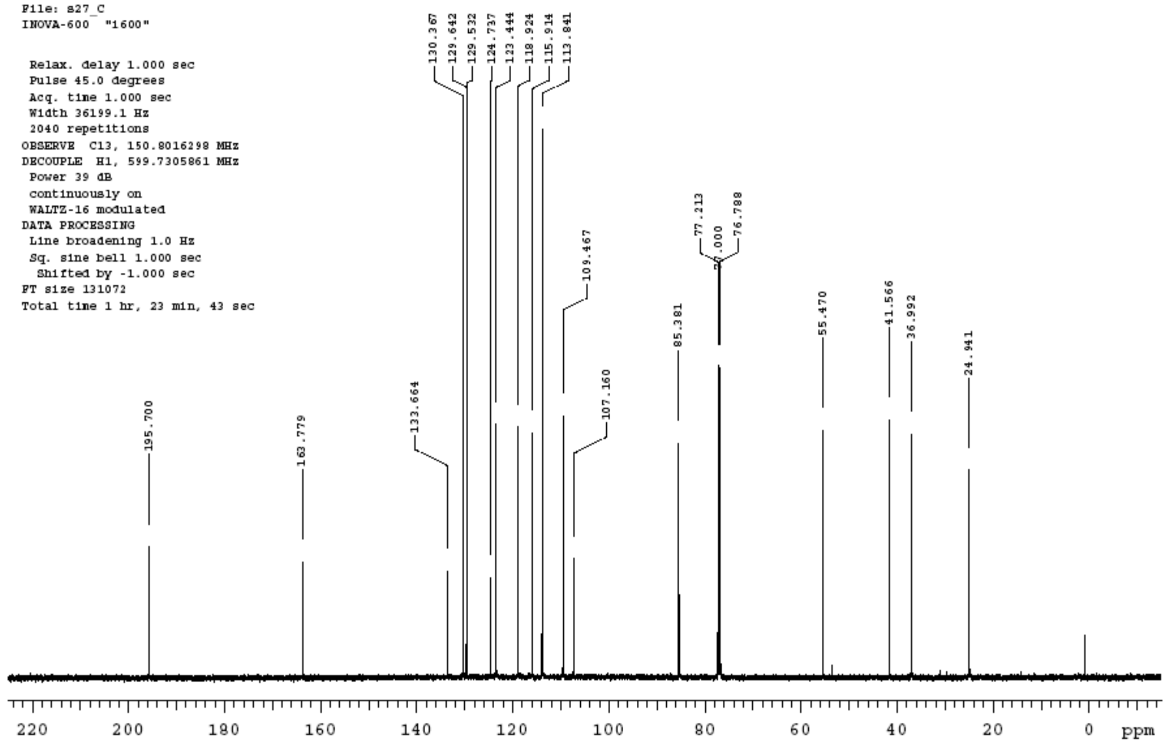

S25_col_Br_Ph

File: home/ricci/Spettri/Simone/S025_col_Br_Ph.fid

Pulse Sequence: s2pul

Solvent: cdcl3
Temp. 25.0 C / 298.1 K
Operator: ricci
File: S025_col_Br_Ph
Mercury-400BB "m400"

Relax. delay 1.000 sec
Pulse 45.0 degrees
Acq. time 2.733 sec
Width 6398.0 Hz
20 repetitions
OBSERVE H1, 399.9246063 MHz
DATA PROCESSING
FT size 65536
Total time 4 min, 38 sec

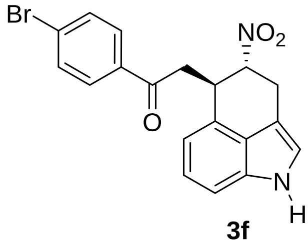

3f

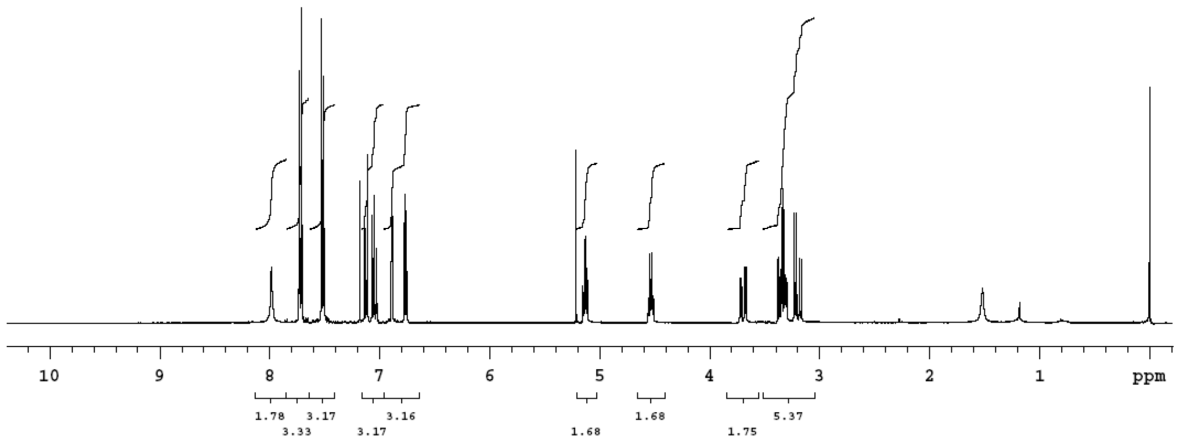

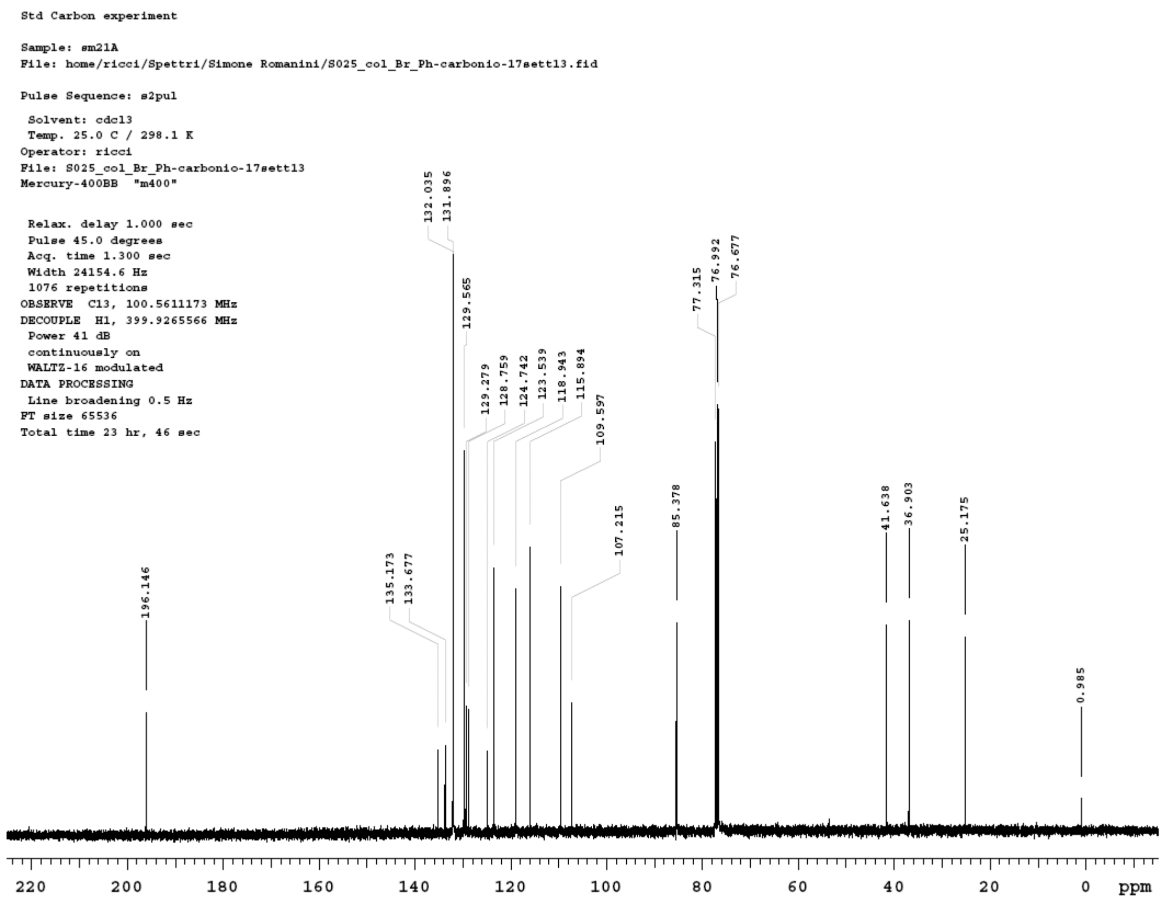

Std Proton parameters

Sample: IM29rilavato
File: home/ricci/Spettri/Simone/S146_crom_protone.fid

Pulse Sequence: s2pul

Solvent: cdcl3
Temp. 25.0 C / 298.1 K
Operator: ricci
File: S146_crom_protone
Mercury-400BB "m400"

Relax. delay 1.000 sec
Pulse 45.0 degrees
Acq. time 2.733 sec
Width 6398.0 Hz
24 repetitions
OBSERVE H1, 399.9245802 MHz
DATA PROCESSING
FT size 65536
Total time 37 min, 3 sec

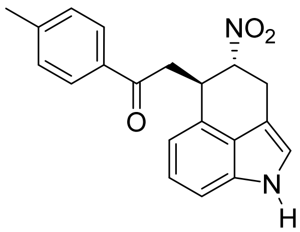

3g

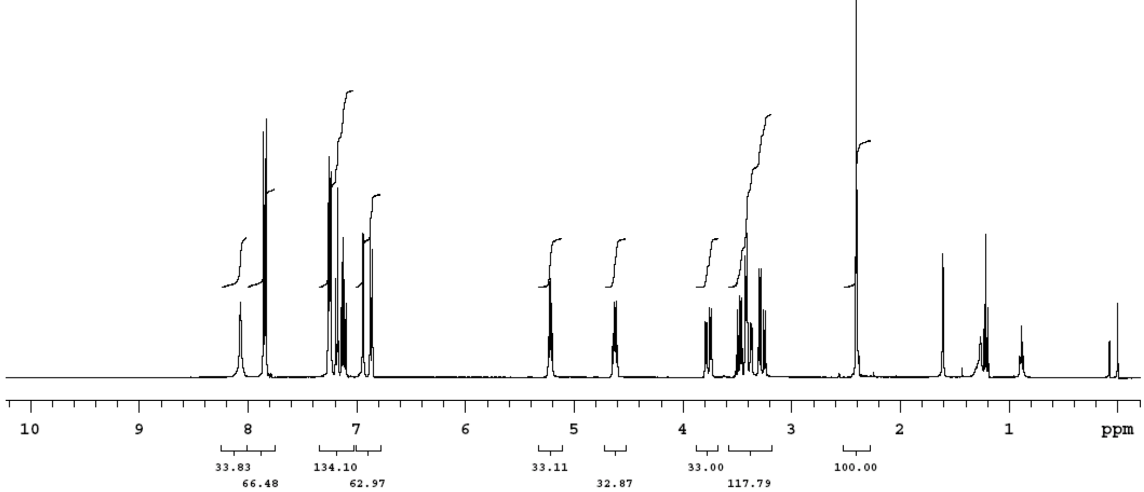

S146_crom_carbonio

Sample: R304_
File: home/ricci/Spettri/Simone Romanini/S146_crom_carbonio.fid

Pulse Sequence: s2pul

Solvent: cdcl3
Temp. 25.0 C / 298.1 K
Operator: ricci
File: S146_crom_carbonio
Mercury-400BB "m400"

Relax. delay 1.000 sec
Pulse 45.0 degrees
Acq. time 1.300 sec
Width 24154.6 Hz
1120 repetitions
OBSERVE C13, 100.5611145 MHz
DECOUPLE H1, 399.9265566 MHz
Power 41 dB
continuously on
WALTZ-16 modulated
DATA PROCESSING
Line broadening 1.0 Hz
FT size 65536
Total time 3 hr, 34 min, 47 sec

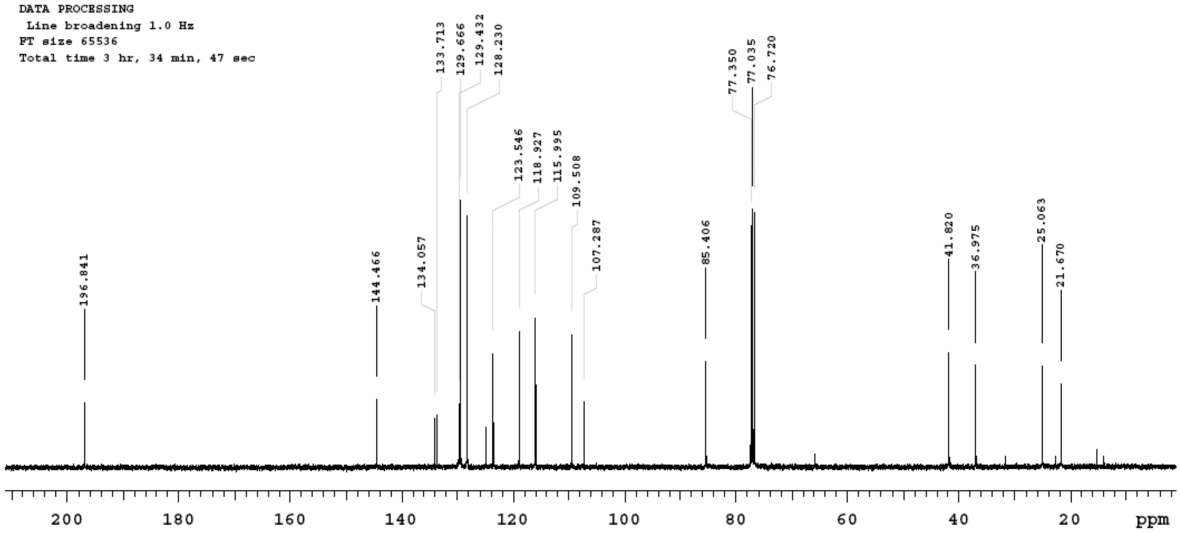

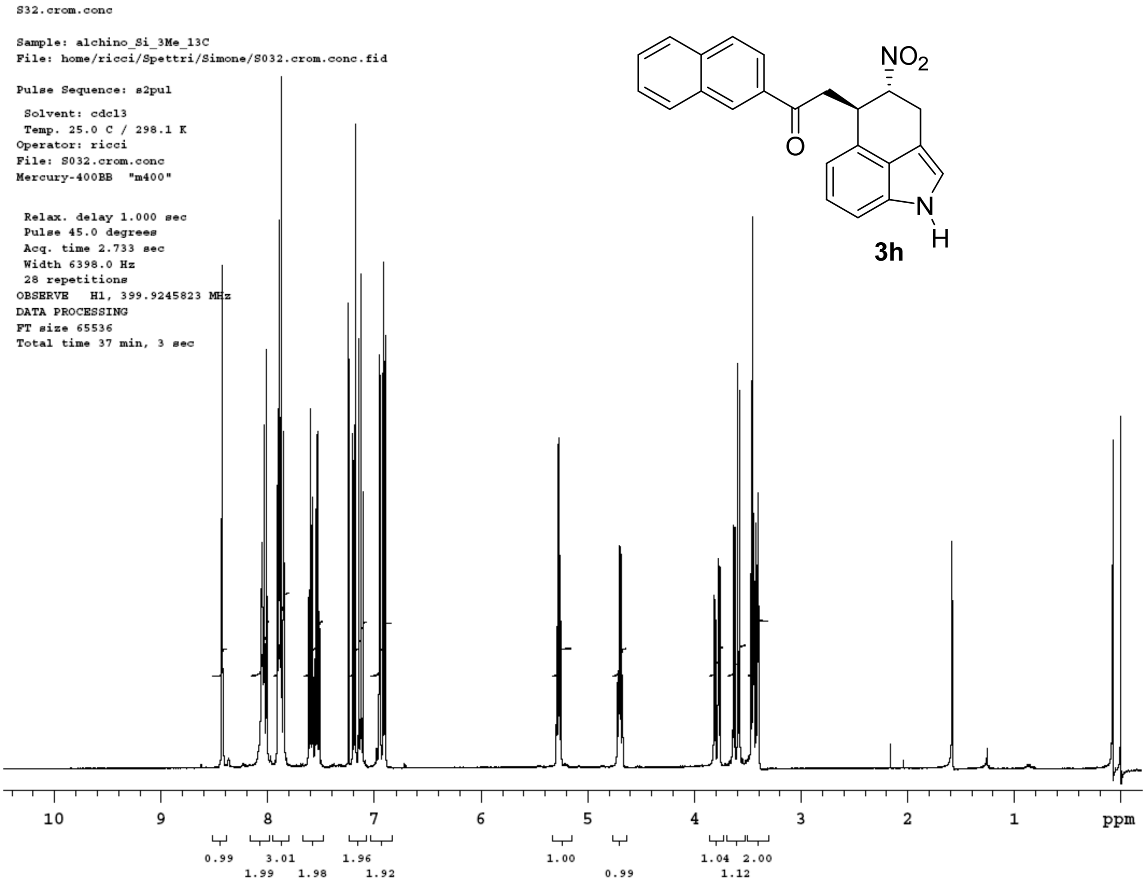
S32.crom.conc
Sample: alchino_Si_3Me_13C
File: home/ricci/Spettri/Simone/S032.crom.conc.fid
Pulse Sequence: s2pul
Solvent: cdcl3
Temp. 25.0 C / 298.1 K
Operator: ricci
File: S032.crom.conc
Mercury-400BB "m400"
Relax. delay 1.000 sec
Pulse 45.0 degrees
Acq. time 2.733 sec
Width 6398.0 Hz
28 repetitions
OBSERVE H1, 399.9245823 MHz
DATA PROCESSING
FT size 65536
Total time 37 min, 3 sec
ppm
0.99 1.99 3.01 1.98 1.96 1.92 1.00 0.99 1.04 1.12 2.00
NO2
O
N
H

3h

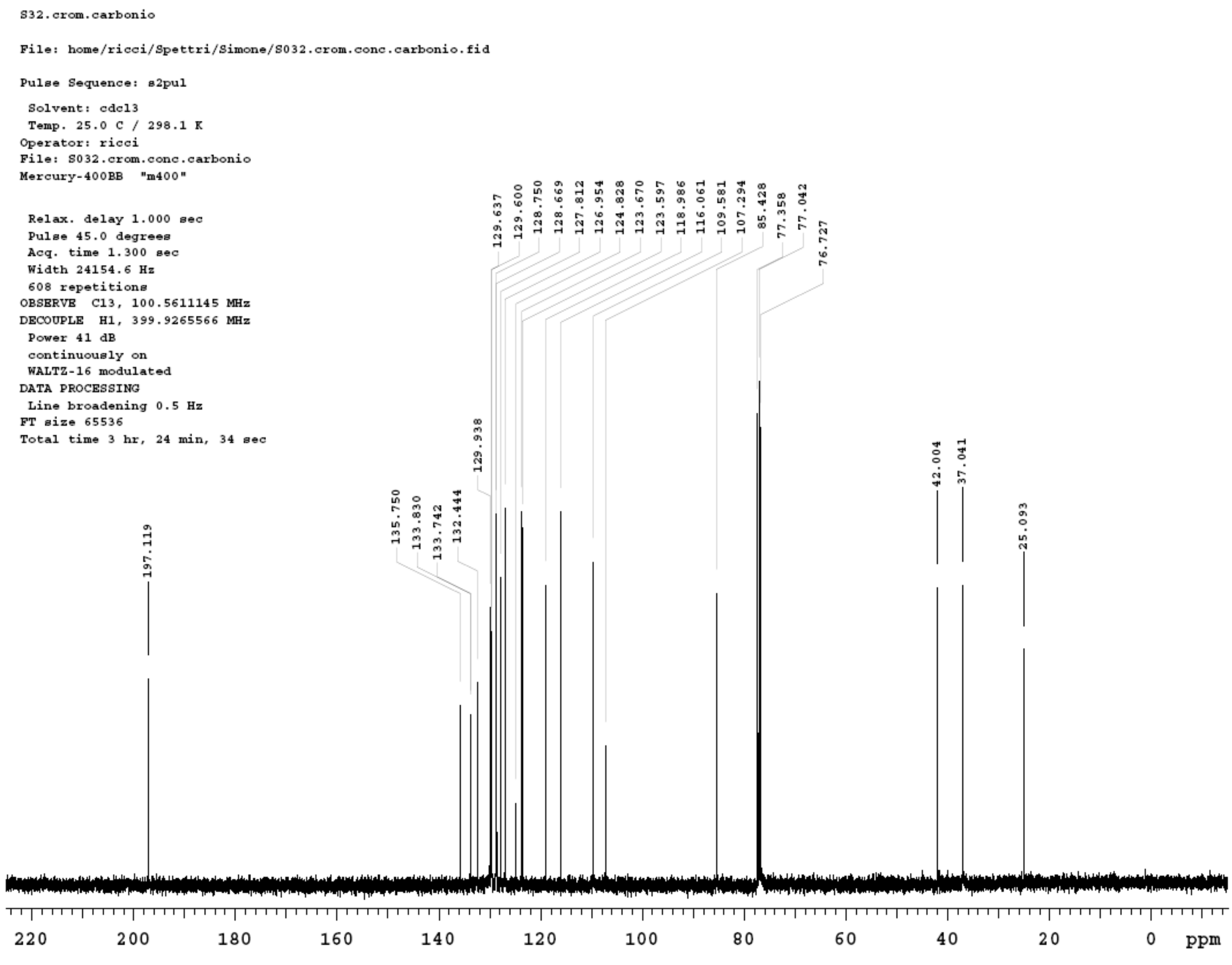
S32.crom.carbonio
File: home/ricci/Spettri/Simone/S032.crom.conc.carbonio.fid
Pulse Sequence: s2pul
Solvent: cdcl3
Temp. 25.0 C / 298.1 K
Operator: ricci
File: S032.crom.conc.carbonio
Mercury-400BB "m400"
Relax. delay 1.000 sec
Pulse 45.0 degrees
Acq. time 1.300 sec
Width 24154.6 Hz
608 repetitions
OBSERVE C13, 100.5611145 MHz
DECOUPLE H1, 399.9265566 MHz
Power 41 dB
continuously on
WALTZ-16 modulated
DATA PROCESSING
Line broadening 0.5 Hz
FT size 65536
Total time 3 hr, 24 min, 34 sec
197.119
135.750
133.830
133.742
132.444
129.938
129.637
129.600
128.750
128.669
127.812
126.954
124.828
123.670
123.597
118.986
116.061
109.581
107.294
85.428
77.358
77.042
76.727
42.004
37.041
25.093
ppm

S155_protone

Sample: R304_
File: home/ricci/Spettri/Simone Romanini/S155_protone.fid

Pulse Sequence: s2pul

Solvent: cdcl3
Temp. 25.0 C / 298.1 K
Operator: ricci
File: S155_protone
Mercury-400BB "m400"

Relax. delay 1.000 sec
Pulse 45.0 degrees
Acq. time 2.733 sec
Width 6398.0 Hz
48 repetitions
OBSERVE H1, 399.9245786 MHz
DATA PROCESSING
FT size 65536
Total time 37 min, 3 sec

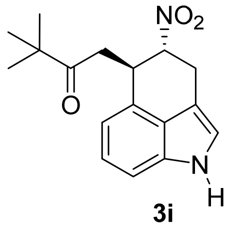

3i

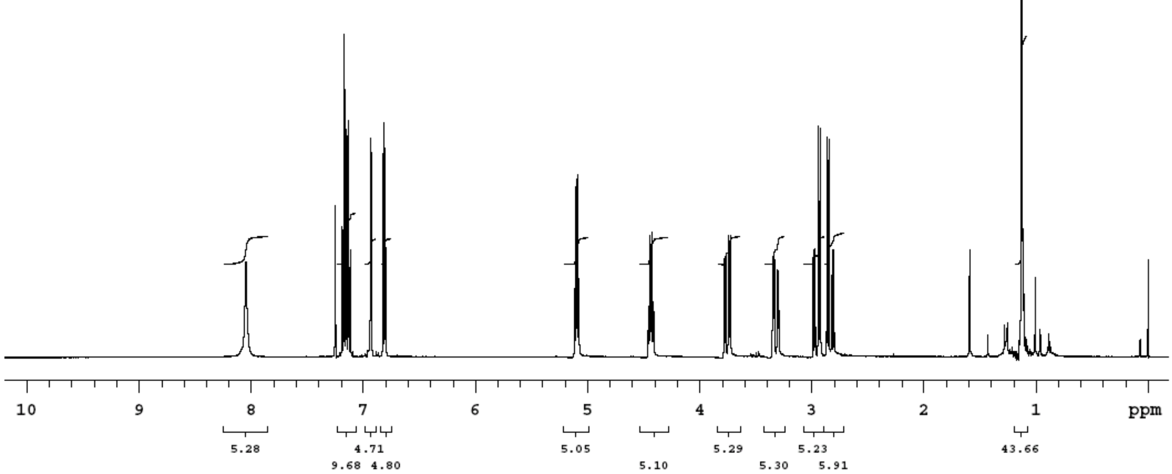

S155_carbonio

File: home/ricci/Spettri/Simone Romanini/S155_carbonio.fid

Pulse Sequence: s2pul

Solvent: cdcl3
Temp. 25.0 C / 298.1 K
Operator: ricci
File: S155_carbonio
Mercury-400BB "m400"

Relax. delay 1.000 sec
Pulse 45.0 degrees
Acq. time 1.300 sec
Width 24154.6 Hz
1120 repetitions
OBSERVE C13, 100.5611145 MHz
DECOUPLE H1, 399.9265566 MHz
Power 41 dB
continuously on
WALTZ-16 modulated
DATA PROCESSING
Line broadening 0.5 Hz
FT size 65536
Total time 3 hr, 24 min, 34 sec

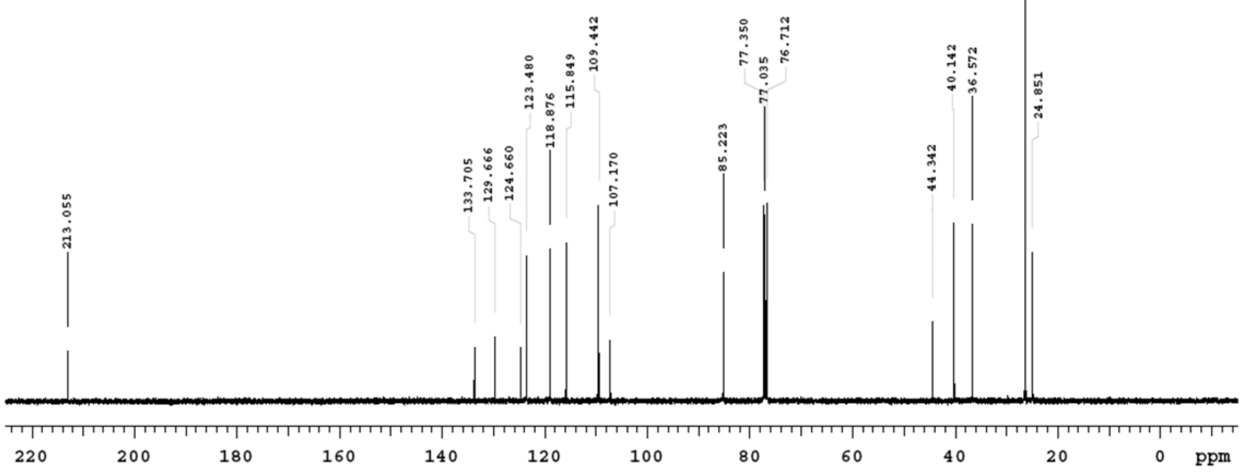

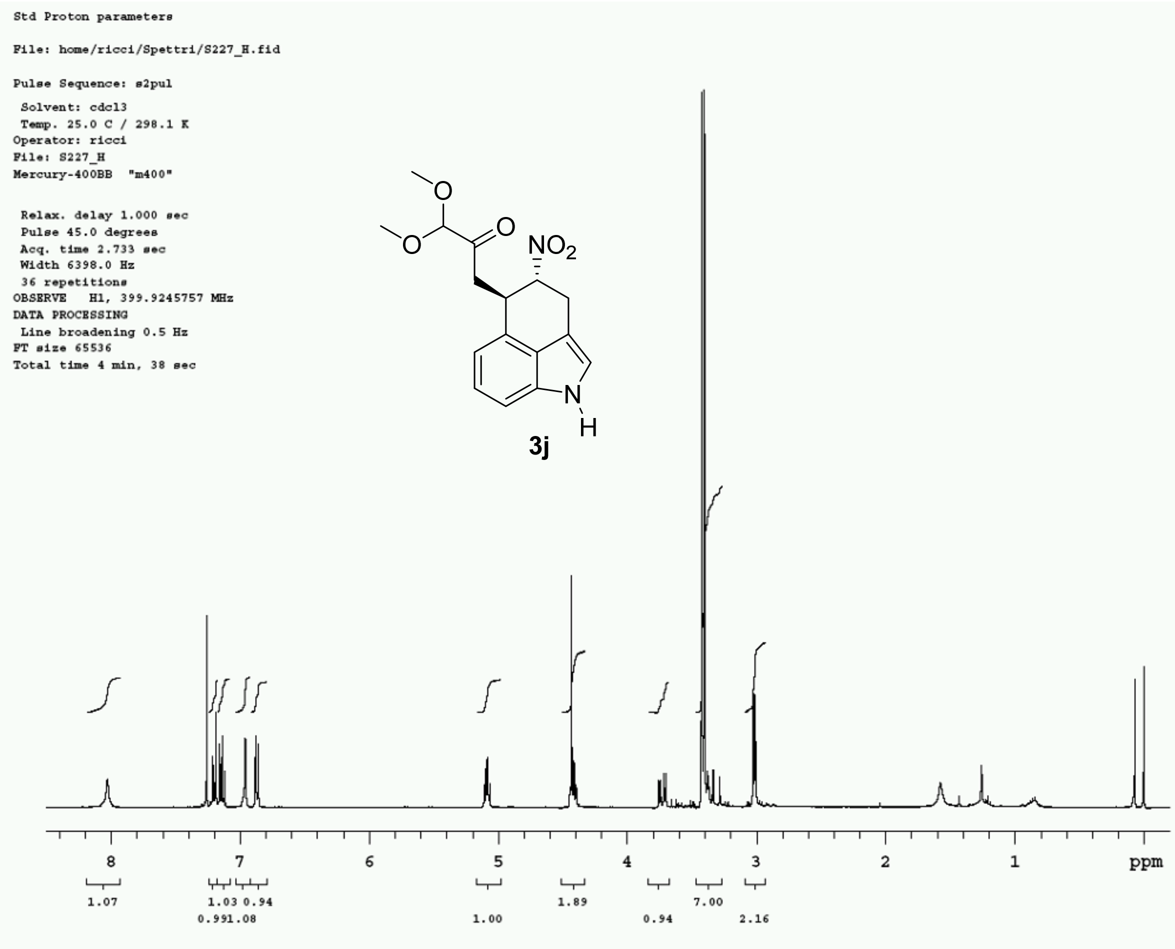
Std Proton parameters
File: home/ricci/Spettri/S227_H.fid
Pulse Sequence: s2pul
Solvent: cdcl3
Temp. 25.0 C / 298.1 K
Operator: ricci
File: S227_H
Mercury-400BB "m400"
Relax. delay 1.000 sec
Pulse 45.0 degrees
Acq. time 2.733 sec
Width 6398.0 Hz
36 repetitions
OBSERVE H1, 399.9245757 MHz
DATA PROCESSING
Line broadening 0.5 Hz
FT size 65536
Total time 4 min, 38 sec
3j
ppm
1.07 1.03 0.94 0.99 1.08 1.00 1.89 0.94 7.00 2.16

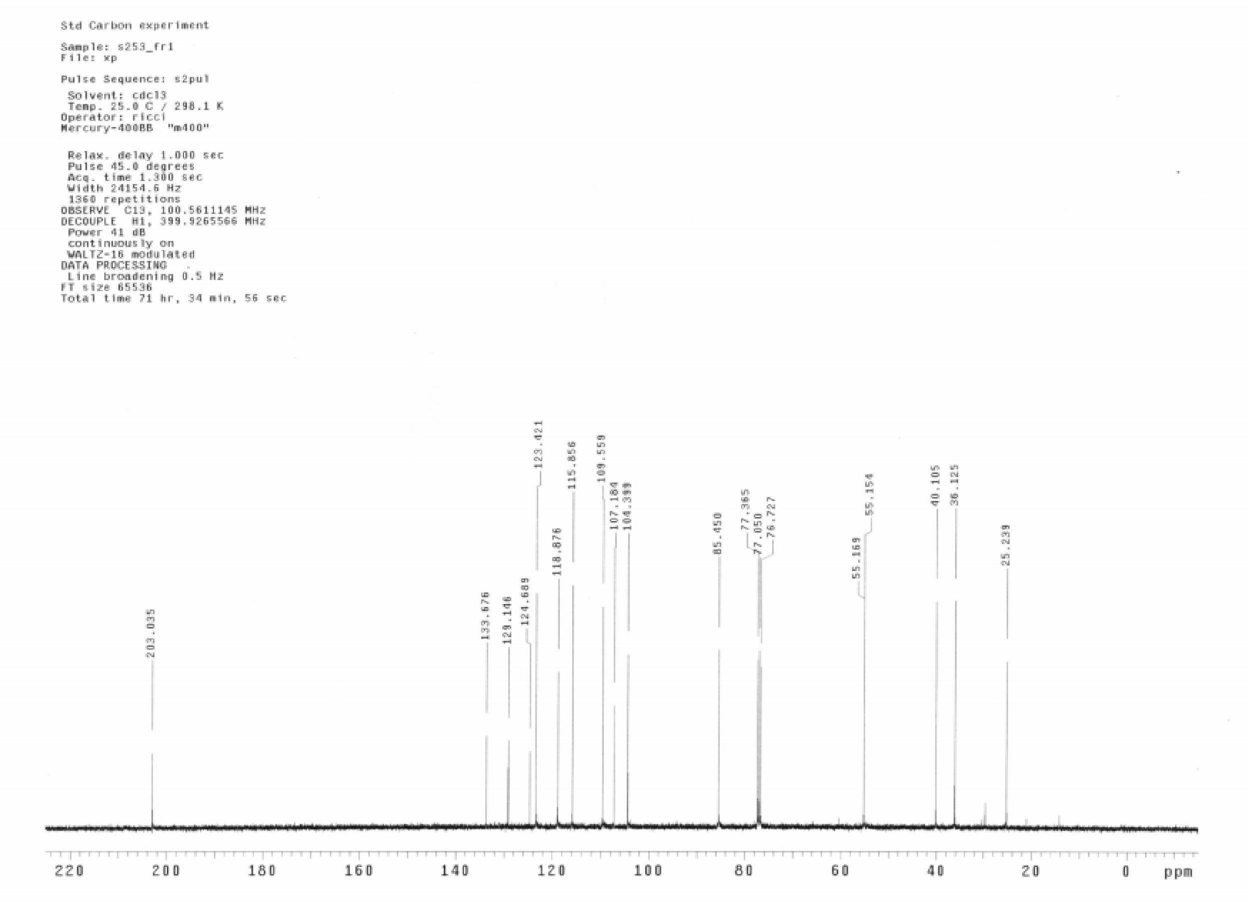
Std Carbon experiment
Sample: s253_fr1
File: xp
Pulse Sequence: s2pul
Solvent: cdcl3
Temp. 25.0 C / 298.1 K
Operator: ricci
Mercury-400BB "m400"
Relax. delay 1.000 sec
Pulse 45.0 degrees
Acq. time 1.300 sec
Width 24154.6 Hz
1360 repetitions
OBSERVE C13, 100.5611145 MHz
DECOUPLE H1, 399.9265566 MHz
Power 41 dB
continuously on
WALTZ-16 modulated
DATA PROCESSING
Line broadening 0.5 Hz
FT size 65536
Total time 71 hr, 34 min, 56 sec
203.035
133.676
129.146
124.689
123.421
118.876
115.856
109.559
107.184
104.399
85.450
77.365
77.050
76.727
55.169
55.154
40.105
36.125
25.239
ppm

s160

Sample: s160
File: home/ricci/Spettri/Simone/s160_H.fid

Pulse Sequence: s2pul

Solvent: cdcl3
Temp. 25.0 C / 298.1 K
Operator: ricci
File: s160_H
Mercury-400BB "m400"

Relax. delay 1.000 sec
Pulse 45.0 degrees
Acq. time 2.733 sec
Width 6398.0 Hz
36 repetitions
OBSERVE H1, 399.9245827 MHz
DATA PROCESSING
FT size 65536
Total time 4 min, 38 sec

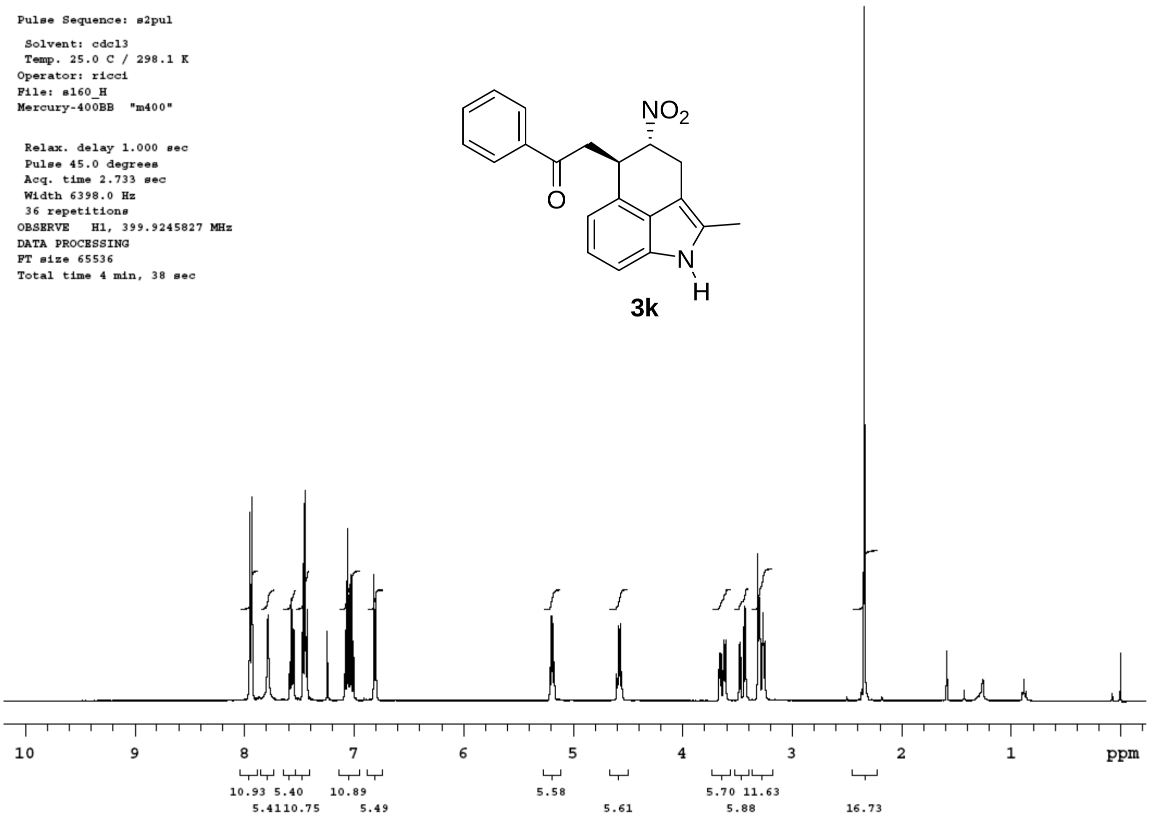

s160_C

File: home/ricci/Spettri/Simone/s160_C.fid

Pulse Sequence: s2pul

Solvent: cdcl3
Temp. 25.0 C / 298.1 K
Operator: ricci
File: s160_C
Mercury-400BB "m400"

Relax. delay 1.000 sec
Pulse 45.0 degrees
Acq. time 1.300 sec
Width 24154.6 Hz
588 repetitions
OBSERVE C13, 100.5611145 MHz
DECOUPLE H1, 399.9265566 MHz
Power 41 dB
continuously on
WALTZ-16 modulated
DATA PROCESSING
Line broadening 0.5 Hz
FT size 65536
Total time 55 min, 14 sec

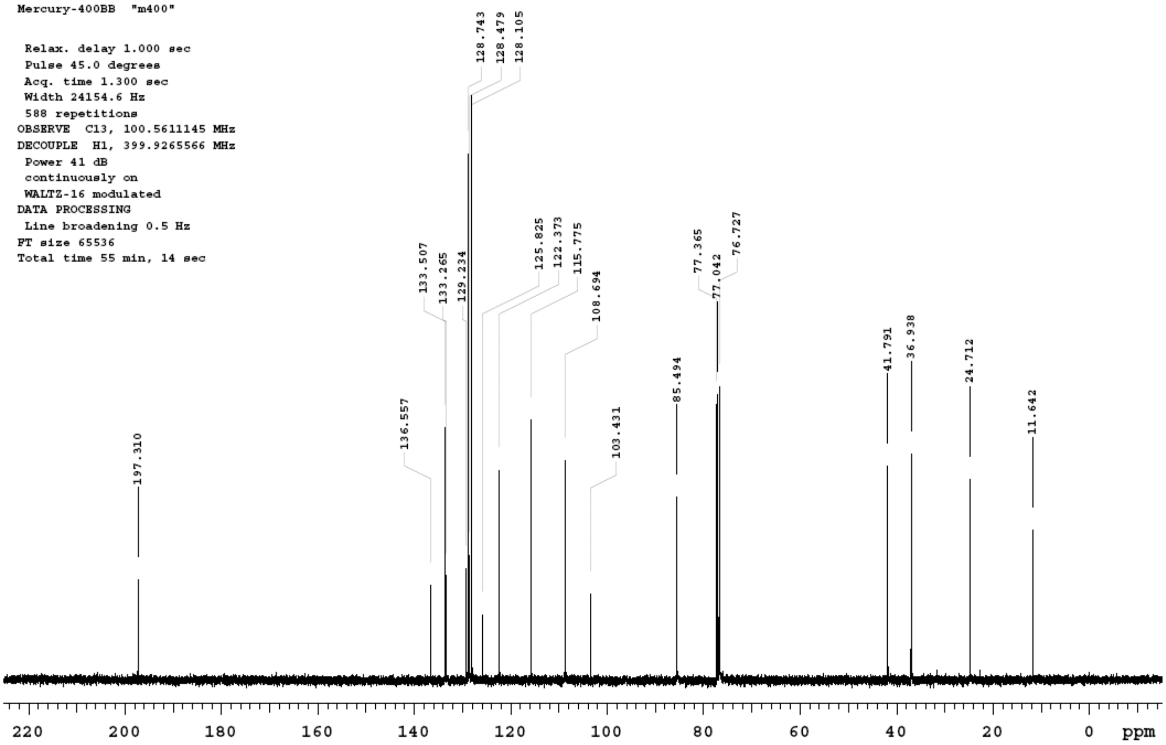

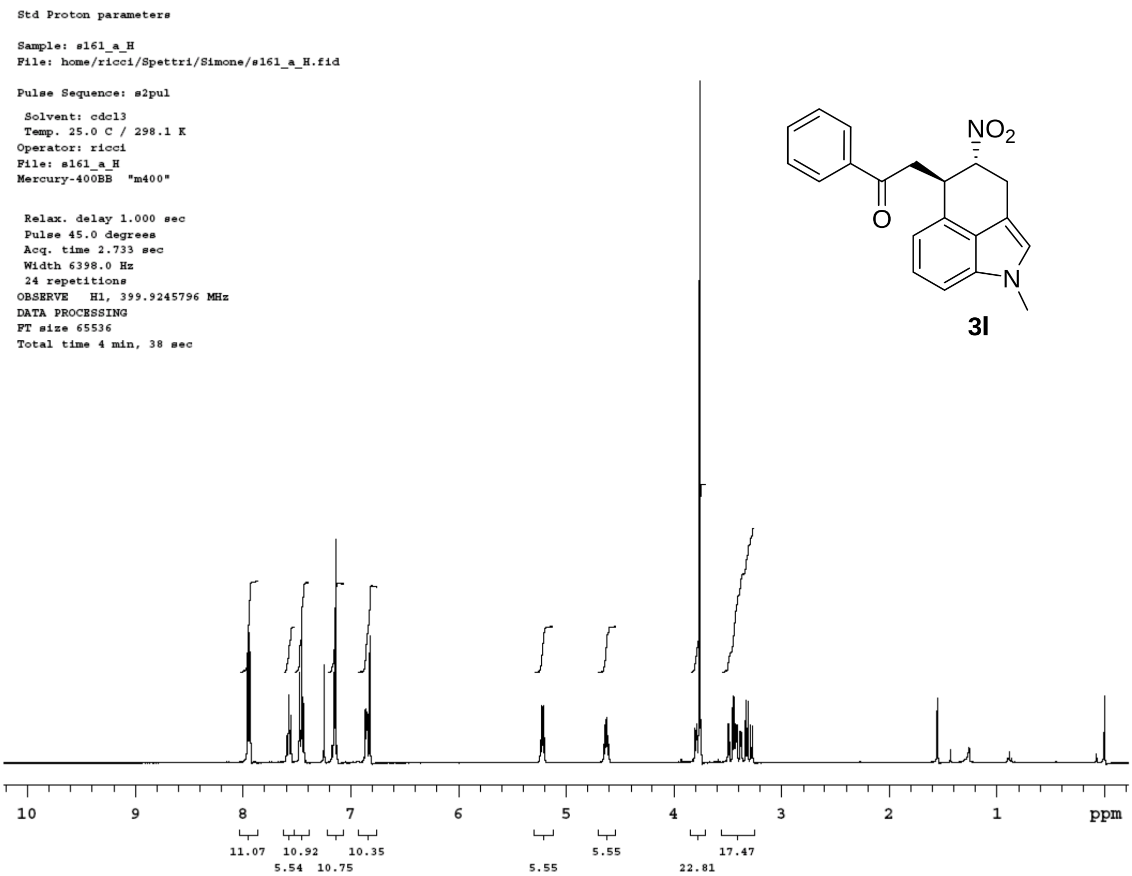
Std Proton parameters
Sample: sl61_a_H
File: home/ricci/Spettri/Simone/sl61_a_H.fid
Pulse Sequence: s2pul
Solvent: cdcl3
Temp. 25.0 C / 298.1 K
Operator: ricci
File: sl61_a_H
Mercury-400BB "m400"
Relax. delay 1.000 sec
Pulse 45.0 degrees
Acq. time 2.733 sec
Width 6398.0 Hz
24 repetitions
OBSERVE H1, 399.9245796 MHz
DATA PROCESSING
FT size 65536
Total time 4 min, 38 sec
NO2
O
N
3l
10
9
8
7
6
5
4
3
2
1
ppm
11.07
10.92
10.35
5.54
10.75
5.55
5.55
22.81
17.47

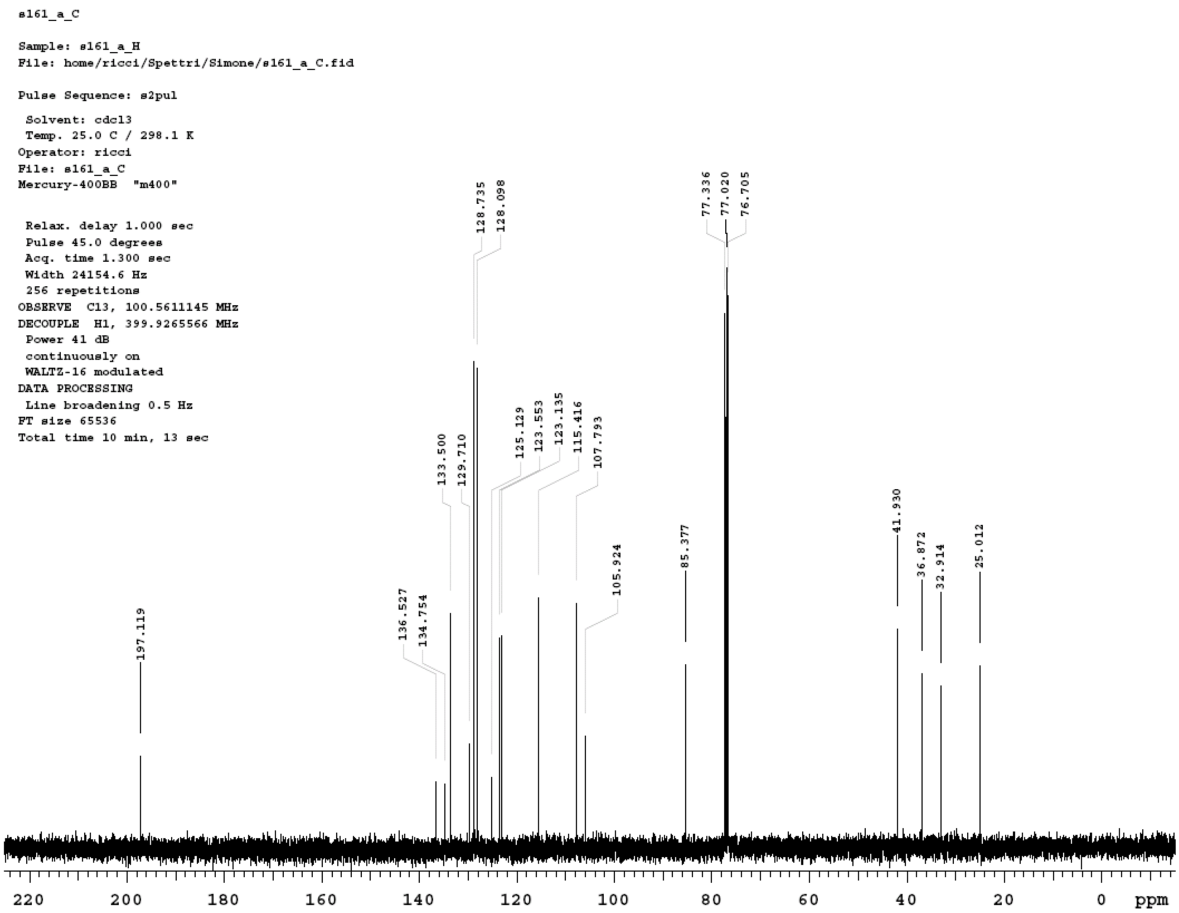
sl61_a_C
Sample: sl61_a_H
File: home/ricci/Spettri/Simone/sl61_a_C.fid
Pulse Sequence: s2pul
Solvent: cdcl3
Temp. 25.0 C / 298.1 K
Operator: ricci
File: sl61_a_C
Mercury-400BB "m400"
Relax. delay 1.000 sec
Pulse 45.0 degrees
Acq. time 1.300 sec
Width 24154.6 Hz
256 repetitions
OBSERVE C13, 100.5611145 MHz
DECOUPLE H1, 399.9265566 MHz
Power 41 dB
continuously on
WALTZ-16 modulated
DATA PROCESSING
Line broadening 0.5 Hz
FT size 65536
Total time 10 min, 13 sec
197.119
136.527
134.754
133.500
129.710
128.735
128.098
125.129
123.553
123.135
115.416
107.793
105.924
85.377
77.336
77.020
76.705
41.930
36.872
32.914
25.012
220
200
180
160
140
120
100
80
60
40
20
0
ppm

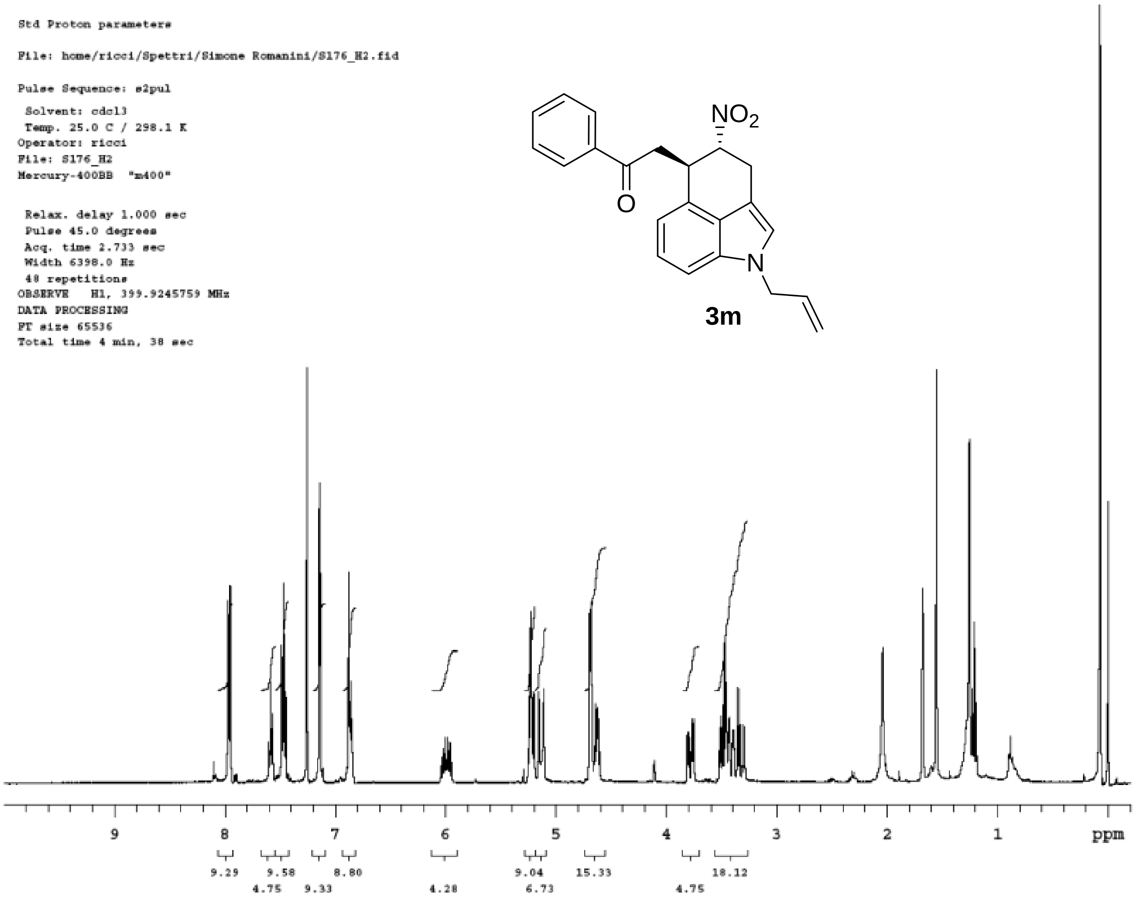
Std Proton parameters
File: home/ricci/Spettri/Simone Romanini/S176_H2.fid
Pulse Sequence: s2pul
Solvent: cdcl3
Temp. 25.0 C / 298.1 K
Operator: ricci
File: S176_H2
Mercury-400BB "m400"
Relax. delay 1.000 sec
Pulse 45.0 degrees
Acq. time 2.733 sec
Width 6398.0 Hz
48 repetitions
OBSERVE H1, 399.9245759 MHz
DATA PROCESSING
FT size 65536
Total time 4 min, 38 sec
NO2
O
N
3m
9
8
7
6
5
4
3
2
1
ppm
9.29
4.75
9.58
9.33
8.80
4.28
9.04
6.73
15.33
4.75
18.12

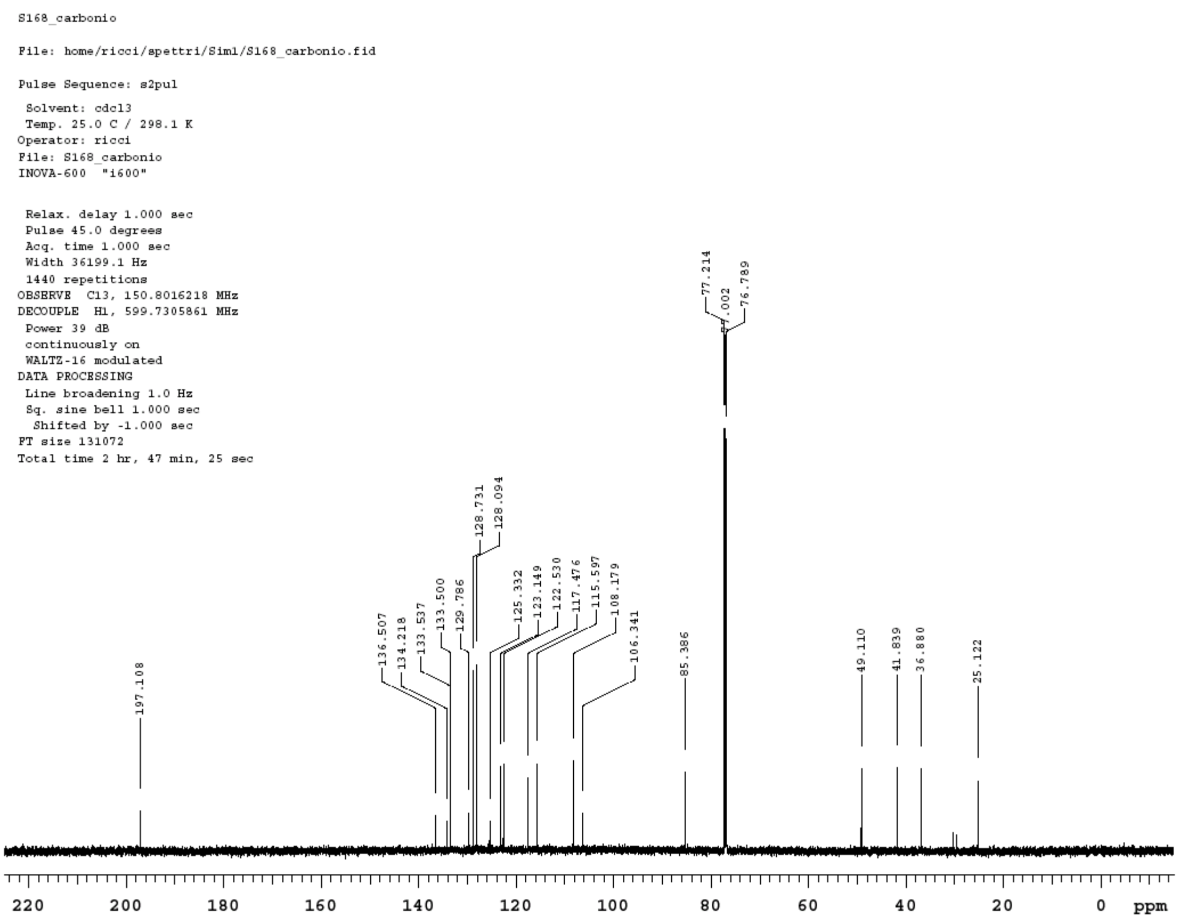
S168_carbonio
File: home/ricci/spettri/Sim1/S168_carbonio.fid
Pulse Sequence: s2pul
Solvent: cdcl3
Temp. 25.0 C / 298.1 K
Operator: ricci
File: S168_carbonio
INOVA-600 "i600"
Relax. delay 1.000 sec
Pulse 45.0 degrees
Acq. time 1.000 sec
Width 36199.1 Hz
1440 repetitions
OBSERVE C13, 150.8016218 MHz
DECOUPLE H1, 599.7305861 MHz
Power 39 dB
continuously on
WALTZ-16 modulated
DATA PROCESSING
Line broadening 1.0 Hz
Sq. sine bell 1.000 sec
Shifted by -1.000 sec
FT size 131072
Total time 2 hr, 47 min, 25 sec
197.108
136.507
134.218
133.537
133.500
129.786
128.731
128.094
125.332
123.149
122.530
117.476
115.597
108.179
106.341
85.386
77.214
77.002
76.789
49.110
41.839
36.880
25.122
220
200
180
160
140
120
100
80
60
40
20
0
ppm

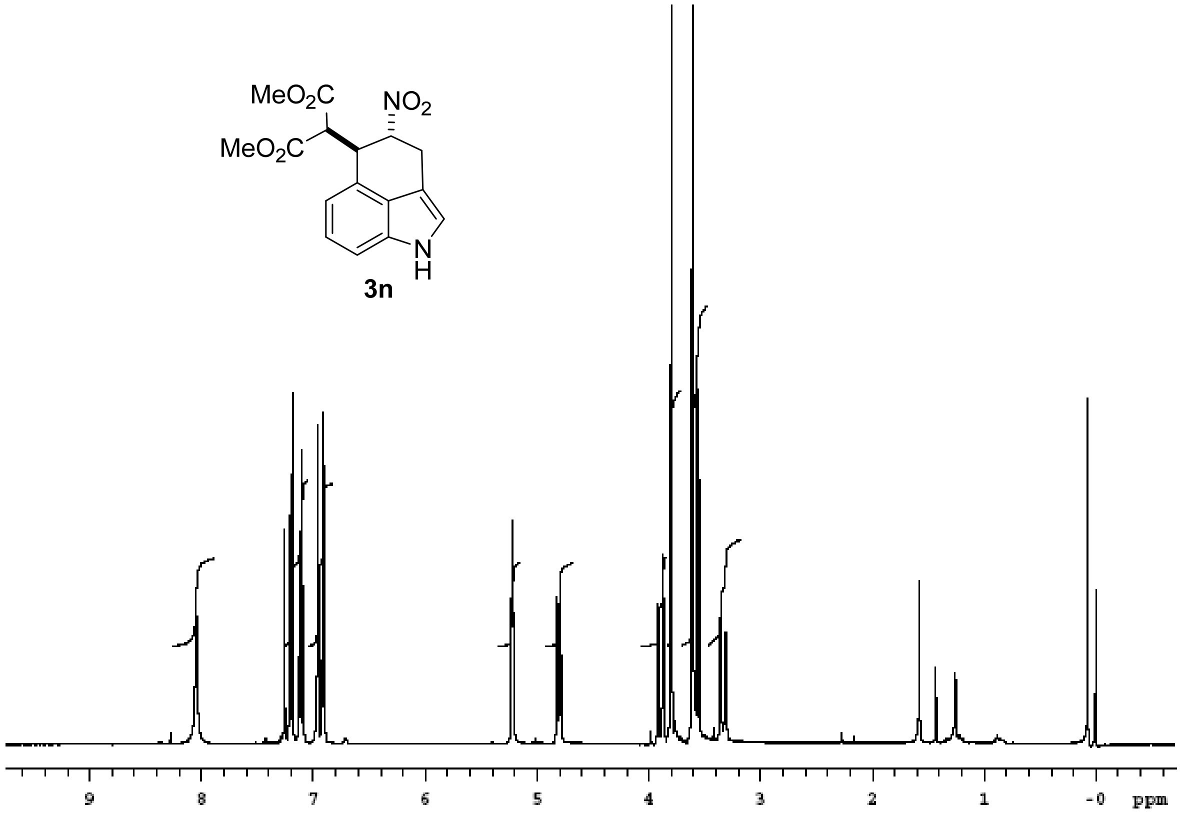
MeO2C
NO2
MeO2C
N
H
3n
9
8
7
6
5
4
3
2
1
-0
ppm

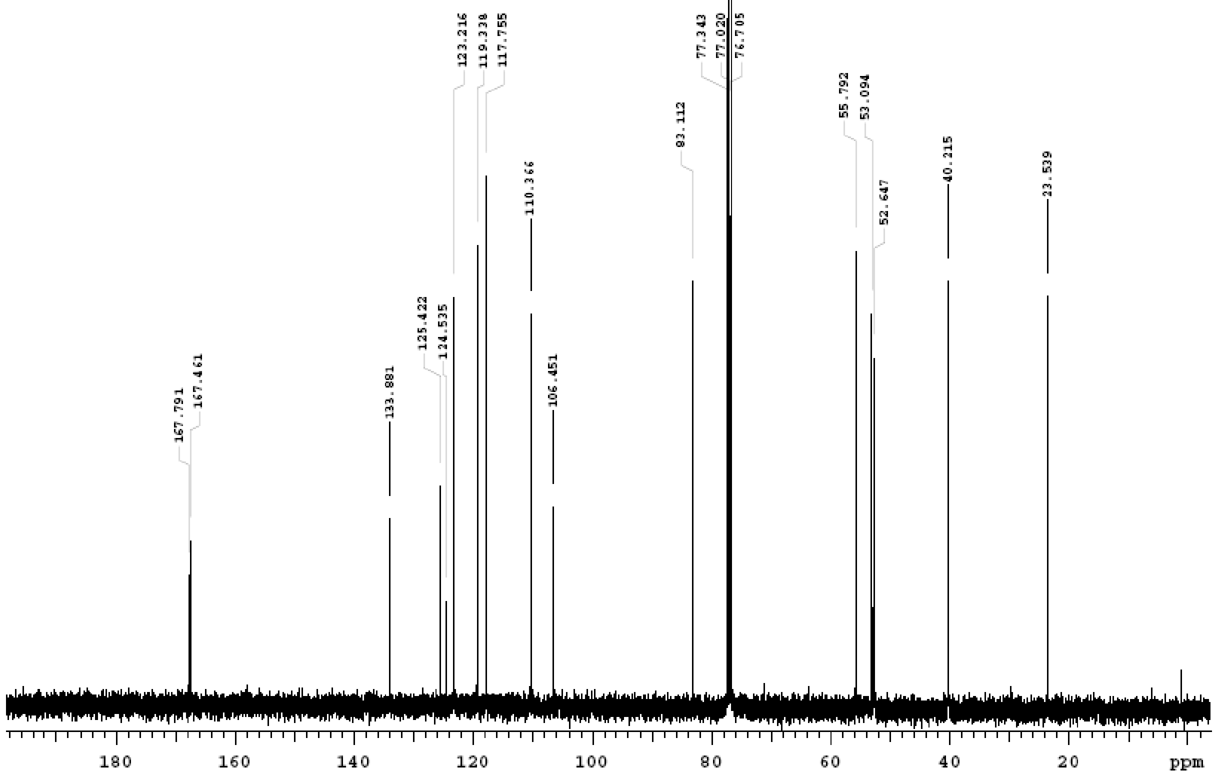
167.791
167.461
133.881
125.422
124.535
123.216
119.338
117.755
110.366
106.451
83.112
77.343
77.020
76.705
55.792
53.094
52.647
40.215
23.539
180
160
140
120
100
80
60
40
20
ppm

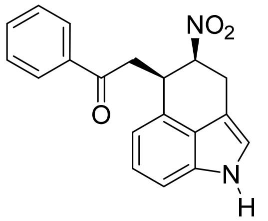

NO2
O
N
H

4a

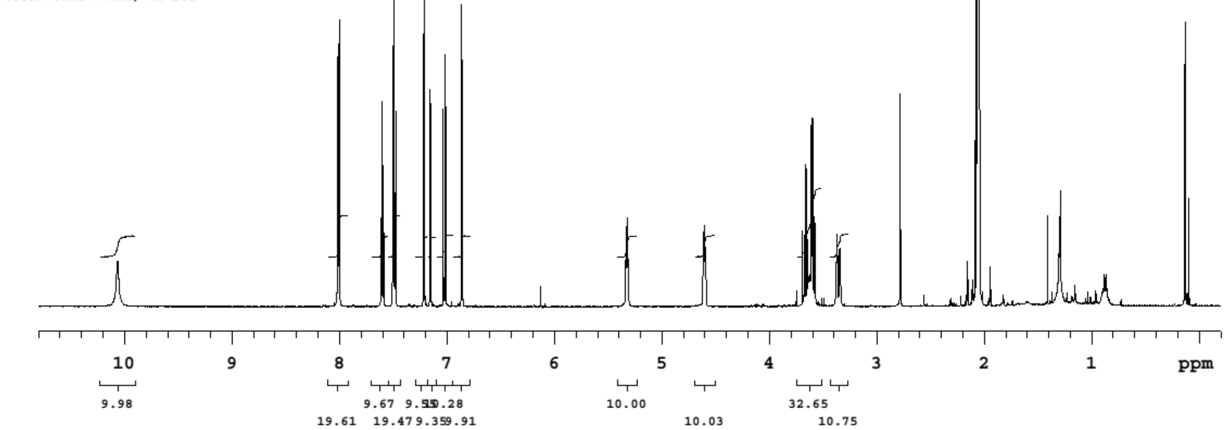

Solvent: Acetone
Temp. 30.0 C / 303.1 K
Operator: lunazzi
File: NACCA-233A-protone30c
INOVA-600
Relax. delay 1.000 sec
Pulse 45.0 degrees
Acq. time 2.990 sec
Width 9611.9 Hz
16 repetitions
OBSERVE H1, 599.7306975 MHz
DATA PROCESSING
FT size 65536
Total time 1 min, 11 sec
10
9
8
7
6
5
4
3
2
1
ppm
9.98
19.61
9.67
19.47
9.35
9.91
10.00
10.03
32.65
10.75

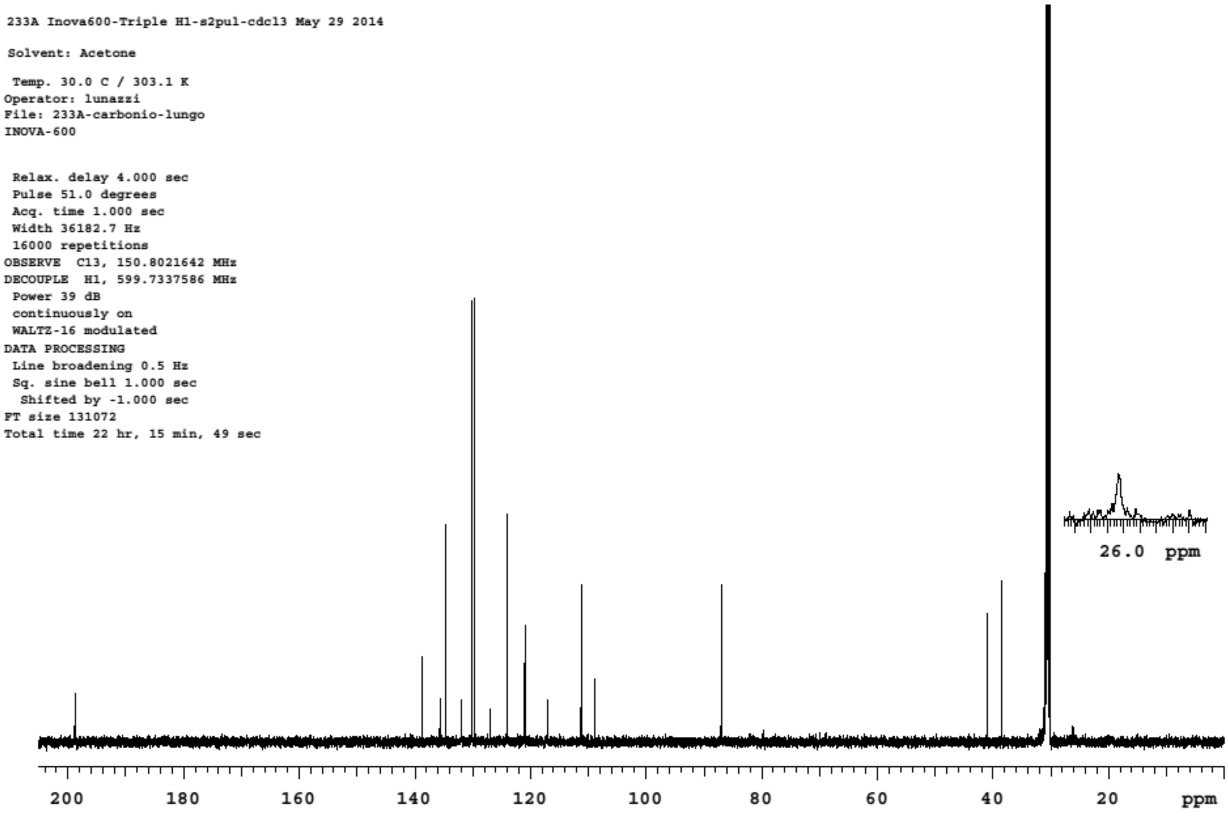

233A Inova600-Triple H1-s2pul-cdcl3 May 29 2014
Solvent: Acetone
Temp. 30.0 C / 303.1 K
Operator: lunazzi
File: 233A-carbonio-lungo
INOVA-600
Relax. delay 4.000 sec
Pulse 51.0 degrees
Acq. time 1.000 sec
Width 36182.7 Hz
16000 repetitions
OBSERVE C13, 150.8021642 MHz
DECOUPLE H1, 599.7337586 MHz
Power 39 dB
continuously on
WALTZ-16 modulated
DATA PROCESSING
Line broadening 0.5 Hz
Sq. sine bell 1.000 sec
Shifted by -1.000 sec
FT size 131072
Total time 22 hr, 15 min, 49 sec
26.0 ppm
200
180
160
140
120
100
80
60
40
20
ppm

Copies of the HPLC traces

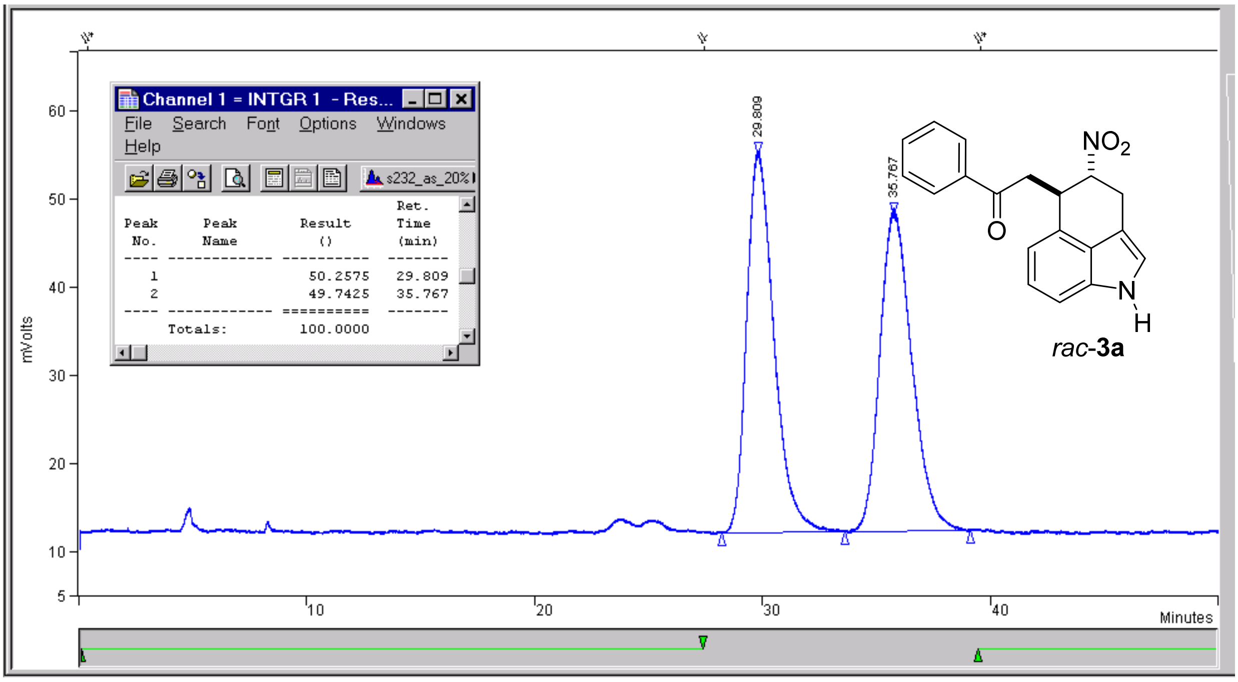

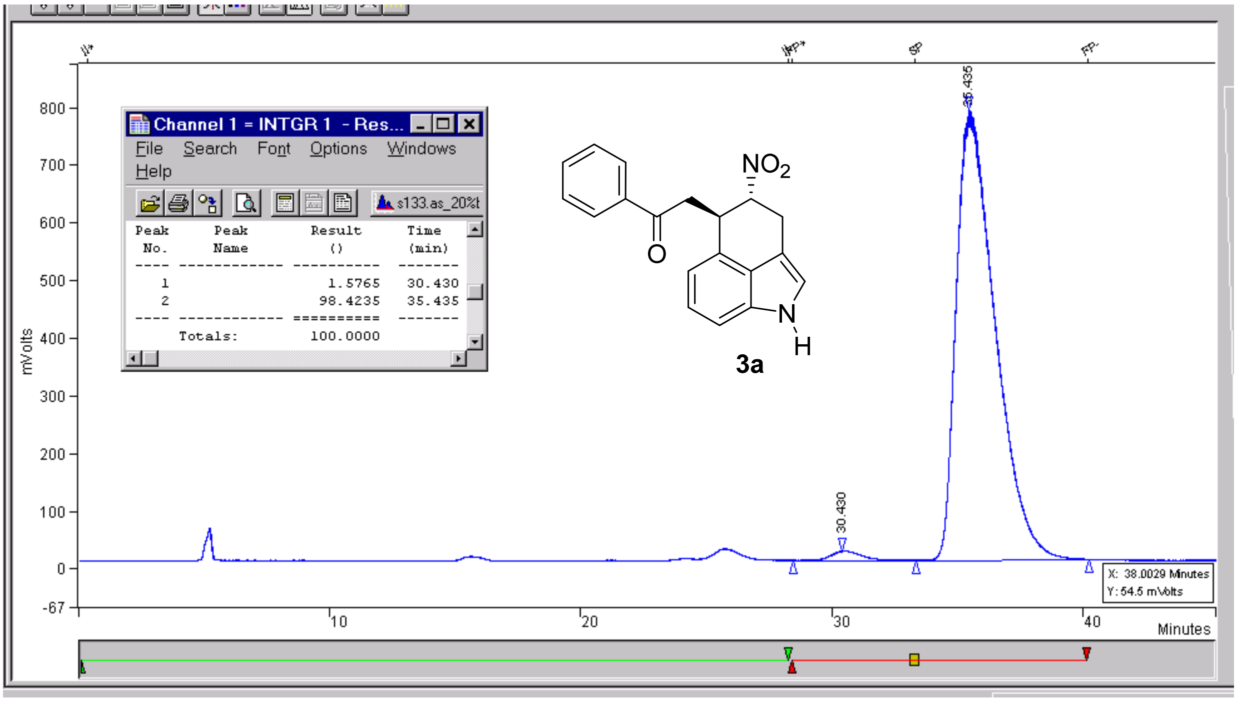

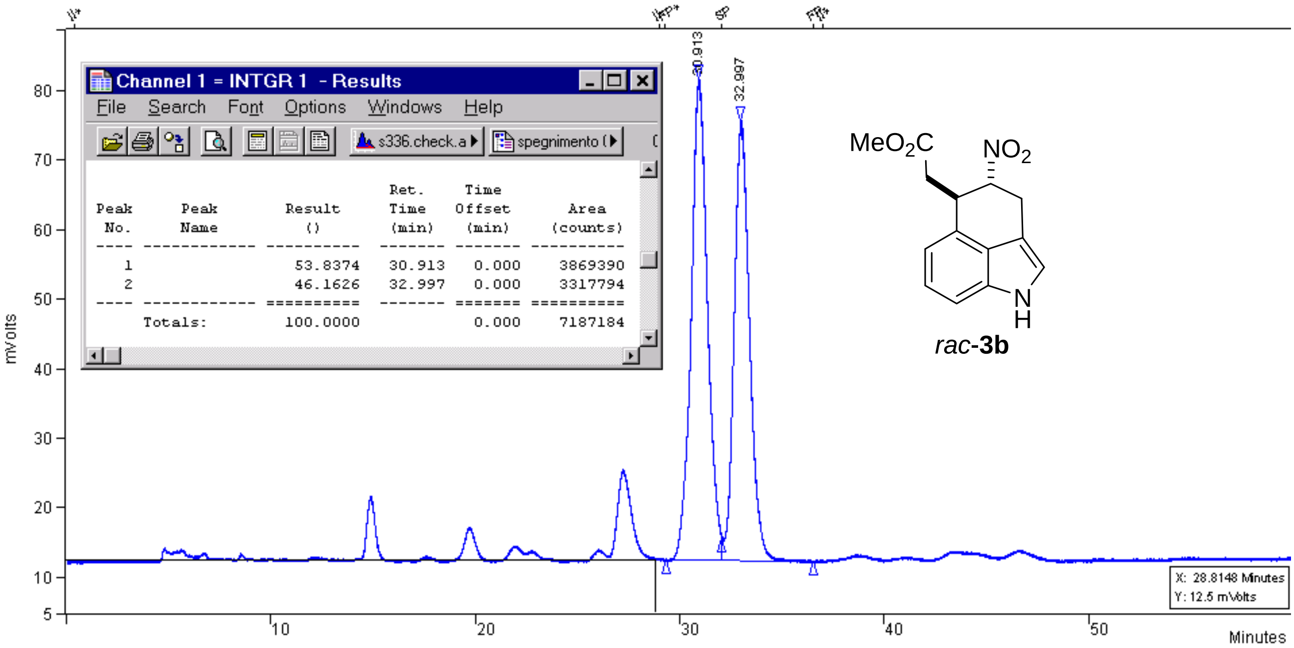

Peak No.	Peak Name	Result ()	Ret. Time (min)	Time Offset (min)	Area (counts)
1		53.8374	30.913	0.000	3869390
2		46.1626	32.997	0.000	3317794
	Totals:	100.0000		0.000	7187184

rac-**3b**

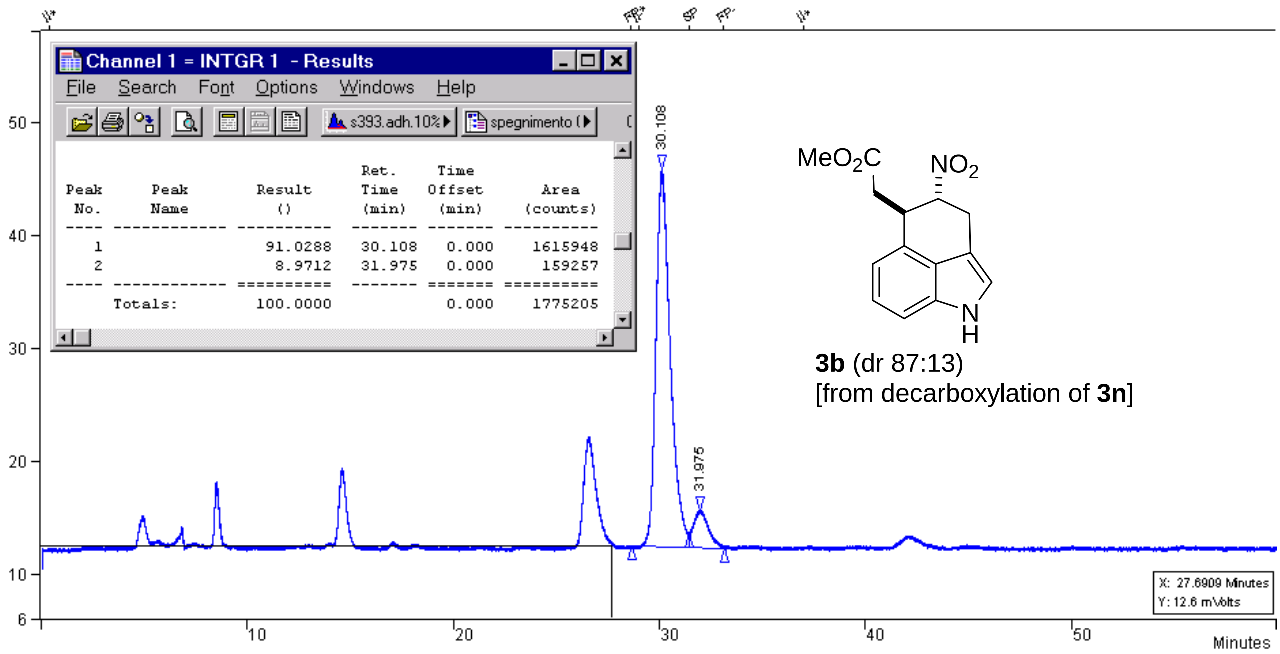

Peak No.	Peak Name	Result ()	Ret. Time (min)	Time Offset (min)	Area (counts)
1		91.0288	30.108	0.000	1615948
2		8.9712	31.975	0.000	159257
	Totals:	100.0000		0.000	1775205

3b (dr 87:13)
[from decarboxylation of **3n**]

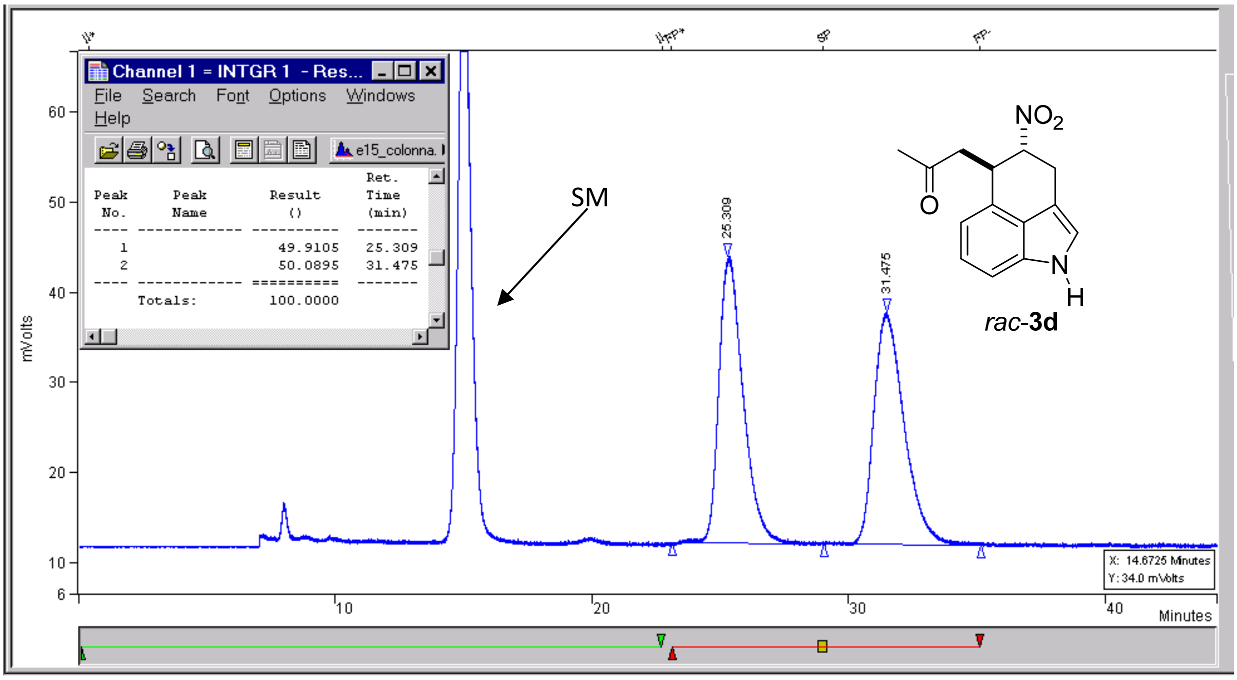

Channel 1 = INTGR 1 - Res...
File Search Font Options Windows Help
e15_colonna.
Peak No. | Peak Name | Result () | Ret. Time (min)
1 | | 49.9105 | 25.309
2 | | 50.0895 | 31.475
Totals: | | 100.0000 |
SM
25.309
31.475
NO_2
O
N
H
rac-3d
mVolts
Minutes
X: 14.6725 Minutes
Y: 34.0 mVolts

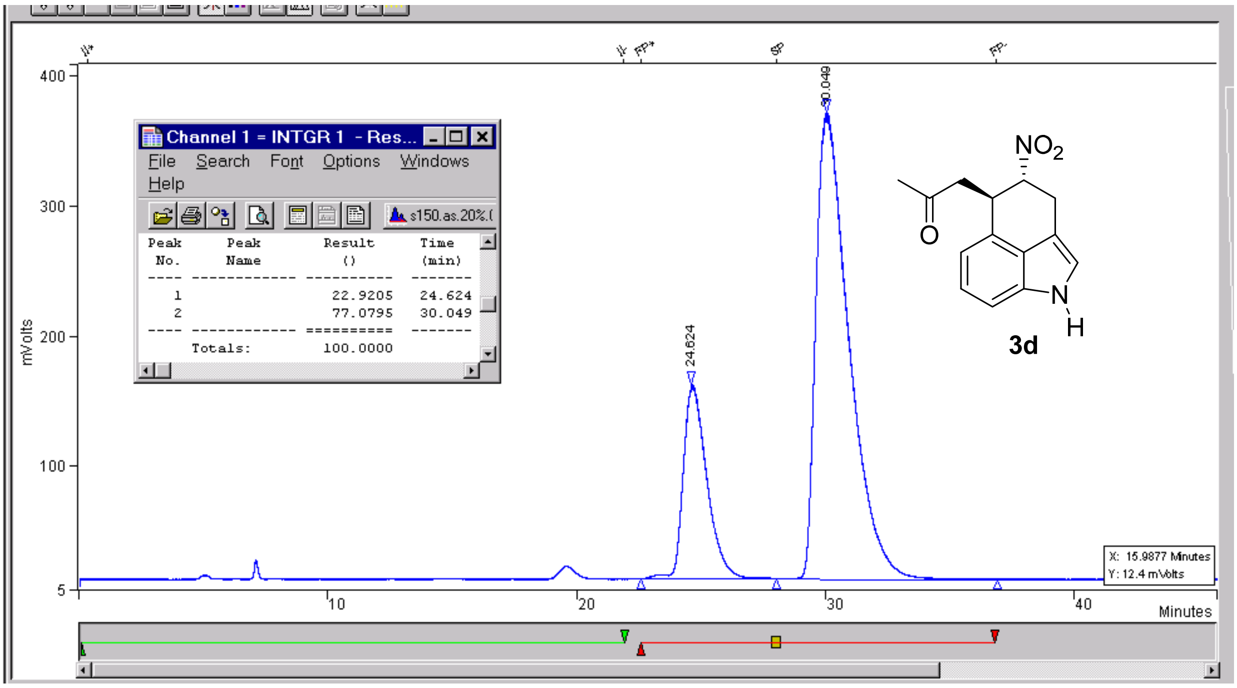

Channel 1 = INTGR 1 - Res...
File Search Font Options Windows Help
s150.as.20%.
Peak No. | Peak Name | Result () | Time (min)
1 | | 22.9205 | 24.624
2 | | 77.0795 | 30.049
Totals: | | 100.0000 |
24.624
30.049
NO_2
O
N
H
3d
mVolts
Minutes
X: 15.9877 Minutes
Y: 12.4 mVolts

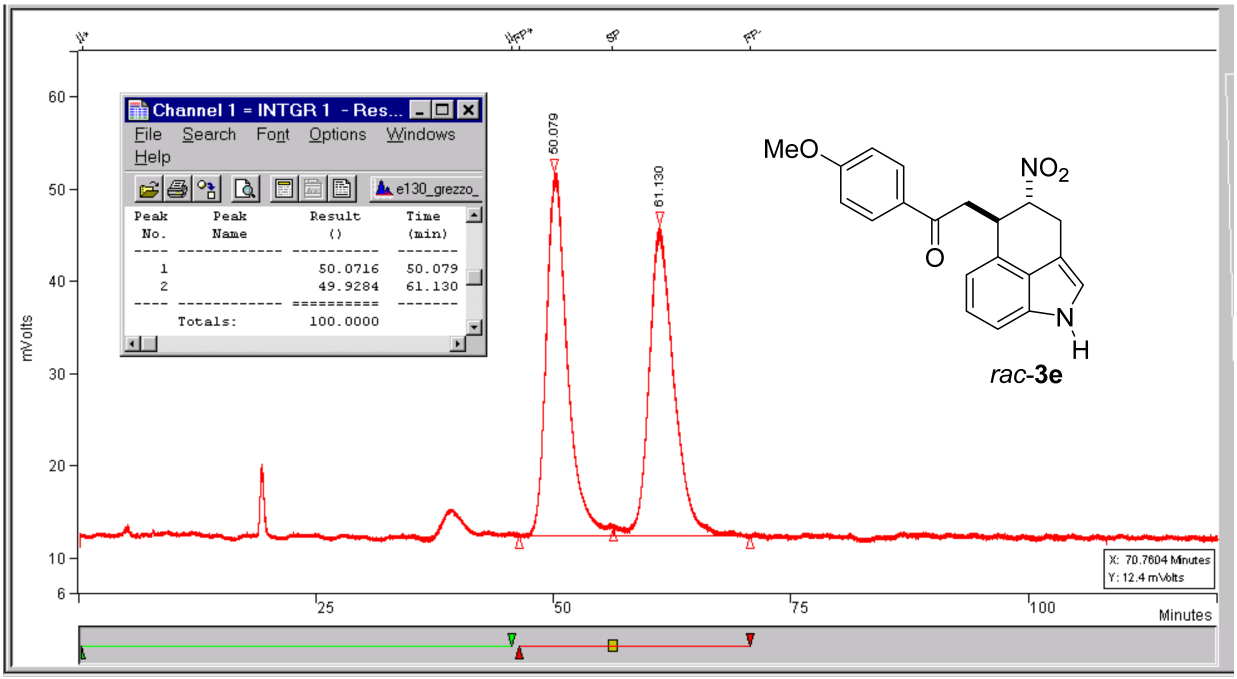
Channel 1 = INTGR 1 - Res...
File Search Font Options Windows Help
e130_grezzo_
Peak No. | Peak Name | Result () | Time (min)
1 | | 50.0716 | 50.079
2 | | 49.9284 | 61.130
Totals: | | 100.0000 |
MeO
NO2
O
N
H
rac-3e
mVolts
Minutes
X: 70.7604 Minutes
Y: 12.4 mVolts

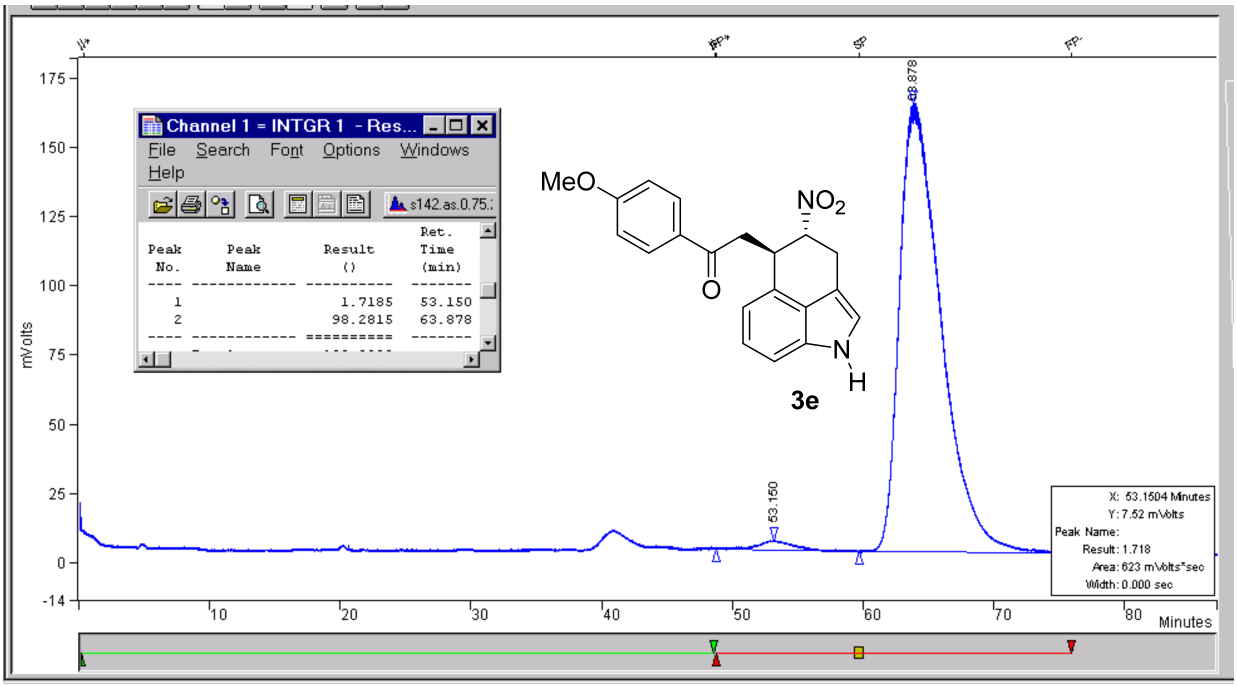
Channel 1 = INTGR 1 - Res...
File Search Font Options Windows Help
s142.as.0.75.
Peak No. | Peak Name | Result () | Ret. Time (min)
1 | | 1.7185 | 53.150
2 | | 98.2815 | 63.878
MeO
NO2
O
N
H
3e
mVolts
Minutes
X: 53.1504 Minutes
Y: 7.52 mVolts
Peak Name:
Result: 1.718
Area: 623 mVolts*sec
Width: 0.000 sec

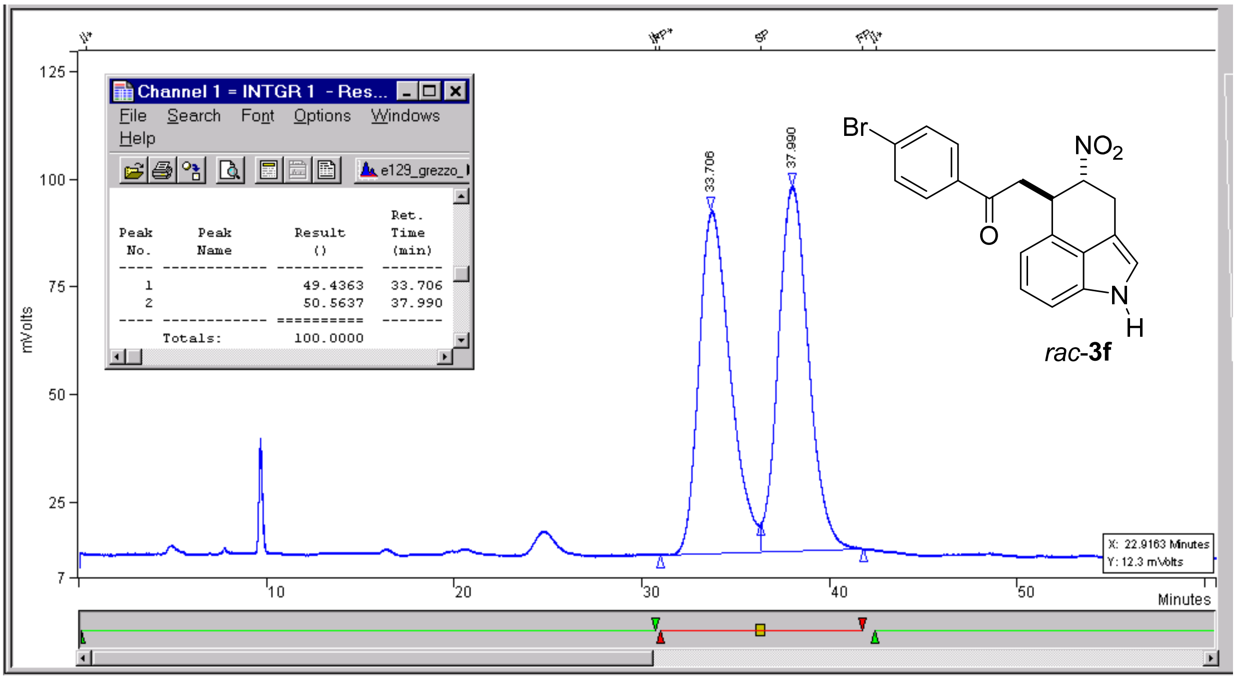
Channel 1 = INTGR 1 - Res...
File Search Font Options Windows Help
e129_grezzo_
Peak No. | Peak Name | Result () | Ret. Time (min)
1 | | 49.4363 | 33.706
2 | | 50.5637 | 37.990
Totals: | | 100.0000 |
33.706
37.990
mVolts
Minutes
X: 22.9163 Minutes
Y: 12.3 mVolts
Br
NO2
O
N
H
rac-3f

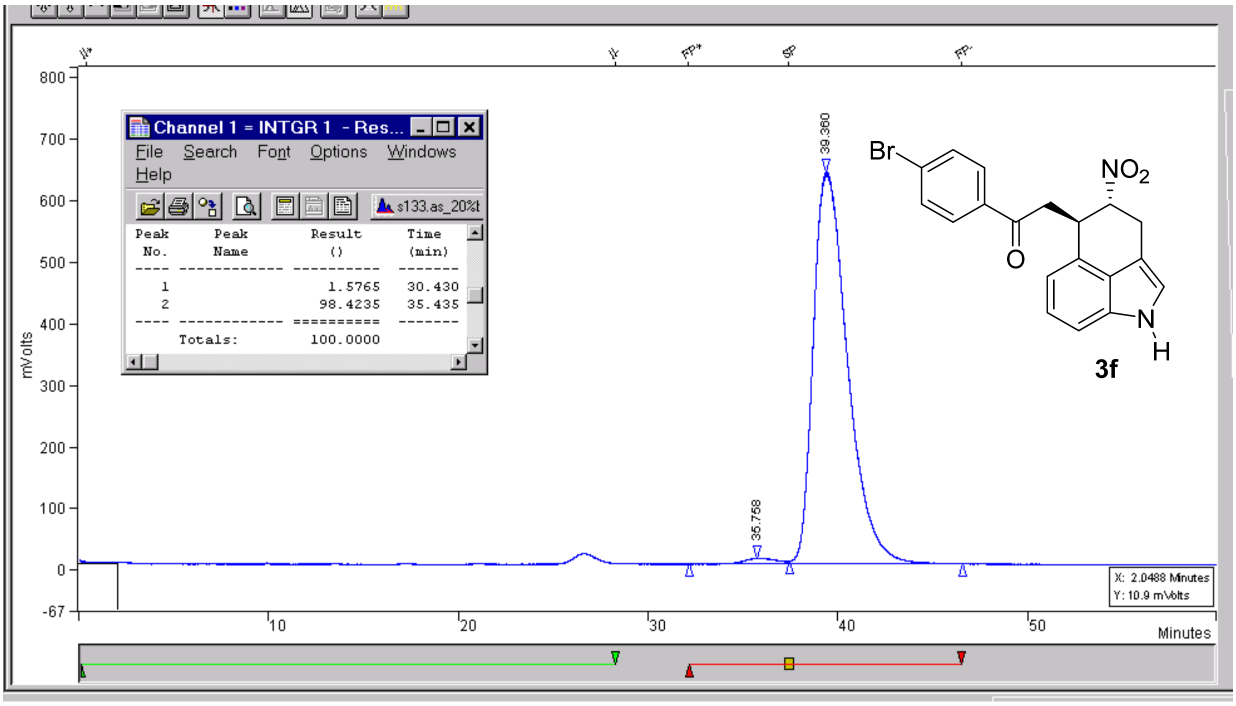
Channel 1 = INTGR 1 - Res...
File Search Font Options Windows Help
s133.as_20%
Peak No. | Peak Name | Result () | Time (min)
1 | | 1.5765 | 30.430
2 | | 98.4235 | 35.435
Totals: | | 100.0000 |
39.360
35.758
mVolts
Minutes
X: 2.0488 Minutes
Y: 10.9 mVolts
Br
NO2
O
N
H
3f

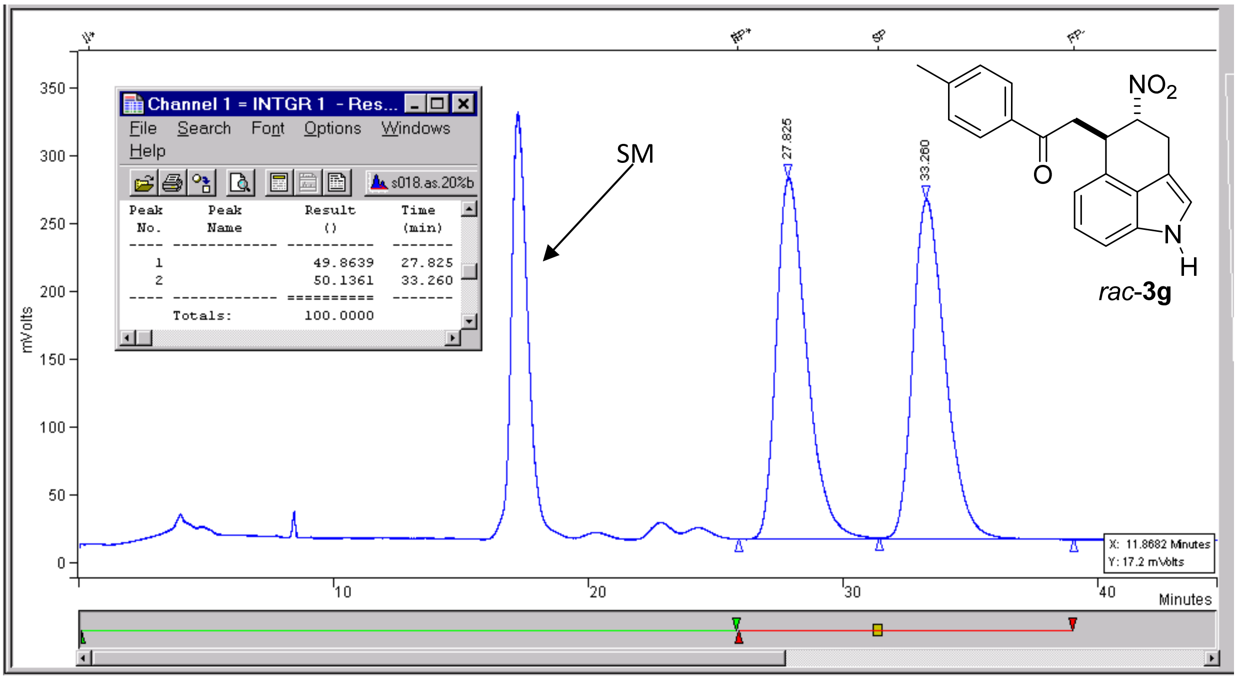

Channel 1 = INTGR 1 - Res...
File Search Font Options Windows Help
s018.as.20%b
Peak No. | Peak Name | Result () | Time (min)
1 | | 49.8639 | 27.825
2 | | 50.1361 | 33.260
Totals: | | 100.0000 |
SM
27.825
33.260
NO_2
O
N
H
rac-3g
mVolts
Minutes
X: 11.8682 Minutes
Y: 17.2 mVolts

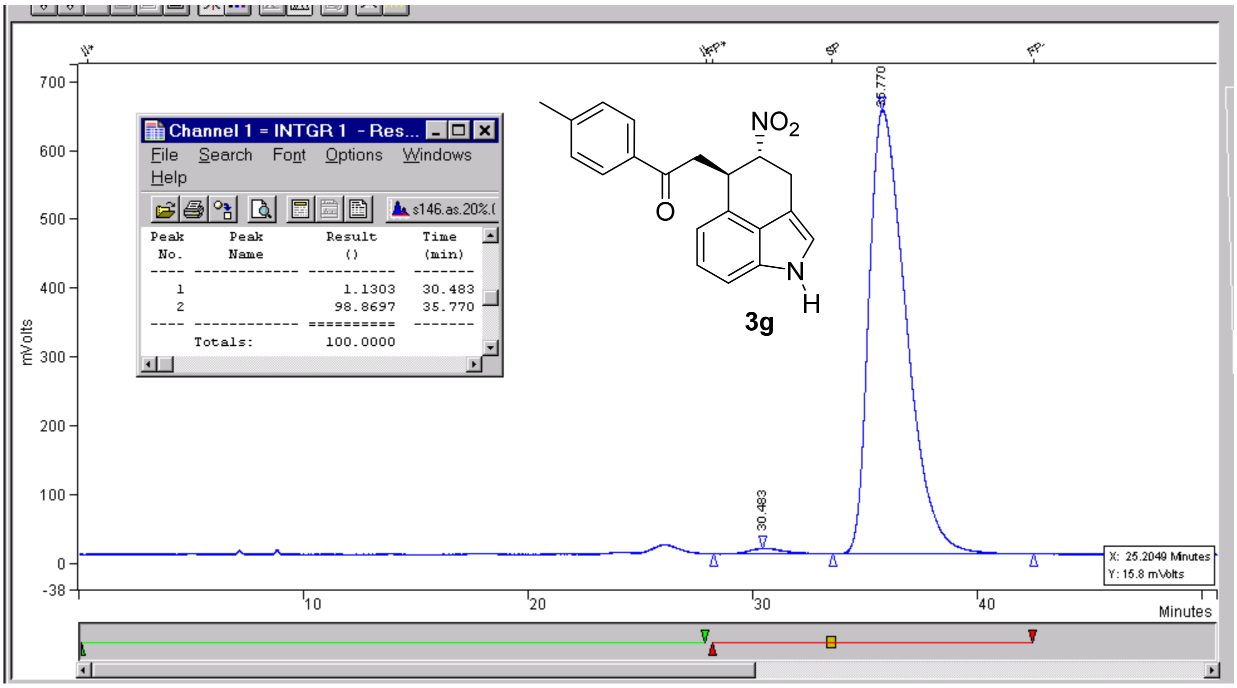

Channel 1 = INTGR 1 - Res...
File Search Font Options Windows Help
s146.as.20%.(
Peak No. | Peak Name | Result () | Time (min)
1 | | 1.1303 | 30.483
2 | | 98.8697 | 35.770
Totals: | | 100.0000 |
30.483
35.770
NO_2
O
N
H
3g
mVolts
Minutes
X: 25.2049 Minutes
Y: 15.8 mVolts

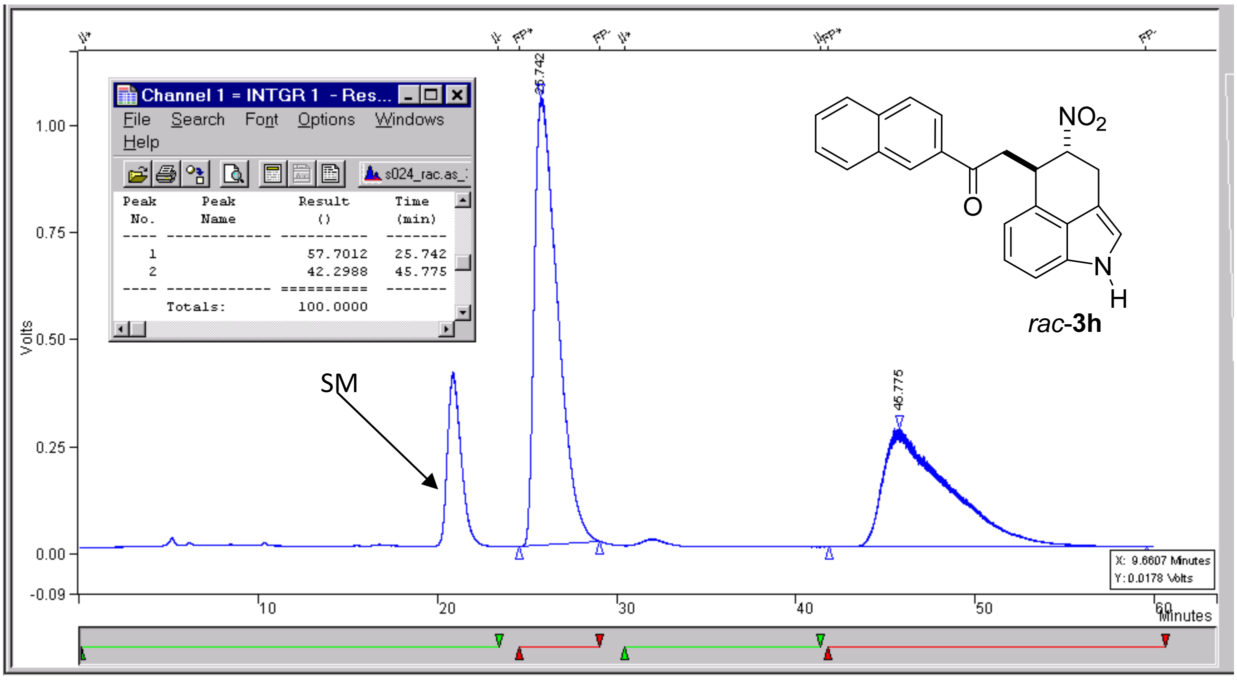
Channel 1 = INTGR 1 - Res...
File Search Font Options Windows Help
s024_rac.as
Peak No. | Peak Name | Result () | Time (min)
1 | | 57.7012 | 25.742
2 | | 42.2988 | 45.775
Totals: 100.0000
SM
25.742
45.775
NO_2
O
N
H
rac-**3h**
Volts
1.00
0.75
0.50
0.25
0.00
-0.09
10
20
30
40
50
60
Minutes
X: 9.6607 Minutes
Y: 0.0178 Volts

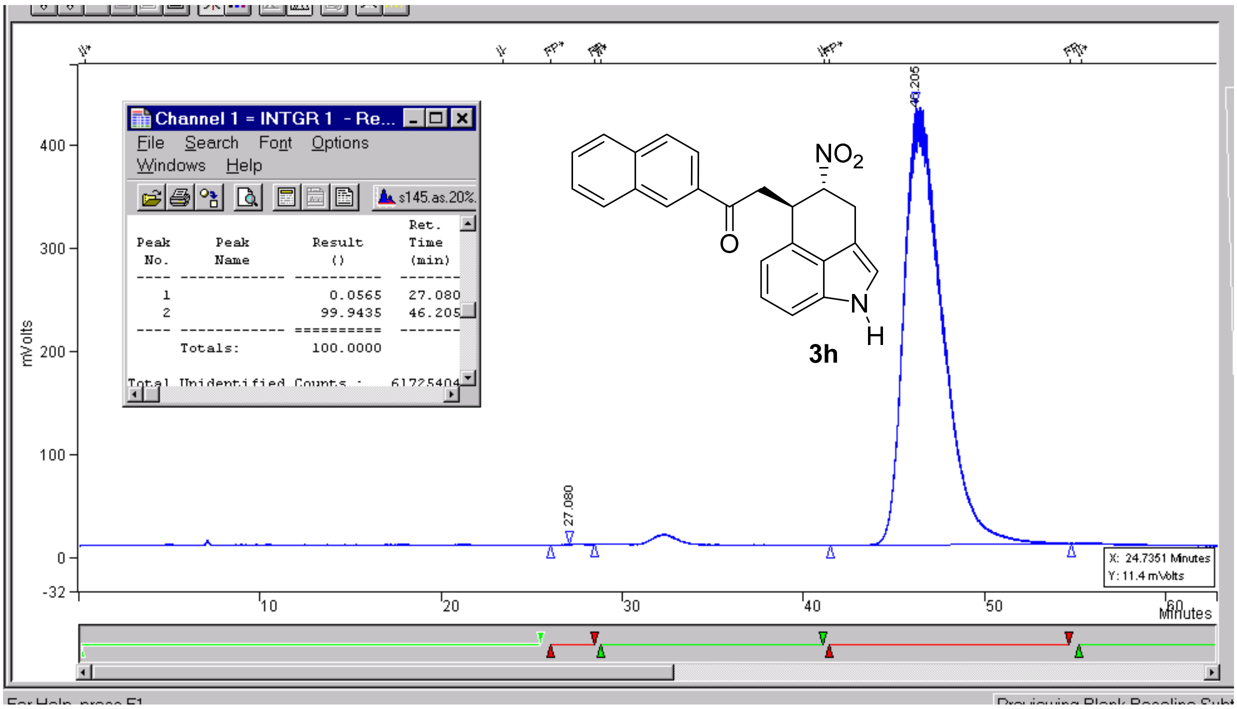
Channel 1 = INTGR 1 - Re...
File Search Font Options Windows Help
s145.as.20%
Peak No. | Peak Name | Result () | Ret. Time (min)
1 | | 0.0565 | 27.080
2 | | 99.9435 | 46.205
Totals: 100.0000
Total Unidentified Counts : 61725404
27.080
46.205
NO_2
O
N
H
3h
mVolts
400
300
200
100
0
-32
10
20
30
40
50
60
Minutes
X: 24.7351 Minutes
Y: 11.4 mVolts

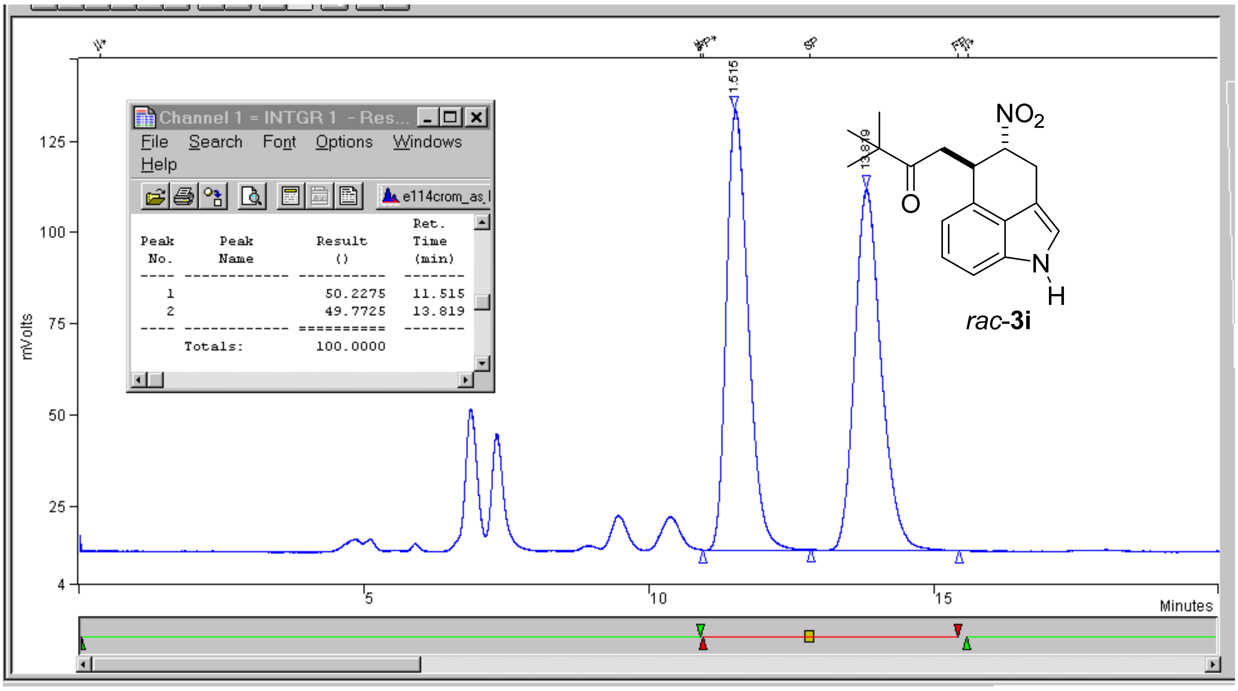
Channel 1 = INTGR 1 - Res...
File Search Font Options Windows Help
e114crom_as_l
Peak No. | Peak Name | Result () | Ret. Time (min)
1 | | 50.2275 | 11.515
2 | | 49.7725 | 13.819
Totals: | | 100.0000 |
11.515
13.819
mVolts
Minutes
NO2
O
N
H
rac-3i

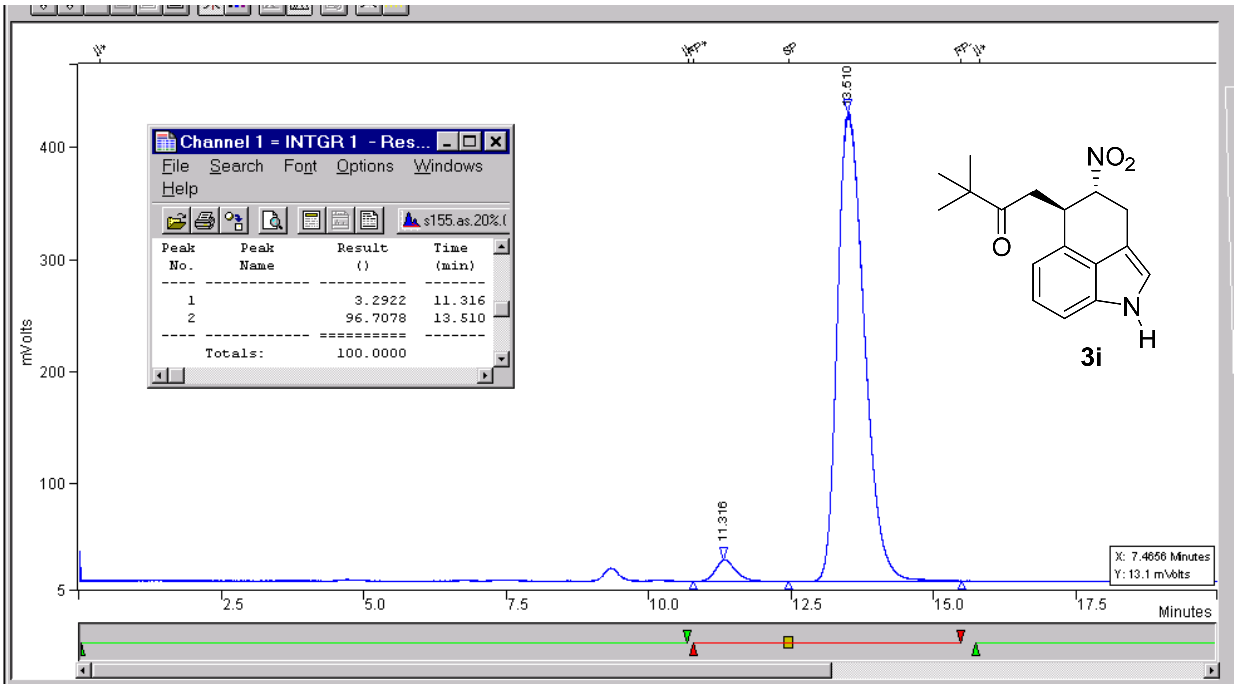
Channel 1 = INTGR 1 - Res...
File Search Font Options Windows Help
s155.as.20%.(
Peak No. | Peak Name | Result () | Time (min)
1 | | 3.2922 | 11.316
2 | | 96.7078 | 13.510
Totals: | | 100.0000 |
13.510
11.316
X: 7.4656 Minutes
Y: 13.1 mVolts
mVolts
Minutes
NO2
O
N
H
3i

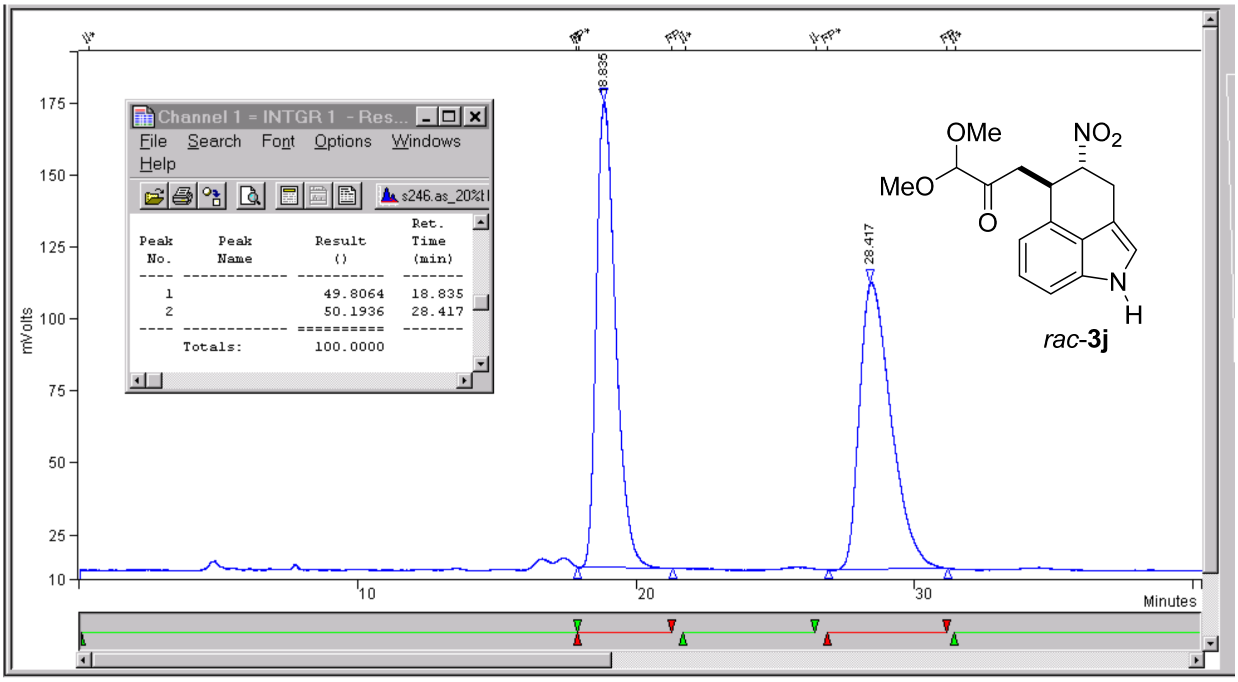
Channel 1 = INTGR 1 - Res...
File Search Font Options Windows Help
s246.as_20%
Peak No. | Peak Name | Result () | Ret. Time (min)
1 | | 49.8064 | 18.835
2 | | 50.1936 | 28.417
Totals: | | 100.0000 |
18.835
28.417
mVolts
Minutes
OMe
MeO
O
NO2
N
H
rac-3j

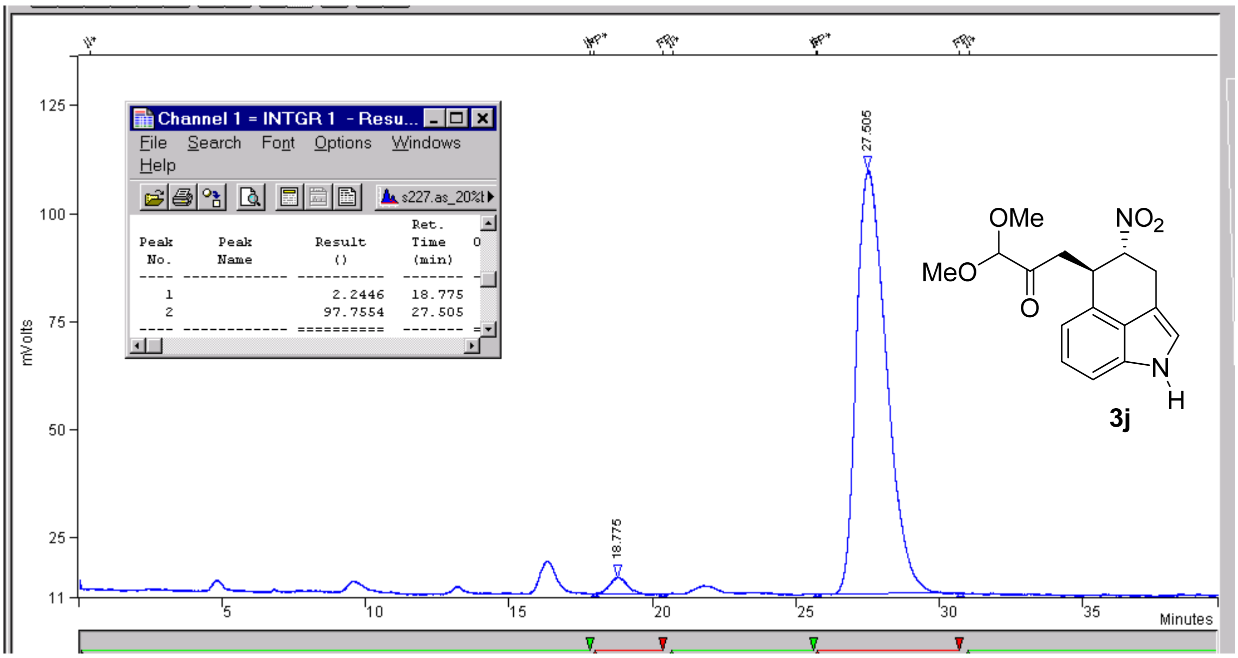
Channel 1 = INTGR 1 - Resu...
File Search Font Options Windows Help
s227.as_20%
Peak No. | Peak Name | Result () | Ret. Time (min)
1 | | 2.2446 | 18.775
2 | | 97.7554 | 27.505
27.505
18.775
mVolts
Minutes
OMe
MeO
O
NO2
N
H
3j

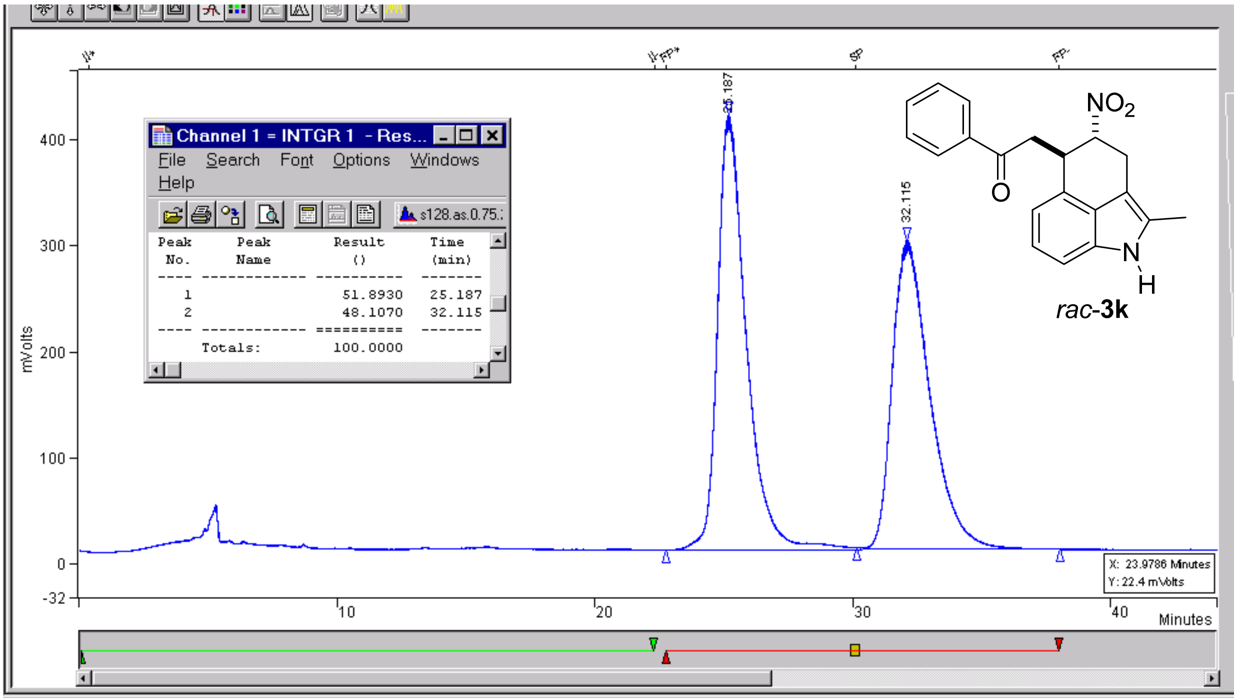
Channel 1 = INTGR 1 - Res...
File Search Font Options Windows Help
s128.as.0.75.
Peak No. | Peak Name | Result () | Time (min)
1 | | 51.8930 | 25.187
2 | | 48.1070 | 32.115
Totals: | | 100.0000 |
25.187
32.115
mVolts
Minutes
X: 23.9786 Minutes
Y: 22.4 mVolts
NO2
O
N
H
rac-3k

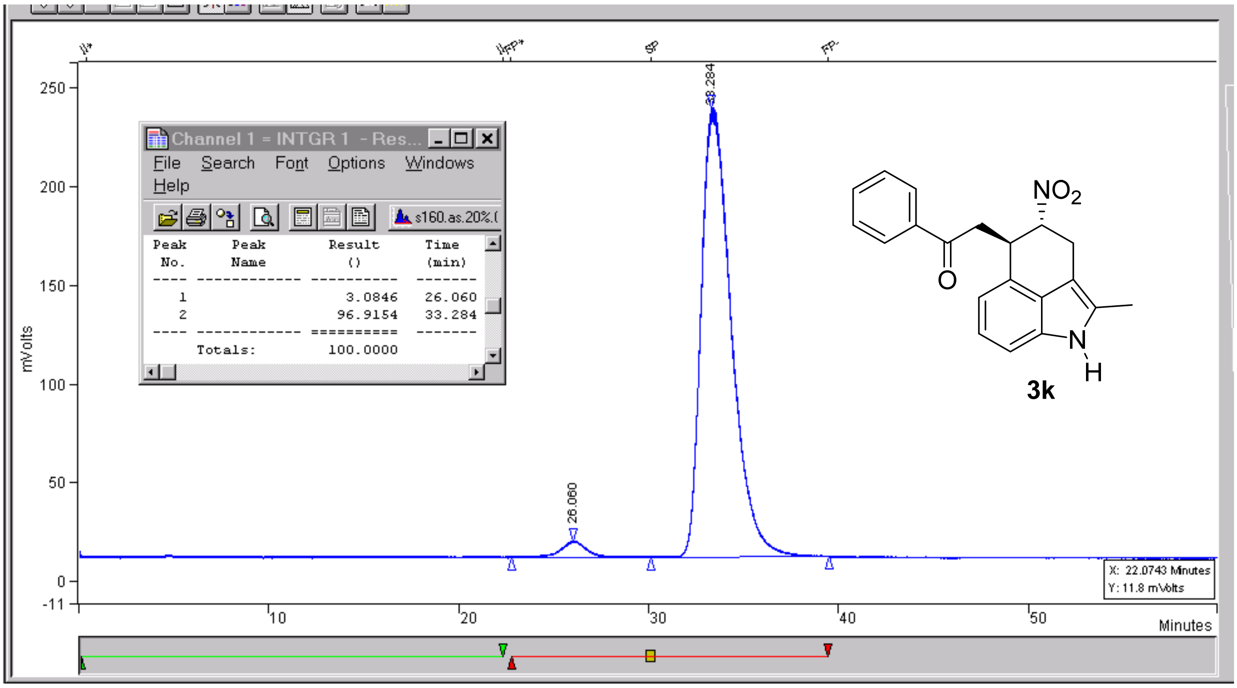
Channel 1 = INTGR 1 - Res...
File Search Font Options Windows Help
s160.as.20%.(
Peak No. | Peak Name | Result () | Time (min)
1 | | 3.0846 | 26.060
2 | | 96.9154 | 33.284
Totals: | | 100.0000 |
26.060
33.284
mVolts
Minutes
X: 22.0743 Minutes
Y: 11.8 mVolts
NO2
O
N
H
3k

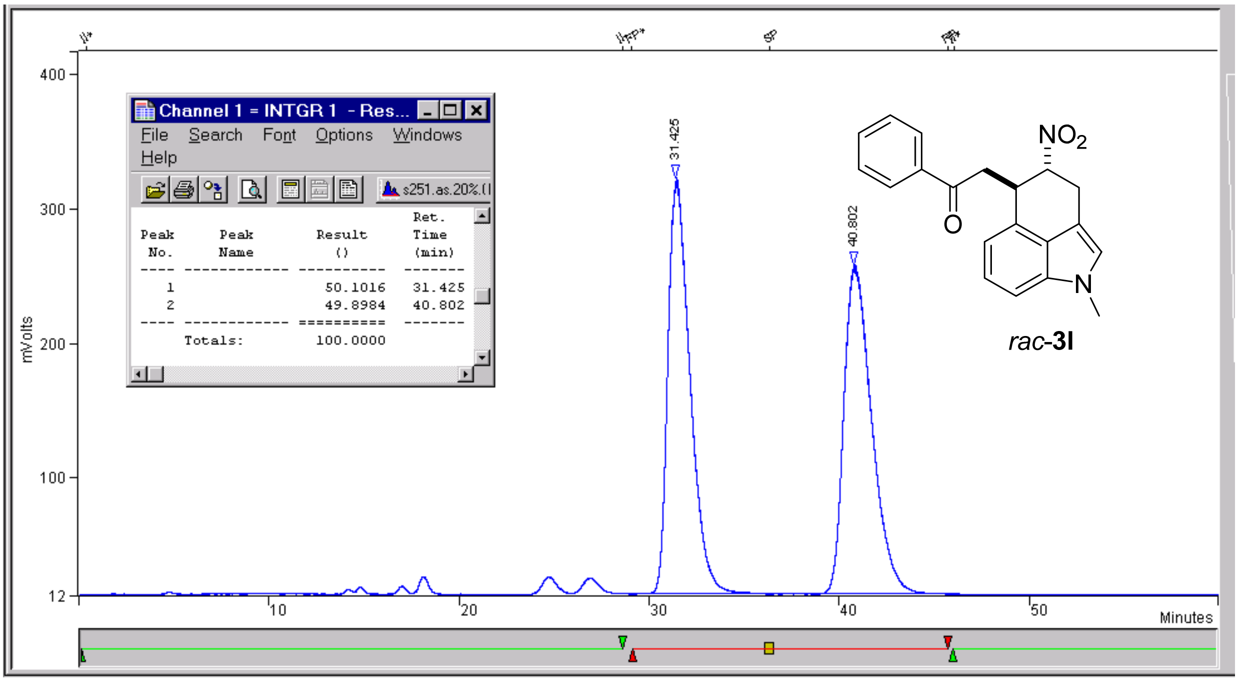

Channel 1 = INTGR 1 - Res...
File Search Font Options Windows Help
Peak No. | Peak Name | Result () | Ret. Time (min)
1 | | 50.1016 | 31.425
2 | | 49.8984 | 40.802
Totals: | | 100.0000 |
31.425
40.802
NO2
O
N
rac-3l
mVolts
Minutes

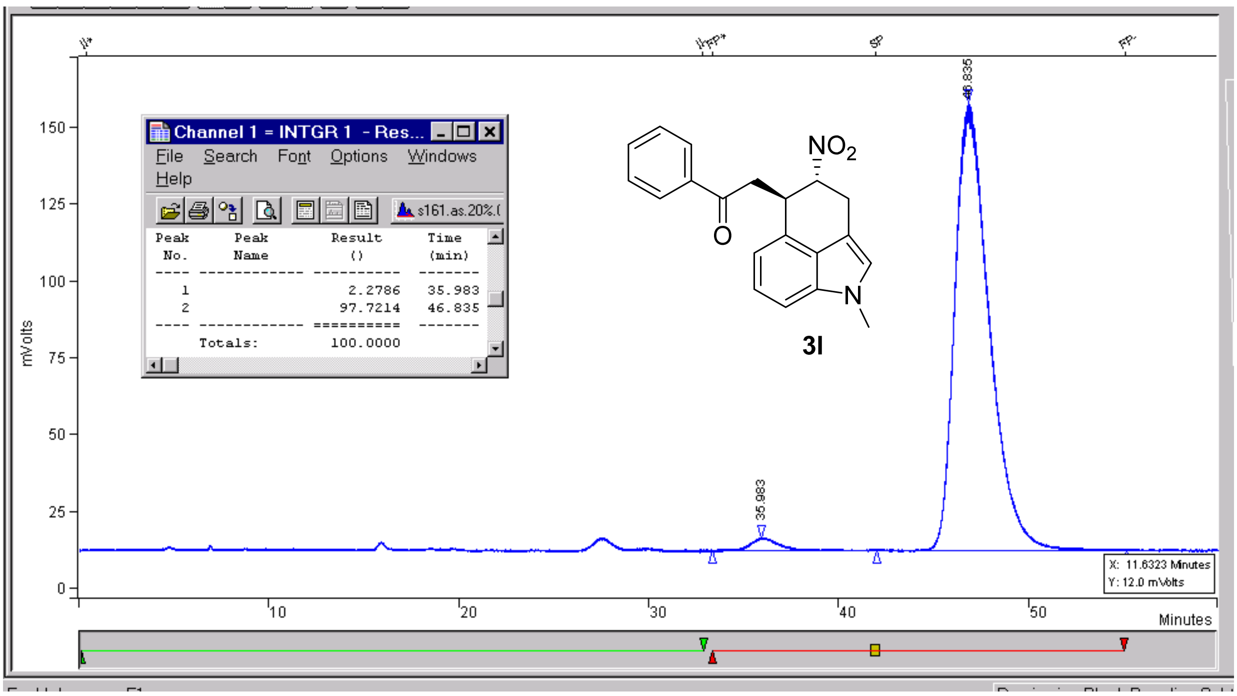

Channel 1 = INTGR 1 - Res...
File Search Font Options Windows Help
Peak No. | Peak Name | Result () | Time (min)
1 | | 2.2786 | 35.983
2 | | 97.7214 | 46.835
Totals: | | 100.0000 |
35.983
46.835
NO2
O
N
3l
mVolts
Minutes
X: 11.6323 Minutes
Y: 12.0 mVolts

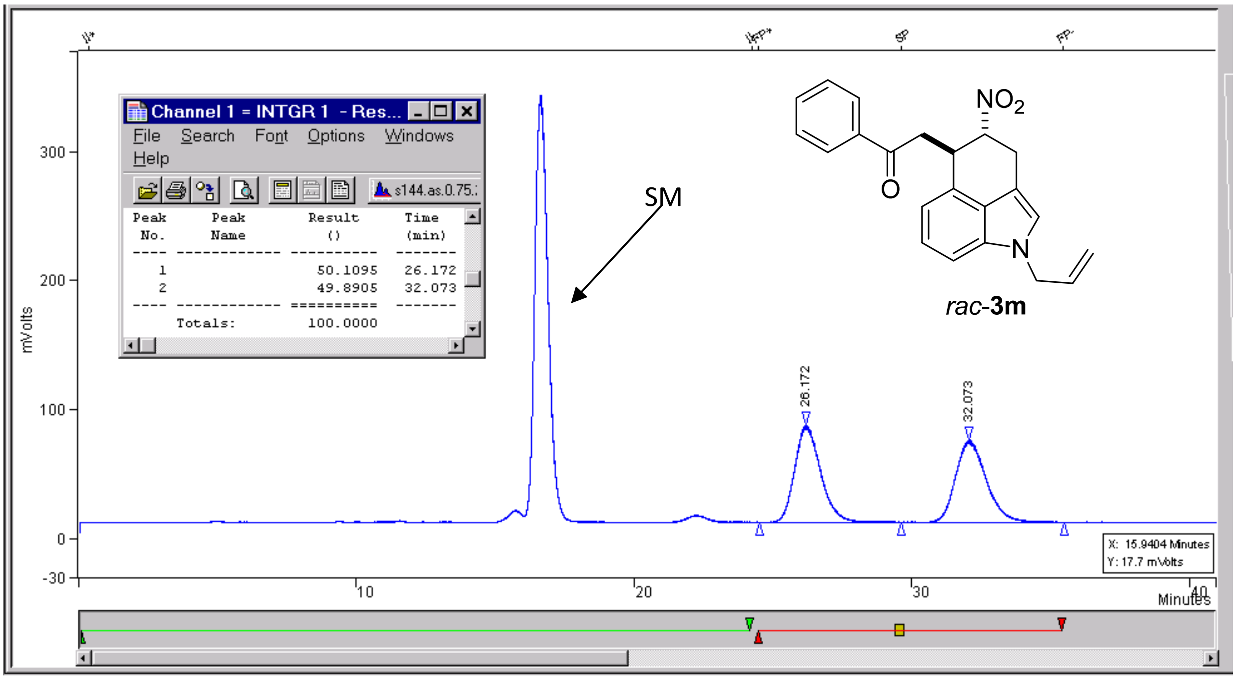
Channel 1 = INTGR 1 - Res...
File Search Font Options Windows Help
s144.as.0.75.
Peak No. | Peak Name | Result () | Time (min)
1 | | 50.1095 | 26.172
2 | | 49.8905 | 32.073
Totals: | | 100.0000 |
SM
NO2
O
N
rac-3m
26.172
32.073
mVolts
300
200
100
0
-30
10
20
30
40
Minutes
X: 15.9404 Minutes
Y: 17.7 mVolts

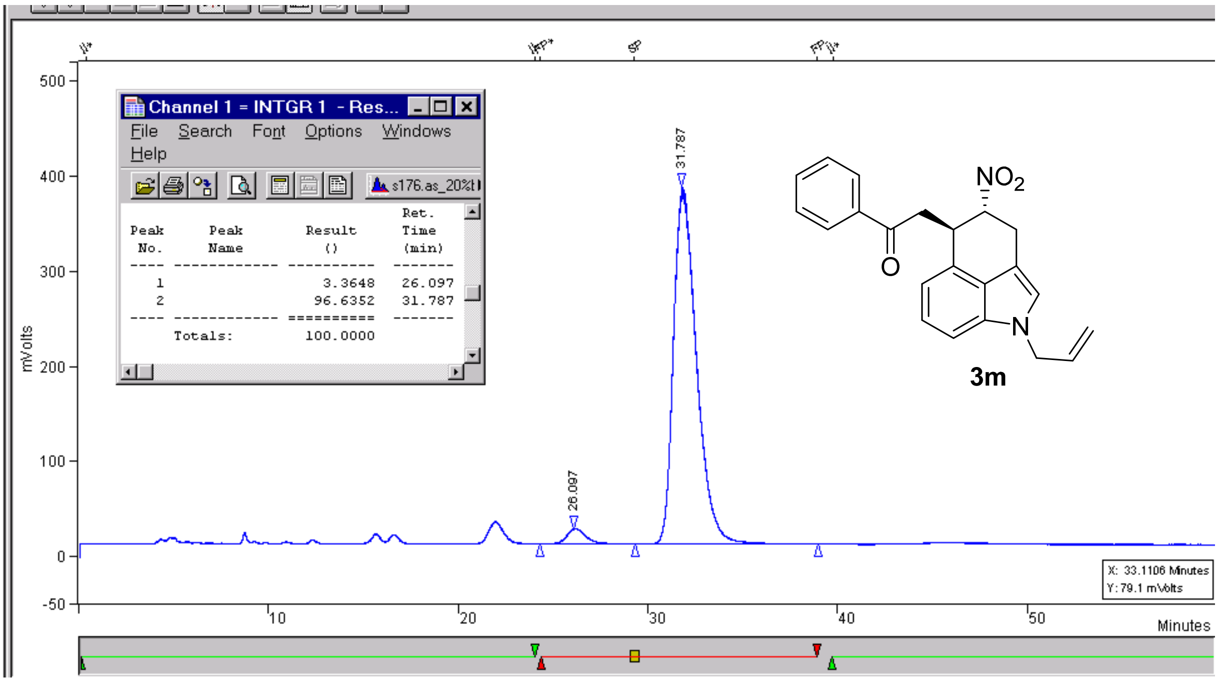
Channel 1 = INTGR 1 - Res...
File Search Font Options Windows Help
s176.as_20%
Peak No. | Peak Name | Result () | Ret. Time (min)
1 | | 3.3648 | 26.097
2 | | 96.6352 | 31.787
Totals: | | 100.0000 |
NO2
O
N
3m
31.787
26.097
mVolts
500
400
300
200
100
0
-50
10
20
30
40
50
Minutes
X: 33.1106 Minutes
Y: 79.1 mVolts

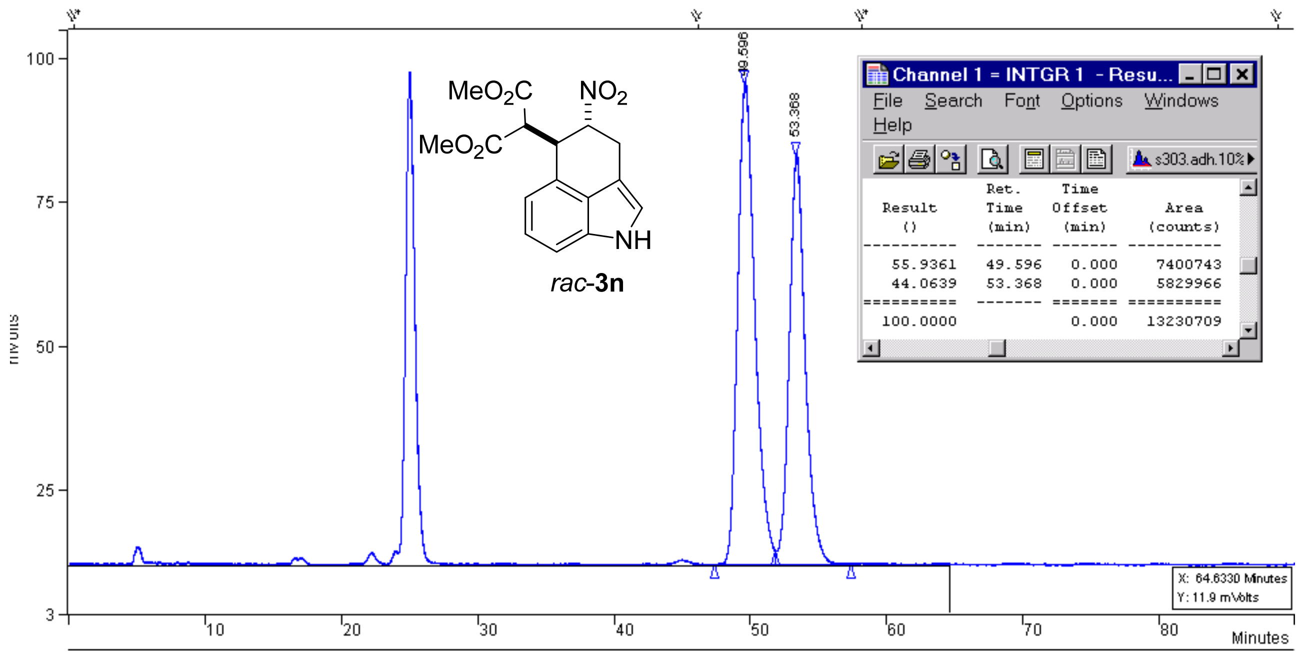

MeO2C NO2
MeO2C
NH
rac-3n
49.596
53.368
Channel 1 = INTGR 1 - Resu...
File Search Font Options Windows Help
s303.adh.10%
Result () | Ret. Time (min) | Time Offset (min) | Area (counts)
55.9361 | 49.596 | 0.000 | 7400743
44.0639 | 53.368 | 0.000 | 5829966
100.0000 | | 0.000 | 13230709
X: 64.6330 Minutes
Y: 11.9 mVolts
100
75
50
25
3
10 20 30 40 50 60 70 80
Minutes

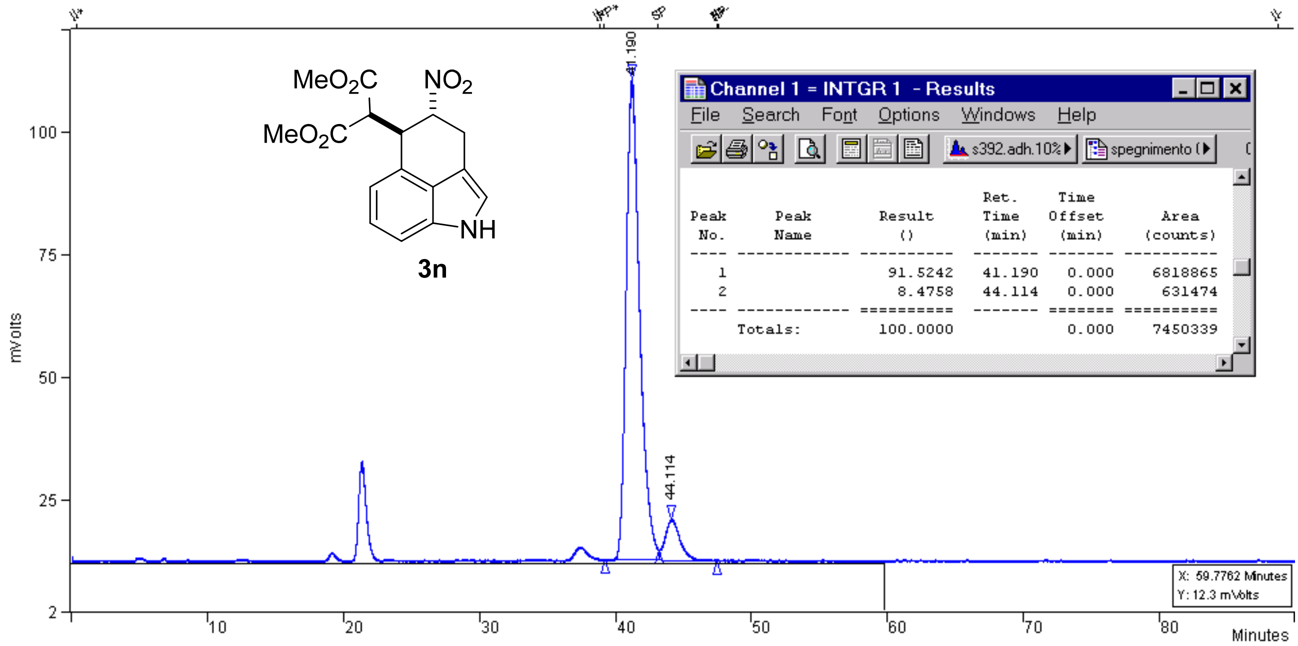

MeO2C NO2
MeO2C
NH
3n
41.190
44.114
Channel 1 = INTGR 1 - Results
File Search Font Options Windows Help
s392.adh.10%
spegnimento
Peak No. | Peak Name | Result () | Ret. Time (min) | Time Offset (min) | Area (counts)
1 | | 91.5242 | 41.190 | 0.000 | 6818865
2 | | 8.4758 | 44.114 | 0.000 | 631474
Totals: | | 100.0000 | | 0.000 | 7450339
X: 59.7762 Minutes
Y: 12.3 mVolts
mVolts
100
75
50
25
2
10 20 30 40 50 60 70 80
Minutes

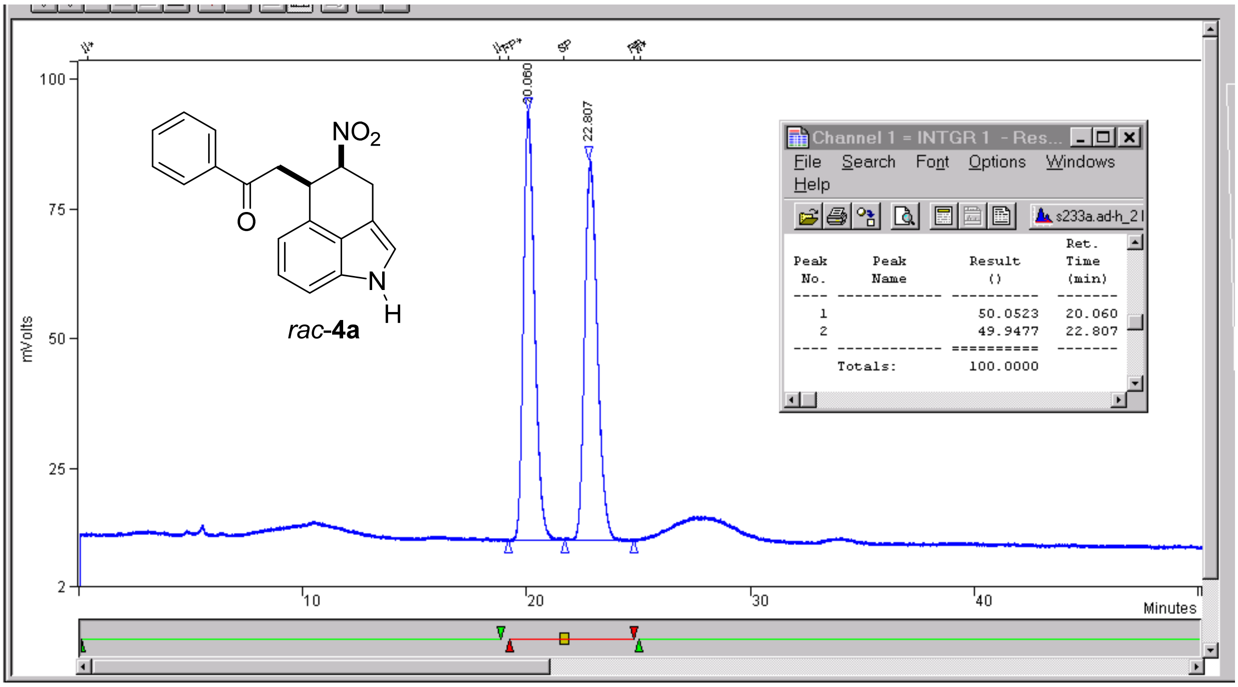
NO2
O
N
H
rac-4a
100
75
50
25
2
mVolts
10
20
30
40
Minutes
20.060
22.807
Channel 1 = INTGR 1 - Res...
File Search Font Options Windows Help
s233a.ad-h_2
Peak No. Peak Name Result () Ret. Time (min)
1 50.0523 20.060
2 49.9477 22.807
Totals: 100.0000

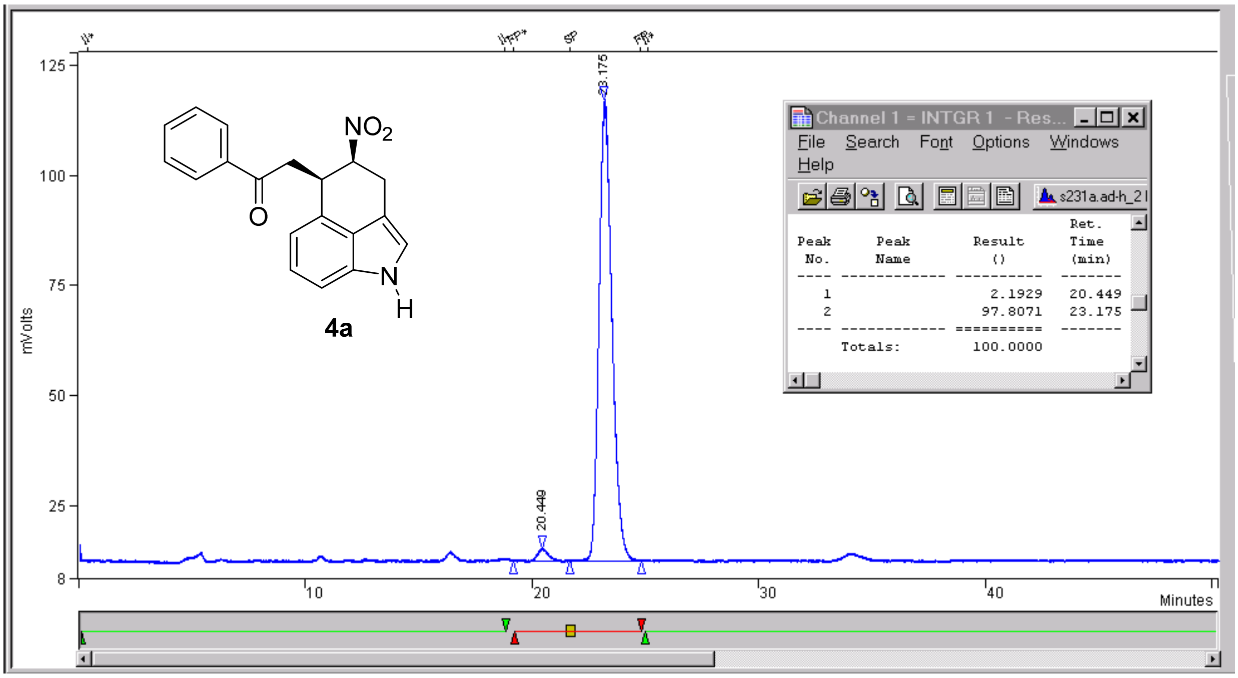
NO2
O
N
H
4a
125
100
75
50
25
8
mVolts
10
20
30
40
Minutes
20.449
23.175
Channel 1 = INTGR 1 - Res...
File Search Font Options Windows Help
s231a.ad-h_2
Peak No. Peak Name Result () Ret. Time (min)
1 2.1929 20.449
2 97.8071 23.175
Totals: 100.0000